

# **Test of New Physics at Neutrino Telescopes**

A thesis submitted in partial fulfilment of  
the requirements for the degree of

**Doctor of Philosophy**

*by*

**Mr. Bhavesh Chauhan**

(Roll No. 14330003)

Under the supervision of

**Prof. Subhendra Mohanty**

Professor

Theoretical Physics Division

Physical Research Laboratory, Ahmedabad, India.



DISCIPLINE OF PHYSICS

INDIAN INSTITUTE OF TECHNOLOGY GANDHINAGAR

2019



**Dedicated to**

*My beloved family.*



## **Declaration**

I declare that this written submission represents my ideas in my own words and wherever others' ideas or words have been included, I have adequately cited and referenced the original sources. I also declare that I have adhered to all principles of academic honesty and integrity and have not misrepresented, fabricated, or falsified any idea/data/fact/source in my submission. I understand that any violation of the above will be cause for disciplinary action by the Institute and can also evoke penal action from the sources which have thus not been properly cited or from whom proper permission has not been taken when needed.

Bhavesh Chauhan

(Roll No: 14330003)

Date:



# CERTIFICATE

It is certified that the work contained in the thesis titled **“Test of New Physics at Neutrino Telescopes”** by Mr. Bhavesh Chauhan (Roll No. 14330003), has been carried out under my supervision and that this work has not been submitted elsewhere for a degree.

Prof. Subhendra Mohanty  
Professor  
Theoretical Physics Division,  
Physical Research Laboratory,  
Ahmedabad, India.  
(Thesis Supervisor)

Date:



# Thesis Approval

The thesis titled

## Test of New Physics at Neutrino Telescopes

by

**Mr. Bhavesh Chauhan**

(Roll No. 14330003)

is approved for the degree of

Doctor of Philosophy

---

Examiner

---

Examiner

---

Supervisor

---

Chairman

Date: \_\_\_\_\_

Place: \_\_\_\_\_



---

## Acknowledgements

*Firstly, I would like to express my most sincere gratitude to my supervisor Prof. Subhendra Mohanty for the constant support during my Ph.D as well as for his guidance and motivation. I have benefited from his immense knowledge and I wish I could have learnt even more. I can not imagine having a better advisor and mentor for my Ph.D.*

*Besides my advisor, I would like to thank the rest of my DSC committee: Prof. Namit Mahajan and Prof. Jitesh Bhatt for their insightful comments and encouragement during the last four years. My sincere thanks also goes to members of the Theoretical Physics division: Prof. Srubabati Goswami, Prof. Hiranmaya Mishra, Prof. Dilip Angom, Dr. Partha Konar, Dr. Navinder Singh, and Dr. Ketan Patel from whom I have learnt a lot. A special mention goes to late Prof. Ramesh whose course on Statistics was extremely influential. I am deeply indebted to my deceased mentor Prof. Champak Das who made sure I knew the ups and downs of a PhD before I started this journey.*

*I am also grateful to my colleague and collaborator, Bharti, for countless stimulating discussions. I acknowledge Coffee Club members Ashish and Priyank for their support and for all the fun we have had over the years. I specially thank Ashish, Priyank, Anshika, and Tanmay for their careful reading of this thesis and useful suggestions and comments. I am also grateful to my other colleagues Soumik, Vishnu, Aman, Nijil, Kaustav, Arvind, Richa, Balbeer, and Akanksha for keeping me on my toes. I thank my seniors Ujjal Dey, Arnab Dasgupta, Girish Kumar, and Rukmani who have guided me with their experience many a times.*

*I reserve my most special gratitude for my mother. Without her emotional and spiritual support, I would not have been able to achieve anything. I thank my younger brother for taking care of the family all this while without which it would have been impossible to dedicate myself to physics.*

*Last but not the least, I would like to acknowledge PRL administration for the financial and logistic support.*

**- Bhavesh Chauhan**



# Abstract

The Standard Model of particle physics is the most successful theory of interactions between elementary particles. But there are enough reasons to believe in particles and symmetries beyond standard model. In this thesis, I have studied two well motivated extensions, leptoquarks and sterile neutrino, in the context of IceCube and ANITA experiments. A TeV scale leptoquark can resolve the observed discrepancy in semi-leptonic decays of B meson (flavor anomalies). The leptoquark can also be resonantly produced in neutrino-nucleon interaction and explain the excess of PeV events at IceCube. We find that a simultaneous explanation using the scalar leptoquark  $R_2 \sim (\mathbf{3}, \mathbf{2}, 7/6)$  is ruled out from LHC searches such as dijet +  $\cancel{E}_T$  and monojet +  $\cancel{E}_T$ . The constraints obtained also limit other resonance based explanation of PeV excess. Moreover, the puzzle of EeV scale  $\tau$  emerging from inside Earth as observed by ANITA can also be explained with leptoquarks. In our framework, the vector leptoquark  $U_1 \sim (\mathbf{3}, \mathbf{1}, 2/3)$ , which can simultaneously address the charged and neutral current mediated flavor anomalies, also couples to a sterile neutrino. The leptoquark mediated interaction between astrophysical neutrino and nucleons in Earth produces a sterile neutrino that propagates without significant attenuation. If the mass of the sterile neutrino is a few GeV, it decays near the surface to  $\tau$  lepton. On the other hand, if the sterile neutrino is very light, the astrophysical flux of sterile neutrinos can pass through Earth and produce a  $\tau$  lepton near the surface by resonant production of leptoquark. These two scenarios significantly enhance the survival probability and provide a combined explanation of flavor and ANITA anomalies. In addition, the new particles proposed are within the reach of future LHC searches and B factories. A major challenge is to explain the flux of sterile neutrinos and one possibility is to consider oscillation from active neutrinos. This is plausible only if the sterile neutrino is very light and has large mixing angles. The existence of eV scale sterile neutrino is also hinted by short baseline experiments such as MiniBooNE and LSND. However, it is in conflict with big bang nucleosynthesis unless one postulates either non standard cosmology or new interactions. One possibility is to consider self-interaction in the sterile sector. Such interactions would result in absorption features in the astrophysical neutrino spectrum which can be tested by IceCube. We have claimed that the lack of

400-800 TeV neutrinos is due to absorption by cosmic sterile neutrino background. The lack of Glashow events is attributed to absorption due to heaviest active neutrino in the cosmic background. Furthermore, the self-interacting sterile neutrino can also act as a portal to hidden and light self-interacting dark matter. A model is proposed where the relic density of dark matter is obtained from freeze-out of coannihilations and self-interaction is loop suppressed. The interesting parameter space that can be tested with supernova neutrinos is in conflict with observation of PeV events at IceCube.

**Keywords:** Sterile Neutrino, Leptoquark, IceCube, ANITA, MiniBooNE, Flavor Anomalies,  $R_{D^{(*)}}$ ,  $R_{K^{(*)}}$ , Dark Matter.

# Contents

<b>Acknowledgements</b>	<b>i</b>
<b>Abstract</b>	<b>iii</b>
<b>Contents</b>	<b>v</b>
<b>List of Figures</b>	<b>vii</b>
<b>List of Tables</b>	<b>xi</b>
<b>1 Introduction</b>	<b>1</b>
<b>2 Hints of New Physics</b>	<b>5</b>
2.1 IceCube HESE anomalies . . . . .	5
2.2 ANITA Anomalous Events . . . . .	9
2.3 MiniBooNE Excess . . . . .	13
2.4 Flavor Anomalies . . . . .	15
2.4.1 LFU violation in charged current transitions . . . . .	16
2.4.2 LFU violation in neutral current transitions . . . . .	18
2.4.3 Resolution to flavor anomalies . . . . .	21
2.5 Self Interacting Dark Matter . . . . .	21
<b>3 Leptoquark for Flavor and IceCube</b>	<b>23</b>
3.1 Model Description . . . . .	24
3.2 $R_2$ for $(g - 2)_\mu$ . . . . .	25
3.3 $R_2$ for $R_{K^{(*)}}$ . . . . .	26
3.4 $R_2$ for IceCube . . . . .	28

3.5	Simultaneous explanation . . . . .	31
3.6	LHC constraints . . . . .	33
3.7	Conclusion . . . . .	36
<b>4</b>	<b>Leptoquark for ANITA</b>	<b>37</b>
4.1	GeV scale sterile neutrino . . . . .	37
4.2	Light Sterile Neutrino . . . . .	43
4.3	Conclusion . . . . .	47
<b>5</b>	<b>Sterile Neutrino for IceCube</b>	<b>49</b>
5.1	Self interacting sterile neutrino . . . . .	49
5.2	Neutrino absorption by cosmic backgrounds . . . . .	52
5.3	Constraints on parameter space . . . . .	55
5.4	Attenuated Flux at IceCube . . . . .	57
5.5	Conclusion . . . . .	58
<b>6</b>	<b>Sterile Neutrino for Light Dark Matter</b>	<b>61</b>
6.1	Model Description . . . . .	61
6.2	Relic Density from Coannihilation . . . . .	64
6.3	One-Loop self interaction . . . . .	68
6.4	Results and Discussion . . . . .	70
6.5	Conclusion . . . . .	73
<b>7</b>	<b>Conclusion</b>	<b>75</b>
	<b>Bibliography</b>	<b>79</b>
	<b>List of publications</b>	<b>113</b>
	<b>Publications attached with thesis</b>	<b>115</b>

# List of Figures

2.1	Neutrino Deep Inelastic Scattering . . . . .	6
2.2	Feynman diagrams for neutrino-quark and antineutrino-electron scattering . . . . .	6
2.3	Diagram for $\bar{B} \rightarrow D^{(*)} \ell^- \bar{\nu}_\ell$ in SM . . . . .	16
2.4	Typical diagram for $\bar{B} \rightarrow K^{(*)} \ell^+ \ell^-$ . <i>Left: Penguin, Right: Box.</i> . . . .	19
3.1	The leptoquark contribution to $b \rightarrow s \mu^- \mu^+$ . . . . .	26
3.2	The NC like ( <i>left</i> ) and CC like ( <i>right</i> ) interaction of the leptoquark . . . . .	29
3.3	The difference in NC-like (solid) and CC-like (dashed) interactions. . . . .	31
3.4	The variation of $\delta$ with $M_2$ for various choice of coupling $\lambda_1$ is shown. The red, green, blue, and black lines correspond to $\lambda_1 = 1, 3, 6,$ and $4\pi$ respectively. . . . .	32
3.5	The parameter space of $(g - 2)_\mu$ for various choicess of coupling $\lambda_1$ is shown along with the constraints from flavor anomalies for $M_1 = 1100$ GeV and $M_2 = 1000$ GeV. . . . .	32
3.6	The solid black line shows the prediction for IceCube using leptoquark and SM interactions. . . . .	33
3.7	Gluon-initiated (top) and quark-initiated (bottom) pair production of scalar leptoquark . . . . .	34
3.8	Single production of scalar leptoquark . . . . .	34
3.9	The dijet+MET constraints are shown in blue and the monojet+MET constraints are shown in red. The parameter space above the curves is ruled out. The contours of $\delta$ are shown and the benchmark point used to generate Fig. 3.6 is shown. . . . .	36

- 4.1 The Feynman diagrams for the processes involved in section 4.1. *Left:* The s-channel neutrino quark interaction mediated by leptoquark  $U_1$  with sterile neutrino in final state. *Right:* The decay mode of sterile neutrino to charged lepton and  $D_s^+$  is shown. The shaded circle represents the effective vertex. . . . . 39
- 4.2 The parameter space that gives  $\epsilon_{LQ} > \epsilon_{SM}$  (*blue*), and  $\epsilon_{LQ} > 1 \times 10^{-6}$  (*dark blue*) for  $l_{\oplus} = 7210$  km is shown. Similar projections for  $l_{\oplus} = 5740$  km is shown by red curves. The gray shaded region is conservatively ruled out from  $B_c^+$  decays and the limits for various  $\mathcal{B}_\ell$  are shown. The top part is excluded using the perturbativity limit  $g_x \leq \sqrt{4\pi}$ . The neutrino energy is fixed to be 2 EeV. The benchmark point considered in the text is shown. . . . . 41
- 4.3 The Feynman diagrams for  $\chi$ -nucleon interaction. (a) The dominant s-channel  $\chi$ -quark interaction. (b) The  $\kappa$ -dependent  $\chi$ -gluon interaction. (c) The  $\kappa$ -independent  $\chi$ -gluon interaction. . . . . 44
- 4.4 The variation of cross section  $\sigma_q$  ( $\sigma_g$ ) with incident sterile neutrino energy is shown in blue (red). The inset shows the difference in magnitude of  $\sigma_g$  for  $\kappa = 0$  and 1 in arbitrary units. . . . . 45
- 4.5 The variation of  $\epsilon_q$ ,  $\epsilon_g$ , and  $\epsilon$  is shown in blue, red, and black respectively. The solid curve is for  $\kappa = 1$  and the dashed curve for  $\kappa = 0$ . The chord length  $l_{\oplus}$  is fixed to be 5740 km (left) and 7210 km (right). Also,  $g_x = 1.2$  for both the plots. The region shown in green is the observed shower energy for the two events. . . . . 45
- 5.1 The Feynman diagrams for the effective potential. The red crosses denote that the interaction is with the thermal background. . . . . 50
- 5.2 *Left:* This plot shows variation of  $R_e$  (blue),  $R_\mu$  (red),  $R_\tau$  (green), and  $R_s$  (dashed black) with neutrino energy. *Right:* This plot shows variation of  $R_1$  (blue),  $R_2$  (red),  $R_3$ (green), and  $R_4$  (dashed black) with neutrino energy. . . . . 54

5.3	The parameter space of masses of sterile neutrino and new gauge boson. The black point shows the benchmark case considered in the paper. <i>Left:</i> $\langle z_s \rangle = 0.6$ , <i>Right:</i> $\langle z_s \rangle = 0.8$ . See text for details. . . . .	56
5.4	The flux without attenuation is shown as dashed grey line. The blue (red) curve is the flux with attenuation for the democratic (maximal) case. . . . .	57
6.1	The annihilation channel for $\chi_1$ whose freeze-out determines the relic density . . . . .	66
6.2	The Feynman diagram for the self interaction of DM. There are seven other "crossed" diagrams. . . . .	69
6.3	The relative strength of self interactions i.e. $\sigma_{SI}(v)/\sigma_{SI}(0)$ is shown as a function of velocity for various choices of parameters. The red curves are for $M_X = 5$ MeV and the blue ones are for $M_X = 20$ MeV. The solid and dashed curves are for $\delta = 1.5$ and $\delta = 2.5$ respectively. . . . .	71
6.4	The allowed parameter space for $m_\chi = 10$ keV (blue), 100 keV (green), and 1 MeV (red) is shown for benchmark models $\xi = 0.5$ and $\xi = 0.3$ . The upper (lower) limit of $M_X$ corresponds to $\sigma_{SI}/m_1 = 0.1(1.0) \text{ cm}^2/g$ . The exclusion limits from IceCube are shown. . . . .	72
6.5	The Feynman diagram for neutrino dark matter scattering . . . . .	72



# List of Tables

2.1	Properties of the anomalous events. . . . .	10
2.2	Current status of LFU in $R_{D^{(*)}}$ . . . . .	17
2.3	Current status of LFU in $R_{K^{(*)}}$ . . . . .	19
4.1	The required value of $\phi_0$ to get $\mathcal{N} = 1$ for various choices of spectral index and chord lengths ( $A \equiv 5740$ km and $B \equiv 7210$ km). . . . .	46
6.1	The BSM fields and their charges under $U(1)_X$ symmetry. . . . .	62



# Chapter 1

## Introduction

The fundamental quest of physical sciences is to understand what our universe is made up of and how does it give rise to the observed phenomenon. At present, nearly 95% of the universe's content eludes complete knowledge, however we understand the remaining 5% very well. The elementary particles that make up the *visible* matter are fermions and the interaction between them arises from exchange of gauge bosons. There are four fundamental forces in nature that are responsible for these interactions: electromagnetic, weak, strong, and gravitational. All but the gravitational one can be understood in terms of a renormalizable quantum field theory based on local internal symmetry i.e. a gauge theory. The theory of strong interaction is called as quantum chromodynamics whereas the electromagnetic and weak interaction can be studied in a single framework called as electroweak theory.

The Standard Model (SM) of particle physics is based on the non-Abelian symmetry group  $SU(3)_C \times SU(2)_L \times U(1)_Y$  which is spontaneously broken to  $SU(3)_C \times U(1)_Q$  when the Higgs boson takes a non-vanishing vacuum expectation value. This symmetry breaking generates mass for fermions, gauge bosons, and the Higgs itself. The neutrinos, photon, and gluon remain massless. This model is also known as Glashow-Weinberg-Salam model [1–3]. The discovery of Higgs boson at LHC in 2012 [4] and subsequent measurements of its branching fractions in conformity with SM has settled SM to be the theory of particle interactions at the weak scale. The SM has passed almost every precision test at particle colliders such as Large Electron-

Positron Collider (LEP) and Large Hadron Collider (LHC). Despite the successes of SM, there are reasons to believe in new physics scenarios at energies above the electroweak scale ( $\sim$  few TeV). On one hand, there are aesthetic problems in the SM such as the lack of gauge coupling unification, hierarchy between electroweak and Planck scale, large number of free parameters, etc. While on the other hand, there are phenomenological problems such as lack of a Dark Matter (DM) candidate, explanation of matter anti-matter asymmetry, non-zero neutrino masses, etc. All of which motivate the need for theories beyond the standard model (BSM) or simply new physics (NP).

The neutrinos have a special place in SM. Unlike other fermions they do not have right handed partners. They only participate in weak interactions and it is not possible to write a renormalizable mass term that also respects the symmetries of SM. However, the observation of neutrino oscillation in atmospheric [5] and solar neutrinos [6, 7] provides unquestionable evidence of non-vanishing masses for neutrinos. We know from these experiments that at least two of the three neutrinos are massive, and any attempt to explain these small masses necessarily evoke particles that are not part of the SM spectrum. The simplest models utilize the *seesaw* mechanism with heavy right-handed neutrinos (type-I) [8–10], scalar triplet (type-II) [11–13], or fermion triplet (type-III) [14]. In these scenarios, the lightness of neutrino masses is associated with the heaviness of new particle, hence the name *seesaw*. A major challenge for neutrino mass models is to provide experimental tests as the new particles are often too heavy to be produced in present day colliders. One can also generate small neutrino mass through loop effects and in these scenarios, the neutrino mass is said to be generated *radiatively* [15–19]. The unknown parameters like the neutrino mass hierarchy and CP-violation in the neutrino sector [20] may be settled in planned experiments such as DUNE [21, 22].

Since neutrinos only have weak interactions, their scattering cross section with other particles is very small. This implies that the astrophysical neutrino will travel almost unattenuated along the line from source to Earth. On the other hand, photons can scatter off the galactic and intergalactic dust. The charged particles are affected

---

by interim magnetic fields which makes the direction reconstruction impossible. They also lose energy via scattering and bremsstrahlung. Because of this, the observation of astrophysical neutrinos can yield accurate information about the source and becomes a useful tool in understanding the origins of Ultra High Energy (UHE) cosmic rays. While the small cross section has its advantages, it also implies that direct detection of these neutrinos is immensely difficult. To give an estimate, a TeV energy neutrino has an interaction length of 2.5 million km in water [23]. One way to observe neutrino interactions is to have detectors with large volume to compensate for the small cross section. Neutrino observatories such as IceCube [24], ANTARES [25] (which is being upgraded to KM3NET [26]), and ANITA [27] are designed to look at the interaction of neutrino with nucleus (and electrons) in water. These observatories are often called *neutrino telescopes* just like their optical counterparts and play a crucial role in multi messenger astronomy.

In the first three years of its operation, the IceCube experiment reported three events where the reconstructed neutrino energy is 1-3 PeV [28]. In the subsequent years, IceCube has regularly observed neutrino with energy in the range 10 - 400 TeV interacting with nucleons in ice [30]. Recently, the ANITA experiment has also observed interactions of neutrino above EeV energy [31]. With these neutrino telescopes, one can not only test the Standard Model interactions, but also probe new physics at scales varying from MeV to TeV. Moreover, there are some anomalies observed by these experiments that can be interpreted as hints of new physics.

Hints of new physics have also been observed in other experiments. The short baseline neutrino oscillation experiments LSND [32] and MiniBooNE [33] have observed evidence for a eV scale sterile neutrino with relatively large mixing angles. But this is in conflict with effective relativistic degrees of freedom during big bang nucleosynthesis which is inferred from abundances of light nuclei like hydrogen and helium [34]. One possibility is to consider alternate cosmologies to  $\Lambda$ CDM, but another resolution is to assume self interaction in the sterile sector mediated by MeV scale gauge boson [35]. Such interactions can give absorption features in the UHE neutrino spectrum

which can be tested by IceCube.

The collider experiments Belle, BaBar, and LHCb, have tested for lepton flavor universality in semi leptonic decay modes of B mesons through clean observables  $R_{D^{(*)}}$  and  $R_{K^{(*)}}$ . Recent measurements have shown significant deviations from SM predictions. These discrepancies can be resolved by postulating TeV scale leptoquarks. Since these leptoquarks mediate neutrino-nucleon interactions, they also have observable consequence for neutrino telescopes. For example, resonant production of leptoquarks can explain the excess of PeV events at IceCube while a leptoquark coupled to sterile neutrino can explain the anomalous events observed by ANITA.

In this thesis, I have studied the role of IceCube and ANITA for testing and validating new physics scenarios, especially leptoquarks and sterile neutrinos, that have been proposed as a solution to anomalies in other experiments.

## Organization of thesis

The thesis is organised as follows. In chapter 2, I provide a brief overview of the anomalies in experiments which have been addressed in this thesis. In chapter 3, I show that common explanation for flavor and IceCube anomalies using leptoquark  $R_2$  is ruled out from LHC searches. In chapter 4, I have discussed two scenarios based on leptoquark  $U_1$  that can significantly enhance the survival probability of Earth emergent  $\tau$  while simultaneously addressing the flavor anomalies. In chapter 5, I have discussed the implication of self-interacting sterile neutrino for IceCube. The astrophysical neutrinos scatter off the sterile neutrino background and result in absorption features in the UHE neutrino spectrum. The lack of 400-800 TeV neutrinos is attributed to resonant absorption and other consequences are explained. In chapter 6, the self-interacting sterile neutrino is used as a portal to dark matter. I have provided a novel production mechanism for sub MeV self interacting dark matter. Constraints from IceCube are discussed. In chapter 7, the conclusions and implications of the thesis are discussed along with future directions.

# Chapter 2

## Hints of New Physics

In this chapter, I will present some of the anomalies observed in experiments that have been addressed in the thesis. In the beginning, I have discussed the anomalies in neutrino based experiments i.e. IceCube, ANITA, and MiniBooNE and I have followed it up with a discussion on collider based Flavor anomalies.

### 2.1 IceCube HESE anomalies

The IceCube Neutrino Observatory (IceCube) is a neutrino telescope located near the Amundsen-Scott south pole station in Antarctica. The detector comprises of 86 strings of 60 Digital Optical Modules (DOMs) each. The string separation is about 125 m and the DOMs on strings are positioned 17 m apart. This array of DOMs starts 1450 m below the Antarctic surface and extends upto 2450 m. At the surface, there is an array of DOMs called IceTop which is used to veto events of atmospheric origin. At the centre, there is a dense array of DOMs called DeepCore which is relevant for study of neutrino oscillation as well as searches for sterile neutrino [36].

Astrophysical Ultra-High Energy (UHE) neutrinos undergo Deep Inelastic Scattering (DIS) with nucleons in the detector volume through SM interactions. A schematic representation of this process is shown in Fig. 2.1. At the quark level, the interactions are mediated by exchange of  $Z$  boson (neutral current) or  $W^\pm$  boson (charged current). The neutrinos can also interact with the electrons in the ice, however this cross section

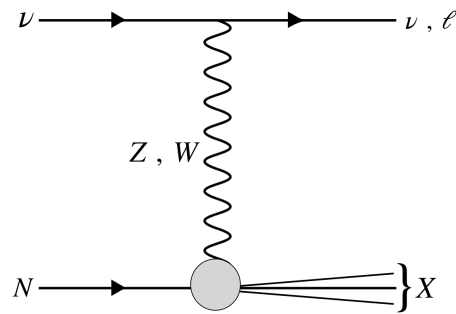


**Figure 2.1:** Neutrino Deep Inelastic Scattering

is relatively small and can be ignored [23]. The exception is when antineutrino-electron interaction resonantly produces the W boson. This happens for a particular neutrino energy of 6.3 PeV, known as Glashow resonance [37], and we expect more events in 3.6 PeV - 7.5 PeV bin as compared to neighbouring bins. The Feynman diagrams for these processes are given in Fig. 2.2.

The neutrino interactions produce relativistic secondary particles inside the detector that emit Cherenkov radiation. The photons are detected by the photo multiplier tubes (PMTs) in DOMs which report the total electromagnetic equivalent energy deposited as well as detection time. This is used to determine the energy and direction of the incident neutrino. Based on the deposited EM equivalent energy, IceCube data is divided into two samples: Medium Energy Starting Events (MESE) with an energy threshold of 1 TeV and High Energy Starting Events (HESE) for neutrino energies larger than 20 TeV. The six year HESE sample contains 82 events in energy range 20 TeV to 10 PeV [30].

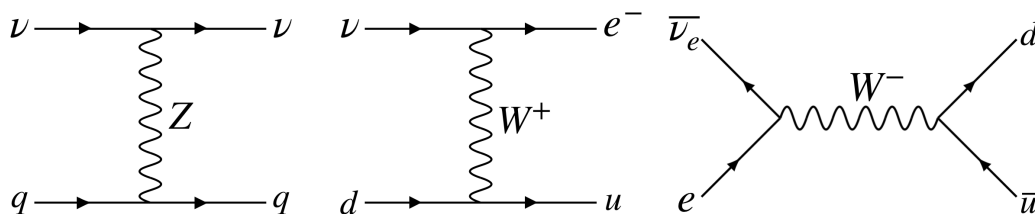


**Figure 2.2:** Feynman diagrams for neutrino-quark and antineutrino-electron scattering

Like other cosmic ray particles, the flux of astrophysical neutrinos is assumed to

have a power-law behaviour and modelled as,

$$\frac{d\phi}{dE_\nu} = \phi_0 \left( \frac{E_\nu}{100 \text{ TeV}} \right)^{-\gamma} \quad (2.1)$$

where  $\phi_0$  is normalization and  $\gamma$  is spectral index. From the Fermi acceleration mechanism at shock fronts, it is expected that  $\gamma = 2.0$  [38]. However, the best fit with six year HESE sample gives [39]

$$\gamma^{6yr} = 2.92^{+0.29}_{-0.33}, \quad (2.2)$$

which is larger (harder) than the best fit for four year sample [30]

$$\gamma^{4yr} = 2.58 \pm 0.25. \quad (2.3)$$

This change can be attributed to the fact that in the last two years of operation, IceCube has not seen any events above 200 TeV. This is often called as the *pile-up* of low energy events. The discrepancy in expected and observed spectral indices leads to the question: Where do astrophysical neutrinos come from? The concurrent measurement of a neutrino event with blazar flaring observed in FermiLAT and other optical telescopes has provided some hints [40]. However, future multi-messenger astronomy will shed more light on the issue.

There are other issues in the HESE sample as well. During the first three years of its operation, IceCube reported three cascade events with deposited energy between 1.0 PeV to 3.0 PeV [28]. In order to explain these events with only SM interactions, one requires a smaller spectral index. However, this leads to a significant number of expected events from Glashow resonance. A larger value of spectral index makes the low-energy events compatible with Glashow resonance, but then the PeV events appear to be an *excess*. Recently, IceCube has reported two highest energy neutrino events from its nine year data [29]. The best estimated neutrino energy for the two events is 8.6 PeV and 5.9 PeV respectively. The first event is a track-like event and the second is a partially contained shower. While the second event may be due to Glashow

resonance, there is no consensus yet due to uncertainties in the energy reconstruction of an uncontained shower. Furthermore, even after six years of observation, no neutrinos with energy in the range 400-800 TeV have been observed. This is also known as the *gap* in IceCube HESE data.

Several new physics scenarios have been proposed to address these issues. The solutions to the PeV excess can be broadly classified as modification to either the neutrino flux, the cross section, or both. In the first class of solutions, cosmological dark matter decays to SM neutrinos at late times [41–46]. This gives a line feature in the astrophysical neutrino spectrum which is broadened due to cosmological redshift. For dark matter mass in the PeV regime, one can explain the PeV excess with large spectral index for astrophysical neutrinos. This is compatible with low-energy events as well as non observation of Glashow resonance. The gap in the IceCube spectrum is also naturally addressed in these models. However, such a heavy dark matter cannot be tested with colliders and direct detection experiments. Moreover, recent observations of 5.9 PeV and 8.6 PeV neutrinos by IceCube is in conflict with minimal dark matter models proposed to address the PeV excess.

The second class of models invoke hypothetical particles that contribute to the neutrino nucleon interaction. A t-channel interaction will modify the cross section for all neutrino energy and cannot explain the excess. The s-channel interaction contribution is dominant when the mediator is resonantly produced and thus can possibly address the PeV excess. The new particle needs to couple to neutrino and quarks simultaneously and thus needs to be a  $SU(3)_C$  (anti) triplet. The known candidate for such interactions are leptoquarks [47–53]. To explain the PeV excess, one needs the colored mediator to be in the mass range 800-1200 GeV. This is within the reach of LHC and can be tested in monojet+ $\cancel{E}_T$  and other modes. The prospect of testability makes these explanations more promising than the first class.

If one assumes a single component flux of astrophysical neutrinos, the gap can be addressed through resonant absorption during propagation. This requires MeV-

scale new physics scenarios that have other interesting implications. The gap has been addressed in well motivated models such as  $\nu$ 2HDM [54] and gauged  $U(1)_{L_\mu-L_\tau}$  [55]. The absence of events near the Glashow resonance can be explained by invoking active neutrino decay,  $\Delta^+$  resonance, novel flux, or neutrino DM interaction [56–59]. The new highest energy events observed by IceCube can challenge some of these claims.

## 2.2 ANITA Anomalous Events

The ANtarctic Impulsive Transient Antenna (ANITA) is a long-duration balloon experiment designed primarily to detect broadband impulsive radio emission from neutrinos in the Antarctic ice [60]. The payload consists of 48 high-gain dual-polarization antennas and flies at a height of approximately 37 km above the Antarctic surface looking for radio signals in the range 200 - 1200 MHz. ANITA is sensitive to Askaryan emission from neutrino-induced showers in ice [61], and can also observe geomagnetic emission from extensive air showers (EAS) induced by cosmic rays or other particles [31]. As Earth's magnetic field is nearly vertical in Antarctica, EAS emission is expected to be horizontally polarized. But the Askaryan emission is vertically polarized for SM interactions of the neutrino. The downward directed EAS are reflected off the ice surface and show a characteristic phase reversal. Till date, ANITA has completed four flights whose durations are 35, 28.5, 22, and 29 days respectively.

There is enough precedence to assume that UHE neutrinos are incident on Earth. They are produced when UHE protons with energy greater than  $5 \times 10^{10}$  GeV are stopped by the cosmic microwave background (CMB) photons through Greisen Zatspin Kuzmin (GZK) mechanism [62, 63]. In this process, the pions are produced through either of the following interactions:

$$p + \gamma_{CMB} \rightarrow \Delta^+ \rightarrow p + \pi^0$$

$$p + \gamma_{CMB} \rightarrow \Delta^+ \rightarrow n + \pi^+$$

where  $\Delta^+$  is produced on shell. The neutral pion decays to photons, but the charged pion decays to neutrino and charged lepton. One of the final products in neutron decay

is neutrino. This results in an isotropic flux of UHE neutrinos on Earth [64].

During its first and third flight, ANITA also observed unexpected upward directed showers apparently emerging well below the horizon [65, 66]. The observed signal is consistent with  $\tau$  induced EAS. The essential details of the two Anomalous ANITA Events (AAEs) are given in Tab. 2.1. The survival probability with SM interactions ( $\epsilon_{SM}$ ) is estimated taking into account the neutrino regeneration effects and  $\tau$  energy losses in Ref. [67].

Property	AAE1	AAE2
Energy ( $E_\tau$ )	$0.6 \pm 0.4$ EeV	$0.56^{+0.3}_{-0.2}$ EeV
Zenith Angle	$117.4 \pm 0.3^\circ$	$125.0 \pm 0.3^\circ$
Chord Length ( $l_\oplus$ )	$5740 \pm 60$ km	$7210 \pm 55$ km
$\epsilon_{SM}$	$4.4 \times 10^{-7}$	$3.2 \times 10^{-8}$

Table 2.1: Properties of the anomalous events.

In order to estimate the number of Earth emergent showers seen by ANITA, we evaluate the  $\tau$  survival probability,  $\epsilon$  (also called efficiency in Ref. [68]), which represents the fraction of incident flux ( $\Phi$ ) that is converted into  $\tau$  near the surface. We use the expression

$$\mathcal{N} = A \cdot \delta T \cdot \delta\Omega \int_{E_{min}}^{E_{max}} dE_\nu \cdot \epsilon \cdot \Phi(E_\nu) \quad (2.4)$$

where the effective area of ANITA ( $A \approx 4 \text{ km}^2$ ) is estimated using the Cherenkov angle [68],  $\delta T$  is the time period, and  $\delta\Omega$  is the acceptance angle. For temporally continuous sources,  $\delta T \approx 25$  days is the combined exposure of ANITA-I (17.25 days) and ANITA-III (7 days) [65, 66]. We have ignored the contribution of ANITA-II (28.5 days) as it was not sensitive to such events. For transient sources,  $\delta T$  will depend on the source and can be smaller. For isotropic sources,  $\delta\Omega \approx 2\pi \text{ sr}$ . But for anisotropic sources,

$$\delta\Omega \approx 2\pi(1 - \cos \delta_\theta) \approx 0.0021 \text{ sr} \quad (2.5)$$

where  $\delta_\theta \sim 1.5^\circ$  is the angular uncertainty relative to parent neutrino direction [66]. The neutrino energy ( $E_\nu$ ) is integrated over the interval which gives correct range of

shower energy. For example, assume that  $\tau$  is produced through interaction of the incident neutrino such that  $E_\tau = E_\nu/4$ . Since the observed shower has energy in the range 0.1 - 1 EeV, one must integrate over 0.4 - 4 EeV. In general,  $\epsilon$  depends on  $E_\nu$  and other model dependent parameters.

We now provide an order-of-magnitude estimate of the required  $\epsilon$  taking  $\delta T = 25$  days. For the isotropic case, we assume that the source of EeV neutrinos is the Greisen-Zatsepin-Kuzmin (GZK) mechanism. We approximate the GZK flux by the upper limit [69] of its saturated value over the range 0.4 - 4 EeV as

$$\bar{\Phi}_{iso} \approx 10^{-25} (\text{GeV cm}^2 \text{ s sr})^{-1} \quad (2.6)$$

which gives  $\mathcal{N} \approx 200\epsilon$ . To get two events, one requires  $\epsilon \sim 0.01$ . Similar estimates were also obtained in Ref. [70] which takes energy dependence into account albeit with larger exposure time. With SM interactions, the authors in Ref. [67] have estimated that  $\epsilon_{SM} \sim 10^{-7}$  for the two reported events. Thus the estimated number of anomalous events from GZK neutrinos with only SM interactions is

$$\mathcal{N}_{iso}^{SM} \sim 2 \times 10^{-5} \quad (2.7)$$

which makes observation of two events extremely unlikely.

One can relax the assumption that the source of EeV neutrinos is the GZK flux. This allows us to postulate that such high energy neutrinos are coming from a localised source in the sky [70]. The upper limit on such anisotropic flux of EeV neutrinos is [71, 72]

$$\bar{\Phi}_{aniso} \approx 3.2 \times 10^{-20} (\text{GeV cm}^2 \text{ s sr})^{-1} \quad (2.8)$$

which is several orders larger than the isotropic case. After accounting for the small solid angle, one can similarly obtain,  $\mathcal{N} \approx 2.1 \times 10^4 \epsilon$ . To get two events, one requires  $\epsilon \sim 10^{-4}$ . Using SM interactions for the incident neutrinos,

$$\mathcal{N}_{aniso}^{SM} \sim 2.1 \times 10^{-3} \quad (2.9)$$

which again makes the two events very unlikely. In this section, we have ignored the energy dependence of  $\epsilon$  as well as  $\Phi$ . Even after taking those into account, the message will remain unchanged. The smallness of  $\epsilon_{SM}$  makes the two event unlikely.

One must also check the compatibility of ANITA with IceCube observations. Even though IceCube has smaller effective area, the long duration of the experiment implies that the expected number of EeV scale up going  $\tau$ -tracks seen by IceCube ( $\mathcal{N}_{IC}$ ) to be larger than expected anomalous events by ANITA ( $\mathcal{N}_{AN}$ ). Using the relative exposures, it has been estimated that  $\mathcal{N}_{IC} \approx 10 \times \mathcal{N}_{AN}$  [68, 70]. In Ref. [67], the authors identify three events in nine year (3142 days) IceCube data that may have origin similar to ANITA. This implies that  $\mathcal{N}_{AN} = 0.3$ . Using Poisson distribution, the probability of observing two such events is around 0.03. The challenge for BSM scenarios is to get  $\mathcal{N}_{AN}$  of this order by enhancing  $\epsilon$  as has been done in the two scenarios studied in Chapter 4 of this thesis.

There have been several attempts in recent times to explain the anomalous events. In Ref. [73], the authors propose that decay of a long-lived DM particle inside Earth. The required mass of DM is of EeV scale which is natural in CPT symmetric universe [74] or high-scale supersymmetry [75]. However, the gravitational capture of such a heavy DM and subsequent decays within the runtime of ANITA is highly unlikely [75].

The other possibility is to consider a flux of sterile neutrino on Earth. If the mixing angle is in the range  $0.1 - 0.01$ , then the up-going sterile neutrino can propagate freely inside Earth and interact close to the Antarctic surface [68, 76]. In these scenarios, the flux of sterile neutrino is generated via oscillations from the active neutrinos. The small mixing angle implies that the flux of active neutrinos is one or two orders of magnitude larger than the sterile neutrino flux. The limits from IceCube and other neutrino observatories on the flux of active neutrinos at these energies is in conflict with the flux required to explain ANITA events [68]. One way to escape these limits is to consider anisotropic flux [70]. The other possibility is to consider DM decaying to sterile neutrinos [77].

Another class of models that address the ANITA events involve a messenger particle that is produced in interactions at one end of the chord, propagates inside Earth without any significant attenuation, and subsequently decays or interacts at the other end. In Ref. [67], the messenger was proposed to be a long lived  $\tilde{\tau}$  produced in neutrino-nucleon interaction. In Ref. [70], a low mass neutralino (mostly bino) in R-parity violating supersymmetry was considered as the messenger. In Ref. [78], a heavier partner of inelastic dark matter was proposed as the messenger. A major challenge in these models is to get enough survival rate after two interactions as I have shown in Chapter 4. Similar inferences were also drawn in Ref. [79]. In Ref. [80], model independent properties of dark matter and the messenger particles were derived.

The anomalous ANITA events have also been addressed with axions [81] and supersymmetric sphalerons [82]. In Ref. [83], a non-particle physics explanation of these events was proposed using the Antarctic subsurface.

## 2.3 MiniBooNE Excess

The Mini Booster Neutrino Experiment (MiniBooNE) [33] looks for anomalous oscillation between muon and electron neutrino in short baseline ( $L/E_\nu \sim 1$  m/MeV). It was designed to investigate the anomaly reported by the Liquid Scintillator Neutrino Detector (LSND) [32] experiment in 1990s. The Booster at FermiLab accelerates protons to 8 GeV and directs it to neutrino beamline. These protons hit a Beryllium target and produce pions inside a magnetic focussing horn. By changing the polarity of horn, either  $\pi^+$  or  $\pi^-$  can be focussed. The decay of  $\pi^+$  produces a beam of  $\nu_\mu$  (neutrino mode) whereas the decay of  $\pi^-$  produces a beam of  $\bar{\nu}_\mu$  (anti-neutrino mode). The muon neutrino and muon antineutrino fluxes peak at approximately 600 MeV and 400 MeV, respectively. The detector consists of a sphere containing 818 tonnes of pure mineral oil ( $CH_2$ ) which is located 541 m away from the source. The inside of the shell is covered with photo multiplier tubes (PMT) each approximately 20 cm in diameter. The  $\nu_e$  and  $\bar{\nu}_e$  produced from oscillation will undergo charged current quasi

inelastic (CCQE) scattering inside the detector. The charged particles thus produced emit both directed Cherenkov radiation and an isotropic scintillation light that is detected by the PMTs.

The probability of  $\nu_\alpha$  converting to  $\nu_\beta$  is given by,

$$P_{\alpha \rightarrow \beta} = \delta_{\alpha\beta} - 4 \sum_{i>j} \text{Re} (U_{\alpha i}^* U_{\beta i} U_{\alpha j} U_{\beta j}^*) \sin^2 \left( \frac{\Delta m_{ij}^2 L}{4E} \right) + 2 \sum_{i>j} \text{Im} (U_{\alpha i}^* U_{\beta i} U_{\alpha j} U_{\beta j}^*) \sin \left( \frac{\Delta m_{ij}^2 L}{2E} \right) \quad (2.10)$$

where  $U$  is the Pontecorvo-Maki-Nakagawa-Sakata (PMNS) matrix and  $\Delta m_{ij}^2 = m_i^2 - m_j^2$  is the squared mass difference of the neutrinos. The third term on the RHS of Eq. (2.10) is related to CP asymmetry and assumed to be zero for remainder of the discussion. In two flavor approximation, the probability of  $\nu_\mu$  converting to  $\nu_e$  is given by the expression,

$$P_{\mu e} = \sin^2 (2\theta) \sin^2 \left( \frac{\Delta m^2 L}{E_\nu} \right) \quad (2.11)$$

where  $\theta$  is the mixing angle. The flux of  $\nu_e$  at MiniBooNE detector is a product of the conversion probability and the flux of  $\nu_\mu$  at the source. There is a background flux of  $\nu_e$  and  $\bar{\nu}_e$  from  $\mu^\pm$  and  $K^{\pm,0}$  decay that needs to be accounted for. The gamma background from neutral current production of  $\pi^0$  and  $\Delta$  radiative decay are constrained. The details of other backgrounds can be found in Ref. [33]. After accounting for all known effects and systematics, MiniBooNE expected 1578 events in neutrino mode and 399 events in antineutrino mode. However, the experiment saw an excess of 381 events in neutrino mode and 79 events in antineutrino mode. This excess, when attributed to oscillation, gives the best fit point as,

$$\Delta m^2 = 0.041 \text{ eV}^2 \quad \text{and} \quad \sin^2 2\theta = 0.92. \quad (2.12)$$

The neutrino mass scale and mixing angles inferred from MiniBooNE are neither compatible with solar nor atmospheric neutrino parameters. Thus, it is associated with a fourth mass eigenstate of the neutrino. However, from decay of the  $Z$  boson and other

experiments, we know that only three neutrinos are charged under the SM gauge group. Hence, this fourth neutrino must be *sterile* i.e. SM gauge singlet.

While the MiniBooNE excess is astonishing at least, the sterile neutrino interpretation is in direct conflict with many other observations. The parameter space favored by MiniBooNE is already ruled out from many experiments like OPERA [84], KARMEN [85], and IceCube [86]. Moreover, existence of such light states with large mixing angles is in direct conflict with cosmology. The determination of effective relativistic degrees of freedom ( $N_{eff}$ ) during the nucleosynthesis era ( $T \sim \text{MeV}$ ) by Planck is compatible with three neutrinos only [87, 88]. The fourth neutrino with large mixing angle will be in thermal equilibrium with other neutrinos and contribute to  $N_{eff}$ . The other conflict with cosmology is that the sum of neutrino mass is constrained to be  $\sum m_\nu < 0.12 \text{ eV}$  [88]. Thus it is nearly impossible to accommodate a eV-scale sterile neutrino with large mixing angles in the standard cosmological scenario.

A non-oscillation solution to the MiniBooNE anomaly was proposed in Ref. [89] using decay of a dark neutrino. However, there are strong limits on such explanation from neutrino scattering experiments [90]. Future runs of MiniBooNE and other experiments will shed more light on the anomaly.

## 2.4 Flavor Anomalies

In SM, there are six *flavors* each of quarks and leptons. For quarks, the neutral current interaction mediated by  $Z$  boson does not distinguish between generations at tree level and considered as flavor diagonal. However, the charged current interaction mediated by  $W^\pm$  boson distinguishes between flavors and depends on the quark mixing matrix known as Cabibbo-Kobayashi-Maskawa (CKM) matrix. For leptons, both neutral and charged current interactions are flavor diagonal as well as independent. This is known as Lepton Flavor Universality (LFU) and has been experimentally established through decays of light mesons,  $\tau$  decays,  $Z$  boson partial decay widths, etc. However, recent tests of LFU in rare decays involving  $b$  quark have shown significant deviations from

SM predictions. In this section, I have provided overview of two flavor anomalies that have garnered attention in recent times.

### 2.4.1 LFU violation in charged current transitions

The collider experiments Belle, BaBar, and LHCb have searched for decay of  $B$  meson involving the quark level transition  $b \rightarrow c$  occurring at tree level. In order to minimize the form factor dependence, one looks at the ratio

$$R_{D^{(*)}} = \frac{\mathcal{B}(\bar{B} \rightarrow D^{(*)} \tau^- \bar{\nu}_\tau)}{\mathcal{B}(\bar{B} \rightarrow D^{(*)} \ell^- \bar{\nu}_\ell)} \quad (2.13)$$

where the denominator is the average value for  $\ell = e$  and  $\ell = \mu$ . The rates in the numerator and denominator are expected to be different due to the large difference in  $\tau$  mass as compared to  $e$  or  $\mu$ . Recently, significant deviation in  $R_{J/\psi}$  was also reported [91]. The SM prediction and the results from various experiments are mentioned in Tab. 2.2. For completeness, I have also included recent results from Belle and the updated average. However, these are not used for obtaining the results in this thesis.

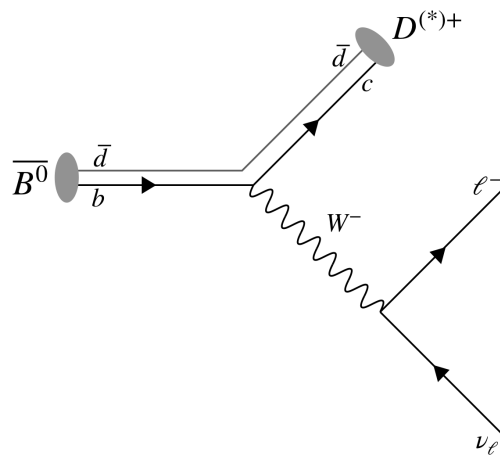


**Figure 2.3:** Diagram for  $\bar{B} \rightarrow D^{(*)} \ell^- \bar{\nu}_\ell$  in SM

As one can see, the experiments have consistently reported 3-3.5 $\sigma$  discrepancy from the SM prediction. While still not at the level of *discovery*, one can attribute this to contribution from new physics. One must note that the recent result from Belle, as

Experiment	$R_D$	$R_{D^*}$
BaBar	$0.440 \pm 0.058 \pm 0.042$ [92, 93]	$0.332 \pm 0.024 \pm 0.018$ [92, 93]
Belle	$0.375 \pm 0.064 \pm 0.026$ [94]	$0.270 \pm 0.035^{+0.028}_{-0.025}$ [95, 96]
LHCb	–	$0.291 \pm 0.019 \pm 0.029$ [97, 98]
<b>HFLAV Average</b>	$0.407 \pm 0.039 \pm 0.024$ [99]	$0.306 \pm 0.013 \pm 0.007$ [99]
Belle (2019)	$0.307 \pm 0.037 \pm 0.016$ [100]	$0.283 \pm 0.018 \pm 0.014$ [100]
<b>HFLAV Average</b>	$0.340 \pm 0.027 \pm 0.013$ [101]	$0.295 \pm 0.011 \pm 0.008$ [101]
<b>SM Prediction</b>	$0.299 \pm 0.003$ [102–110]	$0.258 \pm 0.005$ [102–110]

Table 2.2: Current status of LFU in  $R_{D^{(*)}}$ 

mentioned in Tab. 2.2, has reduced the significance of the discrepancy.

An efficient way of calculating the contribution of SM as well as new physics to these observables is through Effective Field Theory (EFT). The low energy weak effective theory for  $b \rightarrow c\ell\nu$  transition is described by the Lagrangian,

$$\mathcal{L}_{\text{eff}}^{b \rightarrow c\ell\nu} = -\frac{2G_F V_{cb}}{\sqrt{2}} \sum C_i \mathcal{O}_i + \text{h.c.} \quad (2.14)$$

where  $G_F = 1.116 \times 10^{-5} \text{ GeV}^{-2}$  is the Fermi coupling constant,  $\mathcal{O}_i$  are the dimension six effective operators, and  $C_i$  are the Wilson coefficients. The operator basis is similar to Ref. [111] and given by,

$$\begin{aligned} \mathcal{O}_{\text{VL}} &= [\bar{c}\gamma^\mu b] [\bar{\ell}\gamma_\mu P_L \nu] & \mathcal{O}_{\text{VR}} &= [\bar{c}\gamma^\mu b] [\bar{\ell}\gamma_\mu P_R \nu] \\ \mathcal{O}_{\text{AL}} &= [\bar{c}\gamma^\mu \gamma_5 b] [\bar{\ell}\gamma_\mu P_L \nu] & \mathcal{O}_{\text{AR}} &= [\bar{c}\gamma^\mu \gamma_5 b] [\bar{\ell}\gamma_\mu P_R \nu] \\ \mathcal{O}_{\text{SL}} &= [\bar{c}b] [\bar{\ell} P_L \nu] & \mathcal{O}_{\text{SR}} &= [\bar{c}b] [\bar{\ell} P_R \nu] \\ \mathcal{O}_{\text{PL}} &= [\bar{c}\sigma^{\mu\nu}] [\bar{\ell} P_L \nu] & \mathcal{O}_{\text{PR}} &= [\bar{c}\gamma_5 b] [\bar{\ell} P_R \nu] \end{aligned}$$

where the first letter of the subscript denote a vector, axial-vector, scalar, or pseudoscalar operator between quark fields and the second letter denotes chirality operators,  $P_{L,R} = (1 \mp \gamma_5)/2$ , between the lepton fields. Using only SM interactions, one

obtains

$$C_{VL}^{SM} = -C_{AL}^{SM} = 1 \quad (2.15)$$

which can be clearly seen as the contribution coming from exchange of  $W$  boson in the full theory. In presence of New Physics, these Wilson coefficients get correction depending on new interactions. One can write,

$$C_i = C_i^{SM} + \delta C_i \quad (2.16)$$

where the second term on the right side is the contribution from BSM fields. I have used the following simplified expressions for  $R_D$  and  $R_{D^*}$  obtained in Ref. [112] for the analysis done in this thesis:

$$\begin{aligned} R_D = & 0.30 + 0.60 \delta C_{VL} + 0.51 \delta C_{SL} \\ & + 0.30 (\delta C_{VL})^2 + 0.40 (\delta C_{SL})^2 + 0.51 \delta C_{VL} \delta C_{SL} \end{aligned} \quad (2.17)$$

$$\begin{aligned} R_{D^*} = & 0.25 + 0.03 \delta C_{VL} - 0.48 \delta C_{AL} + 0.03 \delta C_{PL} + 0.01 (\delta C_{VL})^2 \\ & + 0.24 (\delta C_{AL})^2 + 0.01 (\delta C_{PL})^2 - 0.03 \delta C_{AL} \delta C_{PL}. \end{aligned} \quad (2.18)$$

The leading term in these expressions is the SM prediction and agrees with the values mentioned in Tab. 2.2. For a given BSM scenario, one has to map the amplitude with new fields on to the operator basis, obtain the additional contribution to the Wilson coefficients, and substitute it into above expression.

## 2.4.2 LFU violation in neutral current transitions

As mentioned earlier, the flavor changing neutral currents (FCNCs) in SM are a consequence of loop process involving  $W^\pm$  boson in penguin and box topologies. It is a very sensitive probe of New Physics as new fields can contribute to FCNCs at the tree level. In last couple of decades, the processes involving  $b \rightarrow s$  and  $b \rightarrow d$  transitions have become an important probe in flavor physics. Since the first measurement of  $b \rightarrow s\gamma$  by CLEO collaboration in 1993 [113], significant theoretical and experimental advances

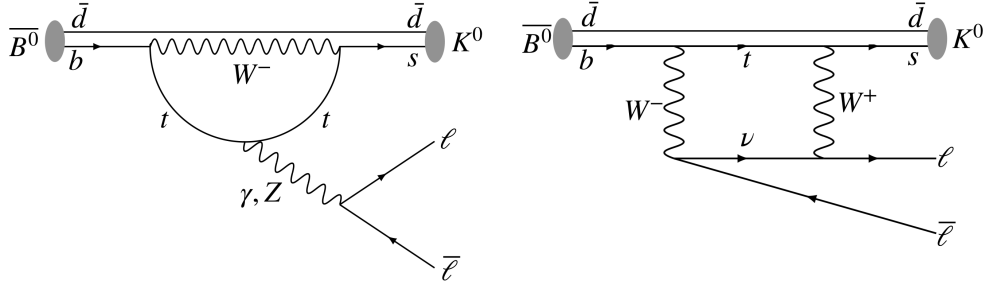


**Figure 2.4:** Typical diagram for  $\bar{B} \rightarrow K^{(*)} \ell^+ \ell^-$ . *Left:* Penguin, *Right:* Box.

have been made in the field. Just like in the previous section, one looks at the ratio,

$$R_{K^{(*)}} = \frac{\mathcal{B}(\bar{B} \rightarrow \bar{K}^{(*)} \mu^+ \mu^-)}{\mathcal{B}(\bar{B} \rightarrow \bar{K}^{(*)} e^+ e^-)}. \quad (2.19)$$

as a test of LFU. The fact that form factor dependence cancels in the above ratio is by no means trivial and was first pointed out in Ref. [114]. The current status of these ratios is mentioned in Tab. 2.3. It should be noted that the experiments have shown

Experiment	$R_K$	$R_{K^*}$
BaBar	$0.74^{+0.40}_{-0.31} \pm 0.06$ [115]	$1.13^{+0.34}_{-0.26} \pm 0.10$ [115]
Belle	$1.03 \pm 0.19 \pm 0.06$ [116]	$0.83 \pm 0.17 \pm 0.08$ [116]
LHCb	$0.745^{+0.090}_{-0.074} \pm 0.036$ [117]	$0.69^{+0.11}_{-0.07} \pm 0.05$ [118]
<b>SM Prediction</b>	$1.00 \pm 0.01$ [119–123]	$0.9964 \pm 0.005$ [119–123]

Table 2.3: Current status of LFU in  $R_{K^{(*)}}$

upto  $4\sigma$  deviation from SM predictions. Note that I have only mentioned the results for the central  $q^2 \in \{1, 6\} \text{ GeV}^2$  where  $q^2$  is the invariant mass squared of the outgoing leptons.

The effective dimension-six Lagrangian for  $b \rightarrow s \ell \ell$  transition is,

$$\mathcal{L}_{\text{eff}}^{b \rightarrow s \ell \ell} = -\frac{4G_F}{\sqrt{2}} V_{tb} V_{ts}^* \sum C_i \mathcal{O}_i \quad (2.20)$$

where I have ignored the double Cabibo suppressed contribution of the up-quark. Since other operators do not contribute to LFU violation, the dominant contribution to  $R_K$

and  $R_{K^*}$  comes from non-universal contribution to the semi-leptonic operators. I have used the basis used in Ref. [124] given by,

$$\begin{aligned}
\mathcal{O}_9 &= (\bar{s}\gamma^\mu P_L b) (\bar{\ell}\gamma_\mu \ell) & \mathcal{O}_{10} &= (\bar{s}\gamma^\mu P_L b) (\bar{\ell}\gamma_\mu \gamma_5 \ell) \\
\mathcal{O}'_9 &= (\bar{s}\gamma^\mu P_R b) (\bar{\ell}\gamma_\mu \ell) & \mathcal{O}'_{10} &= (\bar{s}\gamma^\mu P_R b) (\bar{\ell}\gamma_\mu \gamma_5 \ell) \\
\mathcal{O}_S &= (\bar{s}P_R b) (\bar{\ell}\ell) & \mathcal{O}_P &= (\bar{s}P_R b) (\bar{\ell}\gamma_5 \ell) \\
\mathcal{O}'_S &= (\bar{s}P_L b) (\bar{\ell}\ell) & \mathcal{O}'_P &= (\bar{s}P_L b) (\bar{\ell}\gamma_5 \ell).
\end{aligned}$$

Again, one can write the Wilson coefficients as

$$C_i = C_i^{SM} + \delta C_i \quad (2.21)$$

where the  $\delta C_i$  is the contribution from new physics. I have used the simplified expressions obtained in Ref. [124] for  $R_K$  and  $R_{K^*}$  which are given in Eq. (2.22) and Eq. (2.23) respectively.

$$\begin{aligned}
R_K &= 1 + 0.2427 (\delta C_9) + 0.0274 (\delta C_9)^2 + 0.2427 (\delta C'_9) + 0.0248 (\delta C_9) (\delta C_9)^2 \\
&\quad - 0.2253 (\delta C_{10}) + 0.0275 (\delta C_{10})^2 - 0.225 (\delta C_{10'}) + 0.055 (\delta C_{10}) (\delta C_{10'}) \\
&\quad + 0.0275 (\delta C_{10'})^2 + 0.009 (\delta C_S)^2 + 0.018 (\delta C_S) (\delta C_{S'}) + 0.009 (\delta C_{S'})^2 \\
&\quad - 0.0187 (\delta C_P) + 0.0046 (\delta C_{10} + \delta C'_{10}) (\delta C_P + \delta C_{P'}) + 0.0091 (\delta C_P)^2 \\
&\quad - 0.0187 (\delta C_{P'}) + 0.0182 (\delta C_P) (\delta C_{P'}) + 0.0091 (\delta C_{P'})^2
\end{aligned} \quad (2.22)$$

$$\begin{aligned}
R_{K^*} &= 1 + 0.2194 (\delta C_9) + 0.0321 (\delta C_9)^2 - 0.2004 (\delta C_{9'}) - 0.0476 (\delta C_9) (\delta C'_9) \\
&\quad + 0.0321 (\delta C_{9'})^2 - 0.2622 (\delta C_{10}) + 0.032 (\delta C_{10})^2 + 0.1949 (\delta C_{10'}) \\
&\quad - 0.0475 (\delta C_{10}) (\delta C_{10'}) + 0.032 (\delta C_{10'})^2 + 0.0066 (\delta C_S)^2 \\
&\quad - 0.0132 (\delta C_S) (\delta C_{S'}) + 0.0066 (\delta C_{S'})^2 - 0.0138 (\delta C_P) + 0.0034 (\delta C_{10}) (\delta C_P) \\
&\quad - 0.0034 (\delta C_{10'}) (\delta C_P) + 0.0067 (\delta C_P)^2 + 0.0138 (\delta C_{P'}) - 0.0034 (\delta C_{10}) (\delta C_{P'}) \\
&\quad + 0.0034 (\delta C_{10'}) (\delta C_{P'}) - 0.0134 (\delta C_P) (\delta C_{P'}) + 0.0067 (\delta C_{P'})^2
\end{aligned} \quad (2.23)$$

The leading term in these expressions is the SM prediction and agrees with the values mentioned in Tab. 2.3. Similar to  $R_{D^{(*)}}$ , one has to map the amplitude with contribution of the BSM fields on to the operator basis. The new contribution to the

Wilson coefficients can be substituted in above expression and compared with the experimental data.

### 2.4.3 Resolution to flavor anomalies

The discrepancies in LFU violation observables  $R_{D^{(*)}}$  and  $R_{K^{(*)}}$  have been explained in a wide variety of frameworks such as leptoquarks [125–130], R-parity violating supersymmetry [131–134], and flavor violating  $Z'$  [135–147]. While all of them resolve the anomaly equally well, leptoquarks are of special interest to this thesis as they can be resonantly produced in neutrino-nucleon interactions. The leptoquark mass required to resolve the anomalies in the neutrino sector is  $\mathcal{O}(1)$  TeV which coincides with the mass required to address the flavor anomalies. Moreover, as leptoquarks are (anti) triplet under  $SU(3)_C$ , they can be efficiently produced via gluons at LHC and these models can be tested with present and future searches.

## 2.5 Self Interacting Dark Matter

For the past few decades, the gravitational interaction of DM has been extensively studied and very little doubt remains of its existence [148–152]. However, the particle nature of DM remains a mystery and its mass, spin, and interactions with other elementary particles are still a mystery. The most promising candidate, Weakly Interacting Massive Particles (WIMPs), are exceedingly in tension with recent bounds from null results of terrestrial experiments such as LUX [153] and XENON [154]. Several new candidates have been proposed recently which get the correct relic abundance and are consistent with present detector bounds.

One of the simple solutions is to assume that the DM is light i.e. its mass is in the sub-GeV domain. In this limit, the local DM cannot produce sufficient recoil and thus will remain undetected in the traditional detectors. It has been proposed that electron recoil can be used to probe this parameter space [155–157]. From the model building perspective, it was recently proposed that the 3-to-2 and 4-to-2 annihilations may be

important for MeV and keV scale DM respectively [158]. Several interesting follow ups to this paradigm can be found in [159–169]. For sub-MeV DM, the strongest constraints come from BBN  $N_{eff}$  [170]. To evade these limits, one can assume either that it freezes-in after the BBN [171] or that the dark sector has lower temperature than the SM bath [172–175].

The standard model of cosmology,  $\Lambda$ CDM, has been extremely successful in explaining the observed astrophysical phenomenon at large scales. However, the assumption of cold collisionless DM in simulations does not give correct predictions at Galactic scales. This is popularly known as the *small-scale crisis* of  $\Lambda$ CDM. The most prominent issues are the *core vs. cusp* problem, the *missing satellite* problem, and *too-big-to-fail* problem [176]. While specific resolutions to all the problems is possible, the assumption of self-interacting DM can solve some of these problems simultaneously [177–186]. However, observation of galaxy cluster collisions puts a strong bound on this self interaction.

## Chapter 3

# Leptoquark for Flavor and IceCube

Leptoquarks are bosons (scalar or vector) that couple simultaneously to quarks and leptons. They appear naturally in many BSM models. For example, the squarks in R-parity violating supersymmetry have scalar leptoquark like interactions [187] whereas vector leptoquarks appear as gauge bosons in Grand Unification Theories (GUTs) based on  $SU(5)$  and  $SO(10)$  [188–190]. There are twelve types of leptoquarks based on their transformations under the SM gauge group. Leptoquarks have been used to explain IceCube PeV events [47–53], flavor anomalies [125–130], and the anomalous magnetic moment of muon [191–197] independently. However, simultaneous explanation of all the three observations has not been attempted before. In this chapter, it is shown that a scalar leptoquark of mass close to 1 TeV can explain all the aforementioned discrepancies. However, it will be shown in this chapter that such an explanation is ruled out from LHC searches.

In section 3.1 I have discussed the Lagrangian of leptoquark and the texture of the coupling matrices that is required. In section 3.2-3.4 I have addressed the discrepancies in  $(g - 2)_\mu$ , charged-current flavor anomalies, and IceCube HESE anomalies respectively. In section 3.5, I discuss the parameter space for simultaneous explanation followed by LHC analysis in section 3.6. The last section discusses the conclusions and implications of this chapter.

### 3.1 Model Description

In this chapter, I have considered the scalar leptoquark  $R_2$  with  $SU(3)_C \times SU(2)_L \times U(1)_Y$  quantum numbers  $(\mathbf{3}, \mathbf{2}, 7/6)$ . The interactions with the SM fields is given by [199],

$$\mathcal{L}_\Delta \ni -(y_L)_{ij} \bar{u}_R^i \Delta_a \varepsilon^{ab} (L_L)_b^j + (y_R)_{ij} \bar{Q}_L^i \Delta_a l_R^j + \text{h.c.} \quad (3.1)$$

where  $y_{L(R)}$  are the Yukawa-like couplings of the leptoquark and I have used the notation  $\Delta$  for the leptoquark and  $M_\Delta$  for the mass of the leptoquark. For simplicity, I have assumed that the couplings are real. The kinetic and Higgs interactions are not mentioned for as they are not relevant for the discussion. We can rewrite Eq. (3.1) in terms of the mass eigenstates  $\Delta^{5/3}$  and  $\Delta^{2/3}$  where the superscript denotes the electric charge. In terms of these states, the Lagrangian (3.1) is written as,

$$\mathcal{L}_\Delta \ni (V y_R)_{ij} \bar{u}_i P_R l_j \Delta^{5/3} - (y_L)_{ij} \bar{u}_i P_L l_j \Delta^{5/3} \quad (3.2)$$

$$+ (y_R)_{ij} \bar{d}_i P_R l_j \Delta^{2/3} + (y_L U)_{ij} \bar{u}_i P_L \nu_j \Delta^{2/3} + \text{h.c.} \quad (3.3)$$

where  $V$  and  $U$  are the CKM and PMNS matrices respectively.

The negligible branching fractions of the flavor violating decays of leptons (such as  $\tau \rightarrow \mu\gamma$  and  $\mu \rightarrow e\gamma$ ) put stringent constraints on the inter-generation couplings of the leptoquark. Thus it is assumed that,

$$y_{L(R)}^{qe} = y_{L(R)}^{q\tau} = 0 \quad \forall q. \quad (3.4)$$

It is understood that the couplings are not exactly zero, however they are so small that their contribution to the process is within the experimental limits. It is commonly understood that  $R_2$  contributes to  $R_K$  and  $R_{K^*}$  at tree level and it disagrees with the recent measurements by LHCb [117, 118]. However, if one assumes

$$y_R^{s\mu} = 0 \quad \text{or} \quad y_R^{b\mu} = 0, \quad (3.5)$$

then the tree level contribution is negligible and the leading contribution comes from

a one-loop process [127]. We chose the former solution in Eq. (3.5) as it can also address the discrepancy in  $(g - 2)_\mu$ . If  $y_L^{c\mu} \neq 0$ , the leptoquark mediates  $b \rightarrow cl\bar{\nu}_l$  at tree level and the contribution contradicts with measurement of  $R_{D^{(*)}}$  [127]. Hence, it is also assumed that

$$y_L^{c\mu} = 0. \quad (3.6)$$

In order to avoid undesired contribution to other rare decays of the B meson, such as  $b \rightarrow dl^+l^-$ , it is assumed that

$$y_R^{d\mu} = 0. \quad (3.7)$$

Including all these constraints, the structure of the coupling matrices is,

$$y_L = \begin{pmatrix} 0 & y_L^{u\mu} & 0 \\ 0 & 0 & 0 \\ 0 & y_L^{t\mu} & 0 \end{pmatrix} \quad \text{and} \quad y_R = \begin{pmatrix} 0 & 0 & 0 \\ 0 & 0 & 0 \\ 0 & y_R^{b\mu} & 0 \end{pmatrix}. \quad (3.8)$$

For convenience, I use the notation  $\lambda_1 = y_L^{u\mu}$ ,  $\lambda_2 = y_L^{t\mu}$ , and  $\lambda_3 = y_R^{b\mu}$  for the remainder of this chapter. I will also use  $M_1$  and  $M_2$  to denote the mass of  $\Delta^{5/3}$  and  $\Delta^{2/3}$  respectively. The LHC constraints limit  $M_1 \geq 1100$  GeV. The lower limit is used to constrain the remaining parameters. Thus, there are only four free parameters in our model

$$\{M_2, \lambda_1, \lambda_2, \lambda_3\}. \quad (3.9)$$

In the subsequent sections, the constraints on these model parameters from  $(g - 2)_\mu$ , flavor anomalies, IceCube HESE data, and LHC are obtained.

## 3.2 $\mathbf{R}_2$ for $(\mathbf{g} - 2)_\mu$

The experimentally measured value of the anomalous magnetic moment of muon is slightly larger than the prediction from SM. The difference is [198],

$$\delta a_\mu = a_\mu^{EXP} - a_\mu^{SM} = (2.8 \pm 0.9) \times 10^{-9}. \quad (3.10)$$

In this model, both of the mass eigenstates contribute to  $(g - 2)_\mu$  and I have estimated the contribution using expressions given in Ref. [199]. Using  $M_1 = 1100$  GeV, the leptoquark contribution to  $(g - 2)_\mu$  is given as,

$$a_\mu^\Delta \approx 1.34 \times 10^{-6} \lambda_2 \lambda_3 - 10^{-11} (8.65 \lambda_1^2 + 7.83 \lambda_2^2 + 7.83 \lambda_3^2) + \mathcal{O}(10^{-13}) \quad (3.11)$$

where the approximation is obtained using the benchmark point  $M_2 = 1000$  GeV as the leading contribution does not depend on  $M_2$ . It is also clear that the product  $\lambda_2 \lambda_3 \approx 10^{-3}$  gives the correct estimate for  $(g - 2)_\mu$ . In section 3.5, I have used  $a_\mu^\Delta = \delta a_\mu$  to constrain the parameter space.

### 3.3 $R_2$ for $R_{K^{(*)}}$

The leading contribution of the leptoquark to  $b \rightarrow s\mu^+\mu^-$  is at one-loop and it only contributes to the Wilson coefficients  $\delta C_9$  and  $\delta C_{10}$  (cf. Eq. (2.21)). The Feynman diagram for this process that gives the dominant contribution is given in Fig. 3.1. The other diagram with two leptoquarks is mass suppressed.

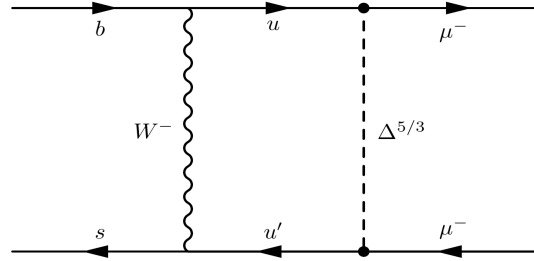


**Figure 3.1:** The leptoquark contribution to  $b \rightarrow s\mu^-\mu^+$

In terms of the simplified notation  $x_i = (m_i/m_W)^2$ , one obtains

$$\delta C_9 = A_1 + A_2 \quad \text{and} \quad \delta C_{10} = -A_1 + A_2 \quad (3.12)$$

where  $A_1$  and  $A_2$  are contribution of left-handed and right-handed couplings respec-

tively and they are given by

$$A_1 = \frac{|\lambda_2|^2}{8\pi\alpha_{em}} F_1(x_t, x_t) \quad \text{and} \quad (3.13)$$

$$A_2 = - \sum_{u, u' \in c, t} (Vy_R)_{u\mu}^* (Vy_R)_{u'\mu} \frac{1}{16\pi\alpha_{em}} \frac{V_{ub}V_{u's}^*}{V_{tb}V_{ts}^*} F_2(x_u, x_{u'}). \quad (3.14)$$

The  $F_i$  are loop functions obtained using *Package-X* 2.0 [200] and their analytical forms are given by the expressions,

$$F_1(x_u, x_{u'}) = \frac{\sqrt{x_u x_{u'}}}{4} \left[ \frac{x_{u'}(x_{u'} - 4) \log x_{u'}}{(x_{u'} - 1)(x_u - x_{u'})(x_{u'} - x_\Delta)} \right. \\ \left. + \frac{x_u(x_u - 4) \log x_u}{(x_u - 1)(x_{u'} - x_u)(x_u - x_\Delta)} - \frac{x_\Delta(x_\Delta - 4) \log x_\Delta}{(x_\Delta - 1)(x_\Delta - x_{u'})(x_\Delta - x_u)} \right] \quad (3.15)$$

and

$$F_2(x_u, x_{u'}) = \frac{x_u^2 \log x_u}{(x_u - x_{u'})(x_u - x_\Delta)} + \frac{x_\Delta(x_u + x_{u'} - x_u x_{u'}) \log x_\Delta}{(x_u - x_\Delta)(x_\Delta - x_{u'})} \\ + \left[ \frac{x_u^2 - 1}{(x_u - x_\Delta)(x_u - x_{u'})} + \frac{x_{u'}^2}{(x_{u'} - x_\Delta)(x_{u'} - x_u)} \right] \log x_{u'}. \quad (3.16)$$

To evaluate  $R_{K^{(*)}}$ , these Wilson coefficients are substituted in Eq. (2.22) and Eq. (2.23). As an intermediate step one obtains,

$$R_K = 1. + 0.49A_1 + 0.06A_1^2 - 0.01A_2 + 0.06A_2^2 \quad (3.17)$$

$$R_{K^*} = 1. + 0.47A_1 + 0.07A_1^2 - 0.14A_2 + 0.07A_2^2 \quad (3.18)$$

from which one can infer that  $-1 < A_1 < 0$  and  $A_2 = 0$  is a solution to the flavor anomalies. This was also the conclusion in Ref. [127].

The measurement of the branching ratio  $\mathcal{B}(B_s \rightarrow \mu^- \mu^+) = 2.8_{-0.6}^{+0.7} \times 10^{-9}$  by LHCb [201] is in close agreement with the SM prediction  $(3.65 \pm 0.23 \times 10^{-9})$  [202] and provides a constraint on the model parameters. From Ref. [203] one obtains,

$$\mathcal{B}(B_s \rightarrow \mu^- \mu^+) = \frac{\tau_{B_s}}{16\pi^3} \frac{\alpha^2 G_F^2}{m_{B_s}^3} f_{B_s}^2 |V_{tb} V_{ts}^*|^2 m_{B_s}^6 m_\mu^2 \left( 1 - \frac{2m_\mu^2}{m_{B_s}^2} \right) |C_{10}|^2 \quad (3.19)$$

and for the model considered in this chapter, one gets the simplified expression

$$\mathcal{B}(B_s \rightarrow \mu^- \mu^+) = 10^{-9}(3.4 + 1.65(A_1 - A_2) + 0.2(A_1 - A_2)^2). \quad (3.20)$$

The branching fraction in Eq. (3.19) also depends on  $C'_{10}$ ,  $C_S^{(\prime)}$  and  $C_P^{(\prime)}$  but these Wilson coefficients are zero in SM and this model. Again, one can see that the solution  $-1 < A_1 < 0$  and  $A_2 = 0$  is consistent with the experiments. In terms of the couplings, one obtains the following simplified expressions,

$$\begin{aligned} R_K = 1. - & (5.16 \times 10^{-2}) \lambda_2^2 + (6.66 \times 10^{-4}) \lambda_2^4 \\ & - (1.66 \times 10^{-5}) \lambda_3^2 + (1.59 \times 10^{-7}) \lambda_3^4 \end{aligned} \quad (3.21)$$

$$\begin{aligned} R_{K^*} = 1. - & (4.96 \times 10^{-2}) \lambda_2^2 + (8.18 \times 10^{-4}) \lambda_2^4 \\ & - (2.34 \times 10^{-4}) \lambda_3^2 + (1.96 \times 10^{-7}) \lambda_3^4 \end{aligned} \quad (3.22)$$

$$\mathcal{B}(B_s \rightarrow \mu^- \mu^+) = 2.01 \times 10^{-10} |4.1 - 0.10 \lambda_2^2 - 1.6 \times 10^{-3} \lambda_3^2|^2. \quad (3.23)$$

One can note that these expressions do not explicitly depend on  $\lambda_1$ . This is due to the fact that the term proportional to  $\lambda_1$  will enter the expression due to u-quark in the loop which is CKM suppressed.

### 3.4 $R_2$ for IceCube

Resonant production of leptoquark in neutrino nucleon interaction has been proposed as a possible explanation of the excess in PeV events at IceCube [48–53]. For the model considered in this chapter, both s-channel and t-channel processes are possible but only the s-channel one dominates due to resonance. The Feynman diagrams for the process are shown in Fig. 3.2. It is important to distinguish between the charged current (CC) like and neutral current (NC) like interactions due to the difference in their deposited energy signature. For CC like, the final state hadrons as well as the charged leptons will contribute to the deposited energy in the detector. For NC like, the neutrino in the final state will carry away a part of the incoming neutrino energy and only the hadrons will contribute to the deposited energy. Thus the incoming neu-

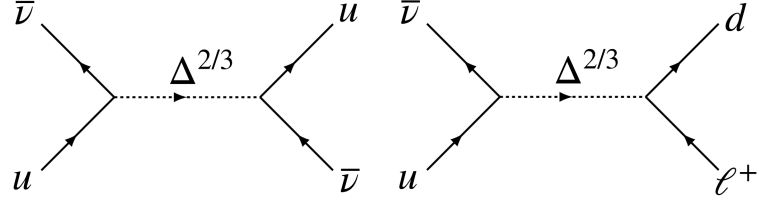


**Figure 3.2:** The NC like (*left*) and CC like (*right*) interaction of the leptoquark

trino energy and deposited energy are often not same and it should be systematically accounted for.

The additional number of events due to leptoquark in the deposited energy interval  $(E_i, E_f)$  is [204]

$$\mathcal{N} = T N_A \int_0^1 dy \int_{E_\nu^{ch}(E_i, y)}^{E_\nu^{ch}(E_f, y)} dE_\nu \mathcal{V}_{eff}(E_{dep}^{ch}) \Omega(E_\nu) \frac{d\phi}{dE_\nu} \frac{d\sigma^{ch}}{dy} \quad (3.24)$$

where  $T = 1347$  days is the total exposure time for four years,  $N_A = 6.023 \times 10^{23} \text{ cm}^{-3}$  water equivalent is the Avogadro's number, and  $ch$  denotes the interaction channel (NC or CC like). As mentioned in chapter 2, for each neutrino or anti-neutrino flavor, an isotropic, power-law flux is assumed which is parametrized as

$$\frac{d\Phi}{dE_\nu} = \phi_0 \left( \frac{E_\nu}{100 \text{ TeV}} \right)^{-\gamma} \quad (3.25)$$

similar to other cosmic rays. The best fit values from four year IceCube HESE data i.e.

$$\phi_0 = (2.2 \pm 0.7) \times 10^{-8} \text{ GeV}^{-1} \text{ s}^{-1} \text{ sr}^{-1} \text{ cm}^{-2} \quad (3.26)$$

$$\gamma^{4yr} = 2.58 \pm 0.25 \quad (3.27)$$

are obtained using likelihood analysis of the data from 10 TeV - 10 PeV [30]. I have used the central values in this analysis.

From the structure of coupling matrices in Eq. (3.8), one can infer that the model has interactions between incoming antineutrino (neutrino) with u- and t- (anti-u- and anti-t-) quarks only. Since the PDF of t-quark is negligible as compared to that of u-

quark, only the interaction with u-quark are considered in this analysis. The differential cross-section for this process is given as [51]

$$\frac{d\sigma^{NC,CC}}{dy} = \frac{\pi}{2} \frac{\Lambda_{NC,CC}^4}{|\Lambda^2|} \frac{\mathcal{U}(M_\Delta^2/s, yM_\Delta^2)}{s} \quad (3.28)$$

where  $s = 2M_N E_\nu$  and  $\mathcal{U}(x, Q^2)$  is the PDF of u-quark in an isoscalar proton. In terms of the *valence* and *sea* quark distributions, one can write [48]

$$\mathcal{U} = \frac{u_{v+s} + d_{v+s}}{2} \quad (3.29)$$

and ignore the contribution of other heavier quarks [23]. I have used the package MSTW [205] for numerical evaluation of the PDFs. In terms of the couplings, one can see that,

$$\Lambda_{NC}^4 = \lambda_1^2 \times (\lambda_1^2 + \lambda_2^2), \quad (3.30)$$

$$\Lambda_{CC}^4 = \lambda_1^2 \times (\lambda_3^2), \text{ and} \quad (3.31)$$

$$\Lambda^2 = \lambda_1^2 + \lambda_2^2 + \lambda_3^2. \quad (3.32)$$

Once the mass of the leptoquark ( $M_2$ ) and the couplings are known, one can evaluate  $\mathcal{N}$  for each bin.

The deposited energy in the detector can be written as a sum of lepton and hadron contribution as [204],

$$E_{dep} = \zeta(1 - y)E_\nu + F_X y E_\nu \quad (3.33)$$

where  $\zeta = 1$  for CC-like and  $\zeta = 0$  for NC-like interactions. The quantity  $F_X$  is parametrised as,

$$F_X = 1 - \left( \frac{yE_\nu}{E_0} \right)^{-m} (1 - f_0) \quad (3.34)$$

where  $E_0 = 0.399$  GeV,  $m = 0.130$ , and  $f_0 = 0.467$  are best-fit values obtained from simulations [206]. The lower limit of integration over neutrino energy in Eq. (3.24) is obtained by numerically inverting Eq. (3.33) using  $E_i = E_{dep}$ . The upper limit is obtained using  $E_f = E_{dep}$ . To illustrate this difference, I have shown the NC-like and CC-like contribution of leptoquark for  $M_\Delta = 600$  GeV in Fig. 3.3. If one does

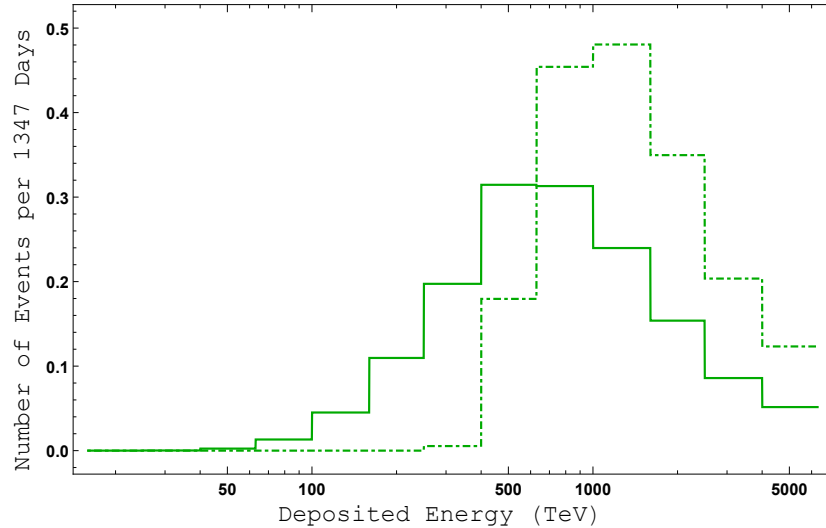


**Figure 3.3:** The difference in NC-like (solid) and CC-like (dashed) interactions.

not distinguish between the neutrino energy and the deposited energy, as has been the case in some earlier papers, one only gets a CC-like contribution. This gives the desired feature that leptoquark only contributes to high energy bins and fits the data well. However, once NC-like contributions are also accounted for, the contribution to low energy bins spoils the fit and the claim is weakened.

In this chapter, the usual  $\chi^2$  analysis is used to obtain the couplings that provide the best fit to the data. The results are shown using the statistic

$$\delta(\lambda_i^2, M_{LQ}) = 100 \times \frac{\chi_{SM}^2 - \chi_{SM+LQ}^2}{\chi_{SM}^2} \quad (3.35)$$

which represents the percentage change in  $\chi^2$ . Only the bins for which non-zero number of events are observed at IceCube are used. As we will see in the next section, the leptoquark contribution to IceCube only depends on  $\lambda_1$  and  $M_2$ . In Fig. 3.4, I have shown the variation of  $\delta$  with  $M_2$  for various choice of coupling  $\lambda_1$ .

### 3.5 Simultaneous explanation

This model has four free parameters as was pointed out before. However, the leptoquark state  $\Delta^{2/3}$  does not contribute significantly to flavor anomalies and hence they

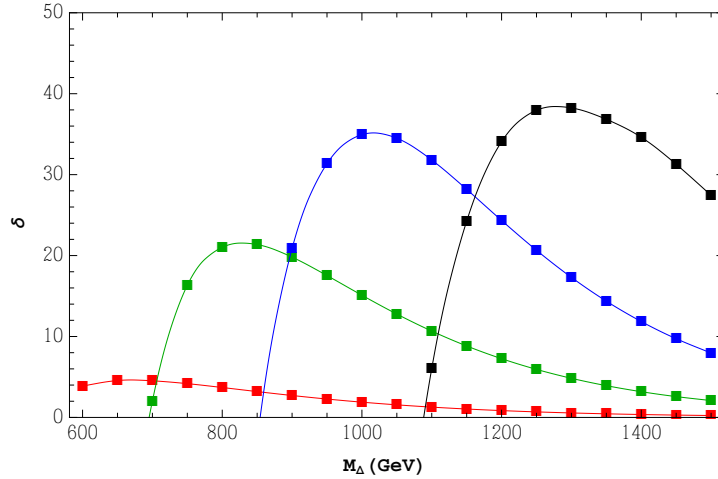


**Figure 3.4:** The variation of  $\delta$  with  $M_2$  for various choice of coupling  $\lambda_1$  is shown. The red, green, blue, and black lines correspond to  $\lambda_1 = 1, 3, 6,$  and  $4\pi$  respectively.

do not depend on  $M_2$ . For  $M_2 \in (600 - 1400)$  GeV, which is also the range studied in the chapter,  $(g - 2)_\mu$  depends very weakly on  $M_2$ . Hence, the flavor anomalies and  $(g - 2)_\mu$  effectively depend only on the three couplings. In Fig. 3.5, I have shown the parameter space that explains the flavor anomalies and  $(g - 2)_\mu$  for  $M_1 = 1100$  GeV and  $M_2 = 1000$  GeV.

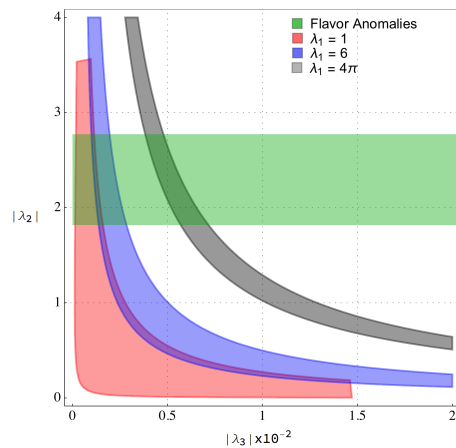


**Figure 3.5:** The parameter space of  $(g - 2)_\mu$  for various choicess of coupling  $\lambda_1$  is shown along with the constraints from flavor anomalies for  $M_1 = 1100$  GeV and  $M_2 = 1000$  GeV.

It can be inferred from Fig. 3.5 that the resolution to flavor anomalies requires  $\lambda_2 \sim \mathcal{O}(1)$  whereas  $(g - 2)_\mu$  constrains  $\lambda_3 \sim \mathcal{O}(10^{-3})$  for  $\lambda_1 < 6$ . Substituting these values in Eqs. (3.30)-(3.32) implies that the leptoquark contribution to IceCube effec-

tively depends on the coupling  $\lambda_1$  and  $M_2$  only. It is also independent of  $M_1$  as the t-channel contribution is ignored. It can be seen that a leptoquark of mass 800 - 1400 GeV can give 20-35% improvement to the fit. In Fig. 3.6, we show the contribution of leptoquark for the benchmark point  $M_{LQ} = 1$  TeV,  $\lambda_1 \approx 6$ , which gives  $\delta \simeq 35$ .

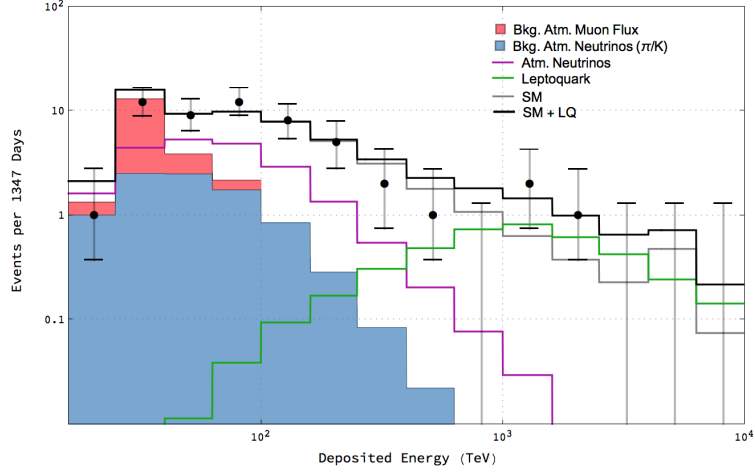


**Figure 3.6:** The solid black line shows the prediction for IceCube using leptoquark and SM interactions.

It is evident that for the aforementioned choices of leptoquark parameters, one can satisfactorily explain the observed excess in the IceCube HESE Data. However, such an explanation requires large couplings and TeV scale leptoquarks. Such a scenario should be testable at LHC and is studied in the next section.

### 3.6 LHC constraints

Since leptoquarks carry color charge, they can be produced in  $pp$  collisions. The typical Feynman diagrams for pair production are shown in Fig. 3.7 and for single production in Fig. 3.8. Subsequent decays of these leptoquarks in the detector will give rise to jets ( $j$ ), leptons ( $l$ ), and neutrino ( $\nu$ ). This results in interesting final states such as  $jjll$ ,  $jjl\nu$ ,  $jl\nu$ ,  $jj\nu$ , and  $j\nu\nu$  which have been extensively studied in Refs. [207–217]. As these neutrinos are not seen by the detector, they are recorded as a Missing Transverse Energy (MET or  $E_T$ ).

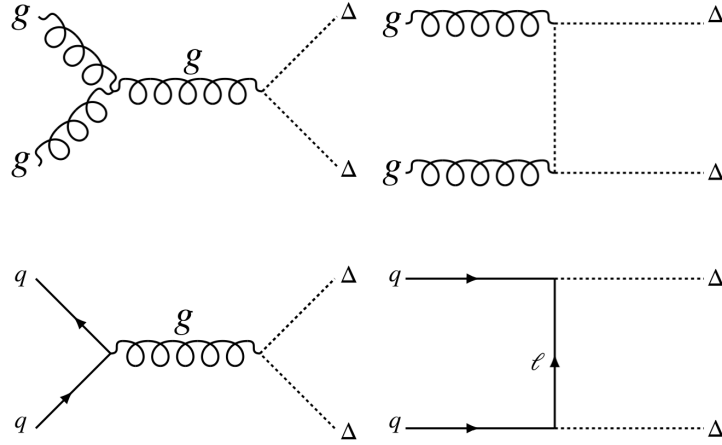


**Figure 3.7:** Gluon-initiated (top) and quark-initiated (bottom) pair production of scalar leptoquark

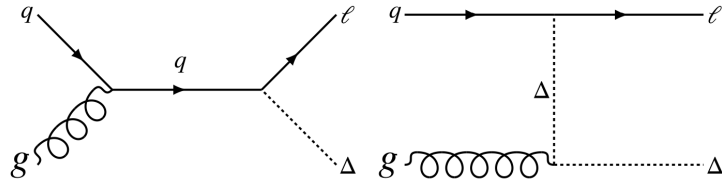


**Figure 3.8:** Single production of scalar leptoquark

For the LHC analysis, we have implemented the model using FeynRules 2.0 [218] and simulate the above processes using MadGraph5 [219]. We use CheckMATE-2 [220] to find the value of statistical parameter  $r$  defined as

$$r = \frac{(S - 1.96\Delta S)}{S_{exp}^{0.95}} \quad (3.36)$$

for several points in the parameter space. Here,  $S$  and  $\Delta S$  represents signal and its uncertainty. The numerator represents 95% confidence limit on number of events obtained using CheckMATE and the denominator represents 95% experimental limits on the number of events. Parameter space with  $r \geq 1$  is excluded and the results are summarized in Fig. 3.9. The various constraints are listed below:

**Two jets and two leptons:** When the leptoquarks are pair produced in pp collisions, each leptoquark can decay into a charged lepton and a quark. Recently, ATLAS

collaboration performed a search for new physics signature of lepton-jet resonances based on  $\sqrt{s} = 13$  TeV data [221] wherein pair production of leptoquarks was studied based on events like  $eejj$  and  $\mu\mu jj$ . The analysis gives an upper limit on branching ratio of first and second generation leptoquark to  $ej$  and  $\mu j$  respectively. Although, our model has inter-generation couplings, we use these limits to constrain the free parameters in our model. We find that,

$$\mathcal{B}(\Delta^{5/3} \rightarrow \mu j) \approx 1 \quad (3.37)$$

as it couples to only second generation of leptons. This puts a lower limit on mass of leptoquark as,

$$M_1 \geq 1100 \text{ TeV}.$$

We use the lower limit to generate other constraints and for flavor analysis. For  $\Delta^{2/3}$  state,

$$\mathcal{B}(\Delta^{2/3} \rightarrow \mu j) \propto \lambda_4^2 \approx 0 \quad (3.38)$$

which does not provide any constraints from this analysis.

**Two jets and MET:** When the leptoquark state  $\Delta^{2/3}$  is pair produced, each can decay into a neutrino and a quark giving rise to a peculiar dijet + MET signature. The parameters  $M_1$  and  $\lambda_2$  are fixed from flavor observables and this process only depends on  $M_2$  and  $\lambda_1$ . We use the 13 TeV ATLAS search [222] to find constraints on this parameter space.

**One jet and MET:** If the leptoquark  $\Delta^{2/3}$  is singly produced, it can decay into a quark and a neutrino giving rise to monojet+MET signal at the LHC. This process only depends on the parameters  $M_2$  and  $\lambda_1$ . We use the 8 TeV ATLAS search [223] to find constraints on this parameter space.

**Other Constraints:** We find that the monojet+MET constraints are strong enough to rule out the entire parameter space that explains IceCube PeV events and tests for other processes are not required. However, in passing, we note that the constraints from

$jl\nu$  final state are much stronger. This maybe relevant for future tests of leptoquark models.

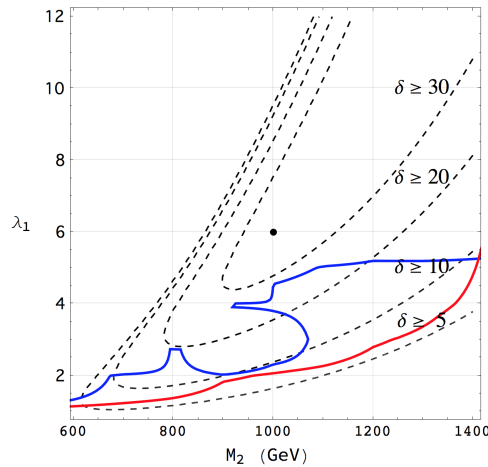


**Figure 3.9:** The dijet+MET constraints are shown in blue and the monojet+MET constraints are shown in red. The parameter space above the curves is ruled out. The contours of  $\delta$  are shown and the benchmark point used to generate Fig. 3.6 is shown.

### 3.7 Conclusion

The discrepancy in anomalous magnetic moment of muon, the observed excess in PeV events at IceCube, and the lepton flavor universality violation in B decays can be successfully addressed within the common framework of scalar leptoquark  $R_2 = (\mathbf{3}, \mathbf{2}, 7/6)$ . In this model, the flavor anomalies  $R_K$  and  $R_{K^*}$  are explained through one-loop contribution of  $R_2$  and one requires a TeV scale leptoquark with  $\mathcal{O}(1)$  couplings. Such a leptoquark invariably couples to first generation quarks and neutrinos through the CKM matrix. It is resonantly produced in neutrino-nucleon interactions and gives significant number of events for deposited energy  $\mathcal{O}(\text{PeV})$ . Due to this, one can reconcile the PeV excess with non-observation of Glashow resonance using a harder spectral index. However, any such coupling will give rise to monojet+MET and dijet+MET signals at LHC and it has been shown in this chapter that these provide severe constraints on the model. We find that all of the interesting parameter space is ruled out and a simultaneous explanation is not possible. While the limits obtained are model dependent, the conclusions can be extended to other similar models e.g. R-parity violating supersymmetry.

# Chapter 4

## Leptoquark for ANITA

In this chapter, I have considered two scenarios wherein a leptoquark, proposed as a resolution to flavor anomalies, also explains the anomalous events observed by ANITA. In the first scenario, I have extended the minimal leptoquark model proposed in Ref. [224] with a sterile neutrino ( $\chi$ ) of mass  $\mathcal{O}(1)$  GeV. The sterile neutrino is produced in UHE neutrino-nucleon interactions mediated by the leptoquark. Due to insignificant interaction with normal matter, it can travel inside Earth without attenuation and decays to  $\tau$  near the south pole. In the second scenario, an astrophysical UHE sterile neutrino propagates freely through the chord of the Earth and produces a  $\tau$  via leptoquark mediated interaction. Interestingly, the same set of interactions also explains  $R_{D^{(*)}}$  as shown in Ref. [225].

### 4.1 GeV scale sterile neutrino

As has been discussed in Refs. [224–226], a vector leptoquark  $U_1$  with  $SU(3)_C \times SU(2)_L \times U(1)_Y$  quantum numbers  $(\mathbf{3}, \mathbf{1}, 2/3)$  can simultaneously explain the flavor anomalies  $R_{D^{(*)}}$  and  $R_{K^{(*)}}$ . It is also one of the few models that admit leptoquark coupling to a sterile neutrino [199]. The Lagrangian of  $U_1$  in the mass basis is,

$$\mathcal{L} \ni -\frac{1}{2}U_{\mu\nu}^\dagger U^{\mu\nu} - ig_s \kappa U_\mu^\dagger T^a U_\nu G^{a\mu\nu} + M_U^2 U_\mu^\dagger U^\mu \quad (4.1)$$

$$- (V \cdot g_L)_{ij} \bar{u}_L^i \gamma^\mu U_{1,\mu} \nu_L^j - (g_L)_{ij} \bar{d}_L^i \gamma^\mu U_{1,\mu} e_L^j \quad (4.2)$$

$$- (g_R)_{ij} \bar{d}_R^i \gamma^\mu U_{1,\mu} e_R^j - (g_\chi)_i \bar{u}_R^i \gamma^\mu U_{1,\mu} \chi_R \quad (4.3)$$

where  $V$  is the CKM matrix and  $\chi$  is the sterile neutrino. If  $\chi$  is sufficiently heavy, its contribution as final state to semi-leptonic B decays is kinematically forbidden. In this way, even if scalar and pseudo-scalar operators are generated by  $\chi$ , their contributions can be neglected and the conclusions in Ref. [226] remain unchanged. The required texture of coupling matrices to explain flavor anomalies is,

$$g_L = \begin{pmatrix} 0 & 0 & 0 \\ 0 & g_{s\mu} & g_{s\tau} \\ 0 & g_{b\mu} & g_{b\tau} \end{pmatrix}, \quad g_R = 0, \quad \text{and} \quad g_\chi = (0 \ g_x \ 0). \quad (4.4)$$

The left-handed couplings ( $g_L$ ) generate the desired Wilson coefficients (i.e.  $\delta C_9 = -\delta C_{10}$  with the correct sign for  $b \rightarrow s\mu\mu$  and  $\delta C_{VL} > 0$  for  $b \rightarrow c\tau\nu$ ). In this way,  $U_1$  is one of the rare solutions that can simultaneously address both the anomalies. The right-handed coupling ( $g_R$ ) is severely constrained as it generates the problematic scalar and pseudoscalar operators. The sterile neutrino ( $\chi$ ) can also couple to other up-type right handed quarks, but these couplings and their constraints have been neglected for simplicity. In this section, the mass of leptoquark  $U_1$  is fixed to be  $M_U = 1.5$  TeV and the couplings to be,

$$g_{s\mu} = -0.012, \quad g_{b\mu} = 0.2, \quad g_{s\tau} = 0.5, \quad g_{b\tau} = 0.5 \quad (4.5)$$

which can explain the flavor anomalies. This choice is within the reach of future LHC searches but allowed from present constraints [226, 227]. The coupling  $g_x$  and mass of the sterile neutrino ( $M_\chi$ ) are considered as free parameters.

The singlet is produced near the surface of Earth through neutrino-nucleon interaction mediated by the leptoquark. The cross section for the process is dominated by the resonant s-channel neutrino-quark interactions. The Feynman diagram is shown in Fig. 4.1 (left). It was pointed out in Ref. [228] that the gluon initiated neutrino interactions are significant for IceCube. But these give an  $\mathcal{O}(1)$  correction to survival probability

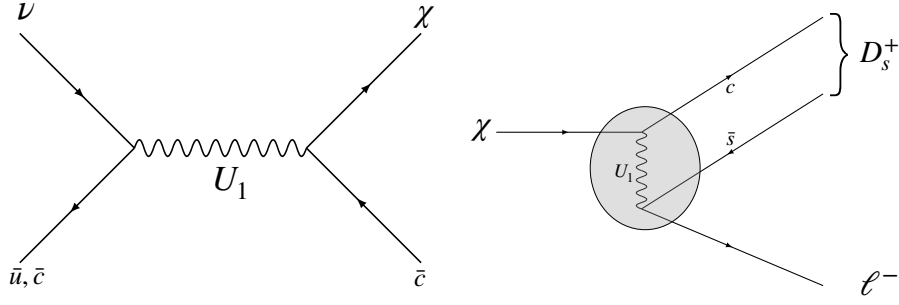


**Figure 4.1:** The Feynman diagrams for the processes involved in section 4.1. *Left:* The s-channel neutrino quark interaction mediated by leptoquark  $U_1$  with sterile neutrino in final state. *Right:* The decay mode of sterile neutrino to charged lepton and  $D_s^+$  is shown. The shaded circle represents the effective vertex.

and has been neglected in this section. The production cross section is approximated using the narrow width limit as,

$$\sigma_{LQ}(E_\nu) = \frac{3\pi}{2} \left( \frac{g_x^2}{g_x^2 + 1.08} \right) \frac{1}{2M_N E_\nu} \int_0^1 dy y^2 \left( (0.11)^2 f_u + (0.5)^2 f_c \right) \quad (4.6)$$

where  $f_q$  is the PDF of  $q$  evaluated at  $x = M_U^2/2M_N E_\nu$  and  $Q = M_U \sqrt{y}$ . I have used ManeParse [229] and NNPDF3.1(sx) [231, 232] datasets to numerically evaluate the PDFs. The factors 1.08, 0.11, and 0.5 in Eq. (4.6) are obtained using central values of CKM parameters [233]. Since the PDFs are evaluated at small- $x$ , the quark and anti-quark PDFs are similar and hence neutrino and anti-neutrino have similar cross sections. The interaction length is obtained from  $\ell_{LQ} = (\rho N_A \sigma_{LQ})^{-1}$  where  $\rho \approx 4\text{gm/cm}^3$  and  $N_A$  is the Avogadro's constant. Even though the density is larger near the centre of Earth, the approximation is valid for the trajectory of messenger particles associated with the anomalous events.

In Ref. [70], three body decay of a singlet was considered. In this analysis, the two body decay width of the sterile neutrino to a pseudoscalar meson and the tau lepton is calculated. The Feynman diagram is shown in Fig. 4.1 (right). Since the decay width is being estimated in the rest frame of a GeV mass sterile neutrino, one can integrate

out the heavy leptoquark and the effective Lagrangian is obtained as,

$$\mathcal{L}_{eff} = \frac{2g_x g_{q\ell}}{M_U^2} [\bar{c} P_L q] [\bar{\ell} P_R \chi] \quad (4.7)$$

where  $q \in \{s, b\}$  and  $\ell \in \{\mu, \tau\}$ . To relate in quark-level and meson-level interactions, one has to use the expression,

$$\langle 0 | \bar{q}_1 \gamma_5 q_2 | P \rangle = i \frac{M_P^2}{M_1 + M_2} f_P \quad (4.8)$$

where  $P$  is a pseudoscalar meson of mass  $M_P$  and  $f_P$  is the associated form factor. The rest frame partial width of the sterile neutrino is,

$$\Gamma_\tau \equiv \Gamma(\chi \rightarrow \tau^- D_s^+) = \frac{1}{16\pi} \left( \frac{g_x g_{s\tau}}{M_U^2} \right)^2 \left( \frac{M_{D_s^+}^2}{M_c + M_s} f_{D_s^+} \right)^2 M_\chi \beta(M_{D_s^+}, M_\tau, M_\chi) \quad (4.9)$$

where the phase space factor is,

$$\beta(a, b, c) = \left[ \left( 1 - \left( \frac{a-b}{c} \right)^2 \right) \left( 1 - \left( \frac{a+b}{c} \right)^2 \right) \right]^{1/2}. \quad (4.10)$$

For numerical analysis I have used,

$$f_{D_s^+} = 257.86 \text{ MeV} \quad M_{D_s^+} = 1.968 \text{ GeV} \quad (4.11)$$

based on the central values reported in [198]. The quarks and lepton masses used are  $M_c = 1.29 \text{ GeV}$ ,  $M_s = 95 \text{ MeV}$ ,  $M_\mu = 105.66 \text{ MeV}$ , and  $M_\tau = 1.77 \text{ GeV}$ . The decay length of  $\chi$  for this mode in Earth's frame is,

$$\ell_D = \gamma c \tau = \frac{1}{\Gamma_\tau} \frac{E_\chi}{M_\chi} \approx \frac{1}{\Gamma_\tau} \frac{E_\nu}{2M_\chi} \quad (4.12)$$

where the last approximation is true for the range of energies involved. In this scenario, the energy of the emergent tau is related to the incident neutrino energy by  $E_\tau = E_\nu/4$  and hence for observed shower energy  $\sim 0.5 \text{ EeV}$ , one requires the incident neutrino to have energy  $E_\nu \sim 2 \text{ EeV}$ .

Using only SM interactions, one can estimate the *bare* survival probability  $\epsilon_0 = e^{-l_{\oplus}/\ell_0}$  where  $l_{\oplus}$  is the length of path traversed (chord) by neutrino inside Earth and for EeV neutrinos,  $\ell_0 \sim 275$  km [67]. This is severely enhanced when one takes neutrino regeneration effects during propagation into account. In Ref. [67], the probability, denoted with  $\epsilon_{SM}$ , is obtained using simulations and mentioned in Tab. 2.1. Due to the leptoquark interactions, the survival probability of the neutrino flux is,

$$\epsilon_{LQ} = \int_0^{l_{\oplus}} dl_1 \int_{l_{\oplus}-l_1-\delta}^{l_{\oplus}-l_1} dl_2 \left[ \frac{e^{-l_2/\ell_D} e^{-l_1/\ell_{LQ}}}{\ell_D \ell_{LQ}} \left( 1 - \int_0^{l_1} \frac{dl_3}{\ell_0} e^{-l_3/\ell_0} \right) \right] \quad (4.13)$$

The above expression is understood as follows. The parentheses denote the fraction neutrinos that survive SM interactions after propagating a distance  $l_1$ . These neutrino undergo leptoquark interactions with the matter and produce a sterile neutrino. The sterile neutrino propagates a distance of  $l_{\oplus} - l_1 - \delta$  before it decays near Antarctic surface in the  $\delta \approx 10$  km window that will produce the observed  $\tau$ .

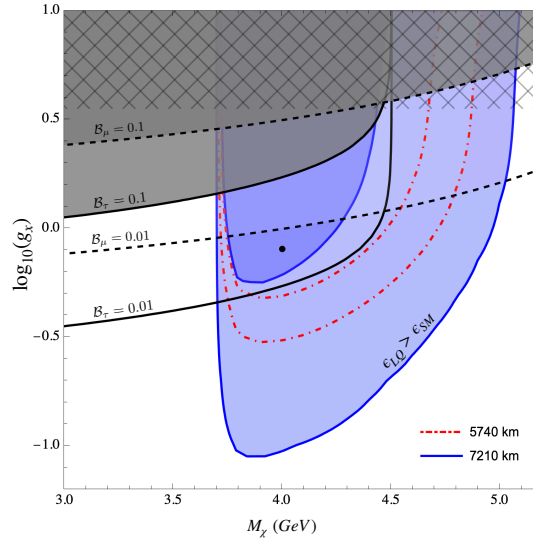


**Figure 4.2:** The parameter space that gives  $\epsilon_{LQ} > \epsilon_{SM}$  (blue), and  $\epsilon_{LQ} > 1 \times 10^{-6}$  (dark blue) for  $l_{\oplus} = 7210$  km is shown. Similar projections for  $l_{\oplus} = 5740$  km is shown by red curves. The gray shaded region is conservatively ruled out from  $B_c^+$  decays and the limits for various  $B_\ell$  are shown. The top part is excluded using the perturbativity limit  $g_x \leq \sqrt{4\pi}$ . The neutrino energy is fixed to be 2 EeV. The benchmark point considered in the text is shown.

In Fig. 4.2, I have shown the parameter space that gives  $\epsilon_{LQ} > \epsilon_{SM}$  and  $\epsilon_{LQ} > 10^{-6}$  for the two values of  $l_{\oplus}$ . The maximum survival probability in this scenario is of the order  $4 \times 10^{-6}$  but accounting for neutrino regeneration effects can increase  $\epsilon_{LQ}$  by few orders. However, complete estimation requires simulation of neutrino propagation which is beyond the scope of this work. The precision measurement of  $B_c^+$  decay modes can test the most interesting part of the parameter space in future. The branching fraction  $\mathcal{B}_{\ell} = Br(B_c^+ \rightarrow \ell^+ \chi)$  for  $\ell \in \{\mu, \tau\}$  is,

$$\mathcal{B}_{\ell} = \frac{\tau_{B_c^+}}{4\pi M_{B_c^+}} \left( \frac{g_x g_{bl}}{M_U^2} \right)^2 \left( \frac{M_{B_c^+}^2}{M_c + M_b} f_{B_c^+} \right)^2 \left( M_{B_c^+}^2 - M_{\ell}^2 - M_{\chi}^2 \right) \beta(M_{\chi}, M_{\ell}, M_{B_c^+}) \quad (4.14)$$

where  $f_{B_c^+} = 0.43$  GeV [225] and  $M_{B_c^+} = 6.275$  GeV [233]. Since the typical branching ratio of leptonic mode is very small, I take the conservative limit of  $\mathcal{B}_{\ell} = 10\%$  for both  $\mu$  and  $\tau$  modes to constrain our parameter space. The limits for  $\mathcal{B}_{\ell} = 1\%$ , which will be accessible in future B-factories, are also indicated.

In this model, for the interesting part of parameter space, the only kinematically allowed choice for the final state meson is  $D_s^+$ . The model also allows for  $\chi \rightarrow \mu^- D_s^+$  but this decay mode is suppressed due to smallness of  $|g_{s\mu}| \sim 0.012$  as compared to  $|g_{s\tau}| \sim 0.5$  (cf. Eq. (4.5)). It is also possible to have  $\chi \rightarrow \nu^- X$  but to get emergent  $\tau$  from this one needs another interaction which makes it less probable. This mode will be important when accounting for regeneration effects using simulation.

To estimate the number of events, consider the benchmark scenario

$$M_{\chi} = 4.0 \text{ GeV} \quad \text{and} \quad g_x = 0.8 \quad (4.15)$$

for which  $\Gamma_{\tau} = 4.64 \times 10^{-16}$  GeV and  $\epsilon_{LQ} \sim (1.5 - 2.0) \times 10^{-6}$ . This gives the expected number of AAE per direction to be 0.03 using the saturated anisotropic flux. In this scenario, larger values of the coupling  $g_x$  seem to be preferable but they would be constrained from determination of  $\mathcal{B}_{\mu}$  in future. To avoid this, one can assume  $g_{b\mu} = 0$  but then the model cannot explain  $R_{K^{(*)}}$ . If simultaneous explanation of both flavor anomalies is not necessary, one can also consider a light sterile neutrino.

## 4.2 Light Sterile Neutrino

In Ref. [225], it is shown that  $U_1$  leptoquark coupled to a light sterile neutrino can also address the flavor anomalies. Unlike the scenario considered in Ref. [226],  $R_{D^{(*)}}$  is explained via right-handed couplings and  $R_{K^{(*)}}$  via left-handed ones. It is concluded that a simultaneous explanation in this model is in tension with big bang nucleosynthesis but  $R_{D^{(*)}}$  can be explained without conflict. The Lagrangian for the leptoquark is similar to Eq. (4.1) but only a handful of Yukawa couplings are required. For completeness, I have mentioned the Lagrangian for the model again in Eq. (4.16). The relevant interactions are,

$$\mathcal{L}_{LQ} = -\frac{1}{2}U_{\mu\nu}^\dagger U^{\mu\nu} - ig_s \kappa U_\mu^\dagger T^a U_\nu G^{a\mu\nu} + M_U^2 U_\mu^\dagger U^\mu + g_{b\tau} \bar{b}_R \gamma^\mu U_{1,\mu} \tau_R + g_x \bar{c}_R \gamma^\mu U_{1,\mu} \chi_R \quad (4.16)$$

where  $g_s$  is the strong coupling constant and  $\kappa = 0$  for a minimally-coupled theory whereas  $\kappa = 1$  for a gauge theory of leptoquark. The flavor anomalies can be explained with the following choice of coupling and leptoquark mass,

$$|g_x g_{b\tau}| \sim 0.62 \left( \frac{M_U}{1 \text{ TeV}} \right)^2. \quad (4.17)$$

Considering the LHC constraints on the model, I chose  $M_U = 1.5 \text{ TeV}$  which is close to the lightest allowed mass for  $\kappa = 1$ . To a good approximation,  $g_{b\tau} \in \{1.1, 1.4\}$  which translates to  $g_x \in (1.0, 1.25)$  using Eq. (4.17). In this limit, the model can be tested in future  $300 \text{ fb}^{-1}$  LHC analysis. The limits are weakened for  $\kappa = 0$ .

To explain the anomalous events, a flux of light sterile neutrinos ( $\chi$ ) is assumed. The sterile neutrinos pass through the Earth almost unattenuated and only a fraction of them interact with the matter in Earth. Through these interactions, they can produce a  $\tau$  near the Antarctic surface. In this section, I have considered both quarks and gluon initiated interactions. The Feynman diagrams for this process are shown in Fig. 4.3

The  $\chi$ -quark interaction is dominated by the s-channel resonant contribution and the cross section can be estimated by

$$\sigma_q = \sigma(\chi c \rightarrow \tau b) = \frac{3\pi}{2} \left( \frac{g_x^2 g_{b\tau}^2}{g_x^2 + g_{b\tau}^2} \right) \frac{1}{2M_N E_\nu} \int_0^1 dy (1-y)^2 f_c. \quad (4.18)$$

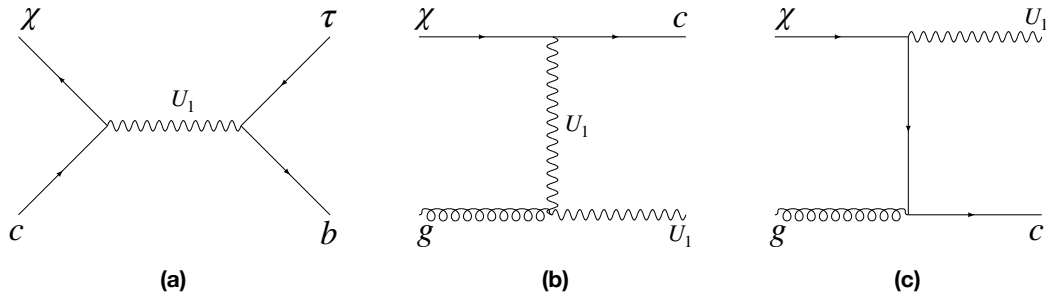


**Figure 4.3:** The Feynman diagrams for  $\chi$ -nucleon interaction. (a) The dominant s-channel  $\chi$ -quark interaction. (b) The  $\kappa$ -dependent  $\chi$ -gluon interaction. (c) The  $\kappa$ -independent  $\chi$ -gluon interaction.

The difference in  $y$ -dependence is due to the  $RR$  nature of interaction as opposed to  $LR$  in the previous case. On the other hand, the  $\chi$ -gluon interaction cross section can be estimated using,

$$\sigma_g = \sigma(\chi g \rightarrow \tau c \bar{b}) \approx \sigma(\chi g \rightarrow c U_1) \times Br(U_1 \rightarrow \tau \bar{b}). \quad (4.19)$$

The model is implemented in FeynRules [218] and compared with the implementation in Ref. [234]. The analytical form of the cross section is obtained using CalcHep [230]. As is shown in Ref. [228], the gluon initiated process are significant for large energies and of the same order of magnitude as the quark initiated processes. The cross section depends on  $\kappa$  as evident from Fig. 4.3. In Fig. 4.4, I have show the variation of  $\sigma_q$  and  $\sigma_g$  with incident sterile neutrino energy. I have also shown the relative strength for  $\kappa = 0$  and 1.

Due to the minimal set of interactions considered in this model, the interaction of  $\chi$  with quarks invariably produces  $\tau$  in the final state. The fraction of incident  $\chi$  that interact with matter in Earth is given as,

$$\epsilon_{q/g} = \int_{l_{\oplus}-\delta}^{l_{\oplus}} dl_1 \frac{e^{-l_1/\ell_{q/g}}}{\ell_{q/g}} \quad (4.20)$$

where  $\ell_{q/g} = (\rho N_A \sigma_{q/g})^{-1}$ . One must note that, for  $\chi$ -quark interactions  $E_{\tau} = E_{\chi}/2$  whereas for  $\chi$ -gluon interaction  $E_{\tau} = E_{\chi}/4$ . By uniformly varying  $E_{\chi}$ , I have shown

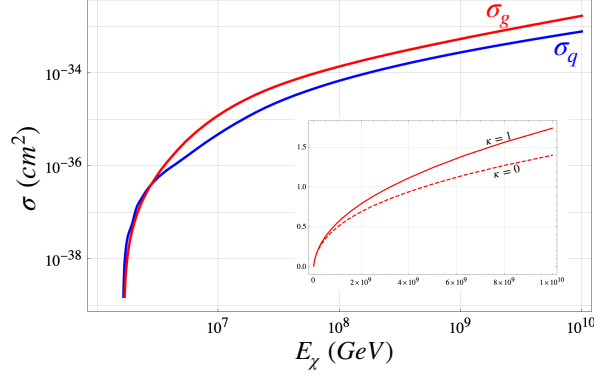


**Figure 4.4:** The variation of cross section  $\sigma_q$  ( $\sigma_g$ ) with incident sterile neutrino energy is shown in blue (red). The inset shows the difference in magnitude of  $\sigma_g$  for  $\kappa = 0$  and 1 in arbitrary units.

show the variation of  $\epsilon = \epsilon_q + \epsilon_g$  with energy of emergent tau in Fig. 4.5. An interesting result of this scenario is that the distribution peaks for tau energy in the same range as seen by ANITA.

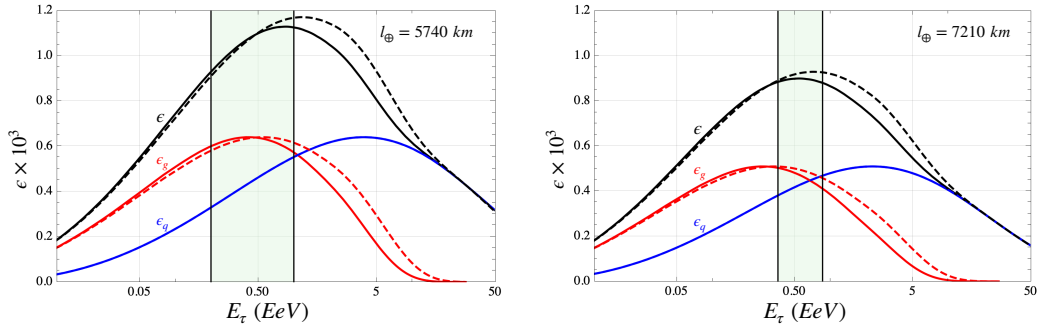


**Figure 4.5:** The variation of  $\epsilon_q$ ,  $\epsilon_g$ , and  $\epsilon$  is shown in blue, red, and black respectively. The solid curve is for  $\kappa = 1$  and the dashed curve for  $\kappa = 0$ . The chord length  $l_{\oplus}$  is fixed to be 5740 km (left) and 7210 km (right). Also,  $g_x = 1.2$  for both the plots. The region shown in green is the observed shower energy for the two events.

In order to estimate the number of events, one needs to know the flux of incident  $\chi$  on Earth. It is clear from the discussion in section 2.2 that this scenario cannot explain AAE with isotropic flux. An anisotropic flux from point-like sources in the sky is assumed and parametrized as

$$\Phi = \phi_0 \times 10^{-20} \left( \frac{E_\chi}{\text{EeV}} \right)^{-\gamma} (\text{GeV cm}^2 \text{ s sr})^{-1} \quad (4.21)$$

where the spectral index  $\gamma$  is unknown. The number of events is then given by,

$$\mathcal{N} \approx \left( \frac{1800}{\text{EeV}} \right) \times \phi_0 \times \left[ \int_{2E_\tau^{\min}}^{2E_\tau^{\max}} dE_\chi \cdot \epsilon_q(E_\chi) \cdot \left( \frac{E_\chi}{\text{EeV}} \right)^{-\gamma} + \int_{4E_\tau^{\min}}^{4E_\tau^{\max}} dE_\chi \cdot \epsilon_g(E_\chi) \cdot \left( \frac{E_\chi}{\text{EeV}} \right)^{-\gamma} \right] \quad (4.22)$$

where the limits of integration are determined by the  $1\sigma$  range of observed  $\tau$  energy. Note that the limits and  $\epsilon_{q/g}$  depend on the chord length in consideration. Keeping  $\mathcal{N} = 1$ , one can obtain the required value of  $\phi_0$  for various choices of  $\gamma$ . The results have been summarised in Tab. 4.1. It can be seen that these values are compatible with the upper bounds mentioned in section 2.2. Note that, for  $\gamma = 0$ , one expects more number of events with shower energies higher than the ones observed by ANITA. Hence, higher values of spectral index is preferred.

	$\gamma = 0$		$\gamma = 1$		$\gamma = 2$		$\gamma = 3$	
	A	B	A	B	A	B	A	B
$\phi_0$	0.19	0.41	0.31	0.71	0.37	1.04	0.33	1.30

Table 4.1: The required value of  $\phi_0$  to get  $\mathcal{N} = 1$  for various choices of spectral index and chord lengths ( $A \equiv 5740$  km and  $B \equiv 7210$  km).

We briefly comment regarding the source of such high energy sterile neutrinos. They can either be produced via the leptoquark interactions, via oscillation of active neutrinos near the source, or via interactions during propagation. If the sterile neutrinos are produced due to oscillation from the active ones, then the flux is proportional to the square of the mixing angle. For large mixing, the cross section will be dominated by SM interactions and the sterile neutrino will be significantly attenuated by Earth. For small mixing, albeit the sterile neutrino propagates freely, the incident flux is smaller and constraints from active neutrino flux become important. On the other hand, if a flux of active neutrinos encounters large magnetic fields during propagation, it can convert to sterile neutrinos via the transition magnetic dipole moment [235]. In this scenario, one anticipates both fluxes to be of the same order of magnitude and offers a testable explanation. Another possibility is the absorption of active neutrino flux by cosmic sterile neutrino background [236] or dark matter [237]. In [77], a flux of

boosted right handed neutrinos was obtained through decay of dark matter.

### 4.3 Conclusion

Since the observation of AAEs, many BSM scenarios have been invoked to explain the discrepancy. In this chapter, I have proposed two models that can significantly enhance the  $\tau$  survival probability while simultaneously addressing the flavor anomalies. In the first scenario, I have extended chiral vector leptoquark model which explains  $R_{D^{(*)}}$  and  $R_{K^{(*)}}$  [224] by a sterile neutrino. The cosmogenic UHE neutrinos interact with the matter in Earth and produce a sterile neutrino that propagates freely inside Earth and decays near the surface to a  $\tau$ . The precise measurement of  $Br(B_c \rightarrow \tau\chi)$ , which is possible in upcoming B factories, will provide a good test of this model.

In the second scenario, a cosmogenic UHE sterile neutrino passes through the Earth almost unattenuated and interacts with the matter in Earth to produce an observable  $\tau$ . The same interactions and parameters also explain  $R_{D^{(*)}}$  anomaly [225]. The interesting result is that the distribution of emergent  $\tau$  energy peaks in the same regime as observed by ANITA. This model has observable signatures in  $300 \text{ fb}^{-1}$  LHC searches.

In summary, the observation of lepton flavor universality violation and Earth emergent  $\tau$  with EeV energy can be explained in a common framework. Moreover, it has testable signatures in upcoming experiments. Future observations by IceCube Gen-II and data from ANITA-IV should be able to shed more light on such BSM hypotheses.



# Chapter 5

## Sterile Neutrino for IceCube

In this chapter, we look at resonant absorption of astrophysical neutrinos from cosmic neutrino background and its signature in the IceCube spectrum. In section 5.1 I have discussed the model for a light sterile neutrino with self interactions. In section 5.2, I have discussed the basics of neutrino absorption and its relevance for IceCube. In section 5.3, I have discussed the parameter space favoured by IceCube, MiniBooNE, and cosmology. In section 5.4, the features of attenuated flux after absorption are discussed. Finally in section 5.5, the conclusion and test of the model with future observations are discussed.

### 5.1 Self interacting sterile neutrino

The existence of a sterile neutrino with mass  $\mathcal{O}(\text{eV})$  and large mixing angles is in conflict with cosmology. The measurement of cosmic microwave background (CMB) anisotropy puts severe constraints on the number of fully thermalised relativistic degrees of freedom ( $N_{eff}$ ) around the epoch of big bang nucleosynthesis (BBN) i.e.  $T_\gamma = 1 \text{ MeV}$  [87]. A simple resolution to this puzzle is to assume self-interactions in the sterile sector [35, 238–242]. Another interesting possibility is to consider neutrino anti-neutrino asymmetry that can also suppress  $N_{eff}$  during BBN [243–245].

In this chapter, we closely follow the model proposed in Ref. [35]. The SM is extended by introducing a left-handed sterile neutrino ( $\nu_s$ ) which is charged under a

new gauge symmetry  $U(1)_X$ . The new gauge boson ( $X_\mu$ ) may acquire its mass through spontaneous symmetry breaking in the hidden sector or Stueckelberg mechanism. For this analysis, we only focus on the sterile neutrino and its interactions. The relevant part of the Lagrangian is the gauge interaction of the sterile neutrino given by,

$$- \mathcal{L}_s = g_X \bar{\nu}_s \gamma^\mu P_L \nu_s X_\mu \quad (5.1)$$

In terms of mass eigenstates,

$$- \mathcal{L}_s = \sum_{i,j} g_{ij} \bar{\nu}_i \gamma^\mu P_L \nu_j X_\mu \quad (5.2)$$

where  $g_{ij} = g_X U_{si}^* U_{sj}$ . The  $4 \times 4$  equivalent of PMNS matrix is parametrised as,

$$U = R_{34} R_{24} R_{14} R_{23} R_{13} R_{12} \quad (5.3)$$

where  $R_{ij}$  is the rotation matrix in the  $i$ - $j$  plane. It is assumed that the elements of the mixing matrix are real for simplicity. The other neutrino mixing angles used are central values of the best-fit from the oscillation measurements [246]:  $\theta_{12} = 33.62^\circ$ ,  $\theta_{23} = 47.2^\circ$ , and  $\theta_{13} = 8.54^\circ$ . There are six free parameters in this model,

$$\mathcal{P} = \{\theta_{14}, \theta_{24}, \theta_{34}, m_4, g_X, M_X\} \quad (5.4)$$

where  $m_4$  is the mass of the fourth (mostly sterile) mass eigenstate and  $M_X$  is the mass of new gauge boson.

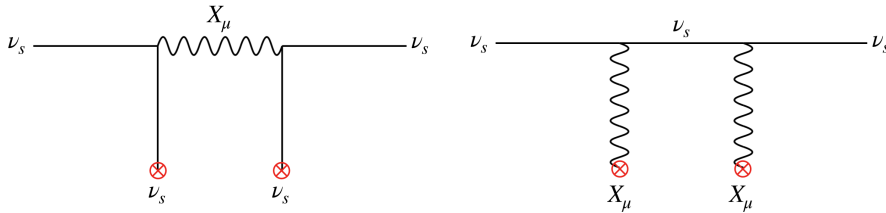


**Figure 5.1:** The Feynman diagrams for the effective potential. The red crosses denote that the interaction is with the thermal background.

Due to the strong (as compared to weak interactions of SM neutrinos) self inter-

action of the sterile neutrino, interactions with the thermal background fields in the plasma become important. The dominant contribution comes from taking thermal propagators in the one-loop bubble diagram. The tadpole contribution is negligible [35]. The relevant Feynman diagrams are shown in Fig. 5.1. As a result, the sterile neutrino sees an effective potential due to the background fields. In other words, the sterile neutrino has an effective *thermal mass* which depends on the number density (or temperature) of the fields in the background. The Effective potential for the sterile neutrino is of the form [35],

$$V_{eff} = \begin{cases} -\frac{28\pi^3\alpha_X ET_s^4}{45M_X^4} & E, T_s \ll M_X \\ +\frac{\pi\alpha_X T_s^2}{2E} & E, T_s \gg M_X \end{cases} \quad (5.5)$$

which modifies the effective mixing angle as,

$$\sin^2(2\theta_m) = \frac{\sin^2(2\theta_0)}{(\cos(2\theta_0) + \frac{2E}{\Delta m^2} V_{eff})^2 + \sin^2(2\theta_0)}. \quad (5.6)$$

As the thermal effective potential is large in the early universe, the mixing is suppressed then. The universe cools down due to expansion and the effective potential is smaller at later times. The mixing angle at late times is the vacuum mixing angle which is allowed to be large. Due to this suppression in early universe, the sterile neutrinos are produced efficiently only at low temperatures i.e. after *recoupling* [247]. The strong limits from BBN can be avoided if  $T_{rec} < 1$  MeV and this provides constraints on the model parameters. Small gauge couplings in the sterile sector are ruled out which is understandable as one needs strong self interactions [239]. Moreover, the mass of the gauge boson required is of  $\mathcal{O}(10)$  MeV. The new gauge boson will also mediate self interactions of *lighter* neutrino mass eigenstates due to the mixing. This will affect their free streaming in the early universe and the scenario is constrained from CMB [248, 249]. Furthermore, the constraints from  $\sum m_\nu$  generally rules out  $m_s > 0.2$  eV but several scenarios have been proposed in Ref. [250] which can evade this. One of the plausible solutions is to add new lighter sterile neutrinos in the model.

## 5.2 Neutrino absorption by cosmic backgrounds

It was shown in Refs. [54, 251–253] that *secret* interaction between neutrinos mediated by an MeV scale boson will give rise to absorption lines in the UHE neutrino spectrum. During propagation through the cosmic media, these neutrinos can get resonantly scattered off the cosmic neutrino background which results in an absorption line. However, due to the redshift during propagation, the lines appear as *troughs* or *dips* in the spectrum. If only SM interactions are considered, the dip is at  $E_\nu \sim 10^{13}$  GeV [254] which is undetectable with present neutrino telescopes. The absorption features of sterile neutrino background were first pointed out in Ref. [255], and Ref. [256] applied it in the context of diffuse supernova background. As mentioned Section 2.1, there is a gap in the IceCube spectrum from 400 TeV to 800 TeV, an excess of PeV events, and lack of Glashow events. In this chapter, I have tried to explain these features through two dips in the IceCube spectrum using resonant absorption by sterile and SM neutrinos in the cosmic background.

Due to recoupling, the neutrino background has all four mass eigenstates in equal proportions and at the same temperature. For the benchmark scenarios considered in the chapter, recoupling is guaranteed [239]. The scattering cross section is,

$$\sigma_{ij} = \sigma(\bar{\nu}_i \nu_j \rightarrow \bar{\nu} \nu) = \frac{1}{6\pi} |g_{ij}|^2 g_X^2 \frac{s}{(s - m_X^2)^2 + m_X^2 \Gamma_X^2} \quad (5.7)$$

where  $\nu_i$  are the mass eigenstates of the four neutrino species and  $\Gamma_X = g_X^2 m_X / 12\pi$  is the decay width of the new boson. The mean free path or interaction length is,

$$\lambda_i(E_i, z) = \left( \sum_j \int \frac{d^3 \mathbf{p}}{(2\pi)^3} f_j(p, z) \sigma_{ij}(p, E_i, z) \right)^{-1} \approx \left( n_\nu(z) \sum_j \sigma_{ij}(p, E_i, z) \right)^{-1} \quad (5.8)$$

where  $f_i$  is the distribution function for the neutrinos given by,

$$f_i(p, z)^{-1} = \exp\left(\frac{p}{T_i(1+z)}\right) + 1 \quad (5.9)$$

and  $T_i = 1.95 K$  for all four components. The approximation in the RHS of Eq. (5.8)

is valid only when the neutrino is non-relativistic. Since the lightest neutrino gives absorption feature for higher energies, it is unobservable with present sensitivity of IceCube. For the remainder of this chapter, we assume normal hierarchy (NH) and neutrino masses to be [20]

$$m_1 = 5 \times 10^{-3} \text{ eV}, \quad m_2 = 1 \times 10^{-2} \text{ eV}, \quad \text{and} \quad m_3 = 5 \times 10^{-2} \text{ eV}. \quad (5.10)$$

The case of inverted hierarchy (IH) is similar. One can see that,

$$m_i \gg \langle p \rangle = 3T_\nu \sim 5.3 \times 10^{-4} \text{ eV} \forall i \quad (5.11)$$

which allows us to approximate the c.m. energy ( $\sqrt{s}$ ) using,

$$s = 2E_i(1+z) \left( \sqrt{p^2 + m_i^2} - p \cos[\theta] \right) \approx 2E_i(1+z)m_i. \quad (5.12)$$

The  $z$  dependence accounts for redshift during propagation. The survival rate of  $i$ -th neutrino mass eigenstate is given as [253, 257],

$$R_i = \exp \left[ - \int_0^{z_s} \frac{1}{\lambda_i(1+z)} \frac{dL}{dz} dz \right] \quad (5.13)$$

where  $z_s$  denotes the redshift distance to the source and,

$$\frac{dL}{dz} = \frac{c}{H_0 \sqrt{\Omega_m(1+z)^3 + \Omega_\Lambda}}. \quad (5.14)$$

We have fixed the cosmological parameters to  $\Omega_m = 0.315$ ,  $\Omega_\Lambda = 0.685$ , and  $H_0 = 67.3 \text{ km/s/Mpc}$  using the best fit values from Planck [88]. We also assume a power-law flux for each neutrino near the source. The flux of neutrino of flavor  $\alpha \in e, \mu, \tau, s$  at Earth is,

$$\phi_\alpha = \sum_{j=1}^4 |U_{\alpha j}|^2 \phi_j R_j = (\phi_0 E_\nu^{-\gamma}) \sum_{j=1}^4 |U_{\alpha j}|^2 R_j \equiv (\phi_0 E_\nu^{-\gamma}) R_\alpha. \quad (5.15)$$

Since the sterile neutrino will not generate any signal at the IceCube detector, the flux

of neutrinos that can be seen by IceCube is simply,

$$\phi = \phi_e + \phi_\mu + \phi_\tau = (\phi_0 E_\nu^{-\gamma}) \left( \sum_{f=e,\mu,\tau} \sum_{j=1}^4 |U_{fj}|^2 R_j \right) \equiv \phi_0 E_\nu^{-\gamma} \langle R(\mathcal{P}, E_\nu) \rangle \quad (5.16)$$

where the parentheses in the last term represent that  $\langle R \rangle$  depends on the model parameters and incident neutrino energy only.

In Fig. 5.2, the variation of  $R_\alpha$  and  $R_i$  is shown for a benchmark scenario. The gauge coupling is fixed to be  $g_X = 0.1$  and the mass of the gauge boson to be  $M_X = 25$  MeV. It is assumed that the neutrino sources are localised around  $z_s \sim 0.3$ . There are three features that are important. Firstly, there are two dips in the interesting range of neutrino energy. The first one is associated with the absorption due to heavy (i.e. mostly sterile) mass eigenstate and the second dip is due to the absorption by the heaviest SM neutrino (i.e.  $m_3$  in NH). Moreover, for a source located at  $z_s$ , the dip in the spectrum occurs for the neutrino energies between  $E_\nu \sim E^{res}/(1+z_s)$  and  $E_\nu \sim E^{res}$  where  $E^{res} = M_X^2/2m_i$  is the neutrino energy for which  $X$  is resonantly produced. The width of the dip is approximately given as,

$$\Delta^i \approx \frac{M_X^2}{2m_i} \frac{z_s}{1+z_s}. \quad (5.17)$$

And lastly, since other neutrinos (both SM and sterile) are lighter, their absorption features occur at much higher neutrino energies. It is thus inconsequential for our analysis whether the lightest neutrino is relativistic or non-relativistic today.

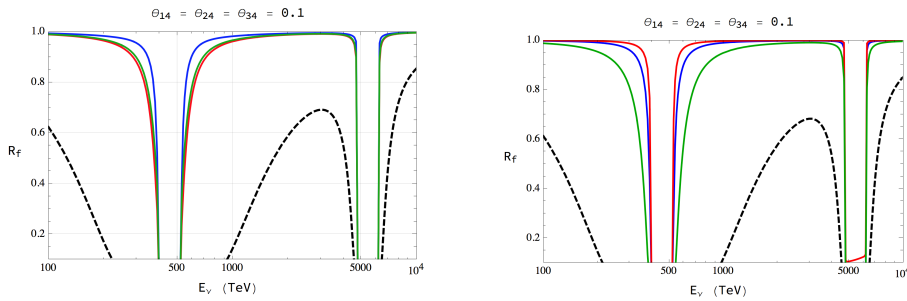


**Figure 5.2:** *Left:* This plot shows variation of  $R_e$  (blue),  $R_\mu$  (red),  $R_\tau$  (green), and  $R_s$  (dashed black) with neutrino energy. *Right:* This plot shows variation of  $R_1$  (blue),  $R_2$  (red),  $R_3$  (green), and  $R_4$  (dashed black) with neutrino energy.

The absorption lines are sensitive to the distance to the source. It can be inferred from Eq. (5.17) that the further the source, the broader will be the absorption line. It is assumed that the UHE neutrinos originate from blazars and non-blazar active galactic nuclei (AGN) like sources as opposed to spatially distributed sources like dark matter decay [40, 258–261]. In future, multi messenger observations will verify this hypothesis. For this analysis it is assumed that the sources are localised around a fixed redshift,  $\langle z_s \rangle$ , which allow for simpler calculations. The detailed analysis considering various possibilities of sources and their distributions is done in Ref. [257] and similar results are obtained. It is interesting to note that any source located very far from Earth (say  $z_s > 5$ ) will broaden absorption lines to an extent where flux at high energies ( $> 200$  TeV) becomes negligible. Such an inference cannot be made in the standard picture without these self-interactions. Thus, if future multi-messenger observations conclude that almost all the sources of UHE neutrinos are localized within a horizon, it will strongly hint at resonant absorption.

### 5.3 Constraints on parameter space

In this section, I examine the  $m_s$ - $M_X$  parameter space that can explain the observed IceCube spectrum. To begin with, if  $E^{res} \sim \text{PeV}$ , one cannot explain the observed PeV events at IceCube unless the sources are very close. Thus in general scenarios, the  $m_3$  absorption line should not lie in the range 800-3000 TeV. This is shown in Fig. 5.3 as region shaded in grey. Because of the redshift broadening during propagation, these constraint depends on  $\langle z_s \rangle$ . I have shown two cases  $\langle z_s \rangle = 0.6$  and  $\langle z_s \rangle = 0.8$ .

As the aim to explain the dip in the spectrum using the fourth neutrino, it is required that,

$$E^{res} \leq 800 \text{ TeV} \quad \text{and} \quad \frac{E^{res}}{1 + \langle z_s \rangle} \geq 400 \text{ TeV}. \quad (5.18)$$

This parameter space allowed is shown as the blue shaded region in Fig. 5.3. Furthermore, to avoid the  $\sum m_\nu$  constraints one need to add very light sterile neutrinos in the full theory [250]. The parameter space that requires one additional particle is towards right of the red solid line in Fig. 5.3. Similarly, the region for two light particles is

towards right of red dashed line. The sterile neutrino mass hinted by MiniBooNE at 68% C.L. is shown as green shaded area and the best fit point is shown as dashed grey line.

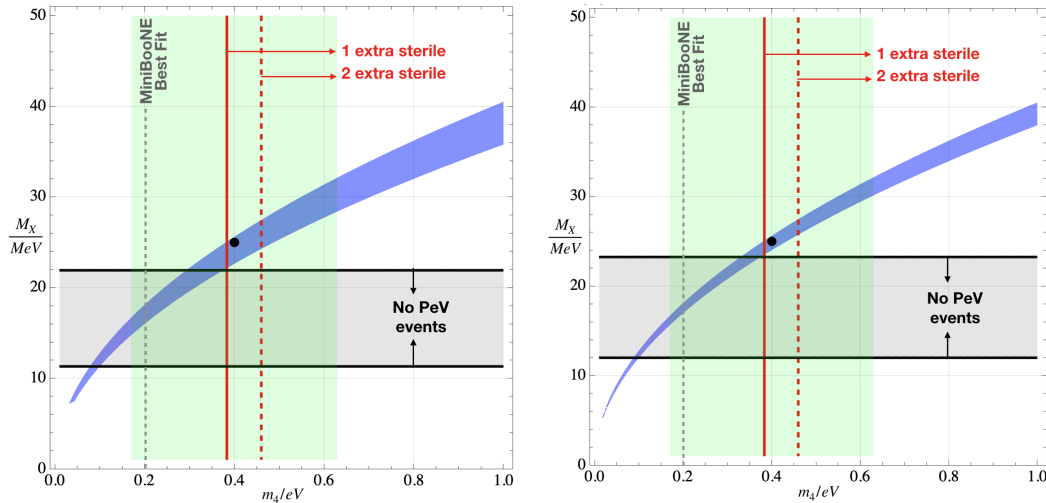


**Figure 5.3:** The parameter space of masses of sterile neutrino and new gauge boson. The black point shows the benchmark case considered in the paper. *Left:*  $\langle z_s \rangle = 0.6$ , *Right:*  $\langle z_s \rangle = 0.8$ . See text for details.

It can be easily concluded from Fig. 5.3 that only a small portion of the parameter space is compatible with all the constraints. I have used the representative point

$$m_4 = 0.4 \text{ eV} \quad \text{and} \quad M_X = 25 \text{ MeV} \quad (5.19)$$

as it requires only one additional light particle. This is also required from anomaly cancellation for the new symmetry. The gauge coupling is constrained from restrictions on the recoupling temperature and a consistent benchmark point  $g_X = 0.1$  is chosen.

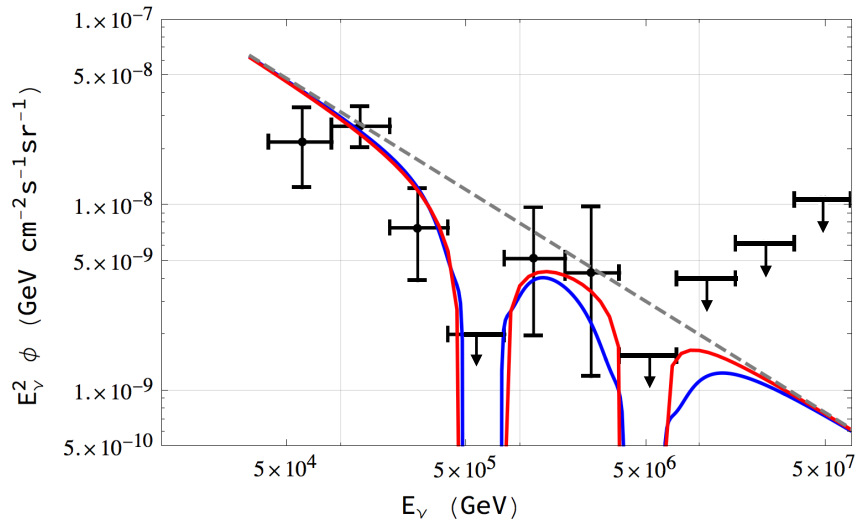


**Figure 5.4:** The flux without attenuation is shown as dashed grey line. The blue (red) curve is the flux with attenuation for the democratic (maximal) case.

## 5.4 Attenuated Flux at IceCube

In the beginning we started with six free parameters for the model. Following the discussion in the previous section, the mass of sterile neutrino and new gauge boson are fixed from IceCube requirements. The strength of the gauge coupling is determined from the recoupling requirements. Thus the only free parameters left are the three mixing angles. If the mixing angles are too small, the interaction length in Eq. (5.8) will be larger than the size of observable universe. For significant absorption, it is estimated that  $\theta \geq 0.01$ . In this section, I have considered two cases,

$$\text{Case I (democratic mixing) : } \theta_{14} = \theta_{24} = \theta_{34} = 0.3$$

$$\text{Case II (maximal mixing) : } \theta_{14} = \theta_{24} = \pi/4 \quad \text{and} \quad \theta_{34} = 0$$

for representative purposes. The maximal case is motivated by the mixing angles required by MiniBooNE. For the neutrino flux parameters, the spectral index is taken to be 2.6 and normalization is fixed from the second bin. Sources are assumed to be distributed around  $z = 0.6$ . The resulting attenuated flux is shown in Fig. 5.4.

In this model, the astrophysical neutrino spectrum has several features that help explaining the observed events by IceCube. To begin with, the absorption line and the

subsequent broadening give rise to a dip from 400-800 TeV. At the end of the absorption feature, the flux increases and this can explain the PeV events without requiring other sources such as dark matter decay. At even higher energies, the absorption feature of the heavy neutrino gives rise to another dip in the spectrum. This can explain the lack of Glashow events even when one considers a small spectral index. At the end of this feature, the flux increases again. The recent observation of high energy neutrino indicates two events in this energy range [29]. Our model uniquely predicts that the neutrino flux increases after the second dip which is compatible with the new events. As more data gets available, one may have to re-evaluate the absorption features of sterile neutrino by either assuming larger spectral index or a different point in the  $m_4 - M_X$  parameter space. With more data, the absorption features of other lighter neutrinos can also be probed. Another prediction of the model is that there is a flux of 400-800 TeV sterile neutrinos on Earth. The direct or indirect detection of these sterile neutrinos is an open question for now. A different point in the parameter space can give rise to flux of sterile neutrinos with energy of  $\mathcal{O}(\text{EeV})$  which may be relevant for ANITA as discussed in chapter 4 of the thesis.

## 5.5 Conclusion

The existence of a eV scale sterile neutrino is hinted by short baseline experiments such as MiniBooNE and LSND. Due to the large vacuum mixing angles required to explain the anomaly, these sterile neutrinos will be fully thermalised with SM neutrinos in the early universe. This would be in tension with the determination of  $N_{eff}$  during big bang nucleosynthesis using CMB data. To reconcile a light sterile neutrino explanation MiniBooNE anomaly with BBN predictions in  $\Lambda\text{CDM}$ , one can introduce gauge or scalar mediated interactions in the sterile sector. For  $\mathcal{O}(0.1)$  coupling, the mediator mass required is of MeV scale for successful recoupling. Since the mixing angles are also large, the astrophysical neutrinos can efficiently scatter off the cosmic background neutrinos - both sterile and active. This leads to absorption like features in the spectrum of UHE neutrinos which can be tested by IceCube.

---

In this chapter, I have shown that the observed gaps in the spectrum at 400-800 TeV as well as beyond 2.6 PeV correspond to resonant absorption by two heaviest neutrino mass eigenstates in the cosmic background. The prediction for this model is that there are peaks in the spectrum beyond 6.3 PeV and dips corresponding to two lighter neutrino mass states. These features can be tested in future IceCube observations. Furthermore, a generic feature of absorption during propagation is that gap in the spectrum widens with distance to the source. This renders IceCube invisible to  $\nu$  sources beyond a certain  $z_{max}$ . Future multi-messenger observations should be able to confirm this horizon.



# Chapter 6

## Sterile Neutrino for Light Dark Matter

In this chapter, I have presented a model for self-interacting light dark matter that is coupled to a self-interacting sterile neutrino similar to the one in previous chapter. In section 6.1, I have discussed details of the model for dark matter. In section 6.2, I have analytically calculated the relic density of a thermally decoupled dark matter through freeze-out of coannihilations. In section 6.3, the cross-section for one loop self interaction is estimated. In section 6.4, the results and implications from IceCube are discussed. In section 6.5, I have mentioned the conclusions of this chapter.

### 6.1 Model Description

In this chapter, it is assumed that in the early universe, dark matter and the sterile neutrino are thermally decoupled from the SM bath similar to Ref. [172, 262–265] and have different temperatures. This temperature asymmetry is characterised by the parameter  $\xi = (T_d/T_{SM}) \leq 1$ . The decoupling can be achieved if the interactions responsible for thermal equilibrium between the two sectors freeze out at high temperatures. For the sterile neutrino, the arguments in the previous chapter assure that even though it has large vacuum mixing angles, the production is not efficient in early universe. In the absence of such interactions, one can also assume that the two sectors have been created at different temperatures during reheating itself [266]. Thus  $\xi$  is a free parameter although it changes with time. Because of this temperature asymmetry, smaller mass for DM is allowed which would otherwise be strictly constrained from

$N_{eff}$  during BBN.

The model considered in the chapter is an extension of the one discussed in the previous chapter. I have added a Dirac fermion which is also charged under the  $U(1)_X$  symmetry. The new gauge boson ( $X_\mu$ ) acquires its mass from spontaneous symmetry breaking. This phase transition also generates a Majorana mass term for DM but not for the sterile neutrino. This *splits* the dark fermion into two Majorana fermions ( $\chi_1$  and  $\chi_2$ ) with a mass gap [267–271]. The lighter of the two Majorana states (say,  $\chi_1$ ) will be the cosmological dark matter. In the mass basis, the coupling of  $X$  boson is purely off-diagonal as the Majorana states cannot carry any conserved quantum number. The new particles and their charge assignments are mentioned in Tab. 6.1. The above charges

Fields	$\psi_1$	$\psi_2$	$\nu_{s1}$	$\nu_{s2}$	$\phi$
$Q_X$	1	-1	$a$	$-a$	2

Table 6.1: The BSM fields and their charges under  $U(1)_X$  symmetry.

assure that the model is anomaly free. The requirement of two sterile neutrinos has been emphasized in the previous chapter. So long as  $a \neq 1$ ,  $\phi$  does not have Yukawa like interaction with the sterile neutrinos. The most general Lagrangian with the BSM fields is,

$$\begin{aligned}
\mathcal{L}_{BSM} = & \bar{\psi}_1(\not{D} - m)\psi_1 + \bar{\psi}_2(\not{D} - m)\psi_2 \\
& + \bar{\nu}_{s1}(\not{D} - m_{s1})\nu_{s1} + \bar{\nu}_{s2}(\not{D} - m_{s2})\nu_{s2} \\
& + y\phi\bar{\psi}_1\psi_2 + h.c. \\
& + (D_\mu\phi)^\dagger(D^\mu\phi) - \frac{1}{4}X^{\mu\nu}X_{\mu\nu} \\
& + \frac{\epsilon}{4}X^{\mu\nu}F_{\mu\nu} + \eta\phi^\dagger\phi H^\dagger H \\
& - \mathcal{V}(\phi)
\end{aligned} \tag{6.1}$$

where  $H$  is the SM Higgs' field and  $X_{\mu\nu} = \partial_\mu X_\nu - \partial_\nu X_\mu$  is the field strength for the new gauge boson. Furthermore,

$$D_\mu = \partial_\mu - ig_X Q_X X_\mu \tag{6.2}$$

is the gauge covariant derivative. The assumption that the dark sector is thermally secluded from the visible sector implies the limits  $\epsilon \rightarrow 0$  and  $\eta \rightarrow 0$ . Since these interactions cannot be generated via loops, one can take these coefficients to be vanishingly small. The potential for the new scalar field has the usual form considered for spontaneous symmetry breaking given by

$$\mathcal{V}(\phi) = -\mu^2 \phi^\dagger \phi + \lambda(\phi^\dagger \phi)^2. \quad (6.3)$$

The symmetry breaking not only gives mass to the new gauge boson, but also generates an off diagonal mass term from the Yukawa-like interaction. In the  $\psi_1 - \psi_2$  basis, the mass matrix is

$$\hat{M} = \begin{pmatrix} m & yv_\phi \\ yv_\phi & m \end{pmatrix} \quad (6.4)$$

which has eigenvalues  $m \pm yv_\phi$ . One can go to the mass eigenstates by the transformation,

$$\psi_1 \rightarrow \frac{\chi_1 + \chi_2}{\sqrt{2}} \text{ and } \psi_2 \rightarrow \frac{\chi_1 - \chi_2}{\sqrt{2}}. \quad (6.5)$$

The Lagrangian for  $\chi_1$  and  $\chi_2$  is,

$$\mathcal{L} = \bar{\chi}_1(\not{\partial} - m_1)\chi_1 + \bar{\chi}_2(\not{\partial} - m_2)\chi_2 + ig_X(\bar{\chi}_1 \not{X} \chi_2 + \bar{\chi}_2 \not{X} \chi_1) + \dots \quad (6.6)$$

where the ellipses denote interactions with the Higgs' scalar of the dark sector. In this basis, the interaction of the gauge boson with  $\chi_1$  and  $\chi_2$  is purely off-diagonal. The role of these off-diagonal interactions for calculation of relic abundance was recently studied in Ref. [272].

In terms of the free parameters, one can fix  $v_\phi$  given the mass of the  $X$  boson. However, by varying  $\lambda$  one can make the scalar sufficiently heavy such that it does not affect the low scale dynamics. The mass gap between the two states is determined by the Yukawa coupling ( $m_2 = m_1 + 2yv_\phi$ ) and can be considered as a free parameter. We fix the the coupling constant  $g_X \approx 1$  ( $\alpha_D = g_X^2/4\pi \approx 0.1$ ) for remainder of this

chapter. The mass hierarchy

$$m_{s1} < m_{s2} \ll m_\chi = m_1 < m_2 = m_1(1 + \delta) \ll M_X \quad (6.7)$$

is natural for eV scale sterile neutrinos, keV scale dark matter, and MeV scale gauge boson. Since the sterile neutrinos recouple after BBN, they do not contribute the  $N_{eff}$ . However, the contribution of DM to the  $N_{eff}$  can be approximated using,

$$N_{eff} = 3.046 + 2 \times \left(\frac{11}{4}\right)^{4/3} \xi^4. \quad (6.8)$$

At the time this work was completed, the Planck data indicated that  $N_{eff} = 3.15 \pm 0.23$  [87]. This implies that to  $\xi \leq 0.45(0.52)$  at  $1\sigma(2\sigma)$  confidence level. The current value reported by Planck is  $N_{eff} = 2.99 \pm 0.17$  [88]. However, in alternative cosmologies the limits can be severe or relaxed depending on the model [273]. In this chapter, I have considered two bench mark scenarios  $\xi = 0.5$  and  $\xi = 0.3$  as the source of this anisotropy is not discussed.

## 6.2 Relic Density from Coannihilation

Following the usual calculation of relic abundance, one must make necessary changes due to the temperature asymmetry. Similar calculation is performed in [172] and the only difference is that I have used hidden sector temperature to define  $x$  while using SM entropy to define  $Y$ . This definition is advantageous in models where the hidden sector entropy is not conserved explicitly (e.g. when a minor component decays into SM particles during late times). In such scenarios, the total entropy density, which is mainly SM entropy, is a good proxy for dilution. Otherwise, the treatment is analogous and one can use either definitions.

The Boltzmann equation for the total number density (6.21) can be expressed in terms of the abundance

$$Y = \frac{n}{s} \quad (6.9)$$

which is free from the dilution due to expansion. Note that  $s$  denotes the total entropy

density of both the dark and the visible sector. Due to temperature asymmetry, one can ignore the contribution of the dark sector for simplicity. Also note that, since the total entropy is conserved,  $\dot{s} + 3Hs = 0$ . During the radiation dominated era, the scale factor  $R \sim t^{1/2}$  which gives us,

$$\frac{dx}{dt} = \frac{\tilde{H}(m_\chi, \xi)}{x} \quad (6.10)$$

where  $x = m_\chi/T_d$  and in terms of Planck Mass  $M_{pl} = 1.22 \times 10^{25}$  keV

$$\tilde{H}(m_\chi, \xi) = 1.66 \sqrt{g_\star} \left( \frac{m_\chi}{x\xi} \right) \frac{1}{\xi^2} \frac{m_\chi^2}{M_{pl}}. \quad (6.11)$$

Using Eq. (6.26) and

$$\tilde{s}(m_\chi, \xi) = \frac{2\pi^2}{45} g_\star^s \left( \frac{m_\chi}{x\xi} \right) \frac{m^3}{\xi^3}, \quad (6.12)$$

the Boltzmann equation for abundance is

$$\frac{dY}{dx} = -\frac{\tilde{s}}{\tilde{H}} \frac{\langle \sigma v \rangle_{eff}}{x^2} (Y^2 - \bar{Y}^2). \quad (6.13)$$

Note that the temperature (hence,  $x$ ) dependence in the effective cross section comes only from the Boltzmann factor and hence one can write,

$$\langle \sigma v \rangle_{eff} = \sigma_0 f(x, \delta) \quad (6.14)$$

where,

$$f(x, \delta) = \frac{(1 + \delta)^2 K_2(x) K_2((1 + \delta)x)}{(K_2(x) + (1 + \delta)^2 K_2((1 + \delta)x))^2}. \quad (6.15)$$

Using the dimensionless quantity  $\lambda = \sigma_0 \tilde{s} / \tilde{H}$  one can simplify Eq. (6.13) as,

$$\frac{dY}{dx} = -\lambda \frac{f(x, \delta)}{x^2} (Y^2 - \bar{Y}^2). \quad (6.16)$$

which can be further simplified using the difference  $\Delta = Y - \bar{Y}$  and approximately solved when  $x \gg x_f$  and  $\Delta \approx Y \gg \bar{Y}$  which gives,

$$\Delta' \approx -\lambda \frac{f(x, \delta)}{x^2} \Delta^2. \quad (6.17)$$

Upon integration from freeze-out to the present day of Eq. (6.17), we get,

$$\frac{1}{Y_\infty} = \frac{1}{\Delta_\infty} = \frac{1}{\Delta_f} + \lambda \int_{x_f}^{\infty} \frac{f(x, \delta)}{x^2} dx = \frac{1}{\Delta_f} + \lambda J \quad (6.18)$$

and the  $J$  integral can be performed numerically once  $x_f$  is determined. It was shown in Ref. [172] that the approximation

$$\Delta_f = c\bar{Y}(x_f, \xi) \quad (6.19)$$

agrees with the numerical solution of Eq. (6.16) if  $c = 0.2$  ( $0.5$ ) for  $\xi = 0.3$  ( $0.8$ ). This gives us the final result,

$$Y_\infty = \frac{c\bar{Y}(x_f, \xi)}{1 + \lambda J(x_f) c\bar{Y}(x_f, \xi)} \quad (6.20)$$

which will be used to determine relic density later. For this analysis, I have considered  $c = 0.2$  as usual and note that any change in  $c$  will proportionately scale the relic density.

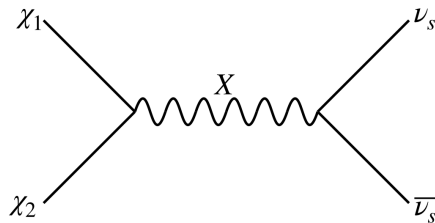


**Figure 6.1:** The annihilation channel for  $\chi_1$  whose freeze-out determines the relic density

In this model, the relic density for  $\chi_1$  is obtained from the coannihilations  $\chi_1\chi_2 \rightarrow \bar{\nu}_s\nu_s$ . The Feynman diagram for the process is shown in Fig. 6.1. I have followed the method outlined in Ref. [274] and important steps have been mentioned in this section. As  $\chi_2$  can decay into  $\chi_1$ , the coupled Boltzmann equations for abundances of  $\chi_1$  and  $\chi_2$  are approximated by a single differential equation for the total number density  $n = n_1 + n_2$  where  $n_1$  and  $n_2$  are the number densities of  $\chi_1$  and  $\chi_2$  respectively [275]. During late times,  $n$  is dominated by  $n_1$  as most of  $\chi_2$  has decayed. The Boltzmann

equation for  $n$  is,

$$\frac{dn}{dt} + 3Hn = -\langle\sigma v\rangle_{eff}(n^2 - \bar{n}^2) \quad (6.21)$$

where bar indicates the equilibrium density and,

$$\langle\sigma v\rangle_{eff} = \sum_{ij} \langle\sigma_{ij}v_{ij}\rangle \frac{\bar{n}_i\bar{n}_j}{\bar{n}^2}. \quad (6.22)$$

Due to the off-diagonal interactions of  $X$  boson, processes such as  $\chi_1\chi_1 \rightarrow \bar{\nu}_s\nu_s$  are forbidden at tree level, and the only annihilation channel is  $\chi_1\chi_2 \rightarrow \bar{\nu}_s\nu_s$ . Thus the effective cross section is given as,

$$\langle\sigma v\rangle_{eff} = 2\langle\sigma_{12}v_{12}\rangle \frac{\bar{n}_1\bar{n}_2}{\bar{n}^2} \approx 2\langle\sigma_{12}v_{12}\rangle \frac{\bar{n}_2}{\bar{n}_1} \quad (6.23)$$

where the approximation obtained by using  $\bar{n}_2 \ll \bar{n}_1$  is only indicative and I have used full expression for the numerical analysis. Recently, utilization of such Boltzmann suppression for light DM has been realised in Refs. [276, 277] however with a small mass-gap ( $\delta < 1$ ). In this chapter, I have considered a significantly large mass gap between the two states ( $\delta \sim 2 - 6$ ). The number density is evaluated with the expression,

$$n_i(m, T) = \frac{T}{2\pi^2} m^2 K_2\left(\frac{m}{T}\right) \quad (6.24)$$

and the thermal averaged cross section in the s-wave limit is given by,

$$\langle\sigma_{12}v_{12}\rangle = \frac{1}{32\pi} \frac{g_X^4}{m_Z^4} (m_1 + m_2)^2. \quad (6.25)$$

One can rewrite Eq. (6.21) using the abundance  $Y = n/s$  where  $s$  denotes the total entropy density of SM and the dark sector. As  $\xi < 1$ , the entropy is dominated by the SM bath and to a very good approximation,

$$s \approx s_{SM} = \frac{2\pi^2}{45} g_*^s(T_{SM}) T_{SM}^3.$$

The equilibrium abundance is given by,

$$\bar{Y}(x, \xi) = \xi^3 \frac{d_\chi}{g_*^s(m_\chi/x\xi)} \frac{45}{4\pi^4} x^2 K_2(x) \quad (6.26)$$

where  $x = m_\chi/T_d$  is a measure of the dark sector temperature. The freeze out occurs when,

$$[\bar{n}\langle\sigma v\rangle_{eff}]_{x_f} = H(\xi, x_f) \quad (6.27)$$

i.e. when the interaction rate becomes less than the Hubble Rate

$$H = 1.66g_*(T)T^2/M_{pl} = 1.66g_*(T/\xi)m_\chi^2/(x^2\xi^2M_{pl}). \quad (6.28)$$

The present day abundance,  $Y_\infty$ , is given as by Eq. (6.20). The relic density of DM is given by,

$$\Omega h^2 = m_\chi s_0 Y_\infty \frac{h^2}{\rho_c} \approx 282 \left(\frac{m_\chi}{\text{keV}}\right) \left(\frac{T_\gamma}{2.75 K}\right)^3 c \bar{Y}(x_f, \xi) \quad (6.29)$$

where the approximation is true in the limit  $\lambda J(x_f)c\bar{Y}(x_f, \xi) \ll 1$ . I have used Eq. (6.27) to numerically determine the freeze-out temperature and enforce that  $x_f \geq 3$  so that the non-relativistic approximation is valid. This restricts us from taking smaller values for  $\xi$  and  $m_1$ . Then the relic density is determined using Eqs. (6.26), (6.20), and (6.29). The result is finally compared with the observed value from Planck [87],

$$\Omega_\chi h^2 = 0.118 \pm 0.002. \quad (6.30)$$

Understanding that such an estimate is only an approximation to solving the complete Boltzmann equations, I have conservatively taken an error of 5% in this analysis.

### 6.3 One-Loop self interaction

One of the features of this model is that the self-interaction of Dark Matter is not a tree level process. At one loop level, there are eight diagrams that contribute to  $\chi_1\chi_1 \rightarrow \chi_1\chi_1$  when  $\chi_2$  and  $X$  are in the loop. A representative diagram is shown in Fig. 6.2. In Refs. [278, 279], the self interaction of inelastic DM was studied in the limit of large  $m_\chi$  and light propagator. In this chapter, I have calculated the self interaction in the limit of small  $m_\chi$  and heavy propagator. Since the loop particles are significantly heavier than the external ones, one can use the decoupling limit where the external momenta are ignored while evaluating the loop.

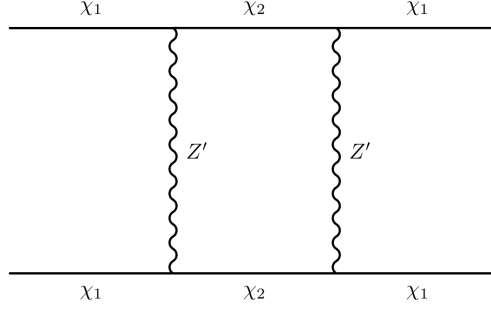


**Figure 6.2:** The Feynman diagram for the self interaction of DM. There are seven other "crossed" diagrams.

In the decoupling limit, the amplitude for the process  $\chi_1(p_1) + \chi_2(p_2) \rightarrow \chi_1(k_1) + \chi_2(k_2)$  is

$$\mathcal{M}_1 \sim \frac{g^4 [\bar{u}(k_1)\gamma^\mu(\not{q} + m_2)\gamma^\alpha u(p_1)] [\bar{v}(p_2)\gamma^\beta(\not{q} + m_2)\gamma^\nu v(k_2)] P_{\alpha\beta} P_{\mu\nu}}{(q^2 - M_X^2)(q^2 - m_2^2)^2} \quad (6.31)$$

where  $q$  is the loop momentum and  $P_{\mu\nu}$  in the unitary gauge is given by,

$$P_{\mu\nu} = -g_{\mu\nu} + \frac{q_\mu q_\nu}{M_X^2}. \quad (6.32)$$

The other crossed amplitudes ( $\mathcal{M}_2 \rightarrow \mathcal{M}_6$ ) are related to  $\mathcal{M}_1$  by  $\beta \leftrightarrow \mu, \beta \leftrightarrow \nu, k_1 \leftrightarrow k_2$ . There are two diagrams corresponding to *s-channel* due to Majorana nature of the incoming fermions. The relative sign of graphs is important for cancellation of the infinities. I have evaluated the loop-integral using *Package-X* 2.0 [200]. The final result can be expressed in the  $\{S, V, T, A, P\}$  basis as,

$$\mathcal{M} = g^4 \sum_{i=S,V,T,A,P} (C_i [\bar{u}(k_1)\Gamma_i u(p_1)] [\bar{v}(p_2)\Gamma_i v(k_2)]) \quad (6.33)$$

$$+ C'_i [\bar{v}(p_2)\Gamma_i u(p_1)] [\bar{u}(k_2)\Gamma_i v(k_1)]) \quad (6.34)$$

Note that the mixed terms (e.g  $V - A$ ) are absent. The only non-zero coefficients are

$$C_A = \frac{6m_2^2 M_X^2 \log\left(\frac{m_2^2}{M_X^2}\right)}{(m_2^2 - M_X^2)^3} - \frac{3(m_2^4 - m_2^2 M_X^2 + 2M_X^4)}{M_X^2 (m_2^2 - M_X^2)^2} \quad (6.35)$$

$$C_T = -\frac{m_2^2(m_2^2 - 3M_X^2)}{M_X^2(m_2^2 - M_X^2)^2} - \frac{2m_2^2M_X^2 \log\left(\frac{m_2^2}{M_X^2}\right)}{(m_2^2 - M_X^2)^3} \quad (6.36)$$

$$C'_S = \frac{6m_2^2(m_2^2 - 3M_X^2)}{M_X^2(m_2^2 - M_X^2)^2} + \frac{12m_2^2M_X^2 \log\left(\frac{m_2^2}{M_X^2}\right)}{(m_2^2 - M_X^2)^3} \quad (6.37)$$

$$C'_A = \frac{3m_2^2M_X^2 \log\left(\frac{m_2^2}{M_X^2}\right)}{(m_2^2 - M_X^2)^3} - \frac{3(m_2^4 - m_2^2M_X^2 + 2M_X^4)}{2M_X^2(m_2^2 - M_X^2)^2} \quad (6.38)$$

In terms of these coefficients, the non-relativistic squared amplitude is

$$|\overline{\mathcal{M}}|^2 = 16m_1^4(3C_A + 2C'_A - 6C_T)^2 - 16m_1^4v^2(C_A + 2C'_A - 6C_T)(3C_A + 2C'_A - 6C_T) \quad (6.39)$$

and the transfer cross section for self interaction is

$$\sigma_{SI} = \int d\Omega(1 - \cos(\theta)) \left( \frac{d\sigma}{d\Omega} = \frac{1}{64\pi^2(4m_\chi^2)} |\overline{\mathcal{M}}|^2 \right) \approx \frac{1}{64\pi m_\chi^2} |\overline{\mathcal{M}}|^2. \quad (6.40)$$

I have checked that the infinities cancel systematically and only a finite part survives.

The self-interaction cross section in the s-wave approximation is given as,

$$\frac{\sigma_{SI}}{m_1} = \frac{9}{256\pi^5} g_X^8 \frac{m_1 \left( m_2^6 + 3m_2^2M_X^4 + 6m_2^2M_X^4 \log\left(\frac{m_2^2}{M_X^2}\right) - 4M_X^6 \right)^2}{M_X^4 (M_X^2 - m_2^2)^6}. \quad (6.41)$$

The velocity dependence of the self interaction is shown in Fig. 6.3. It can be seen that the change is very small for non-relativistic case ( $v < 0.1c$ ). Therefore, we use the estimate  $\frac{\sigma_{SI}(0)}{m_1} = 0.1 - 1 \text{ cm}^2/\text{g}$  to constrain the parameter space.

## 6.4 Results and Discussion

As pointed out before, I have taken  $g_X \approx 1$  for this analysis. In Ref. [280], bounds on mass of warm dark matter from Lyman- $\alpha$  is determined to be  $M_{WDM} \geq \text{few keV}$ . Hence I have only considered  $m_1 > 10 \text{ keV}$  in this work. I have analysed the parameter space in  $\delta - M_X$  plane for  $m_\chi = 10 \text{ keV}$ ,  $100 \text{ keV}$ , and  $1 \text{ MeV}$  that give the correct relic density and strength of self-interactions. One can see that the self-interaction does

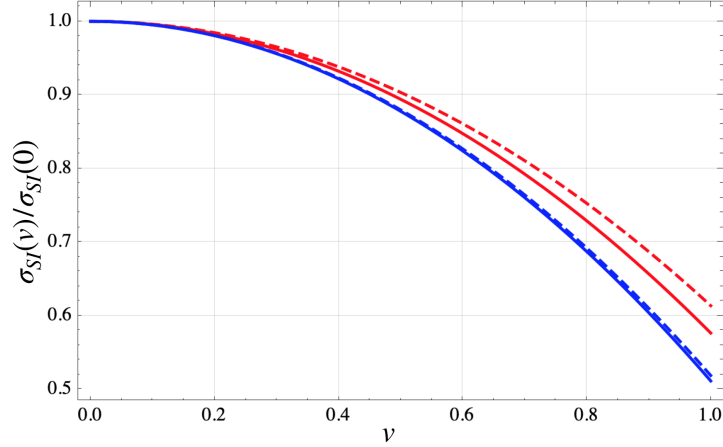


**Figure 6.3:** The relative strength of self interactions i.e.  $\sigma_{SI}(v)/\sigma_{SI}(0)$  is shown as a function of velocity for various choices of parameters. The red curved are for  $M_X = 5$  MeV and the blue ones are for  $M_X = 20$  MeV. The solid and dashed curves are for  $\delta = 1.5$  and  $\delta = 2.5$  respectively.

not depend on  $\xi$  and thus the limits are same for the two benchmark cases. It must be noted that a heavier  $X$  boson is associated with smaller self interaction.

The dependence of relic density on  $\xi$  can be understood as follows. From Eq. (6.26) one can see that  $\bar{Y}$  is a monotonically decreasing function of  $x$ . To compensate for small  $\xi$ , one needs a smaller  $x_f$ . This implies that the effective cross section should be smaller such that freeze-out occurs earlier. This suppression is generated by a smaller Boltzmann factor due to heavier  $m_2$ . In an analogous way, the relic density depends on the numerical factor  $c$ .

As the DM is part of a secluded sector, one does not anticipate any signals in direct detection experiments and colliders. This is consistent with the present status of these terrestrial experiments. Such a dark matter has gravitational signatures and can be probed through structure formation. Due to the self interactions, the DM behaves as warm dark matter and is consistent with the present understanding. In future, as the limits on BBN  $N_{eff}$  are tightened, there will be lesser parameter space for the model.

The  $X$  boson will also mediate self interactions of active neutrinos, the constraints discussed in the previous chapter can also be applied to this model. From the obser-

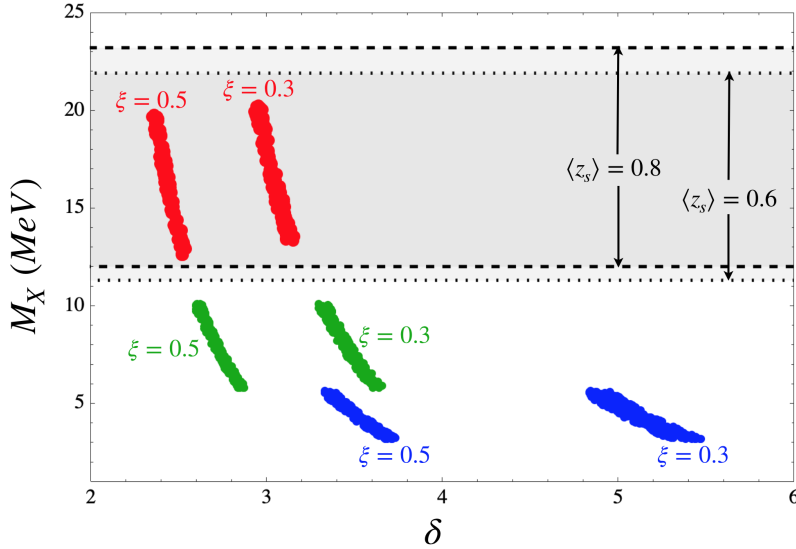


**Figure 6.4:** The allowed parameter space for  $m_\chi = 10$  keV (blue), 100 keV (green), and 1 MeV (red) is shown for benchmark models  $\xi = 0.5$  and  $\xi = 0.3$ . The upper (lower) limit of  $M_X$  corresponds to  $\sigma_{SI}/m_1 = 0.1(1.0)$   $\text{cm}^2/g$ . The exclusion limits from IceCube are shown.

variation of PeV excess, one can rule out the parameter space for  $11.3 \text{ MeV} \leq M_X \leq 21.9 \text{ MeV}$  if  $\langle z_s \rangle = 0.6$  or  $12.0 \text{ MeV} \leq M_X \leq 23.2 \text{ MeV}$  if  $\langle z_s \rangle = 0.8$ . However, these limits can be evaded by assuming small vacuum mixing angles such that the sterile neutrino never fully thermalised. This renders the model less interesting in the context of MiniBooNE anomaly. The other possibility is to assume that the source or PeV neutrinos is nearby. However, there is no evidence to support this claim.

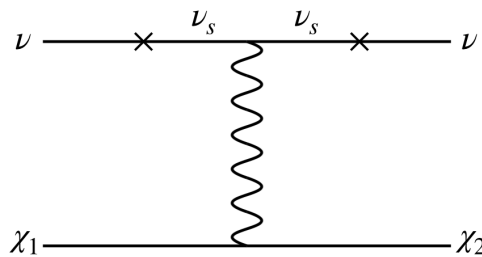


**Figure 6.5:** The Feynman diagram for neutrino dark matter scattering

In this model, the astrophysical neutrinos can interact with the dark matter through interactions mediated by the  $X$  boson. The Feynman diagram for this process is shown in Fig. 6.5. However, one can easily obtain that the threshold neutrino energy above

which these interactions are relevant is given by  $s \geq m_2^2$  where  $s$  is Mandelstam variable associated with the centre of mass energy. In terms of the neutrino energy one can write,

$$E_\nu \geq \frac{m_\chi \delta}{2} (\delta + 2). \quad (6.42)$$

Since the mass of dark matter in this model is 10-1000 keV and  $\delta$  ranges from two to six, the absorption feature for this model will lie in the keV to few MeV range. This is mostly not interesting as there is neither a source nor a detector for keV neutrinos. Moreover, the small parameter space that allows for testing with supernova neutrinos ( $E_\nu \sim \text{MeV}$ ), is already in tension with IceCube.

## 6.5 Conclusion

In this chapter, I investigated a model for secluded dark matter which has strong off-diagonal interactions with a heavier gauge boson. The relic density is obtained by coannihilations to sterile neutrino and self-interactions are a one-loop process. A common parameter space is obtained for sub-MeV dark matter. The light DM must be part of a decoupled sector at a lower temperature in order to be consistent with BBN. The model does not have signature in direct detection experiments or colliders.

Even though the dark matter in this model seems hidden and untestable, a part of the parameter space is ruled out from observation of PeV events at IceCube. This is possible because the gauge boson that mediates interaction between dark matter, also mediates the self-interaction of sterile neutrino. In passing we note that there is a common parameter space with gauge boson mass 5-10 MeV and dark matter mass of  $\mathcal{O}(100)$  keV that can also explain the gap in IceCube spectrum. However, it cannot address the MiniBooNE excess simultaneously.



# Chapter 7

## Conclusion

In this thesis, I have looked at some extensions of the Standard Model that have been proposed as resolution to anomalies in other experiments through neutrino telescopes such as IceCube and ANITA. A TeV scale leptoquark is often proposed as a resolution to the observed discrepancy in some semi-leptonic decay modes of B mesons. The couplings that explain the anomalies, also give rise to novel neutrino-quark interactions at tree level. The contribution of leptoquark mediated process is usually suppressed due to the large mass of the propagator, but it can be significant at resonance. Since this happens for a particular neutrino energy, it is known that a TeV scale leptoquark can explain the excess of PeV events at IceCube. In chapter 3, I tried to find a simultaneous explanation of the two anomalies using the scalar leptoquark  $R_2 \sim (\mathbf{3}, \mathbf{2}, 7/6)$ . However, it was found that any such explanation is ruled out from LHC searches such as dijet +  $\cancel{E}_T$  and monojet +  $\cancel{E}_T$ . The constraints that are obtained in this chapter also limit other resonance based explanation of PeV excess.

The ANITA experiment observed  $\tau$  with energy 0.1 -1 EeV emerging from inside Earth. Due to the small interaction length of SM particles, it is impossible to explain these events without invoking new physics. In chapter 4, I have proposed a framework wherein the vector leptoquark  $U_1 \sim (\mathbf{3}, \mathbf{1}, 2/3)$ , which is the only leptoquark model that can simultaneously address the flavor anomalies  $R_{D^{(*)}}$  and  $R_{K^{(*)}}$ , also couples to a GeV scale sterile neutrino. The leptoquark mediated interaction between astrophysical neutrino and nucleons in Earth produces a sterile neutrino at one end of the chord. The

sterile neutrino propagates inside Earth without significant attenuation and decays near the other end of the chord to  $\tau$  lepton. This scenario significantly enhances the  $\tau$  survival probability as compared to SM even when regeneration effects are not taken into account. On the other hand, if the sterile neutrino is very light, the astrophysical flux of sterile neutrinos can pass through Earth and produce a  $\tau$  lepton near the Antarctic surface via resonant leptoquark mediated interactions. In this scenario as well, the  $\tau$  survival probability is significantly enhanced and provides a combined explanation of flavor and ANITA anomalies. The new particles that proposed in this model are within the reach of future LHC searches and B factories.

In chapter 5, I have studied the signature of cosmologically safe sterile neutrino in IceCube event spectrum. Due to the self interactions in the sterile sector and large mixing angles, the free streaming of astrophysical neutrinos is affected. Such interactions result in absorption features in the neutrino spectrum which can be tested by IceCube. I have claimed that the gap in IceCube HESE data is due to absorption by cosmic sterile neutrino background. The lack of Glashow events is associated with the absorption due to heaviest active neutrino in the cosmic background. In this chapter, we see that a solution which was proposed to reconcile MiniBooNE anomaly and cosmology can have testable signature at IceCube. A part of the parameter space can be ruled out from observation of PeV events.

In chapter 6, I have analysed the proposal that the self interacting sterile neutrino can also act as a portal to hidden and light dark matter. I have proposed a model where the relic density of dark matter is obtained from freeze-out of coannihilations to sterile neutrinos. Due to the off diagonal interactions, the leading contribution to dark matter self-interaction is at one-loop and naturally suppressed. This allows one to consider light dark matter in the 10-1000 keV range. A common parameter space that gives the observed relic density and correct magnitude of self interaction is found. The model does not predict any signal at direct detection experiments, indirect searches, or at colliders. Even for such an extremely safe model, it is seen that a major part of the parameter space is ruled out by IceCube.

---

From the work done in this thesis, I conclude that neutrino telescopes such as IceCube and ANITA play a crucial role in testing and validating new physics scenarios. The BSM models that are proposed to resolve tensions in various terrestrial experiments, both collider based and neutrino oscillation based, can simultaneously address the anomalies in IceCube and ANITA experiments. The minimal models that address these discrepancies successfully can hopefully direct us towards the ultimate goal of particle physics - theory of everything.

One has to admit that the small number of events that are observed at the neutrino telescopes ( $\mathcal{O}(100)$  for IceCube and  $\mathcal{O}(1)$  at ANITA) does not make a definitive argument to invoke new physics. One has to look forward to future experiments such as IceCube Gen-II and KM3NET for more data. Moreover, the results from ANITA IV and future flights will shed more light on the anomalous events. The problem of low statistics can also be remedied by multi-messenger astronomy in future if optical and gravitational counterparts to the neutrino events are also observed.

In future, as more data is collected by IceCube and its successors, the neutrino spectrum at high energies will be available. One must test for the absorption features of sterile neutrino in the new data. The recent observation of 5.9 PeV and 8.6 PeV neutrinos is a weak evidence that the model proposed in chapter 5 correctly reproduces the neutrino spectrum. The model parameters need to be re-evaluated if neutrinos in the energy range 3-5 PeV are observed in future. One must also look for implications of neutrino asymmetry and its effect on the absorption spectrum.

On the other hand, it is becoming increasingly clearer that the best explanation of ANITA anomalous events is through decay of cosmological dark matter to a messenger particle. A very good candidate for EeV dark matter is the gravitino in high scale supersymmetry. If the gravitino decay to sterile neutrino is the dominant mode, then one can naturally evade bounds from IceCube. The phenomenology of such a model and other implications will be considered in future.



# Bibliography

- [1] S. L. Glashow, “*Partial Symmetries of Weak Interactions*,” Nucl. Phys. **22**, 579 (1961). DOI: [10.1016/0029-5582\(61\)90469-2](https://doi.org/10.1016/0029-5582(61)90469-2)
- [2] S. Weinberg, “*A Model of Leptons*,” Phys. Rev. Lett. **19**, 1264 (1967). DOI: [10.1103/PhysRevLett.19.1264](https://doi.org/10.1103/PhysRevLett.19.1264)
- [3] A. Salam, “*Weak and Electromagnetic Interactions*,” Conf. Proc. C **680519**, 367 (1968).
- [4] G. Aad *et al.* [ATLAS Collaboration], “*Observation of a new particle in the search for the Standard Model Higgs boson with the ATLAS detector at the LHC*,” Phys. Lett. B **716**, 1 (2012) DOI: [10.1016/j.physletb.2012.08.020](https://doi.org/10.1016/j.physletb.2012.08.020) arXiv:1207.7214 [hep-ex].
- [5] Y. Fukuda *et al.* [Super-Kamiokande Collaboration], “*Evidence for oscillation of atmospheric neutrinos*,” Phys. Rev. Lett. **81**, 1562 (1998) DOI: [10.1103/PhysRevLett.81.1562](https://doi.org/10.1103/PhysRevLett.81.1562) [hep-ex/9807003].
- [6] R. Davis, Jr., D. S. Harmer and K. C. Hoffman, “*Search for neutrinos from the sun*,” Phys. Rev. Lett. **20**, 1205 (1968). DOI: [10.1103/PhysRevLett.20.1205](https://doi.org/10.1103/PhysRevLett.20.1205)
- [7] Q. R. Ahmad *et al.* [SNO Collaboration], “*Measurement of the rate of  $\nu_e + d \rightarrow p + p + e^-$  interactions produced by  $^8\text{B}$  solar neutrinos at the Sudbury Neutrino Observatory*,” Phys. Rev. Lett. **87**, 071301 (2001) DOI: [10.1103/PhysRevLett.87.071301](https://doi.org/10.1103/PhysRevLett.87.071301) [nucl-ex/0106015].
- [8] P. Minkowski, “ *$\mu \rightarrow e\gamma$  at a Rate of One Out of  $10^9$  Muon Decays?*” Phys. Lett. **67B**, 421 (1977) DOI: [10.1016/0370-2693\(77\)90435-X](https://doi.org/10.1016/0370-2693(77)90435-X)

- [9] M. Gell-Mann, P. Ramond and R. Slansky, “*Complex Spinors and Unified Theories*,” Conf. Proc. C **790927**, 315 (1979) arXiv:1306.4669 [hep-th].
- [10] R. N. Mohapatra and G. Senjanovic, “*Neutrino Mass and Spontaneous Parity Nonconservation*,” Phys. Rev. Lett. **44**, 912 (1980). DOI: [10.1103/PhysRevLett.44.912](https://doi.org/10.1103/PhysRevLett.44.912)
- [11] J. Schechter and J. W. F. Valle, “*Neutrino Masses in  $SU(2) \times U(1)$  Theories*,” Phys. Rev. D **22**, 2227 (1980). DOI: [10.1103/PhysRevD.22.2227](https://doi.org/10.1103/PhysRevD.22.2227)
- [12] G. Lazarides, Q. Shafi and C. Wetterich, “*Proton Lifetime and Fermion Masses in an  $SO(10)$  Model*,” Nucl. Phys. B **181**, 287 (1981). DOI: [10.1016/0550-3213\(81\)90354-0](https://doi.org/10.1016/0550-3213(81)90354-0)
- [13] R. N. Mohapatra and G. Senjanovic, “*Neutrino Masses and Mixings in Gauge Models with Spontaneous Parity Violation*,” Phys. Rev. D **23**, 165 (1981). DOI: [10.1103/PhysRevD.23.165](https://doi.org/10.1103/PhysRevD.23.165)
- [14] R. Foot, H. Lew, X. G. He and G. C. Joshi, “*Seesaw Neutrino Masses Induced by a Triplet of Leptons*,” Z. Phys. C **44** (1989) 441. DOI: [10.1007/BF01415558](https://doi.org/10.1007/BF01415558)
- [15] A. Zee, “*A Theory of Lepton Number Violation, Neutrino Majorana Mass, and Oscillation*,” Phys. Lett. **93B**, 389 (1980) Erratum: [Phys. Lett. **95B**, 461 (1980)]. DOI: [10.1016/0370-2693\(80\)90349-4](https://doi.org/10.1016/0370-2693(80)90349-4), [10.1016/0370-2693\(80\)90193-8](https://doi.org/10.1016/0370-2693(80)90193-8)
- [16] A. Zee, “*Quantum Numbers of Majorana Neutrino Masses*,” Nucl. Phys. B **264**, 99 (1986). DOI: [10.1016/0550-3213\(86\)90475-X](https://doi.org/10.1016/0550-3213(86)90475-X)
- [17] K. S. Babu, “*Model of ‘Calculable’ Majorana Neutrino Masses*,” Phys. Lett. B **203**, 132 (1988). DOI: [10.1016/0370-2693\(88\)91584-5](https://doi.org/10.1016/0370-2693(88)91584-5)
- [18] P. Fileviez Perez and M. B. Wise, “*On the Origin of Neutrino Masses*,” Phys. Rev. D **80**, 053006 (2009) DOI: [10.1103/PhysRevD.80.053006](https://doi.org/10.1103/PhysRevD.80.053006) arXiv:0906.2950 [hep-ph].
- [19] Y. Cai, J. Herrero-Garcia, M. A. Schmidt, A. Vicente and R. R. Volkas, “*From the trees to the forest: a review of radiative neutrino mass models*,” Front. in Phys. **5**, 63 (2017) DOI: [10.3389/fphy.2017.00063](https://doi.org/10.3389/fphy.2017.00063) arXiv:1706.08524 [hep-ph].

- [20] I. Esteban, M. C. Gonzalez-Garcia, A. Hernandez-Cabezudo, M. Maltoni and T. Schwetz, “*Global analysis of three-flavour neutrino oscillations: synergies and tensions in the determination of  $\theta_{23}$ ,  $\delta_{CP}$ , and the mass ordering,*” JHEP **1901**, 106 (2019) DOI: [10.1007/JHEP01\(2019\)106](https://doi.org/10.1007/JHEP01(2019)106) arXiv:1811.05487 [hep-ph].
- [21] R. Acciarri *et al.* [DUNE Collaboration], “*Long-Baseline Neutrino Facility (LBNF) and Deep Underground Neutrino Experiment (DUNE) : Conceptual Design Report, Volume 1: The LBNF and DUNE Projects,*” arXiv:1601.05471 [physics.ins-det].
- [22] R. Acciarri *et al.* [DUNE Collaboration], “*Long-Baseline Neutrino Facility (LBNF) and Deep Underground Neutrino Experiment (DUNE) : Conceptual Design Report, Volume 2: The Physics Program for DUNE at LBNF,*” arXiv:1512.06148 [physics.ins-det].
- [23] R. Gandhi, C. Quigg, M. H. Reno and I. Sarcevic, “*Ultrahigh-energy neutrino interactions,*” Astropart. Phys. **5**, 81 (1996) DOI: [10.1016/0927-6505\(96\)00008-4](https://doi.org/10.1016/0927-6505(96)00008-4) [hep-ph/9512364].
- [24] R. Abbasi *et al.* [IceCube Collaboration], “*The IceCube Data Acquisition System: Signal Capture, Digitization, and Timestamping,*” Nucl. Instrum. Meth. A **601**, 294 (2009) DOI: [10.1016/j.nima.2009.01.001](https://doi.org/10.1016/j.nima.2009.01.001) arXiv:0810.4930 [physics.ins-det].
- [25] S. Adrian-Martinez *et al.* [ANTARES Collaboration], “*Searches for Point-like and extended neutrino sources close to the Galactic Centre using the ANTARES neutrino Telescope,*” Astrophys. J. **786**, L5 (2014) DOI: [10.1088/2041-8205/786/1/L5](https://doi.org/10.1088/2041-8205/786/1/L5) arXiv:1402.6182 [hep-ex].
- [26] S. Adrian-Martinez *et al.* [KM3Net Collaboration], “*Letter of intent for KM3NeT 2.0,*” J. Phys. G **43**, no. 8, 084001 (2016) DOI: [10.1088/0954-3899/43/8/084001](https://doi.org/10.1088/0954-3899/43/8/084001) arXiv:1601.07459 [astro-ph.IM].
- [27] S. W. Barwick *et al.* [ANITA Collaboration], “*Constraints on cosmic neutrino fluxes from the anita experiment,*” Phys. Rev. Lett. **96**, 171101 (2006) DOI: [10.1103/PhysRevLett.96.171101](https://doi.org/10.1103/PhysRevLett.96.171101) [astro-ph/0512265].

- [28] M. G. Aartsen *et al.* [IceCube Collaboration], “*Observation of High-Energy Astrophysical Neutrinos in Three Years of IceCube Data*,” Phys. Rev. Lett. **113**, 101101 (2014) DOI: [10.1103/PhysRevLett.113.101101](https://doi.org/10.1103/PhysRevLett.113.101101) arXiv:1405.5303 [astro-ph.HE].
- [29] M. G. Aartsen *et al.* [IceCube Collaboration], “*Differential limit on the extremely-high-energy cosmic neutrino flux in the presence of astrophysical background from nine years of IceCube data*,” Phys. Rev. D **98**, no. 6, 062003 (2018) DOI: [10.1103/PhysRevD.98.062003](https://doi.org/10.1103/PhysRevD.98.062003) arXiv:1807.01820 [astro-ph.HE].
- [30] M. G. Aartsen *et al.* [IceCube Collaboration], “*The IceCube Neutrino Observatory - Contributions to ICRC 2015 Part II: Atmospheric and Astrophysical Diffuse Neutrino Searches of All Flavors*,” arXiv:1510.05223 [astro-ph.HE].
- [31] H. Schoorlemmer *et al.*, “*Energy and Flux Measurements of Ultra-High Energy Cosmic Rays Observed During the First ANITA Flight*,” Astropart. Phys. **77**, 32 (2016) DOI: [10.1016/j.astropartphys.2016.01.001](https://doi.org/10.1016/j.astropartphys.2016.01.001) arXiv:1506.05396 [astro-ph.HE].
- [32] A. Aguilar-Arevalo *et al.* [LSND Collaboration], “*Evidence for neutrino oscillations from the observation of anti-neutrino(electron) appearance in a anti-neutrino(muon) beam*,” Phys. Rev. D **64**, 112007 (2001) DOI: [10.1103/PhysRevD.64.112007](https://doi.org/10.1103/PhysRevD.64.112007) [hep-ex/0104049].
- [33] A. A. Aguilar-Arevalo *et al.* [MiniBooNE Collaboration], “*Significant Excess of ElectronLike Events in the MiniBooNE Short-Baseline Neutrino Experiment*,” Phys. Rev. Lett. **121**, no. 22, 221801 (2018) DOI: [10.1103/PhysRevLett.121.221801](https://doi.org/10.1103/PhysRevLett.121.221801) arXiv:1805.12028 [hep-ex].
- [34] K. A. Olive and D. Thomas, “*Generalized limits to the number of light particle degrees of freedom from big bang nucleosynthesis*,” Astropart. Phys. **11**, 403 (1999) DOI: [10.1016/S0927-6505\(99\)00009-2](https://doi.org/10.1016/S0927-6505(99)00009-2) [hep-ph/9811444].
- [35] B. Dasgupta and J. Kopp, “*Cosmologically Safe eV-Scale Sterile Neutrinos and Improved Dark Matter Structure*,” Phys. Rev. Lett. **112**, no. 3, 031803 (2014) DOI: [10.1103/PhysRevLett.112.031803](https://doi.org/10.1103/PhysRevLett.112.031803) arXiv:1310.6337 [hep-ph].

- [36] A. Achterberg *et al.* [IceCube Collaboration], “*First Year Performance of The IceCube Neutrino Telescope,*” *Astropart. Phys.* **26**, 155 (2006) DOI: [10.1016/j.astropartphys.2006.06.007](https://doi.org/10.1016/j.astropartphys.2006.06.007) [astro-ph/0604450].
- [37] S. L. Glashow, “*Resonant Scattering of Antineutrinos,*” *Phys. Rev.* **118**, 316 (1960). DOI: [10.1103/PhysRev.118.316](https://doi.org/10.1103/PhysRev.118.316)
- [38] E. Waxman and J. N. Bahcall, “*High-energy neutrinos from astrophysical sources: An Upper bound,*” *Phys. Rev. D* **59**, 023002 (1999) DOI: [10.1103/PhysRevD.59.023002](https://doi.org/10.1103/PhysRevD.59.023002) [hep-ph/9807282].
- [39] D. Williams [IceCube Collaboration], “*Recent Results from IceCube,*” *Int. J. Mod. Phys. Conf. Ser.* **46**, 1860048 (2018). DOI: [10.1142/S2010194518600480](https://doi.org/10.1142/S2010194518600480)
- [40] M. G. Aartsen *et al.* [IceCube and Fermi-LAT and MAGIC and AGILE and ASAS-SN and HAWC and H.E.S.S. and INTEGRAL and Kanata and Kiso and Kapteyn and Liverpool Telescope and Subaru and Swift NuSTAR and VERITAS and VLA/17B-403 Collaborations], “*Multimessenger observations of a flaring blazar coincident with high-energy neutrino IceCube-170922A,*” *Science* **361**, no. 6398, eaat1378 (2018) DOI: [10.1126/science.aat1378](https://doi.org/10.1126/science.aat1378) arXiv:1807.08816 [astro-ph.HE].
- [41] A. Bhattacharya, R. Gandhi, A. Gupta and S. Mukhopadhyay, “*Boosted Dark Matter and its implications for the features in IceCube HESE data,*” *JCAP* **1705**, no. 05, 002 (2017) DOI: [10.1088/1475-7516/2017/05/002](https://doi.org/10.1088/1475-7516/2017/05/002) arXiv:1612.02834 [hep-ph].
- [42] A. Bhattacharya, A. Esmaili, S. Palomares-Ruiz and I. Sarcevic, “*Probing decaying heavy dark matter with the 4-year IceCube HESE data,*” *JCAP* **1707**, no. 07, 027 (2017) DOI: [10.1088/1475-7516/2017/07/027](https://doi.org/10.1088/1475-7516/2017/07/027) arXiv:1706.05746 [hep-ph].
- [43] M. Dhuria and V. Rentala, “*PeV scale Supersymmetry breaking and the IceCube neutrino flux,*” *JHEP* **1809**, 004 (2018) DOI: [10.1007/JHEP09\(2018\)004](https://doi.org/10.1007/JHEP09(2018)004) arXiv:1712.07138 [hep-ph].

- [44] C. Rott, K. Kohri and S. C. Park, “*Superheavy dark matter and IceCube neutrino signals: Bounds on decaying dark matter,*” *Phys. Rev. D* **92**, no. 2, 023529 (2015) DOI: [10.1103/PhysRevD.92.023529](https://doi.org/10.1103/PhysRevD.92.023529) arXiv:1408.4575 [hep-ph].
- [45] P. S. B. Dev, D. Kazanas, R. N. Mohapatra, V. L. Teplitz and Y. Zhang, “*Heavy right-handed neutrino dark matter and PeV neutrinos at IceCube,*” *JCAP* **1608**, no. 08, 034 (2016) DOI: [10.1088/1475-7516/2016/08/034](https://doi.org/10.1088/1475-7516/2016/08/034) arXiv:1606.04517 [hep-ph].
- [46] Y. Sui and P. S. Bhupal Dev, “*A Combined Astrophysical and Dark Matter Interpretation of the IceCube HESE and Throughgoing Muon Events,*” *JCAP* **1807**, no. 07, 020 (2018) DOI: [10.1088/1475-7516/2018/07/020](https://doi.org/10.1088/1475-7516/2018/07/020) arXiv:1804.04919 [hep-ph].
- [47] L. A. Anchordoqui, C. A. Garcia Canal, H. Goldberg, D. Gomez Dumm and F. Halzen, “*Probing leptoquark production at IceCube,*” *Phys. Rev. D* **74**, 125021 (2006) DOI: [10.1103/PhysRevD.74.125021](https://doi.org/10.1103/PhysRevD.74.125021) [hep-ph/0609214].
- [48] V. Barger and W. Y. Keung, “*Superheavy Particle Origin of IceCube PeV Neutrino Events,*” *Phys. Lett. B* **727**, 190 (2013) DOI: [10.1016/j.physletb.2013.10.021](https://doi.org/10.1016/j.physletb.2013.10.021) arXiv:1305.6907 [hep-ph].
- [49] B. Dutta, Y. Gao, T. Li, C. Rott and L. E. Strigari, “*Leptoquark implication from the CMS and IceCube experiments,*” *Phys. Rev. D* **91**, 125015 (2015) DOI: [10.1103/PhysRevD.91.125015](https://doi.org/10.1103/PhysRevD.91.125015) arXiv:1505.00028 [hep-ph].
- [50] N. Mileo, A. de la Puente and A. Szykman, “*Implications of a Electroweak Triplet Scalar Leptoquark on the Ultra-High Energy Neutrino Events at IceCube,*” *JHEP* **1611**, 124 (2016) DOI: [10.1007/JHEP11\(2016\)124](https://doi.org/10.1007/JHEP11(2016)124) arXiv:1608.02529 [hep-ph].
- [51] U. K. Dey and S. Mohanty, “*Constraints on Leptoquark Models from IceCube Data,*” *JHEP* **1604**, 187 (2016) DOI: [10.1007/JHEP04\(2016\)187](https://doi.org/10.1007/JHEP04(2016)187) arXiv:1505.01037 [hep-ph].

- [52] U. K. Dey, S. Mohanty and G. Tomar, “*Leptoquarks: 750 GeV Diphoton Resonance and IceCube Events*,” arXiv:1606.07903 [hep-ph].
- [53] P. S. B. Dev, D. K. Ghosh and W. Rodejohann, “*R-parity Violating Supersymmetry at IceCube*,” Phys. Lett. B **762**, 116 (2016) DOI: [10.1016/j.physletb.2016.08.066](https://doi.org/10.1016/j.physletb.2016.08.066) arXiv:1605.09743 [hep-ph].
- [54] M. Ibe and K. Kaneta, “*Cosmic neutrino background absorption line in the neutrino spectrum at IceCube*,” Phys. Rev. D **90**, no. 5, 053011 (2014) DOI: [10.1103/PhysRevD.90.053011](https://doi.org/10.1103/PhysRevD.90.053011) arXiv:1407.2848 [hep-ph].
- [55] T. Araki, F. Kaneko, Y. Konishi, T. Ota, J. Sato and T. Shimomura, “*Cosmic neutrino spectrum and the muon anomalous magnetic moment in the gauged  $L_\mu - L_\tau$  model*,” Phys. Rev. D **91**, no. 3, 037301 (2015) DOI: [10.1103/PhysRevD.91.037301](https://doi.org/10.1103/PhysRevD.91.037301) arXiv:1409.4180 [hep-ph].
- [56] S. Pakvasa, A. Joshipura and S. Mohanty, “*Explanation for the low flux of high energy astrophysical muon-neutrinos*,” Phys. Rev. Lett. **110**, 171802 (2013) DOI: [10.1103/PhysRevLett.110.171802](https://doi.org/10.1103/PhysRevLett.110.171802) arXiv:1209.5630 [hep-ph].
- [57] S. Sahu and B. Zhang, “*On the non-detection of Glashow resonance in IceCube*,” JHEAp **18**, 1 (2018) DOI: [10.1016/j.jheap.2018.01.003](https://doi.org/10.1016/j.jheap.2018.01.003) arXiv:1612.09043 [hep-ph].
- [58] M. D. Kistler and R. Laha, “*Multi-PeV Signals from a New Astrophysical Neutrino Flux Beyond the Glashow Resonance*,” Phys. Rev. Lett. **120**, no. 24, 241105 (2018) DOI: [10.1103/PhysRevLett.120.241105](https://doi.org/10.1103/PhysRevLett.120.241105) arXiv:1605.08781 [astro-ph.HE].
- [59] S. Mohanty, A. Narang and S. Sadhukhan, “*Cutoff of IceCube Neutrino Spectrum due to  $t$ -channel Resonant Absorption by  $C\nu B$* ,” JCAP **1903**, no. 03, 041 (2019) DOI: [10.1088/1475-7516/2019/03/041](https://doi.org/10.1088/1475-7516/2019/03/041) arXiv:1808.01272 [hep-ph].
- [60] P. W. Gorham *et al.* [ANITA Collaboration], “*The Antarctic Impulsive Transient Antenna Ultra-high Energy Neutrino Detector Design, Performance, and Sensitivity for 2006-2007 Balloon Flight*,” Astropart. Phys. **32**, 10 (2009) DOI: [10.1016/j.astropartphys.2009.05.003](https://doi.org/10.1016/j.astropartphys.2009.05.003) arXiv:0812.1920 [astro-ph].

- [61] G. A. Askar'yan, "Excess negative charge of an electron-photon shower and its coherent radio emission," Sov. Phys. JETP **14**, no. 2, 441 (1962) [Zh. Eksp. Teor. Fiz. **41**, 616 (1961)].
- [62] K. Greisen, "End to the cosmic ray spectrum?," Phys. Rev. Lett. **16**, 748 (1966). DOI: [10.1103/PhysRevLett.16.748](https://doi.org/10.1103/PhysRevLett.16.748)
- [63] G. T. Zatsepin and V. A. Kuzmin, "Upper limit of the spectrum of cosmic rays," JETP Lett. **4**, 78 (1966) [Pisma Zh. Eksp. Teor. Fiz. **4**, 114 (1966)].
- [64] V. S. Berezhinsky and G. T. Zatsepin, "Cosmic rays at ultrahigh-energies (neutrino?)," Phys. Lett. **28B**, 423 (1969). DOI: [10.1016/0370-2693\(69\)90341-4](https://doi.org/10.1016/0370-2693(69)90341-4)
- [65] P. W. Gorham *et al.* [ANITA Collaboration], "Characteristics of Four Upward-pointing Cosmic-ray-like Events Observed with ANITA," Phys. Rev. Lett. **117**, no. 7, 071101 (2016) DOI: [10.1103/PhysRevLett.117.071101](https://doi.org/10.1103/PhysRevLett.117.071101) arXiv:1603.05218 [astro-ph.HE].
- [66] P. W. Gorham *et al.* [ANITA Collaboration], "Observation of an Unusual Upward-going Cosmic-ray-like Event in the Third Flight of ANITA," Phys. Rev. Lett. **121**, no. 16, 161102 (2018) DOI: [10.1103/PhysRevLett.121.161102](https://doi.org/10.1103/PhysRevLett.121.161102) arXiv:1803.05088 [astro-ph.HE].
- [67] D. B. Fox, S. Sigurdsson, S. Shandera, P. Mszros, K. Murase, M. Mostaf and S. Coutu, "The ANITA Anomalous Events as Signatures of a Beyond Standard Model Particle, and Supporting Observations from IceCube," arXiv:1809.09615 [astro-ph.HE].
- [68] G. Y. Huang, "Sterile neutrinos as a possible explanation for the upward air shower events at ANITA," Phys. Rev. D **98**, no. 4, 043019 (2018) DOI: [10.1103/PhysRevD.98.043019](https://doi.org/10.1103/PhysRevD.98.043019) arXiv:1804.05362 [hep-ph].
- [69] K. Kotera, D. Allard and A. V. Olinto, "Cosmogenic Neutrinos: parameter se and detectabilty from PeV to ZeV," JCAP **1010**, 013 (2010) DOI: [10.1088/1475-7516/2010/10/013](https://doi.org/10.1088/1475-7516/2010/10/013) arXiv:1009.1382 [astro-ph.HE].

- [70] J. H. Collins, P. S. Bhupal Dev and Y. Sui, J. H. Collins, P. S. Bhupal Dev and Y. Sui, “*R-parity Violating Supersymmetric Explanation of the Anomalous Events at ANITA*,” Phys. Rev. D **99**, no. 4, 043009 (2019) DOI: [10.1103/PhysRevD.99.043009](https://doi.org/10.1103/PhysRevD.99.043009) arXiv:1810.08479 [hep-ph].
- [71] S. Adrian-Martinez *et al.* [ANTARES and IceCube Collaborations], “*The First Combined Search for Neutrino Point-sources in the Southern Hemisphere With the Antares and Icecube Neutrino Telescopes*,” Astrophys. J. **823**, no. 1, 65 (2016) DOI: [10.3847/0004-637X/823/1/65](https://doi.org/10.3847/0004-637X/823/1/65) arXiv:1511.02149 [hep-ex].
- [72] M. G. Aartsen *et al.* [IceCube Collaboration], “*All-sky Search for Time-integrated Neutrino Emission from Astrophysical Sources with 7 yr of IceCube Data*,” Astrophys. J. **835**, no. 2, 151 (2017) DOI: [10.3847/1538-4357/835/2/151](https://doi.org/10.3847/1538-4357/835/2/151) arXiv:1609.04981 [astro-ph.HE].
- [73] L. A. Anchordoqui, V. Barger, J. G. Learned, D. Marfatia and T. J. Weiler, “*Up-going ANITA events as evidence of the CPT symmetric universe*,” LHEP **1**, no. 1, 13 (2018) DOI: [10.31526/LHEP.1.2018.03](https://doi.org/10.31526/LHEP.1.2018.03) arXiv:1803.11554 [hep-ph].
- [74] L. Boyle, K. Finn and N. Turok, “*CPT-Symmetric Universe*,” Phys. Rev. Lett. **121**, no. 25, 251301 (2018) DOI: [10.1103/PhysRevLett.121.251301](https://doi.org/10.1103/PhysRevLett.121.251301) arXiv:1803.08928 [hep-ph].
- [75] E. Dudas, T. Gherghetta, K. Kaneta, Y. Mambrini and K. A. Olive, “*Gravitino decay in high scale supersymmetry with R -parity violation*,” Phys. Rev. D **98**, no. 1, 015030 (2018) DOI: [10.1103/PhysRevD.98.015030](https://doi.org/10.1103/PhysRevD.98.015030) arXiv:1805.07342 [hep-ph].
- [76] J. F. Cherry and I. M. Shoemaker, “*Sterile neutrino origin for the upward directed cosmic ray showers detected by ANITA*,” Phys. Rev. D **99**, no. 6, 063016 (2019) DOI: [10.1103/PhysRevD.99.063016](https://doi.org/10.1103/PhysRevD.99.063016) arXiv:1802.01611 [hep-ph].
- [77] L. Heurtier, Y. Mambrini and M. Pierre, “*A Dark Matter Interpretation of the ANITA Anomalous Events*,” arXiv:1902.04584 [hep-ph].

- [78] L. Heurtier, D. Kim, J. C. Park and S. Shin, “*Explaining the ANITA Anomaly with Inelastic Boosted Dark Matter,*” Phys. Rev. D **100**, no. 5, 055004 (2019) DOI: [10.1103/PhysRevD.100.055004](https://doi.org/10.1103/PhysRevD.100.055004) arXiv:1905.13223 [hep-ph].
- [79] J. M. Cline, C. Gross and W. Xue, “*Can the ANITA anomalous events be due to new physics?,*” Phys. Rev. D **100**, no. 1, 015031 (2019) DOI: [10.1103/PhysRevD.100.015031](https://doi.org/10.1103/PhysRevD.100.015031) arXiv:1904.13396 [hep-ph].
- [80] D. Hooper, S. Wegsman, C. Deaconu and A. Viereg, “*Superheavy dark matter and ANITAs anomalous events,*” Phys. Rev. D **100**, no. 4, 043019 (2019) DOI: [10.1103/PhysRevD.100.043019](https://doi.org/10.1103/PhysRevD.100.043019) arXiv:1904.12865 [astro-ph.HE].
- [81] I. Esteban, J. Lopez-Pavon, I. Martinez-Soler and J. Salvado, “*Looking at the Axionic Dark Sector with ANITA,*” arXiv:1905.10372 [hep-ph].
- [82] L. A. Anchordoqui and I. Antoniadis, “*Supersymmetric sphaleron configurations as the origin of the perplexing ANITA events,*” Phys. Lett. B **790**, 578 (2019) DOI: [10.1016/j.physletb.2019.02.003](https://doi.org/10.1016/j.physletb.2019.02.003) arXiv:1812.01520 [hep-ph].
- [83] I. M. Shoemaker, A. Kusenko, P. K. Munneke, A. Romero-Wolf, D. M. Schroeder and M. J. Siebert, “*Reflections On the Anomalous ANITA Events: The Antarctic Subsurface as a Possible Explanation,*” arXiv:1905.02846 [astro-ph.HE].
- [84] N. Agafonova *et al.* [OPERA Collaboration], “*Final results of the search for  $\nu_\mu \rightarrow \nu_e$  oscillations with the OPERA detector in the CNGS beam,*” JHEP **1806**, 151 (2018) DOI: [10.1007/JHEP06\(2018\)151](https://doi.org/10.1007/JHEP06(2018)151) arXiv:1803.11400 [hep-ex].
- [85] B. Armbruster *et al.* [KARMEN Collaboration], “*Upper limits for neutrino oscillations muon-anti-neutrino  $\rightarrow$  electron-anti-neutrino from muon decay at rest,*” Phys. Rev. D **65**, 112001 (2002) DOI: [10.1103/PhysRevD.65.112001](https://doi.org/10.1103/PhysRevD.65.112001) [hep-ex/0203021].
- [86] M. G. Aartsen *et al.* [IceCube Collaboration], “*Search for sterile neutrino mixing using three years of IceCube DeepCore data,*” Phys. Rev. D **95**, no. 11, 112002 (2017) DOI: [10.1103/PhysRevD.95.112002](https://doi.org/10.1103/PhysRevD.95.112002) arXiv:1702.05160 [hep-ex].

- [87] P. A. R. Ade *et al.* [Planck Collaboration], “*Planck 2015 results. XIII. Cosmological parameters*,” *Astron. Astrophys.* **594**, A13 (2016) DOI: [10.1051/0004-6361/201525830](https://doi.org/10.1051/0004-6361/201525830) arXiv:1502.01589 [astro-ph.CO].
- [88] N. Aghanim *et al.* [Planck Collaboration], “*Planck 2018 results. VI. Cosmological parameters*,” arXiv:1807.06209 [astro-ph.CO].
- [89] E. Bertuzzo, S. Jana, P. A. N. Machado and R. Zukanovich Funchal, “*Dark Neutrino Portal to Explain MiniBooNE excess*,” *Phys. Rev. Lett.* **121**, no. 24, 241801 (2018) DOI: [10.1103/PhysRevLett.121.241801](https://doi.org/10.1103/PhysRevLett.121.241801) arXiv:1807.09877 [hep-ph].
- [90] C. A. Argelles, M. Hostert and Y. D. Tsai, “*Testing New Physics Explanations of MiniBooNE Anomaly at Neutrino Scattering Experiments*,” arXiv:1812.08768 [hep-ph].
- [91] R. Aaij *et al.* [LHCb Collaboration], “*Measurement of the ratio of branching fractions  $\mathcal{B}(B_c^+ \rightarrow J/\psi\tau^+\nu_\tau)/\mathcal{B}(B_c^+ \rightarrow J/\psi\mu^+\nu_\mu)$* ,” *Phys. Rev. Lett.* **120**, no. 12, 121801 (2018) DOI: [10.1103/PhysRevLett.120.121801](https://doi.org/10.1103/PhysRevLett.120.121801) arXiv:1711.05623 [hep-ex].
- [92] J. P. Lees *et al.* [BaBar Collaboration], “*Evidence for an excess of  $\bar{B} \rightarrow D^{(*)}\tau^-\bar{\nu}_\tau$  decays*,” *Phys. Rev. Lett.* **109**, 101802 (2012) DOI: [10.1103/PhysRevLett.109.101802](https://doi.org/10.1103/PhysRevLett.109.101802) arXiv:1205.5442 [hep-ex].
- [93] J. P. Lees *et al.* [BaBar Collaboration], “*Measurement of an Excess of  $\bar{B} \rightarrow D^{(*)}\tau^-\bar{\nu}_\tau$  Decays and Implications for Charged Higgs Bosons*,” *Phys. Rev. D* **88**, no. 7, 072012 (2013) DOI: [10.1103/PhysRevD.88.072012](https://doi.org/10.1103/PhysRevD.88.072012) arXiv:1303.0571 [hep-ex].
- [94] M. Huschle *et al.* [Belle Collaboration], “*Measurement of the branching ratio of  $\bar{B} \rightarrow D^{(*)}\tau^-\bar{\nu}_\tau$  relative to  $\bar{B} \rightarrow D^{(*)}\ell^-\bar{\nu}_\ell$  decays with hadronic tagging at Belle*,” *Phys. Rev. D* **92**, no. 7, 072014 (2015) DOI: [10.1103/PhysRevD.92.072014](https://doi.org/10.1103/PhysRevD.92.072014) arXiv:1507.03233 [hep-ex].
- [95] S. Hirose *et al.* [Belle Collaboration], “*Measurement of the  $\tau$  lepton polarization*

- and  $R(D^*)$  in the decay  $\bar{B} \rightarrow D^* \tau^- \bar{\nu}_\tau$ ,” Phys. Rev. Lett. **118**, no. 21, 211801 (2017) DOI: [10.1103/PhysRevLett.118.211801](https://doi.org/10.1103/PhysRevLett.118.211801) arXiv:1612.00529 [hep-ex].
- [96] S. Hirose *et al.* [Belle Collaboration], “Measurement of the  $\tau$  lepton polarization and  $R(D^*)$  in the decay  $\bar{B} \rightarrow D^* \tau^- \bar{\nu}_\tau$  with one-prong hadronic  $\tau$  decays at Belle,” Phys. Rev. D **97**, no. 1, 012004 (2018) DOI: [10.1103/PhysRevD.97.012004](https://doi.org/10.1103/PhysRevD.97.012004) arXiv:1709.00129 [hep-ex].
- [97] R. Aaij *et al.* [LHCb Collaboration], “Measurement of the ratio of the  $B^0 \rightarrow D^{*-} \tau^+ \nu_\tau$  and  $B^0 \rightarrow D^{*-} \mu^+ \nu_\mu$  branching fractions using three-prong  $\tau$ -lepton decays,” Phys. Rev. Lett. **120**, no. 17, 171802 (2018) DOI: [10.1103/PhysRevLett.120.171802](https://doi.org/10.1103/PhysRevLett.120.171802) arXiv:1708.08856 [hep-ex].
- [98] R. Aaij *et al.* [LHCb Collaboration], “Test of Lepton Flavor Universality by the measurement of the  $B^0 \rightarrow D^{*-} \tau^+ \nu_\tau$  branching fraction using three-prong  $\tau$  decays,” Phys. Rev. D **97**, no. 7, 072013 (2018) DOI: [10.1103/PhysRevD.97.072013](https://doi.org/10.1103/PhysRevD.97.072013) arXiv:1711.02505 [hep-ex].
- [99] <https://hflav-eos.web.cern.ch/hflav-eos/semi/summer18/RDRDs.html>
- [100] A. Abdesselam *et al.* [Belle Collaboration], “Measurement of  $\mathcal{R}(D)$  and  $\mathcal{R}(D^*)$  with a semileptonic tagging method,” arXiv:1904.08794 [hep-ex].
- [101] <https://hflav-eos.web.cern.ch/hflav-eos/semi/spring19/html/RDsDsstar/RDRDs.html>
- [102] J. A. Bailey *et al.* [MILC Collaboration], “ $B \rightarrow D \ell \nu$  form factors at nonzero recoil and  $-V_{cb}$  from 2+1-flavor lattice QCD,” Phys. Rev. D **92**, no. 3, 034506 (2015) DOI: [10.1103/PhysRevD.92.034506](https://doi.org/10.1103/PhysRevD.92.034506) arXiv:1503.07237 [hep-lat].
- [103] H. Na *et al.* [HPQCD Collaboration], “ $B \rightarrow D \ell \nu$  form factors at nonzero recoil and extraction of  $|V_{cb}|$ ,” Phys. Rev. D **92**, no. 5, 054510 (2015) Erratum: [Phys. Rev. D **93**, no. 11, 119906 (2016)] DOI: [10.1103/PhysRevD.93.119906](https://doi.org/10.1103/PhysRevD.93.119906), [10.1103/PhysRevD.92.054510](https://doi.org/10.1103/PhysRevD.92.054510) arXiv:1505.03925 [hep-lat].
- [104] S. Aoki *et al.*, “Review of lattice results concerning low-energy particle physics,” Eur. Phys. J. C **77**, no. 2, 112 (2017) DOI: [10.1140/epjc/s10052-016-4509-7](https://doi.org/10.1140/epjc/s10052-016-4509-7) arXiv:1607.00299 [hep-lat].

- [105] D. Bigi and P. Gambino, “*Revisiting  $B \rightarrow D\ell\nu$* ,” Phys. Rev. D **94**, no. 9, 094008 (2016) DOI: [10.1103/PhysRevD.94.094008](https://doi.org/10.1103/PhysRevD.94.094008) arXiv:1606.08030 [hep-ph].
- [106] S. Fajfer, J. F. Kamenik and I. Nisandzic, “*On the  $B \rightarrow D^*\tau\bar{\nu}_\tau$  Sensitivity to New Physics*,” Phys. Rev. D **85**, 094025 (2012) DOI: [10.1103/PhysRevD.85.094025](https://doi.org/10.1103/PhysRevD.85.094025) arXiv:1203.2654 [hep-ph].
- [107] A. Abdesselam *et al.* [Belle Collaboration], “*Precise determination of the CKM matrix element  $|V_{cb}|$  with  $\bar{B}^0 \rightarrow D^{*+}\ell^-\bar{\nu}_\ell$  decays with hadronic tagging at Belle*,” arXiv:1702.01521 [hep-ex].
- [108] F. U. Bernlochner, Z. Ligeti, M. Papucci and D. J. Robinson, “*Combined analysis of semileptonic  $B$  decays to  $D$  and  $D^*$ :  $R(D^{(*)})$ ,  $|V_{cb}|$ , and new physics*,” Phys. Rev. D **95**, no. 11, 115008 (2017) Erratum: [Phys. Rev. D **97**, no. 5, 059902 (2018)] DOI: [10.1103/PhysRevD.95.115008](https://doi.org/10.1103/PhysRevD.95.115008), [10.1103/PhysRevD.97.059902](https://doi.org/10.1103/PhysRevD.97.059902) arXiv:1703.05330 [hep-ph].
- [109] D. Bigi, P. Gambino and S. Schacht, “ *$R(D^*)$ ,  $|V_{cb}|$ , and the Heavy Quark Symmetry relations between form factors*,” JHEP **1711**, 061 (2017) DOI: [10.1007/JHEP11\(2017\)061](https://doi.org/10.1007/JHEP11(2017)061) arXiv:1707.09509 [hep-ph].
- [110] S. Jaiswal, S. Nandi and S. K. Patra, “*Extraction of  $|V_{cb}|$  from  $B \rightarrow D^{(*)}\ell\nu_\ell$  and the Standard Model predictions of  $R(D^{(*)})$* ,” JHEP **1712**, 060 (2017) DOI: [10.1007/JHEP12\(2017\)060](https://doi.org/10.1007/JHEP12(2017)060) arXiv:1707.09977 [hep-ph].
- [111] A. Datta, M. Duraisamy and D. Ghosh, “*Diagnosing New Physics in  $b \rightarrow c\tau\nu_\tau$  decays in the light of the recent BaBar result*,” Phys. Rev. D **86**, 034027 (2012) DOI: [10.1103/PhysRevD.86.034027](https://doi.org/10.1103/PhysRevD.86.034027) arXiv:1206.3760 [hep-ph].
- [112] D. Bardhan, P. Byakti and D. Ghosh, “*A closer look at the  $R_D$  and  $R_{D^*}$  anomalies*,” JHEP **1701**, 125 (2017) DOI: [10.1007/JHEP01\(2017\)125](https://doi.org/10.1007/JHEP01(2017)125) arXiv:1610.03038 [hep-ph].
- [113] R. Ammar *et al.* [CLEO Collaboration], “*Evidence for penguins: First observation of  $B \rightarrow K^*(892)\gamma$* ,” Phys. Rev. Lett. **71**, 674 (1993). DOI: [10.1103/PhysRevLett.71.674](https://doi.org/10.1103/PhysRevLett.71.674)

- [114] G. Hiller and F. Kruger, “*More model-independent analysis of  $b \rightarrow s$  processes,*” Phys. Rev. D **69**, 074020 (2004) DOI: [10.1103/PhysRevD.69.074020](https://doi.org/10.1103/PhysRevD.69.074020) [hep-ph/0310219].
- [115] J. P. Lees *et al.* [BaBar Collaboration], “*Measurement of Branching Fractions and Rate Asymmetries in the Rare Decays  $B \rightarrow K^{(*)}l^+l^-$ ,*” Phys. Rev. D **86**, 032012 (2012) DOI: [10.1103/PhysRevD.86.032012](https://doi.org/10.1103/PhysRevD.86.032012) arXiv:1204.3933 [hep-ex].
- [116] J.-T. Wei *et al.* [Belle Collaboration], “*Measurement of the Differential Branching Fraction and Forward-Backward Asymmetry for  $B \rightarrow K^{(*)}l^+l^-$ ,*” Phys. Rev. Lett. **103**, 171801 (2009) DOI: [10.1103/PhysRevLett.103.171801](https://doi.org/10.1103/PhysRevLett.103.171801) arXiv:0904.0770 [hep-ex].
- [117] R. Aaij *et al.* [LHCb Collaboration], “*Test of lepton universality using  $B^+ \rightarrow K^+l^+l^-$  decays,*” Phys. Rev. Lett. **113**, 151601 (2014) DOI: [10.1103/PhysRevLett.113.151601](https://doi.org/10.1103/PhysRevLett.113.151601) arXiv:1406.6482 [hep-ex].
- [118] R. Aaij *et al.* [LHCb Collaboration], “*Test of lepton universality with  $B^0 \rightarrow K^{*0}l^+l^-$  decays,*” JHEP **1708**, 055 (2017) DOI: [10.1007/JHEP08\(2017\)055](https://doi.org/10.1007/JHEP08(2017)055) arXiv:1705.05802 [hep-ex].
- [119] M. Bordone, G. Isidori and A. Pattori, “*On the Standard Model predictions for  $R_K$  and  $R_{K^*}$ ,*” Eur. Phys. J. C **76**, no. 8, 440 (2016) DOI: [10.1140/epjc/s10052-016-4274-7](https://doi.org/10.1140/epjc/s10052-016-4274-7) arXiv:1605.07633 [hep-ph].
- [120] N. Serra, R. Silva Coutinho and D. van Dyk, “*Measuring the breaking of lepton flavor universality in  $B \rightarrow K^*l^+l^-$ ,*” Phys. Rev. D **95**, no. 3, 035029 (2017) DOI: [10.1103/PhysRevD.95.035029](https://doi.org/10.1103/PhysRevD.95.035029) arXiv:1610.08761 [hep-ph].
- [121] W. Altmannshofer, C. Niehoff, P. Stangl and D. M. Straub, “*Status of the  $B \rightarrow K^*\mu^+\mu^-$  anomaly after Moriond 2017,*” Eur. Phys. J. C **77**, no. 6, 377 (2017) DOI: [10.1140/epjc/s10052-017-4952-0](https://doi.org/10.1140/epjc/s10052-017-4952-0) arXiv:1703.09189 [hep-ph].
- [122] S. Jger and J. Martin Camalich, “*Reassessing the discovery potential of the  $B \rightarrow K^*l^+l^-$  decays in the large-recoil region: SM challenges and BSM*”

- opportunities*,” Phys. Rev. D **93**, no. 1, 014028 (2016) DOI: [10.1103/PhysRevD.93.014028](https://doi.org/10.1103/PhysRevD.93.014028) arXiv:1412.3183 [hep-ph].
- [123] B. Capdevila, S. Descotes-Genon, J. Matias and J. Virto, “*Assessing lepton-flavour non-universality from  $B \rightarrow K^* \ell \ell$  angular analyses*,” JHEP **1610**, 075 (2016) DOI: [10.1007/JHEP10\(2016\)075](https://doi.org/10.1007/JHEP10(2016)075) arXiv:1605.03156 [hep-ph].
- [124] D. Bardhan, P. Byakti and D. Ghosh, “*Role of Tensor operators in  $R_K$  and  $R_{K^*}$* ,” Phys. Lett. B **773**, 505 (2017) DOI: [10.1016/j.physletb.2017.08.062](https://doi.org/10.1016/j.physletb.2017.08.062) arXiv:1705.09305 [hep-ph].
- [125] G. Hiller and M. Schmaltz, “ *$R_K$  and future  $b \rightarrow s \ell \ell$  physics beyond the standard model opportunities*,” Phys. Rev. D **90**, 054014 (2014) DOI: [10.1103/PhysRevD.90.054014](https://doi.org/10.1103/PhysRevD.90.054014) arXiv:1408.1627 [hep-ph].
- [126] G. D’Amico, M. Nardecchia, P. Panci, F. Sannino, A. Strumia, R. Torre and A. Urbano, “*Flavour anomalies after the  $R_{K^*}$  measurement*,” JHEP **1709**, 010 (2017) DOI: [10.1007/JHEP09\(2017\)010](https://doi.org/10.1007/JHEP09(2017)010) arXiv:1704.05438 [hep-ph].
- [127] D. Bečirević and O. Sumensari, “*A leptoquark model to accommodate  $R_K^{\text{exp}} < R_K^{\text{SM}}$  and  $R_{K^*}^{\text{exp}} < R_{K^*}^{\text{SM}}$* ,” JHEP **1708**, 104 (2017) DOI: [10.1007/JHEP08\(2017\)104](https://doi.org/10.1007/JHEP08(2017)104) arXiv:1704.05835 [hep-ph].
- [128] G. Hiller and I. Nisandzic, “ *$R_K$  and  $R_{K^*}$  beyond the standard model*,” Phys. Rev. D **96**, no. 3, 035003 (2017) DOI: [10.1103/PhysRevD.96.035003](https://doi.org/10.1103/PhysRevD.96.035003) arXiv:1704.05444 [hep-ph].
- [129] Y. Cai, J. Gargalionis, M. A. Schmidt and R. R. Volkas, “*Reconsidering the One Leptoquark solution: flavor anomalies and neutrino mass*,” JHEP **1710**, 047 (2017) DOI: [10.1007/JHEP10\(2017\)047](https://doi.org/10.1007/JHEP10(2017)047) arXiv:1704.05849 [hep-ph].
- [130] A. Crivellin, D. Müller and T. Ota, “*Simultaneous explanation of  $R(D^0)$  and  $bs^+$  : the last scalar leptoquarks standing*,” JHEP **1709**, 040 (2017) DOI: [10.1007/JHEP09\(2017\)040](https://doi.org/10.1007/JHEP09(2017)040) arXiv:1703.09226 [hep-ph].

- [131] N. G. Deshpande and X. G. He, “Consequences of  $R$ -parity violating interactions for anomalies in  $\bar{B} \rightarrow D^{(*)}\tau\bar{\nu}$  and  $b \rightarrow s\mu^+\mu^-$ ,” Eur. Phys. J. C **77**, no. 2, 134 (2017) DOI: [10.1140/epjc/s10052-017-4707-y](https://doi.org/10.1140/epjc/s10052-017-4707-y) arXiv:1608.04817 [hep-ph].
- [132] D. Das, C. Hati, G. Kumar and N. Mahajan, “Scrutinizing  $R$ -parity violating interactions in light of  $R_{K^{(*)}}$  data,” Phys. Rev. D **96**, no. 9, 095033 (2017) DOI: [10.1103/PhysRevD.96.095033](https://doi.org/10.1103/PhysRevD.96.095033) arXiv:1705.09188 [hep-ph].
- [133] S. Biswas, D. Chowdhury, S. Han and S. J. Lee, “Explaining the lepton non-universality at the LHCb and CMS within a unified framework,” JHEP **1502**, 142 (2015) DOI: [10.1007/JHEP02\(2015\)142](https://doi.org/10.1007/JHEP02(2015)142) arXiv:1409.0882 [hep-ph].
- [134] W. Altmannshofer, P. S. Bhupal Dev and A. Soni, “ $R_{D^{(*)}}$  anomaly: A possible hint for natural supersymmetry with  $R$ -parity violation,” Phys. Rev. D **96**, no. 9, 095010 (2017) DOI: [10.1103/PhysRevD.96.095010](https://doi.org/10.1103/PhysRevD.96.095010) arXiv:1704.06659 [hep-ph].
- [135] A. K. Alok, B. Bhattacharya, A. Datta, D. Kumar, J. Kumar and D. London, “New Physics in  $b \rightarrow s\mu^+\mu^-$  after the Measurement of  $R_{K^*}$ ,” Phys. Rev. D **96**, no. 9, 095009 (2017) DOI: [10.1103/PhysRevD.96.095009](https://doi.org/10.1103/PhysRevD.96.095009) arXiv:1704.07397 [hep-ph].
- [136] F. Sala and D. M. Straub, “A New Light Particle in  $B$  Decays?,” Phys. Lett. B **774**, 205 (2017) DOI: [10.1016/j.physletb.2017.09.072](https://doi.org/10.1016/j.physletb.2017.09.072) arXiv:1704.06188 [hep-ph].
- [137] A. Datta, J. Liao and D. Marfatia, “A light  $Z'$  for the  $R_K$  puzzle and nonstandard neutrino interactions,” Phys. Lett. B **768**, 265 (2017) DOI: [10.1016/j.physletb.2017.02.058](https://doi.org/10.1016/j.physletb.2017.02.058) arXiv:1702.01099 [hep-ph].
- [138] A. Datta, J. Kumar, J. Liao and D. Marfatia, “New light mediators for the  $R_K$  and  $R_{K^*}$  puzzles,” Phys. Rev. D **97**, no. 11, 115038 (2018) DOI: [10.1103/PhysRevD.97.115038](https://doi.org/10.1103/PhysRevD.97.115038) arXiv:1705.08423 [hep-ph].
- [139] A. Celis, J. Fuentes-Martin, A. Vicente and J. Virto, “Gauge-invariant implications of the LHCb measurements on lepton-flavor nonuniversality,” Phys. Rev. D

- 96** (2017) no.3, 035026 DOI: [10.1103/PhysRevD.96.035026](https://doi.org/10.1103/PhysRevD.96.035026) arXiv:1704.05672 [hep-ph].
- [140] M. Ciuchini, A. M. Coutinho, M. Fedele, E. Franco, A. Paul, L. Silvestrini and M. Valli, “*On Flavourful Easter eggs for New Physics hunger and Lepton Flavour Universality violation,*” Eur. Phys. J. C **77**, no. 10, 688 (2017) DOI: [10.1140/epjc/s10052-017-5270-2](https://doi.org/10.1140/epjc/s10052-017-5270-2) arXiv:1704.05447 [hep-ph].
- [141] L. S. Geng, B. Grinstein, S. Jger, J. Martin Camalich, X. L. Ren and R. X. Shi, “*Towards the discovery of new physics with lepton-universality ratios of  $b \rightarrow s\ell\ell$  decays,*” Phys. Rev. D **96**, no. 9, 093006 (2017) DOI: [10.1103/PhysRevD.96.093006](https://doi.org/10.1103/PhysRevD.96.093006) arXiv:1704.05446 [hep-ph].
- [142] T. Hurth, F. Mahmoudi and S. Neshatpour, “*Global fits to  $b \rightarrow s\ell\ell$  data and signs for lepton non-universality,*” JHEP **1412**, 053 (2014) DOI: [10.1007/JHEP12\(2014\)053](https://doi.org/10.1007/JHEP12(2014)053) arXiv:1410.4545 [hep-ph].
- [143] C. W. Chiang, X. G. He, J. Tandean and X. B. Yuan, “ *$R_{K^{(*)}}$  and related  $b \rightarrow s\ell\bar{\ell}$  anomalies in minimal flavor violation framework with  $Z'$  boson,*” Phys. Rev. D **96**, no. 11, 115022 (2017) DOI: [10.1103/PhysRevD.96.115022](https://doi.org/10.1103/PhysRevD.96.115022) arXiv:1706.02696 [hep-ph].
- [144] A. Crivellin, G. D’Ambrosio and J. Heeck, “*Addressing the LHC flavor anomalies with horizontal gauge symmetries,*” Phys. Rev. D **91**, no. 7, 075006 (2015) DOI: [10.1103/PhysRevD.91.075006](https://doi.org/10.1103/PhysRevD.91.075006) arXiv:1503.03477 [hep-ph].
- [145] D. Ghosh, “*Explaining the  $R_K$  and  $R_{K^*}$  anomalies,*” Eur. Phys. J. C **77**, no. 10, 694 (2017) DOI: [10.1140/epjc/s10052-017-5282-y](https://doi.org/10.1140/epjc/s10052-017-5282-y) arXiv:1704.06240 [hep-ph].
- [146] C. Bonilla, T. Modak, R. Srivastava and J. W. F. Valle, “ *$U(1)_{B_3-3L_\mu}$  gauge symmetry as a simple description of  $b \rightarrow s$  anomalies,*” Phys. Rev. D **98**, no. 9, 095002 (2018) DOI: [10.1103/PhysRevD.98.095002](https://doi.org/10.1103/PhysRevD.98.095002) arXiv:1705.00915 [hep-ph].
- [147] J. M. Cline and J. Martin Camalich, “ *$B$  decay anomalies from nonabelian local horizontal symmetry,*” Phys. Rev. D **96**, no. 5, 055036 (2017) DOI: [10.1103/PhysRevD.96.055036](https://doi.org/10.1103/PhysRevD.96.055036) arXiv:1706.08510 [hep-ph].

- [148] K. Garrett and G. Duda, “*Dark Matter: A Primer*,” Adv. Astron. **2011**, 968283 (2011) DOI: [10.1155/2011/968283](https://doi.org/10.1155/2011/968283) arXiv:1006.2483 [hep-ph].
- [149] G. Bertone and D. Hooper, “*A History of Dark Matter*,” G. Bertone and D. Hooper, “*History of dark matter*,” Rev. Mod. Phys. **90**, no. 4, 045002 (2018) DOI: [10.1103/RevModPhys.90.045002](https://doi.org/10.1103/RevModPhys.90.045002) arXiv:1605.04909 [astro-ph.CO].
- [150] M. Lisanti, “*Lectures on Dark Matter Physics*,” DOI: [10.1142/9789813149441\\_0007](https://doi.org/10.1142/9789813149441_0007) arXiv:1603.03797 [hep-ph].
- [151] S. Profumo, “*Astrophysical Probes of Dark Matter*,” DOI: [10.1142/9789814525220\\_0004](https://doi.org/10.1142/9789814525220_0004) arXiv:1301.0952 [hep-ph].
- [152] M. Bauer and T. Plehn, “*Yet Another Introduction to Dark Matter*,” Lect. Notes Phys. **959**, pp. (2019) DOI: [10.1007/978-3-030-16234-4](https://doi.org/10.1007/978-3-030-16234-4) arXiv:1705.01987 [hep-ph].
- [153] D. S. Akerib *et al.* [LUX Collaboration], “*Limits on spin-dependent WIMP-nucleon cross section obtained from the complete LUX exposure*,” Phys. Rev. Lett. **118**, no. 25, 251302 (2017) DOI: [10.1103/PhysRevLett.118.251302](https://doi.org/10.1103/PhysRevLett.118.251302) arXiv:1705.03380 [astro-ph.CO].
- [154] E. Aprile *et al.* [XENON Collaboration], “*Constraining the spin-dependent WIMP-nucleon cross sections with XENON1T*,” Phys. Rev. Lett. **122**, no. 14, 141301 (2019) DOI: [10.1103/PhysRevLett.122.141301](https://doi.org/10.1103/PhysRevLett.122.141301) arXiv:1902.03234 [astro-ph.CO].
- [155] R. Essig, T. Volansky and T. T. Yu, “*New Constraints and Prospects for sub-GeV Dark Matter Scattering off Electrons in Xenon*,” Phys. Rev. D **96**, no. 4, 043017 (2017) DOI: [10.1103/PhysRevD.96.043017](https://doi.org/10.1103/PhysRevD.96.043017) arXiv:1703.00910 [hep-ph].
- [156] G. Cavoto, F. Luchetta and A. D. Polosa, “*Sub-GeV Dark Matter Detection with Electron Recoils in Carbon Nanotubes*,” Phys. Lett. B **776**, 338 (2018) DOI: [10.1016/j.physletb.2017.11.064](https://doi.org/10.1016/j.physletb.2017.11.064) arXiv:1706.02487 [hep-ph].

- [157] Y. Hochberg *et al.*, “*Detection of sub-MeV Dark Matter with Three-Dimensional Dirac Materials*,” Phys. Rev. D **97**, no. 1, 015004 (2018) DOI: [10.1103/PhysRevD.97.015004](https://doi.org/10.1103/PhysRevD.97.015004) arXiv:1708.08929 [hep-ph].
- [158] Y. Hochberg, E. Kuflik, T. Volansky and J. G. Wacker, “*Mechanism for Thermal Relic Dark Matter of Strongly Interacting Massive Particles*,” Phys. Rev. Lett. **113**, 171301 (2014) DOI: [10.1103/PhysRevLett.113.171301](https://doi.org/10.1103/PhysRevLett.113.171301) arXiv:1402.5143 [hep-ph].
- [159] Y. Hochberg, E. Kuflik, H. Murayama, T. Volansky and J. G. Wacker, “*Model for Thermal Relic Dark Matter of Strongly Interacting Massive Particles*,” Phys. Rev. Lett. **115**, no. 2, 021301 (2015) DOI: [10.1103/PhysRevLett.115.021301](https://doi.org/10.1103/PhysRevLett.115.021301) arXiv:1411.3727 [hep-ph].
- [160] N. Bernal, C. Garcia-Cely and R. Rosenfeld, “*WIMP and SIMP Dark Matter from the Spontaneous Breaking of a Global Group*,” JCAP **1504**, no. 04, 012 (2015) DOI: [10.1088/1475-7516/2015/04/012](https://doi.org/10.1088/1475-7516/2015/04/012) arXiv:1501.01973 [hep-ph].
- [161] N. Daci, I. De Bruyn, S. Lowette, M. H. G. Tytgat and B. Zaldivar, “*Simplified SIMPs and the LHC*,” JHEP **1511**, 108 (2015) DOI: [10.1007/JHEP11\(2015\)108](https://doi.org/10.1007/JHEP11(2015)108) arXiv:1503.05505 [hep-ph].
- [162] S. M. Choi and H. M. Lee, “*SIMP dark matter with gauged  $Z_3$  symmetry*,” JHEP **1509**, 063 (2015) DOI: [10.1007/JHEP09\(2015\)063](https://doi.org/10.1007/JHEP09(2015)063) arXiv:1505.00960 [hep-ph].
- [163] M. Hansen, K. Langble and F. Sannino, “*SIMP model at NNLO in chiral perturbation theory*,” Phys. Rev. D **92**, no. 7, 075036 (2015) DOI: [10.1103/PhysRevD.92.075036](https://doi.org/10.1103/PhysRevD.92.075036) arXiv:1507.01590 [hep-ph].
- [164] N. Bernal, X. Chu, C. Garcia-Cely, T. Hambye and B. Zaldivar, “*Production Regimes for Self-Interacting Dark Matter*,” JCAP **1603**, no. 03, 018 (2016) DOI: [10.1088/1475-7516/2016/03/018](https://doi.org/10.1088/1475-7516/2016/03/018) arXiv:1510.08063 [hep-ph].
- [165] N. Bernal and X. Chu, “ *$Z_2$  SIMP Dark Matter*,” JCAP **1601**, 006 (2016) DOI: [10.1088/1475-7516/2016/01/006](https://doi.org/10.1088/1475-7516/2016/01/006) arXiv:1510.08527 [hep-ph].

- [166] Y. Hochberg, E. Kuflik and H. Murayama, “*SIMP Spectroscopy*,” JHEP **1605**, 090 (2016) DOI: [10.1007/JHEP05\(2016\)090](https://doi.org/10.1007/JHEP05(2016)090) arXiv:1512.07917 [hep-ph].
- [167] U. K. Dey, T. N. Maity and T. S. Ray, “*Light Dark Matter through Assisted Annihilation*,” JCAP **1703**, no. 03, 045 (2017) DOI: [10.1088/1475-7516/2017/03/045](https://doi.org/10.1088/1475-7516/2017/03/045) arXiv:1612.09074 [hep-ph].
- [168] N. Bernal, X. Chu and J. Pradler, “*Simply split strongly interacting massive particles*,” Phys. Rev. D **95**, no. 11, 115023 (2017) DOI: [10.1103/PhysRevD.95.115023](https://doi.org/10.1103/PhysRevD.95.115023) arXiv:1702.04906 [hep-ph].
- [169] S. M. Choi, Y. Hochberg, E. Kuflik, H. M. Lee, Y. Mambrini, H. Murayama and M. Pierre, “*Vector SIMP dark matter*,” JHEP **1710**, 162 (2017) DOI: [10.1007/JHEP10\(2017\)162](https://doi.org/10.1007/JHEP10(2017)162) arXiv:1707.01434 [hep-ph].
- [170] D. Green and S. Rajendran, “*The Cosmology of Sub-MeV Dark Matter*,” JHEP **1710**, 013 (2017) DOI: [10.1007/JHEP10\(2017\)013](https://doi.org/10.1007/JHEP10(2017)013) arXiv:1701.08750 [hep-ph].
- [171] A. Berlin, D. Hooper and G. Krnjaic, “*Thermal Dark Matter From A Highly Decoupled Sector*,” Phys. Rev. D **94**, no. 9, 095019 (2016) DOI: [10.1103/PhysRevD.94.095019](https://doi.org/10.1103/PhysRevD.94.095019) arXiv:1609.02555 [hep-ph].
- [172] J. L. Feng, H. Tu and H. B. Yu, “*Thermal Relics in Hidden Sectors*,” JCAP **0810**, 043 (2008) DOI: [10.1088/1475-7516/2008/10/043](https://doi.org/10.1088/1475-7516/2008/10/043) arXiv:0808.2318 [hep-ph].
- [173] R. Foot and S. Vagnozzi, “*Dissipative hidden sector dark matter*,” Phys. Rev. D **91**, 023512 (2015) DOI: [10.1103/PhysRevD.91.023512](https://doi.org/10.1103/PhysRevD.91.023512) arXiv:1409.7174 [hep-ph].
- [174] R. Foot and S. Vagnozzi, “*Diurnal modulation signal from dissipative hidden sector dark matter*,” Phys. Lett. B **748**, 61 (2015) DOI: [10.1016/j.physletb.2015.06.063](https://doi.org/10.1016/j.physletb.2015.06.063) arXiv:1412.0762 [hep-ph].
- [175] R. Foot and S. Vagnozzi, “*Solving the small-scale structure puzzles with dissipative dark matter*,” JCAP **1607**, no. 07, 013 (2016) DOI: [10.1088/1475-7516/2016/07/013](https://doi.org/10.1088/1475-7516/2016/07/013) arXiv:1602.02467 [astro-ph.CO].

- [176] S. Tulin and H. B. Yu, “*Dark Matter Self-interactions and Small Scale Structure*,” Phys. Rept. **730**, 1 (2018) DOI: [10.1016/j.physrep.2017.11.004](https://doi.org/10.1016/j.physrep.2017.11.004) arXiv:1705.02358 [hep-ph].
- [177] D. N. Spergel and P. J. Steinhardt, “*Observational evidence for selfinteracting cold dark matter*,” Phys. Rev. Lett. **84**, 3760 (2000) DOI: [10.1103/PhysRevLett.84.3760](https://doi.org/10.1103/PhysRevLett.84.3760) [astro-ph/9909386].
- [178] M. Vogelsberger and J. Zavala, “*Direct detection of self-interacting dark matter*,” Mon. Not. Roy. Astron. Soc. **430**, 1722 (2013) DOI: [10.1093/mnras/sts712](https://doi.org/10.1093/mnras/sts712) arXiv:1211.1377 [astro-ph.CO].
- [179] M. Rocha, A. H. G. Peter, J. S. Bullock, M. Kaplinghat, S. Garrison-Kimmel, J. Onorbe and L. A. Moustakas, “*Cosmological Simulations with Self-Interacting Dark Matter I: Constant Density Cores and Substructure*,” Mon. Not. Roy. Astron. Soc. **430**, 81 (2013) DOI: [10.1093/mnras/sts514](https://doi.org/10.1093/mnras/sts514) arXiv:1208.3025 [astro-ph.CO].
- [180] A. H. G. Peter, M. Rocha, J. S. Bullock and M. Kaplinghat, “*Cosmological Simulations with Self-Interacting Dark Matter II: Halo Shapes vs. Observations*,” Mon. Not. Roy. Astron. Soc. **430**, 105 (2013) DOI: [10.1093/mnras/sts535](https://doi.org/10.1093/mnras/sts535) arXiv:1208.3026 [astro-ph.CO].
- [181] B. Moore, S. Gelato, A. Jenkins, F. R. Pearce and V. Quilis, “*Collisional versus collisionless dark matter*,” Astrophys. J. **535**, L21 (2000) DOI: [10.1086/312692](https://doi.org/10.1086/312692) [astro-ph/0002308].
- [182] N. Yoshida, V. Springel, S. D. M. White and G. Tormen, “*Collisional dark matter and the structure of dark halos*,” Astrophys. J. **535**, L103 (2000) DOI: [10.1086/312707](https://doi.org/10.1086/312707) [astro-ph/0002362].
- [183] A. Burkert, “*The Structure and evolution of weakly selfinteracting cold dark matter halos*,” Astrophys. J. **534**, L143 (2000) DOI: [10.1086/312674](https://doi.org/10.1086/312674) [astro-ph/0002409].

- [184] M. Y. Khlopov, G. M. Beskin, N. E. Bochkarev, L. A. Pustyl'nik and S. A. Pustyl'nik, “*Observational Physics of Mirror World,*” *Sov. Astron.* **35**, 21 (1991) [*Astron. Zh.* **68**, 42 (1991)].
- [185] S. I. Blinnikov and M. Y. Khlopov, “*On Possible Effects Of 'mirror' Particles,*” *Sov. J. Nucl. Phys.* **36**, 472 (1982) [*Yad. Fiz.* **36**, 809 (1982)].
- [186] S. I. Blinnikov and M. Khlopov, “*Possible astronomical effects of mirror particles,*” *Sov. Astron.* **27**, 371 (1983) [*Astron. Zh.* **60**, 632 (1983)].
- [187] E. Farhi and L. Susskind, “*Technicolor,*” *Phys. Rept.* **74**, 277 (1981). DOI: [10.1016/0370-1573\(81\)90173-3](https://doi.org/10.1016/0370-1573(81)90173-3)
- [188] H. Georgi and S. L. Glashow, “*Unity of All Elementary Particle Forces,*” *Phys. Rev. Lett.* **32**, 438 (1974). DOI: [10.1103/PhysRevLett.32.438](https://doi.org/10.1103/PhysRevLett.32.438)
- [189] H. Georgi, “*The State of the Art - Gauge Theories,*” *AIP Conf. Proc.* **23**, 575 (1975). DOI: [10.1063/1.2947450](https://doi.org/10.1063/1.2947450)
- [190] P. Cox, A. Kusenko, O. Sumensari and T. T. Yanagida, “*SU(5) Unification with TeV-scale Leptoquarks,*” *JHEP* **1703**, 035 (2017) DOI: [10.1007/JHEP03\(2017\)035](https://doi.org/10.1007/JHEP03(2017)035) arXiv:1612.03923 [hep-ph].
- [191] D. Chakraverty, D. Choudhury and A. Datta, “*A Nonsupersymmetric resolution of the anomalous muon magnetic moment,*” *Phys. Lett. B* **506**, 103 (2001) DOI: [10.1016/S0370-2693\(01\)00419-1](https://doi.org/10.1016/S0370-2693(01)00419-1) [hep-ph/0102180].
- [192] G. Couture and H. Konig, “*Bounds on second generation scalar leptoquarks from the anomalous magnetic moment of the muon,*” *Phys. Rev. D* **53**, 555 (1996) DOI: [10.1103/PhysRevD.53.555](https://doi.org/10.1103/PhysRevD.53.555) [hep-ph/9507263].
- [193] E. Coluccio Leskow, G. D'Ambrosio, A. Crivellin and D. Miller, “ *$(g - 2)\mu$ , lepton flavor violation, and Z decays with leptoquarks: Correlations and future prospects,*” *Phys. Rev. D* **95**, no. 5, 055018 (2017) DOI: [10.1103/PhysRevD.95.055018](https://doi.org/10.1103/PhysRevD.95.055018) arXiv:1612.06858 [hep-ph].

- [194] S. Baek and K. Nishiwaki, “*Leptoquark explanation of  $h \rightarrow \mu\tau$  and muon  $(g - 2)$ ,*” Phys. Rev. D **93**, no. 1, 015002 (2016) DOI: [10.1103/PhysRevD.93.015002](https://doi.org/10.1103/PhysRevD.93.015002) arXiv:1509.07410 [hep-ph].
- [195] D. Das, C. Hati, G. Kumar and N. Mahajan, “*Towards a unified explanation of  $R_{D^{(*)}}$ ,  $R_K$  and  $(g - 2)_\mu$  anomalies in a left-right model with leptoquarks,*” Phys. Rev. D **94**, 055034 (2016) DOI: [10.1103/PhysRevD.94.055034](https://doi.org/10.1103/PhysRevD.94.055034) arXiv:1605.06313 [hep-ph].
- [196] K. M. Cheung, “*Muon anomalous magnetic moment and leptoquark solutions,*” Phys. Rev. D **64**, 033001 (2001) DOI: [10.1103/PhysRevD.64.033001](https://doi.org/10.1103/PhysRevD.64.033001) [hep-ph/0102238].
- [197] C. H. Chen, T. Nomura and H. Okada, “*Excesses of muon  $g - 2$ ,  $R_{D^{(*)}}$ , and  $R_K$  in a leptoquark model,*” Phys. Lett. B **774**, 456 (2017) DOI: [10.1016/j.physletb.2017.10.005](https://doi.org/10.1016/j.physletb.2017.10.005) arXiv:1703.03251 [hep-ph].
- [198] C. Patrignani *et al.* [Particle Data Group], “*Review of Particle Physics,*” Chin. Phys. C **40**, no. 10, 100001 (2016). DOI: [10.1088/1674-1137/40/10/100001](https://doi.org/10.1088/1674-1137/40/10/100001)
- [199] I. Doršner, S. Fajfer, A. Greljo, J. F. Kamenik and N. Košnik, “*Physics of leptoquarks in precision experiments and at particle colliders,*” Phys. Rept. **641**, 1 (2016) DOI: [10.1016/j.physrep.2016.06.001](https://doi.org/10.1016/j.physrep.2016.06.001) arXiv:1603.04993 [hep-ph].
- [200] H. H. Patel, “*Package-X 2.0: A Mathematica package for the analytic calculation of one-loop integrals,*” Comput. Phys. Commun. **218**, 66 (2017) DOI: [10.1016/j.cpc.2017.04.015](https://doi.org/10.1016/j.cpc.2017.04.015) arXiv:1612.00009 [hep-ph].
- [201] R. Aaij *et al.* [LHCb Collaboration], “*Measurement of the  $B_s^0 \rightarrow \mu^+\mu^-$  branching fraction and effective lifetime and search for  $B^0 \rightarrow \mu^+\mu^-$  decays,*” Phys. Rev. Lett. **118**, no. 19, 191801 (2017) DOI: [10.1103/PhysRevLett.118.191801](https://doi.org/10.1103/PhysRevLett.118.191801) arXiv:1703.05747 [hep-ex].
- [202] C. Bobeth, M. Gorbahn, T. Hermann, M. Misiak, E. Stamou and M. Steinhauser, “ *$B_{s,d} \rightarrow l^+l^-$  in the Standard Model with Reduced Theoretical Uncertainty,*”

- Phys. Rev. Lett. **112**, 101801 (2014) DOI: [10.1103/PhysRevLett.112.101801](https://doi.org/10.1103/PhysRevLett.112.101801) arXiv:1311.0903 [hep-ph].
- [203] D. Beirevi, O. Sumensari and R. Zukanovich Funchal, “*Lepton flavor violation in exclusive  $b \rightarrow s$  decays*,” Eur. Phys. J. C **76**, no. 3, 134 (2016) DOI: [10.1140/epjc/s10052-016-3985-0](https://doi.org/10.1140/epjc/s10052-016-3985-0) arXiv:1602.00881 [hep-ph].
- [204] S. Palomares-Ruiz, A. C. Vincent and O. Mena, “*Spectral analysis of the high-energy IceCube neutrinos*,” Phys. Rev. D **91**, no. 10, 103008 (2015) DOI: [10.1103/PhysRevD.91.103008](https://doi.org/10.1103/PhysRevD.91.103008) arXiv:1502.02649 [astro-ph.HE].
- [205] A. D. Martin, W. J. Stirling, R. S. Thorne and G. Watt, “*Parton distributions for the LHC*,” Eur. Phys. J. C **63**, 189 (2009) DOI: [10.1140/epjc/s10052-009-1072-5](https://doi.org/10.1140/epjc/s10052-009-1072-5) arXiv:0901.0002 [hep-ph].
- [206] T. A. Gabriel, D. E. Groom, P. K. Job, N. V. Mokhov and G. R. Stevenson, “*Energy dependence of hadronic activity*,” Nucl. Instrum. Meth. A **338**, 336 (1994). DOI: [10.1016/0168-9002\(94\)91317-X](https://doi.org/10.1016/0168-9002(94)91317-X)
- [207] O. J. P. Eboli, R. Zukanovich Funchal and T. L. Lungov, “*Signal and backgrounds for leptoquarks at the CERN LHC*,” Phys. Rev. D **57**, 1715 (1998) DOI: [10.1103/PhysRevD.57.1715](https://doi.org/10.1103/PhysRevD.57.1715) [hep-ph/9709319].
- [208] M. Kramer, T. Plehn, M. Spira and P. M. Zerwas, “*Pair production of scalar leptoquarks at the CERN LHC*,” Phys. Rev. D **71**, 057503 (2005) DOI: [10.1103/PhysRevD.71.057503](https://doi.org/10.1103/PhysRevD.71.057503) [hep-ph/0411038].
- [209] A. Belyaev, C. Leroy, R. Mehdiyev and A. Pukhov, “*Leptoquark single and pair production at LHC with CalcHEP/CompHEP in the complete model*,” JHEP **0509**, 005 (2005) DOI: [10.1088/1126-6708/2005/09/005](https://doi.org/10.1088/1126-6708/2005/09/005) [hep-ph/0502067].
- [210] I. Dorsner, S. Fajfer and A. Greljo, “*Cornering Scalar Leptoquarks at LHC*,” JHEP **1410**, 154 (2014) DOI: [10.1007/JHEP10\(2014\)154](https://doi.org/10.1007/JHEP10(2014)154) arXiv:1406.4831 [hep-ph].

- [211] T. Mandal, S. Mitra and S. Seth, “*Single Productions of Colored Particles at the LHC: An Example with Scalar Leptoquarks,*” JHEP **1507**, 028 (2015) DOI: [10.1007/JHEP07\(2015\)028](https://doi.org/10.1007/JHEP07(2015)028) arXiv:1503.04689 [hep-ph].
- [212] T. Mandal, S. Mitra and S. Seth, “*Pair Production of Scalar Leptoquarks at the LHC to NLO Parton Shower Accuracy,*” Phys. Rev. D **93**, no. 3, 035018 (2016) DOI: [10.1103/PhysRevD.93.035018](https://doi.org/10.1103/PhysRevD.93.035018) arXiv:1506.07369 [hep-ph].
- [213] I. Dorsner, “*Scalar leptoquarks at LHC,*” PoS CORFU **2015**, 051 (2016). DOI: [10.22323/1.263.0051](https://doi.org/10.22323/1.263.0051)
- [214] U. K. Dey, D. Kar, M. Mitra, M. Spannowsky and A. C. Vincent, “*Searching for Leptoquarks at IceCube and the LHC,*” Phys. Rev. D **98**, no. 3, 035014 (2018) DOI: [10.1103/PhysRevD.98.035014](https://doi.org/10.1103/PhysRevD.98.035014) arXiv:1709.02009 [hep-ph].
- [215] P. Bandyopadhyay and R. Mandal, “*Revisiting scalar leptoquark at the LHC,*” Eur. Phys. J. C **78**, 491 (2018) DOI: [10.1140/epjc/s10052-018-5959-x](https://doi.org/10.1140/epjc/s10052-018-5959-x) arXiv:1801.04253 [hep-ph].
- [216] I. Dorner and A. Greljo, “*Leptoquark toolbox for precision collider studies,*” JHEP **1805**, 126 (2018) DOI: [10.1007/JHEP05\(2018\)126](https://doi.org/10.1007/JHEP05(2018)126) arXiv:1801.07641 [hep-ph].
- [217] G. Hiller, D. Loose and I. Niandi, “*Flavorful leptoquarks at hadron colliders,*” Phys. Rev. D **97**, no. 7, 075004 (2018) DOI: [10.1103/PhysRevD.97.075004](https://doi.org/10.1103/PhysRevD.97.075004) arXiv:1801.09399 [hep-ph].
- [218] A. Alloul, N. D. Christensen, C. Degrande, C. Duhr and B. Fuks, “*FeynRules 2.0 - A complete toolbox for tree-level phenomenology,*” Comput. Phys. Commun. **185**, 2250 (2014) DOI: [10.1016/j.cpc.2014.04.012](https://doi.org/10.1016/j.cpc.2014.04.012) arXiv:1310.1921 [hep-ph].
- [219] J. Alwall *et al.*, “*The automated computation of tree-level and next-to-leading order differential cross sections, and their matching to parton shower simulations,*” JHEP **1407**, 079 (2014) DOI: [10.1007/JHEP07\(2014\)079](https://doi.org/10.1007/JHEP07(2014)079) arXiv:1405.0301 [hep-ph].

- [220] D. Dercks, N. Desai, J. S. Kim, K. Rolbiecki, J. Tattersall and T. Weber, “*CheckMATE 2: From the model to the limit*,” *Comput. Phys. Commun.* **221**, 383 (2017) DOI: [10.1016/j.cpc.2017.08.021](https://doi.org/10.1016/j.cpc.2017.08.021) arXiv:1611.09856 [hep-ph].
- [221] M. Aaboud *et al.* [ATLAS Collaboration], “*Search for scalar leptoquarks in pp collisions at  $\sqrt{s} = 13$  TeV with the ATLAS experiment*,” *New J. Phys.* **18**, no. 9, 093016 (2016) DOI: [10.1088/1367-2630/18/9/093016](https://doi.org/10.1088/1367-2630/18/9/093016) arXiv:1605.06035 [hep-ex].
- [222] M. Aaboud *et al.* [ATLAS Collaboration], “*Search for squarks and gluinos in final states with jets and missing transverse momentum at  $\sqrt{s} = 13$  TeV with the ATLAS detector*,” *Eur. Phys. J. C* **76**, no. 7, 392 (2016) DOI: [10.1140/epjc/s10052-016-4184-8](https://doi.org/10.1140/epjc/s10052-016-4184-8) arXiv:1605.03814 [hep-ex].
- [223] G. Aad *et al.* [ATLAS Collaboration], “*Search for new phenomena in final states with an energetic jet and large missing transverse momentum in pp collisions at  $\sqrt{s} = 8$  TeV with the ATLAS detector*,” *Eur. Phys. J. C* **75**, no. 7, 299 (2015) Erratum: [*Eur. Phys. J. C* **75**, no. 9, 408 (2015)] DOI: [10.1140/epjc/s10052-015-3517-3](https://doi.org/10.1140/epjc/s10052-015-3517-3), [10.1140/epjc/s10052-015-3639-7](https://doi.org/10.1140/epjc/s10052-015-3639-7) arXiv:1502.01518 [hep-ex].
- [224] D. Buttazzo, A. Greljo, G. Isidori and D. Marzocca, “*B-physics anomalies: a guide to combined explanations*,” *JHEP* **1711**, 044 (2017) DOI: [10.1007/JHEP11\(2017\)044](https://doi.org/10.1007/JHEP11(2017)044) arXiv:1706.07808 [hep-ph].
- [225] A. Azatov, D. Barducci, D. Ghosh, D. Marzocca and L. Ubaldi, “*Combined explanations of B-physics anomalies: the sterile neutrino solution*,” *JHEP* **1810**, 092 (2018) DOI: [10.1007/JHEP10\(2018\)092](https://doi.org/10.1007/JHEP10(2018)092) arXiv:1807.10745 [hep-ph].
- [226] A. Angelescu, D. Bečirevi, D. A. Faroughy and O. Sumensari, “*Closing the window on single leptoquark solutions to the B-physics anomalies*,” *JHEP* **1810**, 183 (2018) DOI: [10.1007/JHEP10\(2018\)183](https://doi.org/10.1007/JHEP10(2018)183) arXiv:1808.08179 [hep-ph].
- [227] A. Biswas, D. Kumar Ghosh, N. Ghosh, A. Shaw and A. K. Swain, “*Novel collider signature of  $U_1$  Leptoquark and  $B \rightarrow \pi$  observables*,” arXiv:1808.04169 [hep-ph].

- [228] D. Bečirevi, B. Panes, O. Sumensari and R. Zukanovich Funchal, “*Seeking lept-quarks in IceCube,*” JHEP **1806**, 032 (2018) DOI: [10.1007/JHEP06\(2018\)032](https://doi.org/10.1007/JHEP06(2018)032) arXiv:1803.10112 [hep-ph].
- [229] D. B. Clark, E. Godat and F. I. Olness, “*ManeParse : A Mathematica reader for Parton Distribution Functions,*” Comput. Phys. Commun. **216**, 126 (2017) DOI: [10.1016/j.cpc.2017.03.004](https://doi.org/10.1016/j.cpc.2017.03.004) arXiv:1605.08012 [hep-ph].
- [230] A. Belyaev, N. D. Christensen and A. Pukhov, “*CalcHEP 3.4 for collider physics within and beyond the Standard Model,*” Comput. Phys. Commun. **184**, 1729 (2013) DOI: [10.1016/j.cpc.2013.01.014](https://doi.org/10.1016/j.cpc.2013.01.014) arXiv:1207.6082 [hep-ph].
- [231] R. D. Ball *et al.* [NNPDF Collaboration], “*Parton distributions from high-precision collider data,*” Eur. Phys. J. C **77**, no. 10, 663 (2017) DOI: [10.1140/epjc/s10052-017-5199-5](https://doi.org/10.1140/epjc/s10052-017-5199-5) arXiv:1706.00428 [hep-ph].
- [232] R. D. Ball, V. Bertone, M. Bonvini, S. Marzani, J. Rojo and L. Rottoli, “*Parton distributions with small- $x$  resummation: evidence for BFKL dynamics in HERA data,*” Eur. Phys. J. C **78**, no. 4, 321 (2018) DOI: [10.1140/epjc/s10052-018-5774-4](https://doi.org/10.1140/epjc/s10052-018-5774-4) arXiv:1710.05935 [hep-ph].
- [233] M. Tanabashi *et al.* [Particle Data Group], “*Review of Particle Physics,*” Phys. Rev. D **98**, no. 3, 030001 (2018). DOI: [10.1103/PhysRevD.98.030001](https://doi.org/10.1103/PhysRevD.98.030001)
- [234] I. Dorner and A. Greljo, “*Leptoquark toolbox for precision collider studies,*” JHEP **1805**, 126 (2018) DOI: [10.1007/JHEP05\(2018\)126](https://doi.org/10.1007/JHEP05(2018)126) arXiv:1801.07641 [hep-ph].
- [235] J. Barranco, O. G. Miranda, C. A. Moura and A. Parada, “*A reduction in the UHE neutrino flux due to neutrino spin precession,*” Phys. Lett. B **718**, 26 (2012) DOI: [10.1016/j.physletb.2012.10.024](https://doi.org/10.1016/j.physletb.2012.10.024) arXiv:1205.4285 [astro-ph.HE].
- [236] B. Chauhan and S. Mohanty, “*Signature of light sterile neutrinos at IceCube,*” Phys. Rev. D **98**, no. 8, 083021 (2018) DOI: [10.1103/PhysRevD.98.083021](https://doi.org/10.1103/PhysRevD.98.083021) arXiv:1808.04774 [hep-ph].

- [237] S. Karmakar, S. Pandey and S. Rakshit, “*Are We Looking at Neutrino Absorption Spectra at IceCube?*,” arXiv:1810.04192 [hep-ph].
- [238] S. Hannestad, R. S. Hansen and T. Tram, “*How Self-Interactions can Reconcile Sterile Neutrinos with Cosmology*,” Phys. Rev. Lett. **112**, no. 3, 031802 (2014) DOI: [10.1103/PhysRevLett.112.031802](https://doi.org/10.1103/PhysRevLett.112.031802) arXiv:1310.5926 [astro-ph.CO].
- [239] X. Chu, B. Dasgupta and J. Kopp, “*Sterile neutrinos with secret interactions lasting friendship with cosmology*,” JCAP **1510**, no. 10, 011 (2015) DOI: [10.1088/1475-7516/2015/10/011](https://doi.org/10.1088/1475-7516/2015/10/011) arXiv:1505.02795 [hep-ph].
- [240] M. Archidiacono, S. Hannestad, R. S. Hansen and T. Tram, “*Cosmology with self-interacting sterile neutrinos and dark matter - A pseudoscalar model*,” Phys. Rev. D **91**, no. 6, 065021 (2015) DOI: [10.1103/PhysRevD.91.065021](https://doi.org/10.1103/PhysRevD.91.065021) arXiv:1404.5915 [astro-ph.CO].
- [241] M. Archidiacono, S. Hannestad, R. S. Hansen and T. Tram, “*Sterile neutrinos with pseudoscalar self-interactions and cosmology*,” Phys. Rev. D **93**, no. 4, 045004 (2016) DOI: [10.1103/PhysRevD.93.045004](https://doi.org/10.1103/PhysRevD.93.045004) arXiv:1508.02504 [astro-ph.CO].
- [242] M. Archidiacono, S. Gariazzo, C. Giunti, S. Hannestad, R. Hansen, M. Laveder and T. Tram, “*Pseudoscalar sterile neutrino interactions: reconciling the cosmos with neutrino oscillations*,” JCAP **1608**, no. 08, 067 (2016) DOI: [10.1088/1475-7516/2016/08/067](https://doi.org/10.1088/1475-7516/2016/08/067) arXiv:1606.07673 [astro-ph.CO].
- [243] A. Mirizzi, N. Saviano, G. Miele and P. D. Serpico, “*Light sterile neutrino production in the early universe with dynamical neutrino asymmetries*,” Phys. Rev. D **86**, 053009 (2012) DOI: [10.1103/PhysRevD.86.053009](https://doi.org/10.1103/PhysRevD.86.053009) arXiv:1206.1046 [hep-ph].
- [244] N. Saviano, A. Mirizzi, O. Pisanti, P. D. Serpico, G. Mangano and G. Miele, “*Multi-momentum and multi-flavour active-sterile neutrino oscillations in the early universe: role of neutrino asymmetries and effects on nucleosynthesis*,” Phys. Rev. D **87**, 073006 (2013) DOI: [10.1103/PhysRevD.87.073006](https://doi.org/10.1103/PhysRevD.87.073006) arXiv:1302.1200 [astro-ph.CO].

- [245] A. Mirizzi, G. Mangano, N. Saviano, E. Borriello, C. Giunti, G. Miele and O. Pisanti, “*The strongest bounds on active-sterile neutrino mixing after Planck data,*” *Phys. Lett. B* **726**, 8 (2013) DOI: [10.1016/j.physletb.2013.08.015](https://doi.org/10.1016/j.physletb.2013.08.015) arXiv:1303.5368 [astro-ph.CO].
- [246] I. Esteban, M. C. Gonzalez-Garcia, M. Maltoni, I. Martinez-Soler and T. Schwetz, “*Updated fit to three neutrino mixing: exploring the accelerator-reactor complementarity,*” *JHEP* **1701**, 087 (2017) DOI: [10.1007/JHEP01\(2017\)087](https://doi.org/10.1007/JHEP01(2017)087) arXiv:1611.01514 [hep-ph].
- [247] N. Saviano, O. Pisanti, G. Mangano and A. Mirizzi, “*Unveiling secret interactions among sterile neutrinos with big-bang nucleosynthesis,*” *Phys. Rev. D* **90**, no. 11, 113009 (2014) DOI: [10.1103/PhysRevD.90.113009](https://doi.org/10.1103/PhysRevD.90.113009) arXiv:1409.1680 [astro-ph.CO].
- [248] A. Mirizzi, G. Mangano, O. Pisanti and N. Saviano, “*Collisional production of sterile neutrinos via secret interactions and cosmological implications,*” *Phys. Rev. D* **91**, no. 2, 025019 (2015) DOI: [10.1103/PhysRevD.91.025019](https://doi.org/10.1103/PhysRevD.91.025019) arXiv:1410.1385 [hep-ph].
- [249] F. Forastieri, M. Lattanzi, G. Mangano, A. Mirizzi, P. Natoli and N. Saviano, “*Cosmic microwave background constraints on secret interactions among sterile neutrinos,*” *JCAP* **1707**, no. 07, 038 (2017) DOI: [10.1088/1475-7516/2017/07/038](https://doi.org/10.1088/1475-7516/2017/07/038) arXiv:1704.00626 [astro-ph.CO].
- [250] X. Chu, B. Dasgupta, M. Dentler, J. Kopp and N. Saviano, “*Sterile Neutrinos with Secret Interactions – Cosmological Discord?,*” *JCAP* **1811**, no. 11, 049 (2018) DOI: [10.1088/1475-7516/2018/11/049](https://doi.org/10.1088/1475-7516/2018/11/049) arXiv:1806.10629 [hep-ph].
- [251] K. C. Y. Ng and J. F. Beacom, “*Cosmic neutrino cascades from secret neutrino interactions,*” *Phys. Rev. D* **90**, no. 6, 065035 (2014) Erratum: [*Phys. Rev. D* **90**, no. 8, 089904 (2014)] DOI: [10.1103/PhysRevD.90.065035](https://doi.org/10.1103/PhysRevD.90.065035), [10.1103/PhysRevD.90.089904](https://doi.org/10.1103/PhysRevD.90.089904) arXiv:1404.2288 [astro-ph.HE].
- [252] K. Ioka and K. Murase, “*IceCube PeVEeV neutrinos and secret interactions*

- of neutrinos*,” PTEP **2014**, no. 6, 061E01 (2014) DOI: [10.1093/ptep/ptu090](https://doi.org/10.1093/ptep/ptu090) arXiv:1404.2279 [astro-ph.HE].
- [253] K. Blum, A. Hook and K. Murase, “*High energy neutrino telescopes as a probe of the neutrino mass mechanism*,” arXiv:1408.3799 [hep-ph].
- [254] T. J. Weiler, “*Resonant Absorption of Cosmic Ray Neutrinos by the Relic Neutrino Background*,” Phys. Rev. Lett. **49**, 234 (1982). DOI: [10.1103/PhysRevLett.49.234](https://doi.org/10.1103/PhysRevLett.49.234)
- [255] J. F. Cherry, A. Friedland and I. M. Shoemaker, “*Short-baseline neutrino oscillations, Planck, and IceCube*,” arXiv:1605.06506 [hep-ph].
- [256] Y. S. Jeong, S. Palomares-Ruiz, M. H. Reno and I. Sarcevic, “*Probing secret interactions of eV-scale sterile neutrinos with the diffuse supernova neutrino background*,” JCAP **1806**, no. 06, 019 (2018) DOI: [10.1088/1475-7516/2018/06/019](https://doi.org/10.1088/1475-7516/2018/06/019) arXiv:1803.04541 [hep-ph].
- [257] A. DiFranzo and D. Hooper, “*Searching for MeV-Scale Gauge Bosons with IceCube*,” Phys. Rev. D **92**, no. 9, 095007 (2015) DOI: [10.1103/PhysRevD.92.095007](https://doi.org/10.1103/PhysRevD.92.095007) arXiv:1507.03015 [hep-ph].
- [258] F. Krau *et al.*, “*TANAMI Blazars in the IceCube PeV Neutrino Fields*,” Astron. Astrophys. **566**, L7 (2014) DOI: [10.1051/0004-6361/201424219](https://doi.org/10.1051/0004-6361/201424219) arXiv:1406.0645 [astro-ph.HE].
- [259] S. Sahu, L. S. Miranda and A. Rosales De Len, “*Blazar origin of some IceCube events*,” PoS NEUTEL **2017**, 079 (2018). DOI: [10.22323/1.307.0079](https://doi.org/10.22323/1.307.0079)
- [260] L. S. Miranda, A. R. de Len and S. Sahu, “*Blazar origin of some IceCube events*,” Eur. Phys. J. C **76**, no. 7, 402 (2016) DOI: [10.1140/epjc/s10052-016-4247-x](https://doi.org/10.1140/epjc/s10052-016-4247-x) arXiv:1510.00048 [astro-ph.HE].
- [261] D. Hooper, T. Linden and A. Viereg, “*Active Galactic Nuclei and the Origin of IceCube’s Diffuse Neutrino Flux*,” JCAP **1902**, 012 (2019) DOI: [10.1088/1475-7516/2019/02/012](https://doi.org/10.1088/1475-7516/2019/02/012) arXiv:1810.02823 [astro-ph.HE].

- [262] S. Das and K. Sigurdson, “*Cosmological Limits on Hidden Sector Dark Matter,*” Phys. Rev. D **85**, 063510 (2012) DOI: [10.1103/PhysRevD.85.063510](https://doi.org/10.1103/PhysRevD.85.063510) arXiv:1012.4458 [astro-ph.CO].
- [263] A. Berlin, D. Hooper and G. Krnjaic, “*PeV-Scale Dark Matter as a Thermal Relic of a Decoupled Sector,*” Phys. Lett. B **760**, 106 (2016) DOI: [10.1016/j.physletb.2016.06.037](https://doi.org/10.1016/j.physletb.2016.06.037) arXiv:1602.08490 [hep-ph].
- [264] K. Sigurdson, “*Hidden Hot Dark Matter as Cold Dark Matter,*” arXiv:0912.2346 [astro-ph.CO].
- [265] S. Hannestad and R. J. Scherrer, “*Selfinteracting warm dark matter,*” Phys. Rev. D **62**, 043522 (2000) DOI: [10.1103/PhysRevD.62.043522](https://doi.org/10.1103/PhysRevD.62.043522) [astro-ph/0003046].
- [266] E. Hardy and J. Unwin, “*Symmetric and Asymmetric Reheating,*” JHEP **1709**, 113 (2017) DOI: [10.1007/JHEP09\(2017\)113](https://doi.org/10.1007/JHEP09(2017)113) arXiv:1703.07642 [hep-ph].
- [267] D. Tucker-Smith and N. Weiner, “*Inelastic dark matter,*” Phys. Rev. D **64**, 043502 (2001) DOI: [10.1103/PhysRevD.64.043502](https://doi.org/10.1103/PhysRevD.64.043502) [hep-ph/0101138].
- [268] D. Tucker-Smith and N. Weiner, “*The Status of inelastic dark matter,*” Phys. Rev. D **72**, 063509 (2005) DOI: [10.1103/PhysRevD.72.063509](https://doi.org/10.1103/PhysRevD.72.063509) [hep-ph/0402065].
- [269] Y. Cui, D. E. Morrissey, D. Poland and L. Randall, “*Candidates for Inelastic Dark Matter,*” JHEP **0905**, 076 (2009) DOI: [10.1088/1126-6708/2009/05/076](https://doi.org/10.1088/1126-6708/2009/05/076) arXiv:0901.0557 [hep-ph].
- [270] D. S. M. Alves, S. R. Behbahani, P. Schuster and J. G. Wacker, “*Composite Inelastic Dark Matter,*” Phys. Lett. B **692**, 323 (2010) DOI: [10.1016/j.physletb.2010.08.006](https://doi.org/10.1016/j.physletb.2010.08.006) arXiv:0903.3945 [hep-ph].
- [271] S. Chang, N. Weiner and I. Yavin, “*Magnetic Inelastic Dark Matter,*” Phys. Rev. D **82**, 125011 (2010) DOI: [10.1103/PhysRevD.82.125011](https://doi.org/10.1103/PhysRevD.82.125011) arXiv:1007.4200 [hep-ph].

- [272] K. R. Dienes, J. Kumar, B. Thomas and D. Yaylali, “*Off-Diagonal Dark-Matter Phenomenology: Exploring Enhanced Complementarity Relations in Non-Minimal Dark Sectors,*” Phys. Rev. D **96**, no. 11, 115009 (2017) DOI: [10.1103/PhysRevD.96.115009](https://doi.org/10.1103/PhysRevD.96.115009) arXiv:1708.09698 [hep-ph].
- [273] L. Feng, J. F. Zhang and X. Zhang, “*Searching for sterile neutrinos in dynamical dark energy cosmologies,*” Sci. China Phys. Mech. Astron. **61**, no. 5, 050411 (2018) DOI: [10.1007/s11433-017-9150-3](https://doi.org/10.1007/s11433-017-9150-3) arXiv:1706.06913 [astro-ph.CO].
- [274] K. Griest and D. Seckel, “*Three exceptions in the calculation of relic abundances,*” Phys. Rev. D **43**, 3191 (1991). DOI: [10.1103/PhysRevD.43.3191](https://doi.org/10.1103/PhysRevD.43.3191)
- [275] J. Edsjo and P. Gondolo, “*Neutralino relic density including coannihilations,*” Phys. Rev. D **56**, 1879 (1997) DOI: [10.1103/PhysRevD.56.1879](https://doi.org/10.1103/PhysRevD.56.1879) [hep-ph/9704361].
- [276] R. T. D’Agnolo and J. T. Ruderman, “*Light Dark Matter from Forbidden Channels,*” Phys. Rev. Lett. **115**, no. 6, 061301 (2015) DOI: [10.1103/PhysRevLett.115.061301](https://doi.org/10.1103/PhysRevLett.115.061301) arXiv:1505.07107 [hep-ph].
- [277] R. T. D’Agnolo, D. Pappadopulo and J. T. Ruderman, “*Fourth Exception in the Calculation of Relic Abundances,*” Phys. Rev. Lett. **119**, no. 6, 061102 (2017) DOI: [10.1103/PhysRevLett.119.061102](https://doi.org/10.1103/PhysRevLett.119.061102) arXiv:1705.08450 [hep-ph].
- [278] M. Blennow, S. Clementz and J. Herrero-Garcia, “*Self-interacting inelastic dark matter: A viable solution to the small scale structure problems,*” JCAP **1703**, no. 03, 048 (2017) DOI: [10.1088/1475-7516/2017/03/048](https://doi.org/10.1088/1475-7516/2017/03/048) arXiv:1612.06681 [hep-ph].
- [279] K. Schutz and T. R. Slatyer, “*Self-Scattering for Dark Matter with an Excited State,*” JCAP **1501**, no. 01, 021 (2015) DOI: [10.1088/1475-7516/2015/01/021](https://doi.org/10.1088/1475-7516/2015/01/021) arXiv:1409.2867 [hep-ph].
- [280] C. Yche, N. Palanque-Delabrouille, J. Baur and H. du Mas des Bourboux, “*Constraints on neutrino masses from Lyman-alpha forest power spectrum with*

---

*BOSS and XQ-100*,” JCAP **1706**, no. 06, 047 (2017) DOI: [10.1088/1475-7516/2017/06/047](https://doi.org/10.1088/1475-7516/2017/06/047) arXiv:1702.03314 [astro-ph.CO].



# List of Publications

## Thesis related Publications

1. **Bhavesh Chauhan**, Bharti Kindra, and Ashish Narang  
*Discrepancies in simultaneous explanation of flavor anomalies and IceCube PeV events using leptoquarks*  
Phys. Rev. D **97**, 095007 (2018). arXiv:1706.04598
2. **Bhavesh Chauhan** and Subhendra Mohanty  
*Leptoquark resolution to both flavor and ANITA anomalies*  
Phys. Rev. D **99** (2019), 095018, arXiv:1812.00919 [hep-ph]
3. **Bhavesh Chauhan** and Subhendra Mohanty  
*Signature of light sterile neutrino at IceCube*  
Phys. Rev. D **98** (2018), 083021, arXiv:1808.04774 [hep-ph]
4. **Bhavesh Chauhan**  
*Sub-MeV self interacting dark matter*  
Phys. Rev. D **97**, 123017 (2018), arXiv:1711.02970 [hep-ph]

## Other Publications

5. **Bhavesh Chauhan** and Subhendra Mohanty  
*Constraints on leptophilic light dark matter from internal heat flux of Earth*  
Phys. Rev. D **94** (2016), 035024, arXiv:1603.06350 [hep-ph]
6. **Bhavesh Chauhan** and Bharti Kindra  
*Invoking chiral vector leptoquark to explain LFU violation in B Decays*  
arXiv:1709.09989 [hep-ph] (under revision)

7. **Bhavesh Chauhan** and Subhendra Mohanty

*Constraints on leptophilic light dark matter from internal heat flux of Earth*

Springer Proc . Phys . **203** (2018) , 501-503.

# Publications attached with thesis

1. **Bhavesh Chauhan**, Bharti Kindra, and Ashish Narang

*Discrepancies in simultaneous explanation of flavor anomalies and IceCube PeV events using leptoquarks*

Phys. Rev. D **97**, 095007 (2018). arXiv:1706.04598 [hep-ph]

DOI: [10.1103/PhysRevD.97.095007](https://doi.org/10.1103/PhysRevD.97.095007)

2. **Bhavesh Chauhan** and Subhendra Mohanty

*Leptoquark resolution to both flavor and ANITA anomalies*

Phys. Rev. D **99** (2019), 095018, arXiv:1812.00919 [hep-ph]

DOI: [10.1103/PhysRevD.99.095018](https://doi.org/10.1103/PhysRevD.99.095018)

3. **Bhavesh Chauhan** and Subhendra Mohanty

*Signature of light sterile neutrino at IceCube*

Phys. Rev. D **98** (2018), 083021, arXiv:1808.04774 [hep-ph]

DOI: [10.1103/PhysRevD.98.083021](https://doi.org/10.1103/PhysRevD.98.083021)

4. **Bhavesh Chauhan**

*Sub-MeV self interacting dark matter*

Phys. Rev. D **97**, 123017 (2018), arXiv:1706.04598 [hep-ph]

DOI: [10.1103/PhysRevD.97.123017](https://doi.org/10.1103/PhysRevD.97.123017)



## Discrepancies in simultaneous explanation of flavor anomalies and IceCube PeV events using leptoquarks

Bhavesh Chauhan,<sup>1,2,\*</sup> Bharti Kindra,<sup>1,2,†</sup> and Ashish Narang<sup>1,2,‡</sup>

<sup>1</sup>Physical Research Laboratory, Ahmedabad, India

<sup>2</sup>Indian Institute of Technology, Gandhinagar, India



(Received 4 July 2017; revised manuscript received 14 February 2018; published 7 May 2018)

Leptoquarks have been suggested to solve a variety of discrepancies between the expected and observed phenomenon. In this paper, we show that the scalar doublet leptoquark with hypercharge  $7/6$  can simultaneously explain the recent measurement of  $R_K$ ,  $R_{K^*}$ , the excess in anomalous magnetic moment of muon, and the observed excess in IceCube high energy starting events data. For an appropriate choice of couplings, the flavor anomalies are generated at one-loop level and IceCube data is explained via resonant production of the leptoquark. Several constraints from LHC searches are imposed on the model parameter space.

DOI: [10.1103/PhysRevD.97.095007](https://doi.org/10.1103/PhysRevD.97.095007)

### I. INTRODUCTION

Leptoquarks are the solution to the problem of matter unification which appear naturally in many theories beyond the Standard Model (SM). For example, scalar quarks in R-Parity Violating Supersymmetry (RPV) have leptoquark-like Yukawa couplings [1] whereas vector leptoquarks arise in Grand Unification Theories (GUT) based on  $SU(5)$  and  $SO(10)$  [2–4]. The unique feature of leptoquarks is that they couple simultaneously to SM quarks and leptons, thus providing ample testing grounds and applications to variety of discrepancies between theory and experiments.

The latest measurement of  $R_{K^*}$  and  $R_K$  by LHCb, has pointed towards  $\approx 2.5\sigma$  deviation from the standard model [5,6]. These are clear hints of Lepton Flavor Universality (LFU) violation which can be explained in a wide variety of frameworks including, but not limited to, leptoquarks [7–12], RPV [13–16], E6 [17], flavor violating  $Z'$  [18–30], etc. In the past, leptoquarks have been used to explain the anomalous magnetic moment of muon [31–36], flavor anomalies [7–12], and IceCube PeV events [37–43] independently. However, simultaneous explanation of all the three observations has not been possible due to the different range of leptoquark masses required to solve the individual problems. In this work, we show that a scalar leptoquark of

mass close to 1 TeV can explain the aforementioned discrepancies. However, such an explanation would be extremely disfavored by LHC data. While the particular results are model dependent, one can make qualitative predictions about a more general model.

In Sec. II we describe the model of leptoquark and motivate the texture of the coupling matrices that has been used in this paper. In Sec. III we explain the excess in  $(g-2)_\mu$  using this model. In Sec. IV we explain the recent measurement of  $R_K$  and  $R_{K^*}$  within our framework, followed by the explanation for IceCube High Energy Starting Events (HESE) in Sec. V. In Sec. VI we discuss the results of this analysis and obtain the parameter space for simultaneous explanation. In the next section, we do the LHC analysis for the benchmark point and obtain the constraints. In the end, we conclude with some model-dependent and model-independent statements.

### II. MODEL DESCRIPTION

In this paper, we consider the scalar leptoquark  $\Delta = (3, 2, 7/6)$  whose interactions with the SM fields is given as [44]

$$\mathcal{L}_\Delta \ni -(y_L)_{ij} \bar{u}_R^i \Delta_a \varepsilon^{ab} (L_L)_b^j + (y_R)_{ij} \bar{Q}_L^{ia} \Delta_a l_R^j + \text{H.c.}, \quad (1)$$

where  $y_{L(R)}$  are the Yukawa-like couplings of the leptoquark. For simplicity, we have assumed the couplings to be real. We have not shown the kinetic and Higgs interactions for brevity; however, they are relevant for the discussion that follows. We refer the reader to Ref. [44] for a comprehensive analysis. We can rewrite (1) in terms of the mass eigenstates  $\Delta^{5/3}$  and  $\Delta^{2/3}$ , where the superscript denotes electric charge. In terms of these states, the Lagrangian (1) is written as

\*bhavesh@prl.res.in

†bharti@prl.res.in

‡ashish@prl.res.in

Published by the American Physical Society under the terms of the Creative Commons Attribution 4.0 International license. Further distribution of this work must maintain attribution to the author(s) and the published article's title, journal citation, and DOI. Funded by SCOAP<sup>3</sup>.

$$\mathcal{L}_\Delta \ni (Vy_R)_{ij}\bar{u}_i P_R l_j \Delta^{5/3} - (y_L)_{ij}\bar{u}_i P_L l_j \Delta^{5/3} \quad (2)$$

$$+ (y_R)_{ij}\bar{d}_i P_R l_j \Delta^{2/3} + (y_L U)_{ij}\bar{u}_i P_L \nu_j \Delta^{2/3} + \text{H.c.}, \quad (3)$$

where  $V$  and  $U$  are the Cabibbo-Kabayashi-Masakawa matrix and Pontecorvo-Maki-Nakagawa-Sakata matrix, respectively. In common literature [44], this model is also known as  $\mathbf{R}_2$ .

The observed negligible branching ratios of the flavor violating decays of leptons (for example,  $\tau \rightarrow \mu\gamma$  and  $\mu \rightarrow e\gamma$ ) put stringent constraints on the intergeneration couplings of the leptoquark. For all practical purposes, this implies that

$$y_{L(R)}^{qe} = y_{L(R)}^{q\tau} = 0 \quad \forall q. \quad (4)$$

It has been argued in previous works that this leptoquark model results in  $R_K \approx 1$ , and  $R_{K^*} \approx 1$  because of the tree level contribution to  $b \rightarrow s\mu\mu$  [10]. This clearly contradicts the recent measurements by LHCb. It was pointed out in [9] that, if one assumes

$$y_R^{s\mu} = 0 \quad \text{or} \quad y_R^{b\mu} = 0, \quad (5)$$

then the tree level contribution is negligible and the leading contribution comes from a one-loop process. It will be shown in Sec. IV that this results in  $R_K < 1$ , and  $R_{K^*} < 1$  which is in agreement with the latest experiments. We chose the former solution as it is also favored by  $(g-2)_\mu$ . As mentioned in [9], nonzero  $y_L^{c\mu}$  results in tree level contribution to  $b \rightarrow cl\bar{\nu}_l$  which contradicts the observed  $R(D)$  and  $R(D^*)$ . Hence, we also assume that

$$y_L^{c\mu} = 0. \quad (6)$$

In order to avoid undesired contribution to other rare decays of the B meson, such as  $b \rightarrow dl^+l^-$ , we assume that

$$y_R^{d\mu} \approx 0. \quad (7)$$

With these constraints, the coupling matrices are

$$y_L = \begin{pmatrix} 0 & y_L^{u\mu} & 0 \\ 0 & 0 & 0 \\ 0 & y_L^{t\mu} & 0 \end{pmatrix}, \quad y_R = \begin{pmatrix} 0 & 0 & 0 \\ 0 & 0 & 0 \\ 0 & y_R^{b\mu} & 0 \end{pmatrix}. \quad (8)$$

For brevity, we will use  $y_L^{u\mu} = \lambda_1$ ,  $y_L^{t\mu} = \lambda_2$ , and  $y_R^{b\mu} = \lambda_3$  for the remainder of this paper. We will also use  $M_1$  ( $M_2$ ) to denote the mass of  $\Delta^{5/3}$  ( $\Delta^{2/3}$ ).

In subsequent sections, it will be pointed out that the LHC constraints limit  $M_1 \geq 1100$  GeV. For our analysis, we take the lower limit and generate constraints on the remaining parameters. If future searches increase the lower limit considerably, the expressions will change accordingly. Having said that, there are only four free parameters in our model

$$\{M_2, \lambda_1, \lambda_2, \lambda_3\}. \quad (9)$$

In the subsequent sections, we investigate various constraints on the model parameters coming from  $(g-2)_\mu$ , flavor anomalies, IceCube data, and LHC.

### III. $(g-2)_\mu$

The experimentally measured value of the anomalous magnetic moment of muon is slightly larger than the prediction from the Standard Model. This discrepancy has been attributed to a variety of new physics scenarios [31–33,45,46]. At present, the difference is [47]

$$\delta a_\mu = a_\mu^{\text{EXP}} - a_\mu^{\text{SM}} = (2.8 \pm 0.9) \times 10^{-9}. \quad (10)$$

In this model, both of the mass eigenstates contribute to  $(g-2)_\mu$  and one can estimate the contribution using expressions given in [44]. Keeping  $M_1 = 1100$  GeV, the leptoquark contribution to  $(g-2)_\mu$  is given as

$$\begin{aligned} a_\mu^\Delta &= 1.34 \times 10^{-6} \lambda_2 \lambda_3 \\ &- \frac{10^{-9}}{(M_2/\text{GeV})^2} (6.11\lambda_1^2 + 5.53\lambda_2^2 - 9.4 \times 10^4 \lambda_2 \lambda_3 \\ &+ 5.53\lambda_3^2) + \dots \end{aligned} \quad (11)$$

$$\approx 1.34 \times 10^{-6} \lambda_2 \lambda_3$$

$$- 10^{-11} (8.65\lambda_1^2 + 7.83\lambda_2^2 + 7.83\lambda_3^2) + \mathcal{O}(10^{-13}), \quad (12)$$

where the approximation is obtained using the benchmark point  $M_2 = 1000$  GeV. From the above expressions one can see that the leading contribution does not depend on  $M_2$ . It is also clear that the product  $\lambda_2 \lambda_3 \approx 10^{-3}$  gives the correct estimate for  $(g-2)_\mu$ . In Sec. VI we use  $a_\mu^\Delta = \delta a_\mu$  to constrain the parameter space of the model.

### IV. FLAVOR ANOMALIES

In the last two decades, loop-induced  $b \rightarrow s$  transitions have been playing an active role in understanding the physics beyond the Standard Model. Starting from the first observation of  $B \rightarrow K^* \gamma$ , many decays involving  $b \rightarrow s$  transitions have been observed. Two of the key observables for LFU violating decays of the B meson are  $R_K$  and  $R_{K^*}$ , defined as

$$R_{K^{(*)}} = \frac{\mathcal{BR}(B \rightarrow K^{(*)} \mu\mu)_{q^2 \in [q_1^2, q_2^2]}}{\mathcal{BR}(B \rightarrow K^{(*)} ee)_{q^2 \in [q_1^2, q_2^2]}}. \quad (13)$$

It was shown in [48] that, within the SM, the hadronic uncertainties in these expressions cancel, which results in  $R_K, R_{K^*} \approx 1$ . However recent measurement of  $R_{K^*}$  by LHCb has reported 2.1–2.3 $\sigma$  and 2.3–2.5 $\sigma$  deviations in

the low- $q^2$  (0.045–1.1 GeV<sup>2</sup>) and central- $q^2$  (1.1–6 GeV<sup>2</sup>) regions, respectively [6]. A deviation of 2.6 $\sigma$  from SM has also been reported in  $R_K$  [5]. We use the standard prescription of effective Hamiltonian to evaluate the contribution of the leptoquark to  $R_K$  and  $R_{K^*}$ .

The most general effective Hamiltonian for  $b \rightarrow sl^-l^+$  is given as

$$\mathcal{H}_{\text{eff}} = -\frac{4G_f}{\sqrt{2}} V_{tb} V_{ts}^* \left[ \sum_{i=1}^6 C_i \mathcal{O}_i + \sum_{i=7}^{T5} (C_i \mathcal{O}_i + C'_i \mathcal{O}'_i) \right], \quad (14)$$

where  $\mathcal{O}_i$  are the operators and  $C_i$  are the Wilson Coefficients (WCs) which can be written as

$$C_i = C_i^{\text{SM}} + \delta C_i, \quad (15)$$

where  $\delta C_i$  represent the shifts due to new physics. Global analyses have been performed to fit  $\delta C_i$  to the experimental results which yield interesting correlations between various WCs [49,50]. The operators relevant for the model are

$$\begin{aligned} \mathcal{O}_9 &= \frac{e^2}{(4\pi)^2} (\bar{s} \gamma_\mu P_L b) (\bar{\mu} \gamma^\mu \mu), \quad \text{and} \\ \mathcal{O}_{10} &= \frac{e^2}{(4\pi)^2} (\bar{s} \gamma_\mu P_L b) (\bar{\mu} \gamma^\mu \gamma_5 \mu). \end{aligned} \quad (16)$$

$$A_2 = - \sum_{u, u' \in c, t} (V_{YR})_{u\mu}^* (V_{YR})_{u'\mu} \frac{1}{16\pi\alpha_{em}} \frac{V_{ub} V_{u's}^*}{V_{tb} V_{ts}^*} \mathcal{F}_2(x_u, x_{u'}), \quad (19)$$

$$\mathcal{F}_1(x_u, x_{u'}) = \frac{\sqrt{x_u x_{u'}}}{4} \left[ \frac{x_{u'}(x_{u'} - 4) \log x_{u'}}{(x_{u'} - 1)(x_u - x_{u'})(x_{u'} - x_\Delta)} + \frac{x_u(x_u - 4) \log x_u}{(x_u - 1)(x_{u'} - x_u)(x_u - x_\Delta)} - \frac{x_\Delta(x_\Delta - 4) \log x_\Delta}{(x_\Delta - 1)(x_\Delta - x_{u'})(x_\Delta - x_u)} \right], \quad (20)$$

$$\mathcal{F}_2(x_u, x_{u'}) = \frac{x_u^2 \log x_u}{(x_u - x_{u'})(x_u - x_\Delta)} + \frac{x_\Delta(x_u + x_{u'} - x_u x_{u'}) \log x_\Delta}{(x_u - x_\Delta)(x_\Delta - x_{u'})} + \left[ \frac{x_u^2 - 1}{(x_u - x_\Delta)(x_u - x_{u'})} + \frac{x_{u'}^2}{(x_{u'} - x_\Delta)(x_{u'} - x_u)} \right] \log x_{u'}. \quad (21)$$

The contribution of up-quark is CKM suppressed. We have used *Package-X* [52] and the unitary gauge to evaluate the loop-functions  $\mathcal{F}_1$  and  $\mathcal{F}_2$ .

To evaluate  $R_K$  and  $R_{K^*}$  from the WCs, we use the simplified expressions from [53] and obtain

$$R_K = 1. + 0.49A_1 + 0.06A_1^2 - 0.01A_2 + 0.06A_2^2 \quad (22)$$

$$R_{K^*} = 1. + 0.47A_1 + 0.07A_1^2 - 0.14A_2 + 0.07A_2^2. \quad (23)$$

Immediately one can observe that the solution  $-1 < A_1 < 0$  and  $A_2 = 0$  is consistent with the latest results. This was also the conclusion in [9].

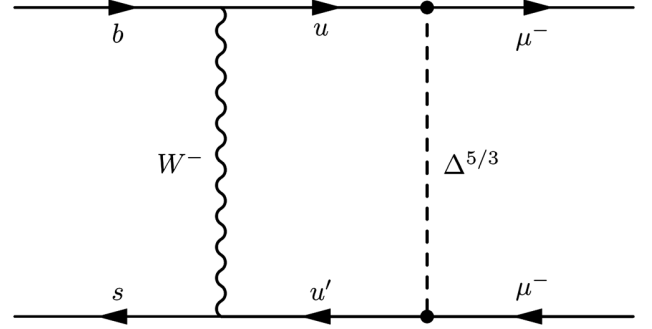


FIG. 1. The box diagram contributing to  $b \rightarrow s\mu^-\mu^+$ .

The expressions for all other operators can be found in [51]. As usual, the doubly CKM suppressed contributions from  $V_{ub} V_{us}^*$  have been neglected.

For the model in consideration, the leptoquark contributes to  $b \rightarrow s\mu^+\mu^-$  at one-loop level (Fig. 1) and results in nonzero  $\delta C_9$  and  $\delta C_{10}$  only. Using  $x_i = (m_i/m_W)^2$ , we can write

$$\delta C_9 = A_1 + A_2 \quad \text{and} \quad \delta C_{10} = -A_1 + A_2, \quad (17)$$

where,

$$A_1 = \frac{|\lambda_2|^2}{8\pi\alpha_{em}} \mathcal{F}_1(x_t, x_t), \quad (18)$$

Recent measurement  $B_s \rightarrow \mu^-\mu^+$  by LHCb is in close agreement with the SM and provides a constraint on the model [54]. In the operator basis (14), the branching ratio of  $B_s \rightarrow \mu^-\mu^+$  can be written as [55]

$$\begin{aligned} \mathcal{BR}(B_s \rightarrow \mu^-\mu^+) &= \frac{\tau_{B_s} \alpha^2 G_F^2}{16\pi^3} f_{B_s}^2 |V_{tb} V_{ts}^*|^2 m_{B_s}^6 m_\mu^2 \left( 1 - \frac{2m_\mu^2}{m_{B_s}^2} \right) |\mathcal{C}_{10}|^2. \end{aligned} \quad (24)$$

In general, this process gets contributions from  $C'_{10}$ ,  $C_S^{(\prime)}$  and  $C_P^{(\prime)}$  as well. However, we are ignoring them as these WCs are zero in the SM as well as the model under

consideration. In the SM,  $\mathcal{B}(B_s \rightarrow \mu^+ \mu^-)$  is  $(3.65 \pm 0.23) \times 10^{-9}$  [56] while LHCb has measured it to be  $2.8_{-0.6}^{+0.7} \times 10^{-9}$  [54]. For the model considered in this paper, (24) is

$$\begin{aligned} \mathcal{BR}(B_s \rightarrow \mu^- \mu^+) \\ = 10^{-9}(3.4 + 1.65(A_1 - A_2) + 0.2(A_1 - A_2)^2), \end{aligned} \quad (25)$$

using parameters given in [55]. Again, one can see that the solution  $-1 < A_1 < 0$  and  $A_2 = 0$  is consistent with the experiments. With these expressions, one can write the observables in terms of the couplings as,

$$\begin{aligned} R_K = 1. - (5.16 \times 10^{-2})\lambda_2^2 + (6.66 \times 10^{-4})\lambda_2^4 \\ - (1.66 \times 10^{-5})\lambda_3^2 + (1.59 \times 10^{-7})\lambda_3^4 \end{aligned} \quad (26)$$

$$\begin{aligned} R_{K^*} = 1. - (4.96 \times 10^{-2})\lambda_2^2 + (8.18 \times 10^{-4})\lambda_2^4 \\ - (2.34 \times 10^{-4})\lambda_3^2 + (1.96 \times 10^{-7})\lambda_3^4 \end{aligned} \quad (27)$$

$$\begin{aligned} \mathcal{BR}(B_s \rightarrow \mu^- \mu^+) \\ = 2.01 \times 10^{-10} |4.1 - 0.10\lambda_2^2 - 1.6 \times 10^{-3}\lambda_3^2|^2. \end{aligned} \quad (28)$$

In passing, one can note that these expressions do not explicitly depend on  $\lambda_1$ . This is due to the fact that the term proportional to  $\lambda_1$  will enter the expression due to u-quark in the loop which is CKM suppressed. Henceforth, the term ‘‘flavor anomalies’’ will be used to refer to  $R_K$  and  $R_{K^*}$  with imposed constraints from  $\mathcal{BR}(B_s \rightarrow \mu^- \mu^+)$ .

## V. ICECUBE PEV EVENTS

During the first four years of its operation, the IceCube neutrino observatory at the South pole has observed more numbers of PeV events than expected. This has resulted in a lot of interesting studies in various fields [57–59]. Resonant production of leptoquark by interactions of astrophysical neutrinos with partons has been proposed as a possible explanation of the excess in PeV events at IceCube [38–43]. In the model considered in this paper, the following neutrino interactions are possible:

Neutral Current (NC) Like:  $\bar{\nu}_i u \xrightarrow{\Delta^{2/3}} \bar{\nu}_j u$ ;  $\bar{\nu}_j t$   $i, j = e, \mu, \tau$

Charged Current (CC) Like:  $\bar{\nu}_i u \xrightarrow{\Delta^{2/3}} \mu d$ ;  $\mu b$   $i = e, \mu, \tau$ .

It is important to distinguish between the CC and NC interactions due to the difference in their deposited energy signatures [60,61]. Ideally speaking, one should also distinguish between shower and track events as the observed PeV events are only shower type. However, one can attribute this to the smallness of statistics and hence we do not consider this difference.

The number of events due to leptoquark contribution in the deposited energy interval  $(E_i, E_f)$  is [41,60]

$$\mathcal{N} = TN_A \int_0^1 dy \int_{E_i^{ch}(E_i, y)}^{E_f^{ch}(E_f, y)} dE_\nu \mathcal{V}_{\text{eff}}(E_{dep}^{ch}) \Omega(E_\nu) \frac{d\phi}{dE_\nu} \frac{d\sigma^{ch}}{dy}, \quad (29)$$

where  $T = 1347$  days is the total exposure time,  $N_A = 6.023 \times 10^{23} \text{ cm}^{-3}$  water equivalent is the Avogadro’s Number, and  $ch$  denotes the interaction channel (NC or CC). Other terms in the expression are discussed in [60]. For each neutrino or antineutrino flavor, an isotropic, power-law flux parametrized as

$$\frac{d\Phi}{dE_\nu} = \phi_0 \left( \frac{E_\nu}{100 \text{ TeV}} \right)^\gamma \quad (30)$$

is assumed. The best fit values from IceCube [62],

$$\phi_0 = (2.2 \pm 0.7) \times 10^{-8} \text{ GeV}^{-1} \text{ s}^{-1} \text{ sr}^{-1} \text{ cm}^{-2} \quad (31)$$

$$\gamma = -2.58 \pm 0.25, \quad (32)$$

are obtained using likelihood analysis of the data from 10 TeV–10 PeV. We use the central values in our analysis.

It is evident from the structure of coupling matrices (8) that the model only admits interactions between incoming antineutrino (neutrino) with u- and t- (anti-u- and anti-t-) quarks. It is seen that the Parton Distribution Function (PDF) of t-quark is negligible as compared to that of u-quark. Hence, we only consider interaction with u-quark in our analysis. The differential cross section for this process is given as [41]

$$\frac{d\sigma^{\text{NC/CC}}}{dy} = \frac{\pi \Lambda_{\text{NC/CC}}^4 \mathcal{U}(M_\Delta^2/s, yM_\Delta^2)}{2 |\Lambda^2| s}, \quad (33)$$

where  $s = 2M_N E_\nu$ , and  $\mathcal{U}(x, Q^2)$  is the PDF of u-quark in an isoscalar proton evaluated at energy  $Q^2$ . In terms of the *valence* and *sea* quark distributions, one can write [38]

$$\mathcal{U} = \frac{u_{v+s} + d_{v+s}}{2}. \quad (34)$$

We have used the Mathematica package MSTW [63] to obtain these PDFs.

The dependence of event rate on couplings is captured by

$$\Lambda_{\text{NC}}^4 = \lambda_1^2 (\lambda_1^2 + \lambda_2^2) \quad (35)$$

$$\Lambda_{\text{CC}}^4 = \lambda_1^2 (\lambda_3^2) \quad (36)$$

$$\Lambda^2 = \lambda_1^2 + \lambda_2^2 + \lambda_3^2. \quad (37)$$

Given the mass of the leptoquark ( $M_2$ ) and the couplings, we are now in a position to estimate the contribution of leptoquark to the IceCube HESE events. We use the standard  $\chi^2$  analysis to estimate the couplings that provide

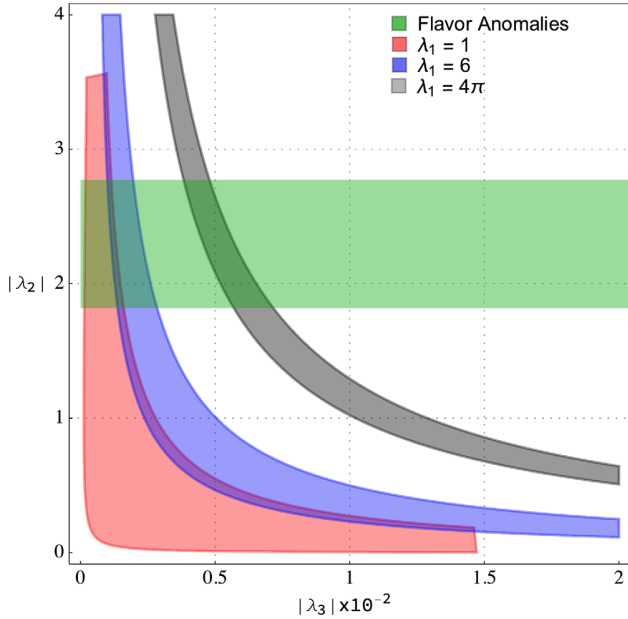


FIG. 2. The parameter space of  $(g-2)_\mu$  various choice of coupling  $\lambda_1$  is shown along with the constraints from flavor anomalies for  $M_1 = 1100$  GeV and  $M_2 = 1000$  GeV.

the best fit to the data. In order to estimate whether adding leptoquark contribution results in a better or worse fit to data, we use the statistic

$$\delta(\lambda_i^2, M_{LQ}) = 100 \times \frac{\chi_{SM}^2 - \chi_{SM+LQ}^2}{\chi_{SM}^2}, \quad (38)$$

which represents the percentage change in  $\chi^2$ . We only use the data for which nonzero numbers of events are observed at IceCube.

## VI. A SIMULTANEOUS EXPLANATION

In this model, we have four free parameters as was pointed out before. However, the leptoquarks state  $\Delta^{2/3}$  does not feature in any explanation of the flavor anomalies and hence these do not depend on  $M_2$ . It is also seen that for  $M_2 \in (600-1400)$  GeV, the dependence of  $(g-2)_\mu$  on  $M_2$  is very weak. Hence, the flavor anomalies and  $(g-2)_\mu$  effectively depend only on the three free couplings in the model. In Fig. 2, we have shown the parameter space that explains the flavor anomalies a  $(g-2)_\mu$  for  $M_1 = 1100$  GeV and  $M_2 = 1000$  GeV.

It can be seen from Fig. 2 that the resolution to flavor anomalies requires  $\lambda_2 \sim \mathcal{O}(1)$ , whereas  $(g-2)_\mu$  constrains  $\lambda_3 \sim \mathcal{O}(10^{-3})$  for  $\lambda_1 < 6$ . Using this, and Eqs. (32)–(36), one sees that the number of events at IceCube only depends on the coupling  $\lambda_1$ . Since  $\Delta^{5/3}$  does not feature in the explanation for IceCube, these predictions are independent of  $M_1$  and only depend on  $M_2$ . In Fig. 3, we show the

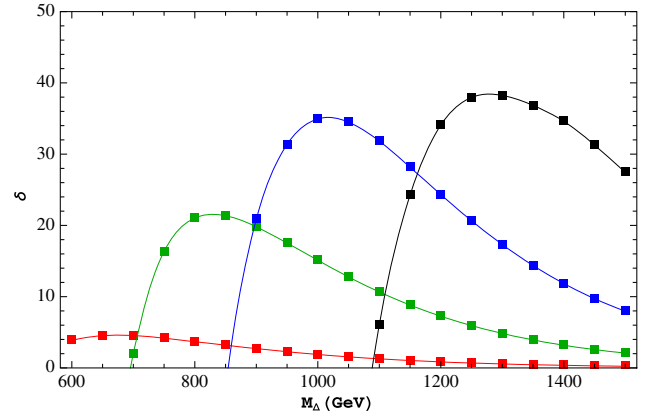


FIG. 3. The variation of  $\delta$  with  $M_2$  for various choice of coupling  $\lambda_1$  is shown. The red, green, blue, and black lines correspond to  $\lambda_1 = 1, 3, 6$ , and  $4\pi$ , respectively.

variation of the statistic  $\delta$  with  $M_2$  for various choice of coupling  $\lambda_1$ . It can be seen that a leptoquark of mass 800–1400 GeV can give 20–35% improvement to the fit. In Fig. 4, we show the contribution of leptoquark for the benchmark point  $M_{LQ} = 1$  TeV,  $\lambda_1 \approx 6$ . which gives  $\delta \approx 35$ .

It is evident that for the aforementioned choices of leptoquark parameters, one can satisfactorily explain the observed excess in the IceCube HESE Data. However, such an explanation requires large couplings and TeV scale leptoquarks. Such a scenario should be testable at LHC and is the subject of study in the next section.

## VII. LHC CONSTRAINTS

Since leptoquarks carry color charge, they can be singly or pair produced in pp collisions. Subsequent decays of these leptoquarks in the detector will give rise to jets, leptons, and neutrinos. This gives very interesting final states of the form  $jjll$ ,  $jjl\nu$ ,  $jl\nu$ ,  $jj\nu$ ,  $j\nu\nu$ , etc. and has been

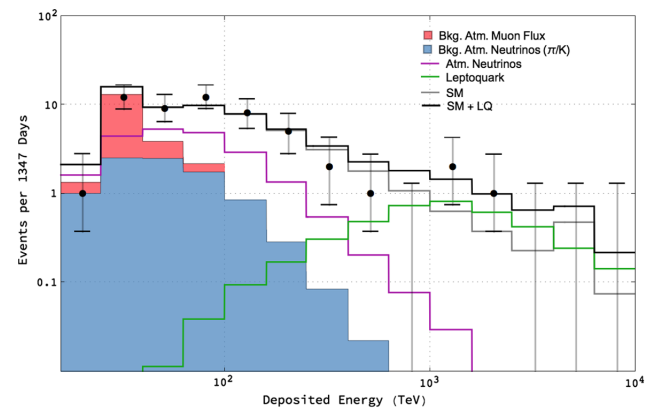


FIG. 4. The solid black line shows the prediction for IceCube using leptoquark and SM interactions.

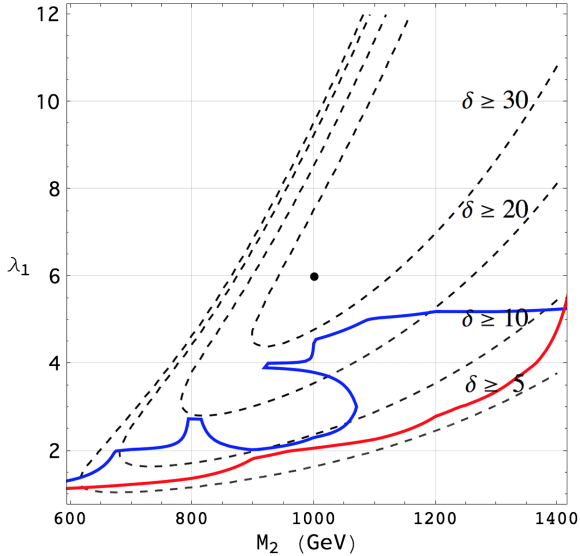


FIG. 5. The Dijet constraints are shown in blue and the Monojet constraints are shown in red. The parameter space above the curves is ruled out. The contours of  $\delta$  are shown and the benchmark point used to generate Fig. 4 is shown.

the subject of various studies [64–74]. As these neutrinos are not seen by the detector, they appear as a Missing Transverse Energy (MET). For the LHC analysis, we have implemented the model using FEYNRULES (v2) [75] and simulate the above processes using MADGRAPH (v5) [76] which uses PYTHIA (v8) [77] for parton showering. We then use CHECKMATE (v2) [78] to find the value of statistical parameter,  $r$ , defined as

$$r = \frac{(S - 1.96\Delta S)}{S_{\text{exp}}^{0.95}}, \quad (39)$$

for several points in the parameter space. Here,  $S$  and  $\Delta S$  represents signal and its uncertainty. The numerator represents 95% confidence limits on the number of events obtained using CHECKMATE and the denominator represents 95% experimental limits on the number of events. The approximate functional form is obtained using linear interpolation. Parameter space with  $r \geq 1$  is excluded and the results are summarized in Fig. 5.

*Constraints from jjll:* When the leptoquarks are pair produced in pp collisions, each leptoquark can decay into a charged lepton and a quark. Recently, ATLAS Collaboration performed a search for a new physics signature of lepton-jet resonances based on  $\sqrt{s} = 13$  TeV data [79], wherein pair production of leptoquarks was studied based on events like  $eejj$  and  $\mu\mu jj$ . The analysis gives an upper limit on the branching ratio of first and second generation leptoquark to  $ej$  and  $\mu j$ , respectively. Although, our model has intergeneration

couplings, we use these limits to constrain the free parameters in our model. We find that

$$\mathcal{BR}(\Delta^{5/3} \rightarrow \mu j) \approx 1 \quad (40)$$

as it couples to only the second generation of leptons. This puts a lower limit on the mass of leptoquark, as

$$M_1 \geq 1100 \text{ TeV}.$$

We use the lower limit to generate other constraints and for flavor analysis. For the  $\Delta^{2/3}$  state,

$$\mathcal{BR}(\Delta^{2/3} \rightarrow \mu j) \propto \lambda_4^2 \approx 0, \quad (41)$$

which does not provide any constraints from this analysis.

*Constraints from jj $\nu\nu$ :* When the leptoquark state  $\Delta^{2/3}$  is pair produced, each can decay into a neutrino and a quark giving rise to a peculiar Dijet + MET signature. The parameters  $M_1$  and  $\lambda_2$  are fixed from flavor observables and this process only depends on  $M_2$  and  $\lambda_1$ . We use the 13 TeV ATLAS search [80] to find constraints on this parameter space.

*Constraints from j $\nu\nu$ :* If the leptoquark  $\Delta^{2/3}$  is singly produced, it can decay into a quark and a neutrino giving rise to Monojet signal at the LHC. Again, this process only depends on the parameters  $M_2$  and  $\lambda_1$ . We use the 8 TeV ATLAS search [81] to find constraints on this parameter space.

*Other Constraints:* We find that the Monojet constraints are strong enough to rule out the entire parameter space that explains IceCube PeV events and we do not provide results for other processes. However, in passing, we note that the constraints from  $j\nu$  final state are much stronger. This maybe relevant for future tests of leptoquark models.

## VIII. CONCLUSION

The discrepancy in the anomalous magnetic moment of muon, the observed excess in PeV events at IceCube, and the lepton flavor universality violation in B decays are some of the biggest challenges facing the Standard Model. A simultaneous explanation for these problems is desirable. An *ad hoc* solution such as leptoquarks, if it can successfully address these issues, will shed more light on the unification scenarios that contain them. One such attempt was made in this paper using a scalar doublet leptoquark. The peculiar feature of this model is that the flavor anomalies are explained at one-loop level. Because of the loop suppression, one does not require either very small couplings or very heavy leptoquarks. We find that one can explain the B-anomalies  $R_K$  and  $R_{K^*}$  with  $\mathcal{O}(1)$  coupling and TeV scale leptoquark. In the past, similar parameters have been invoked to explain IceCube events and a unified explanation seemed possible. However, we find that in order to explain IceCube data, one *needs* leptoquark coupling to first generation quarks and neutrinos. This coupling will give rise to Monojet and Dijet signals at LHC, both of which are

severely constrained. Because of this, any attempt to explain IceCube events using such leptoquarks would be in conflict with LHC data. This conclusion was also reached for a Scalar Triplet in [38], and for Scalar Singlet in [71]. Any unification scenario that has leptoquarklike states, IceCube explanation in such theories (e.g. R-Parity Violating MSSM [43]) should also be in conflict.

## ACKNOWLEDGMENTS

The authors would like to thank Professor Namit Mahajan and Professor Subhendra Mohanty for invaluable discussions and suggestions. The authors also thank the anonymous referee for pointing out the important LHC constraints on the model.

- 
- [1] E. Farhi and L. Susskind, Technicolor, *Phys. Rep.* **74**, 277 (1981).
- [2] H. Georgi and S.L. Glashow, Unity of All Elementary Particle Forces, *Phys. Rev. Lett.* **32**, 438 (1974).
- [3] H. Georgi, The state of the art gauge theories, *AIP Conf. Proc.* **23**, 575 (1975).
- [4] P. Cox, A. Kusenko, O. Sumensari, and T.T. Yanagida, SU(5) unification with TeV-scale leptoquarks, *J. High Energy Phys.* **03** (2017) 035.
- [5] R. Aaij *et al.*, Test of Lepton Universality Using  $B^+ \rightarrow K^+ \ell^+ \ell^-$  Decays, *Phys. Rev. Lett.* **113**, 151601 (2014).
- [6] R. Aaij *et al.*, Test of lepton universality with  $B^0 \rightarrow K^{*0} \ell^+ \ell^-$  decays (unpublished).
- [7] G. Hiller and M. Schmaltz,  $R_K$  and future  $b \rightarrow s \ell \ell$  physics beyond the standard model opportunities, *Phys. Rev. D* **90**, 054014 (2014).
- [8] G. D'Amico, M. Nardecchia, P. Panci, F. Sannino, A. Strumia, R. Torre, and A. Urbano, Flavor anomalies after the  $R_{K^*}$  measurement (unpublished).
- [9] D. Bećirević and O. Sumensari, A leptoquark model to accommodate  $R_K^{\text{exp}} < R_K^{\text{SM}}$  and  $R_{K^*}^{\text{exp}} < R_{K^*}^{\text{SM}}$  (unpublished).
- [10] G. Hiller and I. Nisandzic,  $R_K$  and  $R_{K^*}$  beyond the Standard Model (unpublished).
- [11] Y. Cai, J. Gargalionis, M. A. Schmidt, and R. R. Volkas, Reconsidering the one leptoquark solution: Flavor anomalies and neutrino mass, <http://inspirehep.net/record/1389798?ln=en> (unpublished).
- [12] A. Crivellin, D. Müller, and T. Ota, Simultaneous explanation of  $R(D^{(*)})$  and  $b \rightarrow s \mu^+ \mu^-$ : The last scalar leptoquarks standing (unpublished).
- [13] N. G. Deshpande and X.-G. He, Consequences of R-parity violating interactions for anomalies in  $\bar{B} \rightarrow D^{(*)} \tau \bar{\nu}$  and  $b \rightarrow s \mu^+ \mu^-$ , *Eur. Phys. J. C* **77**, 134 (2017).
- [14] D. Das, C. Hati, G. Kumar, and N. Mahajan, Scrutinizing R-parity violating interactions in light of  $R_{K^{(*)}}$  data (unpublished).
- [15] S. Biswas, D. Chowdhury, S. Han, and S. J. Lee, Explaining the lepton nonuniversality at the LHCb and CMS within a unified framework, *J. High Energy Phys.* **02** (2015) 142.
- [16] W. Altmannshofer, P. S. Bhupal Dev, and A. Soni,  $R_{D^{(*)}}$  anomaly: A possible hint for natural supersymmetry with R-parity violation (unpublished).
- [17] C. Hati, G. Kumar, and N. Mahajan,  $\bar{B} \rightarrow D^{(*)} \tau \bar{\nu}$  excesses in ALRSM constrained from  $B$ ,  $D$  decays and  $D^0 - \bar{D}^0$  mixing, *J. High Energy Phys.* **01** (2016) 117.
- [18] A. K. Alok, B. Bhattacharya, A. Datta, D. Kumar, J. Kumar, and D. London, New physics in  $b \rightarrow s \mu^+ \mu^-$  after the measurement of  $R_{K^*}$  (unpublished).
- [19] F. Sala and D. M. Straub, A new light particle in B decays? (unpublished).
- [20] A. Datta, J. Liao, and D. Marfatia, A light  $Z'$  for the  $R_K$  puzzle and nonstandard neutrino interactions, *Phys. Lett. B* **768**, 265 (2017).
- [21] A. Datta, J. Kumar, J. Liao, and D. Marfatia, New light mediators for the  $R_K$  and  $R_{K^*}$  puzzles (unpublished).
- [22] A. Celis, J. Fuentes-Martin, A. Vicente, and J. Virto, Gauge-invariant implications of the LHCb measurements on lepton-flavor nonuniversality (unpublished).
- [23] M. Ciuchini, A. M. Coutinho, M. Fedele, E. Franco, A. Paul, L. Silvestrini, and M. Valli, On flavorful Easter eggs for new physics hunger and lepton flavor universality violation (unpublished).
- [24] L.-S. Geng, B. Grinstein, S. Jäger, J. M. Camalich, X.-L. Ren, and R.-X. Shi, Towards the discovery of new physics with lepton-universality ratios of  $b \rightarrow s \ell \ell$  decays (unpublished).
- [25] T. Hurth, F. Mahmoudi, and S. Neshatpour, Global fits to  $b \rightarrow s \ell \ell$  data and signs for lepton nonuniversality, *J. High Energy Phys.* **12** (2014) 053.
- [26] C.-W. Chiang, X.-G. He, J. Tandean, and X.-B. Yuan,  $R_{K^{(*)}}$  and related  $b \rightarrow s \ell \bar{\ell}$  anomalies in minimal flavor violation framework with  $Z'$  boson (unpublished).
- [27] A. Crivellin, G. D'Ambrosio, and J. Heeck, Addressing the LHC flavor anomalies with horizontal gauge symmetries, *Phys. Rev. D* **91**, 075006 (2015).
- [28] D. Ghosh, Explaining the  $R_K$  and  $R_{K^*}$  anomalies (unpublished).
- [29] C. Bonilla, T. Modak, R. Srivastava, and J. W. F. Valle,  $U(1)_{B_3-3L_\mu}$  gauge symmetry as the simplest description of  $b \rightarrow s$  anomalies (unpublished).
- [30] J. M. Cline and J. M. Camalich,  $B$  decay anomalies from non-Abelian local horizontal symmetry (unpublished).
- [31] G. Couture and H. Konig, Bounds on second generation scalar leptoquarks from the anomalous magnetic moment of the muon, *Phys. Rev. D* **53**, 555 (1996).
- [32] E. C. Leskow, G. D'Ambrosio, A. Crivellin, and D. Müller,  $(g-2)\mu$ , lepton flavor violation, and  $Z$  decays with leptoquarks: Correlations and future prospects, *Phys. Rev. D* **95**, 055018 (2017).
- [33] S. Baek and K. Nishiwaki, Leptoquark explanation of  $h \rightarrow \mu \tau$  and muon  $(g-2)$ , *Phys. Rev. D* **93**, 015002 (2016).

- [34] D. Das, C. Hati, G. Kumar, and N. Mahajan, Towards a unified explanation of  $R_{D^{(*)}}$ ,  $R_K$  and  $(g-2)_\mu$  anomalies in a left-right model with leptoquarks, *Phys. Rev. D* **94**, 055034 (2016).
- [35] K.-m. Cheung, Muon anomalous magnetic moment and leptoquark solutions, *Phys. Rev. D* **64**, 033001 (2001).
- [36] C.-H. Chen, T. Nomura, and H. Okada, Excesses of muon  $g-2$ ,  $R_{D^{(*)}}$ , and  $R_K$  in a leptoquark model (unpublished).
- [37] V. Barger and W.-Y. Keung, Superheavy particle origin of IceCube PeV neutrino events, *Phys. Lett. B* **727**, 190 (2013).
- [38] N. Mileo, A. de la Puente, and A. Szykman, Implications of an electroweak triplet scalar leptoquark on the ultra-high energy neutrino events at IceCube, *J. High Energy Phys.* **11** (2016) 124.
- [39] U. K. Dey and S. Mohanty, Constraints on leptoquark models from IceCube data, *J. High Energy Phys.* **04** (2016) 187.
- [40] B. Dutta, Y. Gao, T. Li, C. Rott, and L. E. Strigari, Leptoquark implication from the CMS and IceCube experiments, *Phys. Rev. D* **91**, 125015 (2015).
- [41] L. A. Anchordoqui, C. A. Garcia Canal, H. Goldberg, D. G. Dumm, and F. Halzen, Probing leptoquark production at IceCube, *Phys. Rev. D* **74**, 125021 (2006).
- [42] U. K. Dey, S. Mohanty, and G. Tomar, Leptoquarks: 750 GeV diphoton resonance and IceCube events (unpublished).
- [43] P. S. Bhupal Dev, D. K. Ghosh, and W. Rodejohann, R-parity violating supersymmetry at IceCube, *Phys. Lett. B* **762**, 116 (2016).
- [44] I. Doršner, S. Fajfer, A. Greljo, J. F. Kamenik, and N. Košnik, Physics of leptoquarks in precision experiments and at particle colliders, *Phys. Rep.* **641**, 1 (2016).
- [45] D. Chakraverty, D. Choudhury, and A. Datta, A non-supersymmetric resolution of the anomalous muon magnetic moment, *Phys. Lett. B* **506**, 103 (2001).
- [46] G. Bélanger, C. Delaunay, and S. Westhoff, A dark matter relic from muon anomalies, *Phys. Rev. D* **92**, 055021 (2015).
- [47] C. Patrignani *et al.* (Particle Data Group), Review of particle physics, *Chin. Phys. C* **40**, 100001 (2016).
- [48] G. Hiller and F. Kruger, More model-independent analysis of  $b \rightarrow s$  processes, *Phys. Rev. D* **69**, 074020 (2004).
- [49] B. Capdevila, A. Crivellin, S. Descotes-Genon, J. Matias, and J. Virto, Patterns of new physics in  $b \rightarrow s\ell^+\ell^-$  transitions in the light of recent data (unpublished).
- [50] D. Bardhan, P. Byakti, and D. Ghosh, Role of tensor operators in  $R_K$  and  $R_{K^*}$  (unpublished).
- [51] W. Altmannshofer, P. Ball, A. Bharucha, A. J. Buras, D. M. Straub, and M. Wick, Symmetries and asymmetries of  $B \rightarrow K^*\mu^+\mu^-$  decays in the Standard Model and beyond, *J. High Energy Phys.* **01** (2009) 019.
- [52] H. H. Patel, Package-X 2.0: A Mathematica package for the analytic calculation of one-loop integrals, *Comput. Phys. Commun.* **218**, 66 (2017).
- [53] L.-S. Geng, B. Grinstein, S. Jäger, J. M. Camalich, X.-L. Ren, and R.-X. Shi, Towards the discovery of new physics with lepton-universality ratios of  $b \rightarrow s\ell\ell$  decays (unpublished).
- [54] R. Aaij *et al.*, Measurement of the  $B_s^0 \rightarrow \mu^+\mu^-$  Branching Fraction and Effective Lifetime and Search for  $B^0 \rightarrow \mu^+\mu^-$  Decays, *Phys. Rev. Lett.* **118**, 191801 (2017).
- [55] D. Bečirević, O. Sumensari, and R. Z. Funchal, Lepton flavor violation in exclusive  $b \rightarrow s$  decays, *Eur. Phys. J. C* **76**, 134 (2016).
- [56] C. Bobeth, M. Gorbahn, T. Hermann, M. Misiak, E. Stamou, and M. Steinhauser,  $B_{s,d} \rightarrow l^+l^-$  in the Standard Model with reduced theoretical uncertainty, *Phys. Rev. Lett.* **112**, 101801 (2014).
- [57] C. Rott, K. Kohri, and S. C. Park, Superheavy dark matter and IceCube neutrino signals: Bounds on decaying dark matter, *Phys. Rev. D* **92**, 023529 (2015).
- [58] N. Hiroshima, R. Kitano, K. Kohri, and K. Murase, High-energy neutrinos from multi-body decaying dark matter (unpublished).
- [59] A. Bhattacharya, A. Esmaili, S. Palomares-Ruiz, and I. Sarcevic, Probing decaying heavy dark matter with the 4-year IceCube HESE data (unpublished).
- [60] S. Palomares-Ruiz, A. C. Vincent, and O. Mena, Spectral analysis of the high-energy IceCube neutrinos, *Phys. Rev. D* **91**, 103008 (2015).
- [61] R. Gandhi, C. Quigg, M. H. Reno, and I. Sarcevic, Ultrahigh-energy neutrino interactions, *Astropart. Phys.* **5**, 81 (1996).
- [62] M. G. Aartsen *et al.*, in *Proceedings, 34th International Cosmic Ray Conference (ICRC 2015): The Hague, The Netherlands, 2015* (2015).
- [63] A. D. Martin, W. J. Stirling, R. S. Thorne, and G. Watt, Parton distributions for the LHC, *Eur. Phys. J. C* **63**, 189 (2009).
- [64] O. J. P. Eboli, R. Zukanovich Funchal, and T. L. Lungov, Signal and backgrounds for leptoquarks at the CERN LHC, *Phys. Rev. D* **57**, 1715 (1998).
- [65] M. Kramer, T. Plehn, M. Spira, and P. M. Zerwas, Pair production of scalar leptoquarks at the CERN LHC, *Phys. Rev. D* **71**, 057503 (2005).
- [66] A. Belyaev, C. Leroy, R. Mehdiev, and A. Pukhov, Leptoquark single and pair production at LHC with CalcHEP/CompHEP in the complete model, *J. High Energy Phys.* **09** (2005) 005.
- [67] I. Dorsner, S. Fajfer, and A. Greljo, Cornering scalar leptoquarks at LHC, *J. High Energy Phys.* **10** (2014) 154.
- [68] T. Mandal, S. Mitra, and S. Seth, Single productions of colored particles at the LHC: An example with scalar leptoquarks, *J. High Energy Phys.* **07** (2015) 028.
- [69] T. Mandal, S. Mitra, and S. Seth, Pair production of scalar leptoquarks at the LHC to NLO parton shower accuracy, *Phys. Rev. D* **93**, 035018 (2016).
- [70] I. Dorsner, Scalar leptoquarks at LHC, *Proc. Sci., CORFU2015* (2016) 051.
- [71] U. K. Dey, D. Kar, M. Mitra, M. Spannowsky, and A. C. Vincent, Searching for leptoquarks at IceCube and the LHC (unpublished).
- [72] P. Bandyopadhyay and R. Mandal, Revisiting scalar leptoquark at the LHC (unpublished).
- [73] I. Dorsner and A. Greljo, Leptoquark toolbox for precision collider studies (unpublished).
- [74] G. Hiller, D. Loose, and I. Nisandzic, Flavorful leptoquarks at hadron colliders (unpublished).
- [75] A. Alloul, N. D. Christensen, C. Degrande, C. Duhr, and B. Fuks, FeynRules 2.0—A complete toolbox for tree-level phenomenology, *Comput. Phys. Commun.* **185**, 2250 (2014).

- [76] J. Alwall, R. Frederix, S. Frixione, V. Hirschi, F. Maltoni, O. Mattelaer, H. S. Shao, T. Stelzer, P. Torrielli, and M. Zaro, The automated computation of tree-level and next-to-leading order differential cross sections, and their matching to parton shower simulations, *J. High Energy Phys.* **07** (2014) 079.
- [77] T. Sjostrand, S. Ask, J. R. Christiansen, R. Corke, N. Desai, P. Ilten, S. Mrenna, S. Prestel, C. O. Rasmussen, and P. Z. Skands, An introduction to PYTHIA 8.2, *Comput. Phys. Commun.* **191**, 159 (2015).
- [78] M. Drees, H. Dreiner, D. Schmeier, J. Tattersall, and J. S. Kim, CheckMATE: Confronting your favorite new physics model with LHC data, *Comput. Phys. Commun.* **187**, 227 (2015).
- [79] M. Aaboud *et al.*, Search for scalar leptoquarks in pp collisions at  $\sqrt{s} = 13$  TeV with the ATLAS experiment, *New J. Phys.* **18**, 093016 (2016).
- [80] M. Aaboud *et al.*, Search for squarks and gluinos in final states with jets and missing transverse momentum at  $\sqrt{s} = 13$  TeV with the ATLAS detector, *Eur. Phys. J. C* **76**, 392 (2016).
- [81] G. Aad *et al.*, Search for new phenomena in final states with an energetic jet and large missing transverse momentum in pp collisions at  $\sqrt{s} = 8$  TeV with the ATLAS detector, *Eur. Phys. J. C* **75**, 299 (2015); Erratum, *Eur. Phys. J. C* **75**, 408E (2015)].



## Leptoquark solution for both the flavor and ANITA anomalies

Bhavesh Chauhan\*

*Physical Research Laboratory, Ahmedabad 380009, India  
and Indian Institute of Technology Gandhinagar, Palaj 382355, India*

Subhendra Mohanty†

*Physical Research Laboratory, Ahmedabad 380009, India*



(Received 31 January 2019; published 17 May 2019)

The ANITA experiment has seen anomalous Earth emergent showers of EeV energies which cannot be explained with Standard Model interactions. In addition, tests of lepton flavor universality in  $R(D^{(*)})$  and  $R(K^{(*)})$  have shown significant deviations from theoretical predictions. It is known that, among single leptoquark solutions, only the chiral vector leptoquark  $U_1 \sim (\mathbf{3}, \mathbf{1}, 2/3)$  can simultaneously address the discrepancies. In this paper, we show that the leptoquark motivated by flavor anomalies coupled to a sterile neutrino can also explain the ANITA anomalous events. We consider two scenarios, (a) the sterile neutrino, produced via resonant leptoquark mediated neutrino-nucleon interactions, propagates through the Earth without significant attenuation and decays near the surface to a  $\tau$  lepton; and (b) a cosmogenic sterile neutrino interacts with the matter near the surface of Earth and generates a  $\tau$  lepton. These two scenarios give significantly large survival probabilities even when regeneration effects are not taken into account. In the second scenario, the distribution of emergent tau energy peaks in the same energy range as seen by ANITA.

DOI: [10.1103/PhysRevD.99.095018](https://doi.org/10.1103/PhysRevD.99.095018)

### I. INTRODUCTION

The ANtarctic Impulsive Transient Antenna (ANITA) instrument is designed to detect interaction of ultrahigh energy neutrinos via the Askaryan effect in ice. During its first and third flight, it also observed unexpected upward directed showers apparently emerging well below the horizon [1–3]. The observed signal is consistent with  $\tau$  induced showers. The essential details of the two anomalous ANITA events (AAEs) are given in Table I. The survival probability ( $\epsilon$ ) is estimated taking into account the neutrino regeneration effects and  $\tau$  energy losses in [4] using only Standard Model (SM) interactions.

The small survival probabilities within SM indicate that new physics scenarios should be invoked to explain these events. In the past, the AAEs have been explained in the framework of sterile neutrinos [5,6], supersymmetry [4,7,8], and  $CPT$  symmetric universe [9]. However, each of these explanations has their own limitations [7].

Similarly, collider experiments such as LHCb, Belle, and BABAR have observed hints of lepton flavor universality violation (LFUV) in semileptonic decays of the B meson. In particular, the ratios

$$R(D^{(*)}) = \frac{\mathcal{BR}(\bar{B} \rightarrow D^{(*)} \tau^- \bar{\nu}_\tau)}{\mathcal{BR}(\bar{B} \rightarrow D^{(*)} \ell^- \bar{\nu}_\ell)}, \quad (1)$$

$$R(K^{(*)}) = \frac{\mathcal{BR}(\bar{B} \rightarrow \bar{K}^{(*)} \mu^+ \mu^-)}{\mathcal{BR}(\bar{B} \rightarrow \bar{K}^{(*)} e^+ e^-)}, \quad (2)$$

where  $\ell = e, \mu$  are known to have very weak dependence on hadronic form factors and provide excellent probes of LFUV [10]. The experimentally measured value of the observables  $R(D^{(*)})$  [11,12] and  $R(K^{(*)})$  [13,14] is consistently below SM prediction and together are dubbed as “flavor anomalies” in this paper. These discrepancies can

\*bhavesh@prl.res.in  
†mohanty@prl.res.in

*Published by the American Physical Society under the terms of the Creative Commons Attribution 4.0 International license. Further distribution of this work must maintain attribution to the author(s) and the published article’s title, journal citation, and DOI. Funded by SCOAP<sup>3</sup>.*

TABLE I. Properties of the anomalous events.

Property	AAE1	AAE2
Energy ( $E_\tau$ )	$0.6 \pm 0.4$ EeV	$0.56_{-0.2}^{+0.3}$ EeV
Zenith Angle	$117.4 \pm 0.3^\circ$	$125.0 \pm 0.3^\circ$
Chord Length ( $l_\oplus$ )	$5740 \pm 60$ km	$7210 \pm 55$ km
$\epsilon_{\text{SM}}$	$4.4 \times 10^{-7}$	$3.2 \times 10^{-8}$

be explained in several extensions of SM, for example with leptoquarks [15–29].

It was proposed in [4] that a long lived BSM particle, which is produced in ultrahigh energy (UHE) neutrino nucleon interactions, propagates freely through the chord of Earth, and decays to a  $\tau$  near the surface can explain the AAEs. A natural candidate for this is  $\tilde{\tau}$  (stau) in R-parity conserving supersymmetry [4] and neutralino (mostly bino) in R-parity violating supersymmetry [7]. In this paper, we consider two scenarios wherein a leptoquark, proposed as a resolution to flavor anomalies, also explains AAEs. In the first scenario, we extend the minimal leptoquark model of [15] with a heavy sterile neutrino ( $\chi$ ). The SM singlet  $\chi$  is produced in UHE neutrino-nucleon interactions mediated by the leptoquark. The sterile neutrino can travel inside Earth without significant attenuation and decays near the south pole. One of the decay products is the  $\tau$  particle whose shower is seen by ANITA. In the second scenario, an cosmogenic UHE sterile neutrino propagates freely through the chord of the Earth and produces a  $\tau$  via leptoquark mediated interaction. Interestingly, the same leptoquark interaction also explains  $R(D^{(*)})$  through  $b \rightarrow c\tau\chi$  as shown in [18].

In Sec. II, we estimate the number of AAEs for isotropic and anisotropic flux. In Sec. III, we provide details of the leptoquark model and discuss the two scenarios in detail before we conclude in Sec. IV.

## II. ANITA ANOMALOUS EVENTS

In order to estimate the number of Earth emergent showers seen by ANITA, we evaluate the survival probability  $\epsilon$  (also called efficiency in [6]) which represents the fraction of incident flux  $\Phi$  that is converted into  $\tau$  near the surface. We use the expression

$$\mathcal{N} = A \cdot \delta T \cdot \delta\Omega \int_{E_{\min}}^{E_{\max}} dE_\nu \cdot \epsilon \cdot \Phi(E_\nu), \quad (3)$$

where the effective area of ANITA  $A \approx 4 \text{ km}^2$  is estimated using the Cherenkov angle [6],  $\delta T$  is the time period, and  $\delta\Omega$  is the acceptance angle. For a temporally continuous source,  $\delta T \approx 25$  days is the combined exposure of ANITA-I (17.25 days) and ANITA-III (7 days) [1,2]. We have ignored the contribution of ANITA-II (28.5 days) as it was not sensitive to such events. For transient sources,  $\delta T$  will depend on the source and can be smaller. For isotropic source,  $\delta\Omega \approx 2\pi$  sr. However, for anisotropic source,

$$\delta\Omega \approx 2\pi(1 - \cos \delta_\theta) \approx 0.0021 \text{ sr}, \quad (4)$$

where  $\delta_\theta \sim 1.5^\circ$  is the angular uncertainty relative to parent neutrino direction [2]. The neutrino energy ( $E_\nu$ ) is integrated over the range which gives correct range of shower

energy. For example, if  $\tau$  is produced through interaction of the incident neutrino such that  $E_\tau = E_\nu/4$ . Since the observed shower has energy in the range 0.1–1 EeV, one must integrate over 0.4–4 EeV. In general,  $\epsilon$  depends on  $E_\nu$  and model parameters.

We now provide an order-of-magnitude estimate of the required  $\epsilon$  taking  $\delta T = 25$  days. For the isotropic case, we assume that the source of EeV neutrinos is the Greisen-Zatsepin-Kuzmin (GZK) mechanism. We approximate the GZK flux by the upper limit of its saturated value over the range 0.4–4 EeV as,

$$\bar{\Phi}_{\text{iso}} \approx 10^{-25} \text{ (GeV cm}^2 \text{ s sr)}^{-1}, \quad (5)$$

which gives  $\mathcal{N} \approx 200\epsilon$ . To get two events, one requires  $\epsilon \sim 0.01$ . Similar estimates were also obtained in [7] which takes energy dependence into account albeit with larger exposure time. With the Standard Model interactions, the authors in [4] have estimated that  $\epsilon_{\text{SM}} \sim 10^{-7}$  for the two reported events. Thus the estimated number of anomalous events from GZK neutrinos with only SM interactions is,

$$\mathcal{N}_{\text{iso}}^{\text{SM}} \sim 2 \times 10^{-5}, \quad (6)$$

which makes observation of two events extremely unlikely.

One can relax the assumption that the source of EeV neutrinos is the GZK flux. This allows us to postulate that such high energy neutrinos are coming from a localized source in the sky. The upper limit on such anisotropic flux of EeV neutrinos is,

$$\bar{\Phi}_{\text{aniso}} \approx 3.2 \times 10^{-20} \text{ (GeV cm}^2 \text{ s sr)}^{-1}, \quad (7)$$

which is several orders larger than the isotropic case. After accounting for the small solid angle one can similarly obtain,  $\mathcal{N} \approx 2.1 \times 10^4 \epsilon$ . To get two events, one requires  $\epsilon \sim 10^{-4}$ . Using SM interactions for the incident neutrinos,

$$\mathcal{N}_{\text{aniso}}^{\text{SM}} \sim 2.1 \times 10^{-3}, \quad (8)$$

which again makes the two events very unlikely. In this section, we have ignored the energy dependence of  $\epsilon$  as well as  $\Phi$ . Even after taking those into account, the message will remain unchanged. The smallness of  $\epsilon_{\text{SM}}$  makes the two event unlikely.

One must also check the compatibility of IceCube with ANITA observations. Even though IceCube has smaller effective area, the long duration of the experiment implies that the expected number of EeV scale up going  $\tau$ -tracks seen by IceCube ( $\mathcal{N}_{\text{IC}}$ ) to be larger than expected anomalous events by ANITA ( $\mathcal{N}_{\text{AN}}$ ). Using the relative exposures, it has been estimated that  $\mathcal{N}_{\text{IC}} \approx 10 \times \mathcal{N}_{\text{AN}}$  [6,7]. In [4], the authors identify three events in nine year (3142 days) IceCube data that may have origin similar to ANITA. This implies that  $\mathcal{N}_{\text{AN}} = 0.3$ . Using Poisson

distribution, the probability of observing two such events is around 0.03. The challenge for BSM scenarios is to get  $\mathcal{N}_{\text{AN}}$  of this order by enhancing  $\epsilon$  as has been done in the two scenarios studied in this paper.

### III. LEPTOQUARK RESOLUTION OF AAE

As has been discussed [18,19], a vector leptoquark  $U_1$  with  $SU(3)_C \times SU(2)_L \times U(1)_Y$  quantum numbers  $(\mathbf{3}, \mathbf{1}, 2/3)$  can simultaneously explain the flavor anomalies. It is also one of the handful models that admit leptoquark coupling to a sterile neutrino [30]. The interaction of  $U_1$  with fermions in the mass basis is,

$$-\mathcal{L} \supset (V \cdot g_L)_{ij} \bar{u}_L^i \gamma^\mu U_{1,\mu} \nu_L^j + (g_L)_{ij} \bar{d}_L^i \gamma^\mu U_{1,\mu} e_L^j + (g_R)_{ij} \bar{d}_R^i \gamma^\mu U_{1,\mu} e_R^j + (g_\chi)_i \bar{u}_R^i \gamma^\mu U_{1,\mu} \chi_R, \quad (9)$$

where  $V$  is the Cabibbo-Kobayashi-Maskawa (CKM) matrix and the contribution of Pontecorvo-Maki-Nakagawa-Sakata (PMNS) matrix is ignored.

#### A. Heavy sterile neutrino

In this section, we assume that the sterile neutrino is sufficiently heavy so that its contribution to semi-leptonic B decays is kinematically forbidden. Even though the interaction of up-type quarks with a sterile neutrino can generate dangerous scalar and pseudoscalar operators, their contributions can be neglected and the conclusions in [19] remain unchanged. The required texture of coupling matrices is,

$$g_L = \begin{pmatrix} 0 & 0 & 0 \\ 0 & g_{s\mu} & g_{s\tau} \\ 0 & g_{b\mu} & g_{b\tau} \end{pmatrix} \quad g_R = 0. \quad g_\chi = \begin{pmatrix} 0 & g_x & 0 \end{pmatrix}. \quad (10)$$

The left-handed coupling ( $g_L$ ) generates the desired Wilson coefficients (i.e.,  $\delta\mathcal{C}_9 = -\delta\mathcal{C}_{10}$  with the correct sign for  $b \rightarrow s\mu\mu$  and  $g_{V_L} > 0$  for  $b \rightarrow c\tau\nu$ ). In this way,  $U_1$  is one of the rare solutions that can simultaneously address both the anomalies. The right-handed coupling ( $g_R$ ) is severely constrained as it generates scalar and pseudoscalar operators that are disfavored. The sterile neutrino  $\chi$  can also couple to other up-type right handed quarks, but we have neglected those couplings and their constraints for simplicity. In this section, we will assume the mass of leptoquark  $U_1$  to be  $M_U = 1.5$  TeV and the couplings to be,

$$g_{s\mu} = -0.012, \quad g_{b\mu} = 0.2, \quad g_{s\tau} = 0.5, \quad g_{b\tau} = 0.5, \quad (11)$$

which can explain the flavor anomalies. Such a choice is within the reach of future LHC searches but allowed from present limits [19,20]. We treat the coupling  $g_x$  and mass of the sterile neutrino ( $M_\chi$ ) as free parameters of the theory.

The singlet is produced near the surface of Earth through neutrino-nucleon interaction mediated by the leptoquark.

It is assumed that the cross section for the process is dominated by the resonant s-channel neutrino-quark interactions. It has been pointed out in [31] that the gluon initiated process can also give significant contributions. However, this will give an  $\mathcal{O}(1)$  correction to survival probability and has been neglected for the heavy sterile neutrino case. The production cross section can be approximated in the narrow width limit as,

$$\sigma_{LQ}(E_\nu) = \frac{3\pi}{2} \left( \frac{g_x^2}{g_x^2 + 1.08} \right) \times \frac{1}{2M_N E_\nu} \int_0^1 dy y^2 ((0.11)^2 f_u + (0.5)^2 f_c), \quad (12)$$

where  $f_q$  is the parton distribution function (PDF) of  $q$  evaluated at  $x = M_U^2/2M_N E_\nu$  and  $Q = M_U \sqrt{y}$ . We have used ManeParse [32] and NNPDF3.1(sx) [33,34] datasets for the PDFs. The numerical factors (1.08, 0.11, and 0.5) are obtained using the central value of CKM parameters [35]. Note that the PDFs are evaluated at small- $x$  where the quark and antiquark PDFs are similar and hence neutrino and antineutrino have a similar cross section. The interaction length is estimated as,  $\ell_{LQ} = (\rho N_A \sigma_{LQ})^{-1}$  where we have used  $\rho \approx 4g/\text{cm}^3$  and  $N_A = 6.022 \times 10^{23} \text{ cm}^{-3}$  in water-equivalent units. Even though the density is larger near the center of Earth, the approximation for density is valid for the chord lengths relevant for AAE.

As opposed to previous studies with three body decay of a singlet [7], in this paper we estimate the two body decay width of the sterile neutrino to a pseudoscalar meson and the tau lepton. Since the decay width is being estimated in the rest frame of sterile neutrino of mass few GeV, one can integrate out the heavy leptoquark and write the effective Lagrangian as,

$$\mathcal{L}_{\text{eff}} = \frac{2g_x g_{q\ell}}{M_U^2} [\bar{c} P_L q] [\bar{\ell} P_R \chi], \quad (13)$$

where  $q \in \{s, b\}$  and  $\ell \in \{\mu, \tau\}$ . We also use the expression,

$$\langle 0 | \bar{q}_1 \gamma_5 q_2 | P \rangle = i \frac{M_P^2}{M_1 + M_2} f_P, \quad (14)$$

where  $P$  is a pseudoscalar meson of mass  $M_P$  and  $f_P$  is the associated form factor. The rest frame partial width of the sterile neutrino is,

$$\Gamma_\tau \equiv \Gamma(\chi \rightarrow \tau^- D_s^+) = \frac{1}{16\pi} \left( \frac{g_x g_{s\tau}}{M_U^2} \right)^2 \times \left( \frac{M_{D_s^+}^2}{M_c + M_s} f_{D_s^+} \right)^2 M_\chi \beta(M_{D_s^+}, M_\tau, M_\chi) \quad (15)$$

where the phase space factor is,

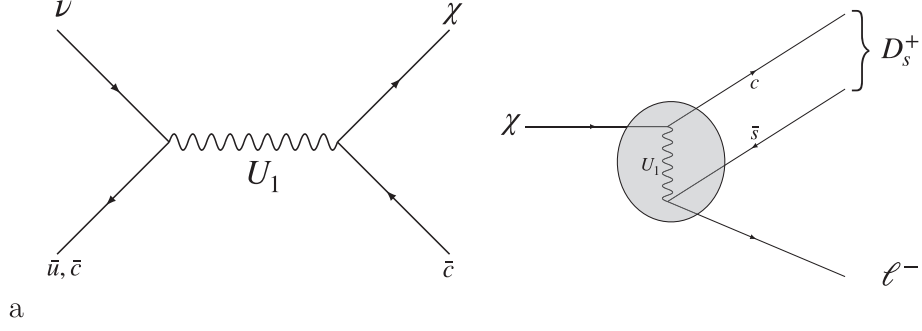


FIG. 1. The Feynman diagrams for the process involved in Model A. Left: The s-channel neutrino quark interaction mediated by leptoquark  $U_1$  that produces sterile neutrino in final state is shown. Right: The decay mode of sterile neutrino to charged lepton and  $D_s^+$  is shown. The shaded circle represents the effective vertex.

$$\beta(a, b, c) = \left[ \left( 1 - \left( \frac{a-b}{c} \right)^2 \right) \left( 1 - \left( \frac{a+b}{c} \right)^2 \right) \right]^{1/2}. \quad (16)$$

For numerical estimation we use,

$$f_{D_s^+} = 257.86 \text{ MeV} \quad M_{D_s^+} = 1.968 \text{ GeV} \quad (17)$$

and the quarks and lepton masses used are  $M_c = 1.29 \text{ GeV}$ ,  $M_s = 95 \text{ MeV}$ ,  $M_\mu = 105.66 \text{ MeV}$ , and  $M_\tau = 1.77 \text{ GeV}$  respectively. The relevant Feynman diagrams for the production and decay are shown in Fig. 1. The associated decay length of  $\chi$  in Earth's frame is estimated as,

$$\ell_D = \gamma c \tau = \frac{1}{\Gamma_\tau} \frac{E_\chi}{M_\chi} \approx \frac{1}{\Gamma_\tau} \frac{E_\nu}{2M_\chi}, \quad (18)$$

where the last approximation is true for the range of energies involved. In this scenario,  $E_\tau = E_\nu/4$  and hence for shower energy  $\sim 0.5 \text{ EeV}$ , one requires the incident neutrino to have energy  $E_\nu \sim 2 \text{ EeV}$ .

With only SM interactions, one can estimate the bare survival probability  $\epsilon_0 = e^{-l_\oplus/\ell_0}$  where  $l_\oplus$  is the length of path traversed by neutrino inside Earth and for EeV neutrinos,  $\ell_0 \sim 275 \text{ km}$  [4]. However, this is severely modified when one takes neutrino regeneration effects during propagation. In [4], the probability is obtained using simulations and mentioned in Table I. We denote these probabilities with  $\epsilon_{\text{SM}}$ . Due to the additional leptoquark interactions, the survival probability of the neutrino flux can be estimated using,

$$\epsilon_{LQ} = \int_0^{l_\oplus} dl_1 \int_{l_\oplus - l_1 - \delta}^{l_\oplus - l_1} dl_2 \left[ \frac{e^{-l_2/\ell_D} e^{-l_1/\ell_{LQ}}}{\ell_D \ell_{LQ}} \left( 1 - \int_0^{l_1} \frac{dl_3}{\ell_0} e^{-l_3/\ell_0} \right) \right] \quad (19)$$

The above expression can be understood as follows. The parentheses denote the fraction neutrinos that survives SM

interactions after propagating a distance  $l_1$ . These neutrino undergo leptoquark interactions with the matter and produce a sterile neutrino. The sterile neutrino propagates a distance of  $l_\oplus - l_1 - \delta$  before it decays near the surface of Earth in the  $\delta \approx 10 \text{ km}$  window that will produce the observed  $\tau$ .

In Fig. 2 we have shown the parameter space that gives  $\epsilon_{LQ} > \epsilon_{\text{SM}}$ , and  $\epsilon_{LQ} > 1 \times 10^{-6}$  for the two values of  $l_\oplus$ . We find that the maximum survival probability in this scenario is of the order  $4 \times 10^{-6}$ . It is understood that neutrino regeneration effects can dramatically increase  $\epsilon_{LQ}$

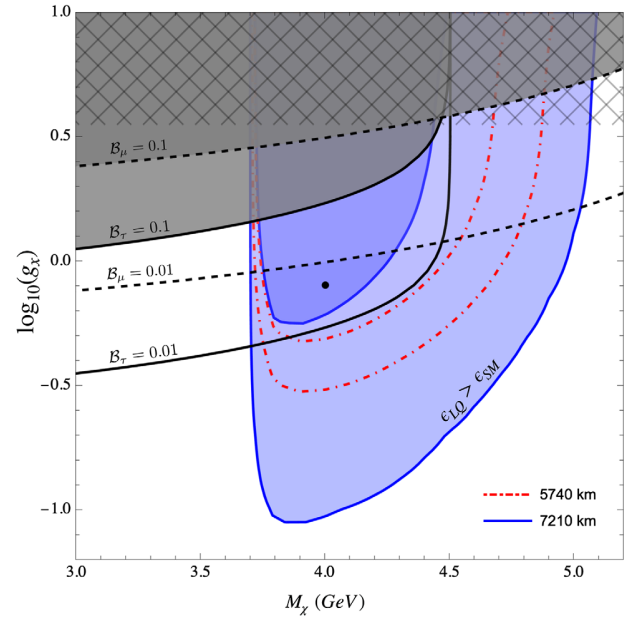


FIG. 2. The parameter space that gives  $\epsilon_{LQ} > \epsilon_{\text{SM}}$  (blue), and  $\epsilon_{LQ} > 1 \times 10^{-6}$  (dark blue) for  $l_\oplus = 7210 \text{ km}$  is shown. Similar projections for  $l_\oplus = 5740 \text{ km}$  is shown by red curves. The gray shaded region is conservatively ruled out from  $B_c^+$  decays and the limits for various  $B_e$  are shown. The top part is excluded using the perturbativity limit  $g_x \leq \sqrt{4\pi}$ . The neutrino energy is fixed to be  $2 \text{ EeV}$ . The benchmark point considered in the text is shown.

similar to SM. However, complete estimation requires simulation of neutrino propagation which is beyond the scope of this work. Moreover, we find that the precision measurement of  $B_c^+$  decay modes can probe the most interesting part of the parameter space. We evaluate the branching fraction  $\mathcal{B}_\ell = \text{Br}(B_c^+ \rightarrow \ell^+ \chi)$  for  $\ell \in \{\mu, \tau\}$  to be,

$$\mathcal{B}_\ell = \frac{\tau_{B_c^+}}{4\pi M_{B_c^+}} \left( \frac{g_x g_{b\ell}}{M_U^2} \right)^2 \left( \frac{M_{B_c^+}^2}{M_c + M_b} f_{B_c^+} \right)^2 \times (M_{B_c^+}^2 - M_\ell^2 - M_\chi^2) \beta(M_\chi, M_\ell, M_{B_c^+}), \quad (20)$$

where  $f_{B_c^+} = 0.43$  GeV [18] and  $M_{B_c^+} = 6.275$  GeV [35]. Since the typical branching ratio of leptonic mode is very small, we take the conservative limit of  $\mathcal{B}_\ell = 10\%$  for both  $\mu$  and  $\tau$  modes to constrain our parameter space. We also show limits for  $\mathcal{B}_\ell = 1\%$  which will be accessible in future B-factories and can test the model.

In this model, for the parameter space that we are interested in, the only kinematically allowed choice for the final state meson is  $D_s^+$ . The model also allows for  $\chi \rightarrow \mu^- D_s^+$  however this decay mode is suppressed due to smallness of  $|g_{s\mu}| \sim 0.012$  as compared to  $|g_{s\tau}| \sim 0.5$  as seen in Eq. (11). We also have  $\chi \rightarrow \nu^- X$  but to get emergent  $\tau$  one needs to account for another interaction in (19) which makes it less probable. This mode will be important when regeneration effects are evaluated using simulation and is beyond the scope of this paper.

To estimate the number of events, we consider the benchmark scenario

$$M_\chi = 4.0 \text{ GeV} \quad g_x = 0.8 \quad (21)$$

for which  $\Gamma_\tau = 4.64 \times 10^{-16}$  GeV and the survival fraction is  $\epsilon_{LQ} \sim (1.5 - 2.0) \times 10^{-6}$ . This gives the expected number of AAE per direction to be 0.03 using the saturated anisotropic flux.

In this scenario, larger values of the coupling  $g_x$  seem to be preferable. However, they would be constrained from future measurements of  $\mathcal{B}_\mu$ . One can avoid these constraints if  $g_{b\mu} = 0$ , but then the model cannot explain  $R(K^{(*)})$ . If

one is willing to give up simultaneous explanation of both flavor anomalies, another interesting possibility opens up, i.e., light sterile neutrino.

## B. Light sterile neutrino

In [18], it is shown that  $U_1$  leptoquark coupled to a light sterile neutrino can also explain the flavor anomalies. However, as opposed to [19],  $R(D^{(*)})$  is explained via right-handed couplings and  $R(K^{(*)})$  via left-handed ones. It is seen that a simultaneous explanation in this scenario is in tension with big bang nucleosynthesis but  $R(D^{(*)})$  can be explained successfully. The Lagrangian for the leptoquark is,

$$\mathcal{L}_{LQ} = -\frac{1}{2} U_{\mu\nu}^\dagger U^{\mu\nu} - i g_s \kappa U_\mu^\dagger T^a U_\nu G^{a\mu\nu} + M_U^2 U_\mu^\dagger U^\mu + g_{b\tau} \bar{b}_R \gamma^\mu U_{1,\mu} \tau_R + g_x \bar{c}_R \gamma^\mu U_{1,\mu} \chi_R, \quad (22)$$

where  $g_s$  is the strong coupling constant and  $\kappa = 0(1)$  for a minimally coupled (gauge) theory. The excess can be explained with the following choice of coupling and leptoquark mass,

$$|g_x g_{b\tau}| \sim 0.62 \left( \frac{M_U}{1 \text{ TeV}} \right)^2. \quad (23)$$

Considering the LHC constraints on the model, we chose  $M_U = 1.5$  TeV which is close to the lightest allowed mass for  $\kappa = 1$ . To a good approximation,  $g_{b\tau} \in \{1.1, 1.4\}$  which translates to  $g_x \in (1.0, 1.25)$  using (23). In this limit, the model has signatures in future 300 fb $^{-1}$  analysis. These limits are considerably weakened for  $\kappa = 0$ . One can refer to [18] for detailed discussion of the model and other constraints.

To explain AAE, we assume a flux of light sterile neutrinos ( $\chi$ ) incident on Earth. These sterile neutrinos can pass through the Earth almost unattenuated, however, a fraction of them can interact with the matter in Earth and produce a  $\tau$  near the surface. In this section, we consider both  $\chi$ -quark and  $\chi$ -gluon interactions. The relevant Feynman diagrams are shown in Fig. 3.

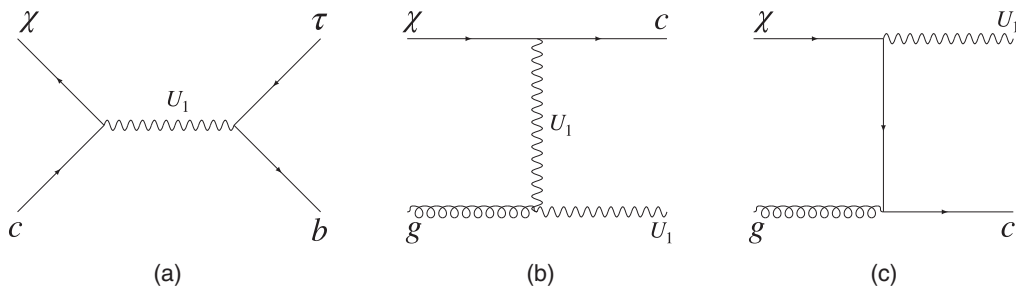


FIG. 3. The Feynman diagrams for  $\chi$ -nucleon interaction. (a) The dominant s-channel  $\chi$ -quark interaction. (b) The  $\kappa$ -dependent  $\chi$ -gluon interaction. (c) The  $\kappa$ -independent  $\chi$ -gluon interaction.

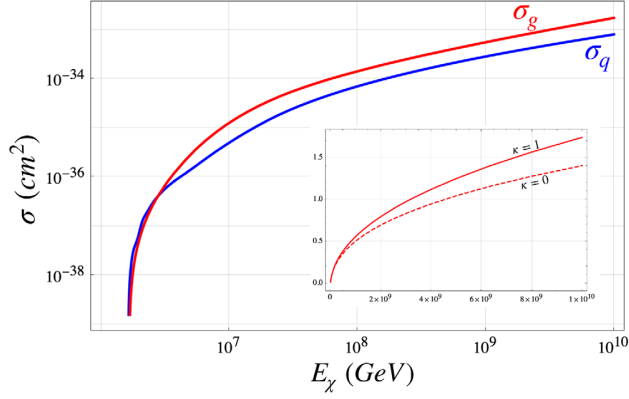


FIG. 4. The variation of cross section  $\sigma_q$  ( $\sigma_g$ ) with incident sterile neutrino energy is shown in blue (red). The inset shows the difference in magnitude of  $\sigma_g$  for  $\kappa = 0$  and 1 in arbitrary units.

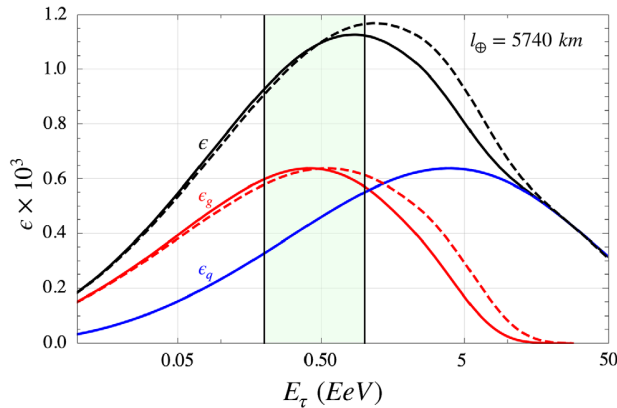
The  $\chi$ -quark interaction is dominated by the s-channel resonant contribution and the cross section can be estimated by

$$\sigma_q = \sigma(\chi c \rightarrow \tau b) = \frac{3\pi}{2} \left( \frac{g_x^2 g_{b\tau}^2}{g_x^2 + g_{b\tau}^2} \right) \times \frac{1}{2M_N E_\nu} \int_0^1 dy (1-y)^2 f_c. \quad (24)$$

The difference in  $y$ -dependence is due to the  $RR$  nature of interaction as opposed to  $LR$  in the previous case. On the other hand, the  $\chi$ -gluon interaction cross section can be estimated using,

$$\sigma_g = \sigma(\chi g \rightarrow \tau c \bar{b}) \approx \sigma(\chi g \rightarrow c U_1) \times \text{Br}(U_1 \rightarrow \tau \bar{b}). \quad (25)$$

We implemented the model in FEYNRULES [36,37] and the cross section is calculated using CALCHEP [38]. As was shown in [31], the gluon initiated process are significant for large energies and of the same order of magnitude as the



quark initiated processes. The cross section depends on  $\kappa$  as evident from Fig. 3(b). In Fig. 4, we show the variation of  $\sigma_q$  and  $\sigma_g$  with incident sterile neutrino energy. We also show the relative strength for  $\kappa = 0$  and 1.

The fraction of incident  $\chi$  that interact with matter in Earth is given by,

$$\epsilon_{q/g} = \int_{l_\oplus - \delta}^{l_\oplus} dl_1 \frac{e^{-l_1/\ell_{q/g}}}{\ell_{q/g}} \quad (26)$$

where  $\ell_{q/g} = (\rho N_A \sigma_{q/g})^{-1}$ . One must note that, for  $\chi$ -quark interactions  $E_\tau = E_\chi/2$  whereas for  $\chi$ -gluon interaction  $E_\tau = E_\chi/4$ . By uniformly varying  $E_\chi$ , we show the variation of  $\epsilon = \epsilon_q + \epsilon_g$  with energy of emergent tau in Fig. 5. An interesting result of this scenario is that the distribution peaks for tau energy in the same range as seen by ANITA.

In order to estimate the number of events, one needs to know the flux of incident  $\chi$  on Earth. It is clear from the discussion in Sec. II that this scenario cannot explain AAE with isotropic flux. We assume anisotropic flux from point-like sources in the sky and parametrize the incident flux as,

$$\Phi = \phi_0 \times 10^{-20} \left( \frac{E_\chi}{\text{EeV}} \right)^{-\gamma} \quad (\text{GeV cm}^2 \text{ s sr})^{-1}, \quad (27)$$

where the spectral index  $\gamma$  is unknown. The number of events is then given by,

$$\mathcal{N} \approx \left( \frac{1800}{\text{EeV}} \right) \times \phi_0 \times \left[ \int_{2E_\tau^{\min}}^{2E_\tau^{\max}} dE_\chi \cdot \epsilon_q(E_\chi) \cdot \left( \frac{E_\chi}{\text{EeV}} \right)^{-\gamma} + \int_{4E_\tau^{\min}}^{4E_\tau^{\max}} dE_\chi \cdot \epsilon_g(E_\chi) \cdot \left( \frac{E_\chi}{\text{EeV}} \right)^{-\gamma} \right], \quad (28)$$

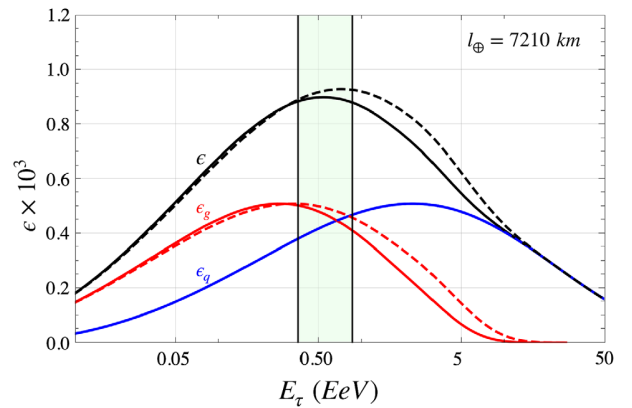


FIG. 5. The variation of  $\epsilon_q$ ,  $\epsilon_g$ , and  $\epsilon$  is shown in blue, red, and black respectively. The solid curve is for  $\kappa = 1$  and the dashed curve for  $\kappa = 0$ . The chord length  $l_\oplus$  is fixed to be 5740 km (left) and 7210 km (right). We fix  $g_x = 1.2$  for both the plots. The region shown in green is the observed shower energy for the two events.

TABLE II. The required value of  $\phi_0$  to get  $\mathcal{N} = 1$  for various choices of spectral index and chord lengths ( $A \equiv 5740$  km and  $B \equiv 7210$  km).

	$\gamma = 0$		$\gamma = 1$		$\gamma = 2$		$\gamma = 3$	
	A	B	A	B	A	B	A	B
$\phi_0$	0.19	0.41	0.31	0.71	0.37	1.04	0.33	1.30

where the limits of integration are determined by the  $1\sigma$  range of observed  $\tau$  energy. Note that the limits and  $\epsilon_{q/g}$  depend on the chord length in consideration. Keeping  $\mathcal{N} = 1$ , one can obtain the required value of  $\phi_0$  for various choices of  $\gamma$ . The results have been summarized in Table II. It can be seen that these values are compatible with the upper bounds mentioned in Sec. II. Note that, for  $\gamma = 0$ , one expects more number of events with shower energies higher than the ones observed by ANITA. Hence, higher values of spectral index is preferred.

We briefly comment regarding the source of such high energy sterile neutrinos. They can either be produced via the leptoquark interactions, via oscillation of active neutrinos near the source, or via interactions during propagation. If the sterile neutrinos are produced due to oscillation from the active ones, then the flux is proportional to the square of the mixing angle. For large mixing, the cross section will be dominated by SM interactions and the sterile neutrino will be significantly attenuated by Earth. For small mixing, albeit the sterile neutrino propagates freely, the incident flux is smaller and constraints from active neutrino flux becomes important. On the other hand, if a flux of active neutrinos encounters large magnetic fields during propagation, it can convert to sterile neutrinos via the transition magnetic dipole moment [39]. In this scenario, one anticipates both fluxes to be of the same order of magnitude and offers a lucrative testable explanation.

Another possibility is the absorption of active neutrino flux by cosmic sterile neutrino background [40], cosmic neutrino background [41], or dark matter [42]. In [43], a flux of boosted right handed neutrinos was obtained through decay of dark matter.

#### IV. CONCLUSION

Since the observation of AAEs, many BSM scenarios have been invoked to explain the discrepancy. In this paper we have proposed two models that can significantly enhance the  $\tau$  survival probability while simultaneously addressing the flavor anomalies. In the first scenario, we have extended chiral vector leptoquark model which explains  $R(D^{(*)})$  and  $R(K^{(*)})$  [15] by a sterile neutrino. The cosmogenic UHE neutrinos interact with the matter in Earth and produce a sterile neutrino that propagates freely inside Earth and decays near the surface to a  $\tau$ . The precise measurement of  $\text{Br}(B_c \rightarrow \tau\chi)$ , which is possible in upcoming B factories, will provide a good test of this model.

In the second scenario, a cosmogenic UHE sterile neutrino passes through the Earth almost unattenuated and interacts with the matter in Earth to produce an observable  $\tau$ . The same interactions and parameters also explain the  $R(D^{(*)})$  anomaly [18]. The interesting result is that the distribution of emergent  $\tau$  energy peaks in the same regime as observed by ANITA. This model has observable signatures in  $300 \text{ fb}^{-1}$  LHC searches.

In summary, the observation of lepton flavor universality violation and Earth emergent  $\tau$  with EeV energy can be explained in a common framework. Moreover, it has testable signatures in upcoming experiments. Future observations by IceCube Gen-II and data from ANITA-IV should be able to shed more light on such BSM hypotheses.

- 
- [1] P. W. Gorham *et al.* (ANITA Collaboration), *Phys. Rev. Lett.* **117**, 071101 (2016).
  - [2] P. W. Gorham *et al.* (ANITA Collaboration), *Phys. Rev. Lett.* **121**, 161102 (2018).
  - [3] H. Schoorlemmer *et al.*, *Astropart. Phys.* **77**, 32 (2016).
  - [4] D. B. Fox, S. Sigurdsson, S. Shandera, P. Mszros, K. Murase, M. Mostaf, and S. Coutu, [arXiv:1809.09615](https://arxiv.org/abs/1809.09615).
  - [5] J. F. Cherry and I. M. Shoemaker, *Phys. Rev. D* **99**, 063016 (2019).
  - [6] G. Y. Huang, *Phys. Rev. D* **98**, 043019 (2018).
  - [7] J. H. Collins, P. S. Bhupal Dev, and Y. Sui, *Phys. Rev. D* **99**, 043009 (2019).
  - [8] L. A. Anchordoqui and I. Antoniadis, *Phys. Lett. B* **790**, 578 (2019).
  - [9] L. A. Anchordoqui, V. Barger, J. G. Learned, D. Marfatia, and T. J. Weiler, *Lett. High Energy Phys.* **1**, 13 (2018).
  - [10] G. Hiller and F. Kruger, *Phys. Rev. D* **69**, 074020 (2004).
  - [11] M. Huschle *et al.* (Belle Collaboration), *Phys. Rev. D* **92**, 072014 (2015).
  - [12] S. Hirose *et al.* (Belle Collaboration), *Phys. Rev. Lett.* **118**, 211801 (2017).
  - [13] R. Aaij *et al.* (LHCb Collaboration), *Phys. Rev. D* **97**, 072013 (2018).
  - [14] R. Aaij *et al.* (LHCb Collaboration), *J. High Energy Phys.* **08** (2017) 055.
  - [15] D. Buttazzo, A. Greljo, G. Isidori, and D. Marzocca, *J. High Energy Phys.* **11** (2017) 044.
  - [16] N. Assad, B. Fornal, and B. Grinstein, *Phys. Lett. B* **777**, 324 (2018).
  - [17] A. Crivellin, C. Greub, D. Miller, and F. Saturnino, *Phys. Rev. Lett.* **122**, 011805 (2019).

- [18] A. Azatov, D. Barducci, D. Ghosh, D. Marzocca, and L. Ubaldi, *J. High Energy Phys.* **10** (2018) 092.
- [19] A. Angelescu, D. Beirevi, D.A. Faroughy, and O. Sumensari, *J. High Energy Phys.* **10** (2018) 183.
- [20] A. Biswas, D. Kumar Ghosh, N. Ghosh, A. Shaw, and A. K. Swain, [arXiv:1808.04169](https://arxiv.org/abs/1808.04169) [Phys. Rev. D (to be published)].
- [21] B. Bhattacharya, A. Datta, D. London, and S. Shivashankara, *Phys. Lett. B* **742**, 370 (2015).
- [22] M. Bauer and M. Neubert, *Phys. Rev. Lett.* **116**, 141802 (2016).
- [23] S. Fajfer and N. Konik, *Phys. Lett. B* **755**, 270 (2016).
- [24] Y. Sakaki, M. Tanaka, A. Tayduganov, and R. Watanabe, *Phys. Rev. D* **88**, 094012 (2013).
- [25] L. Calibbi, A. Crivellin, and T. Li, *Phys. Rev. D* **98**, 115002 (2018).
- [26] A. Crivellin, D. Mller, and T. Ota, *J. High Energy Phys.* **09** (2017) 040.
- [27] E. Coluccio Leskow, G. D'Ambrosio, A. Crivellin, and D. Mller, *Phys. Rev. D* **95**, 055018 (2017).
- [28] M. Blanke and A. Crivellin, *Phys. Rev. Lett.* **121**, 011801 (2018).
- [29] B. Chauhan and B. Kindra, [arXiv:1709.09989](https://arxiv.org/abs/1709.09989).
- [30] I. Dorner, S. Fajfer, A. Greljo, J. F. Kamenik, and N. Konik, *Phys. Rep.* **641**, 1 (2016).
- [31] D. Bečirević, B. Panes, O. Sumensari, and R. Zukanovich Funchal, *J. High Energy Phys.* **06** (2018) 032.
- [32] D.B. Clark, E. Godat, and F.I. Olness, *Comput. Phys. Commun.* **216**, 126 (2017).
- [33] R. D. Ball *et al.* (NNPDF Collaboration), *Eur. Phys. J. C* **77**, 663 (2017).
- [34] R. D. Ball, V. Bertone, M. Bonvini, S. Marzani, J. Rojo, and L. Rottoli, *Eur. Phys. J. C* **78**, 321 (2018).
- [35] M. Tanabashi *et al.* (Particle Data Group), *Phys. Rev. D* **98**, 030001 (2018).
- [36] A. Alloul, N. D. Christensen, C. Degrande, C. Duhr, and B. Fuks, *Comput. Phys. Commun.* **185**, 2250 (2014).
- [37] I. Dorner and A. Greljo, *J. High Energy Phys.* **05** (2018) 126.
- [38] A. Belyaev, N. D. Christensen, and A. Pukhov, *Comput. Phys. Commun.* **184**, 1729 (2013).
- [39] J. Barranco, O. G. Miranda, C. A. Moura, and A. Parada, *Phys. Lett. B* **718**, 26 (2012).
- [40] B. Chauhan and S. Mohanty, *Phys. Rev. D* **98**, 083021 (2018).
- [41] S. Mohanty, A. Narang, and S. Sadhukhan, *J. Cosmol. Astropart. Phys.* **03** (2019) 041.
- [42] S. Karmakar, S. Pandey, and S. Rakshit, [arXiv:1810.04192](https://arxiv.org/abs/1810.04192).
- [43] L. Heurtier, Y. Mambrini, and M. Pierre, [arXiv:1902.04584](https://arxiv.org/abs/1902.04584) [Phys. Rev. D (to be published)].

## Signature of light sterile neutrinos at IceCube

Bhavesh Chauhan<sup>\*</sup>

*Physical Research Laboratory, Ahmedabad 380009, India  
and Indian Institute of Technology Gandhinagar, Palaj 382355, Gandhinagar, India*

Subhendra Mohanty<sup>†</sup>

*Physical Research Laboratory, Ahmedabad 380009, India*



(Received 30 August 2018; published 25 October 2018)

The MiniBooNE collaboration has recently reported evidence for a light sterile neutrino with large mixing angles, thus corroborating the measurement by LSND twenty years ago. Such a state would be directly in conflict with Planck measurement of big bang nucleosynthesis  $N_{\text{eff}}$  unless there is self-interaction in the sterile sector. Our objective is to investigate if such interactions could result in resonant absorption in the cosmogenic neutrino spectrum and its consequences for the IceCube experiment. We show that it is possible to give independent bounds on sterile neutrino parameter space from IceCube observations with the dips in the spectrum corresponding to the neutrino masses.

DOI: [10.1103/PhysRevD.98.083021](https://doi.org/10.1103/PhysRevD.98.083021)

### I. INTRODUCTION

The MiniBooNE collaboration has recently reported excess in the electron neutrino and antineutrino appearance channels that is consistent with the sterile neutrino hypothesis [1]. The best-fit point,

$$\Delta m_{41}^2 = 0.041 \text{ eV}^2 \quad \text{and} \quad \sin^2(2\theta_{\mu e}) = 0.958, \quad (1)$$

is consistent with the earlier measurements by the LSND collaboration [2]. In fact, the combined significance of the two data sets is  $6.1\sigma$ . These results, however, are in tension with data from disappearance experiments like MINOS+ and IceCube. Other experiments like KARMEN and OPERA have not been able to confirm this excess, but they do not rule it out completely either [3].

The existence of such light states with large mixing angles is also in conflict with cosmology. The Planck measurement cosmic microwave background (CMB) anisotropy puts severe constraints on the number of thermalized relativistic degrees of freedom ( $N_{\text{eff}}$ ) around the epoch of big bang nucleosynthesis (BBN), i.e.,  $T_\gamma = 1 \text{ MeV}$  [4]. One possible resolution to this puzzle is to assume self-interactions in the sterile sector [5–10].

Because of the large thermal effective potential, the mixing between sterile and active neutrino is suppressed in the early universe but is allowed to be large today. Hence the sterile neutrinos are produced efficiently only at low temperatures after recoupling [11]. This provides a very strong constraint that the  $T_{\text{rec}} < 1 \text{ MeV}$ , which rules out small gauge couplings in the sterile sector [6]. Because of mixing, the lighter neutrinos also interact with the new gauge boson, which affects their free streaming in the early universe, which is constrained from CMB [12,13]. It was recently pointed out that taking constraints from  $\sum m_\nu$  rules out any viable parameter space for  $m_s > 0.2 \text{ eV}$  [14]. However, the authors also propose several scenarios that weaken these new constraints. For gauge coupling in the range 0.1–1, one requires a gauge boson of mass 10–50 MeV to reconcile sterile neutrinos with cosmology. Moreover, such interactions can also be mediators to dark matter, which can simultaneously solve the small-scale crisis of  $\Lambda\text{CDM}$  [10,15,16].

It was shown in [17] that MeV scale secret interaction of neutrinos gives rise to absorption lines in the very high energy neutrino spectrum. Such lines can be seen by neutrino telescopes like IceCube. The IceCube HESE data have featured a prominent gap in the spectrum for neutrino energies in the range 400–800 TeV [18–20]. In the past, several authors have tried to explain this gap using resonant absorption in well-motivated models such as  $\nu 2\text{HDM}$  [17] and gauged  $U(1)_{L_\mu-L_\tau}$  [21]. Recently it was also proposed that one can explain the absence of Glashow resonance using t-channel resonant absorption [22]. All these explanations assume a flavor-universal single power law flux for incoming neutrinos. The IceCube data can also be

<sup>\*</sup>bhavesh@prl.res.in

<sup>†</sup>mohanty@prl.res.in

*Published by the American Physical Society under the terms of the Creative Commons Attribution 4.0 International license. Further distribution of this work must maintain attribution to the author(s) and the published article's title, journal citation, and DOI. Funded by SCOAP<sup>3</sup>.*

explained by decaying dark matter [23–28], leptoquark like states [29–33], and by modifying assumptions of the source. The leptoquark explanation is highly constrained from LHC data [33–35].

In this paper, we look at resonant absorption of cosmogenic neutrinos from both cosmic neutrino and sterile neutrino background. In Sec. II we describe the model for sterile neutrino with self-interactions. In Sec. III, we discuss the basics of neutrino absorption and explain a few benchmark scenarios. In Sec. IV we look at the six-year IceCube data and provide some constraints on the model. We also provide the parameter space favored by IceCube independent of other short baseline experiments. In Sec. V we provide the results and discuss certain aspects of the analysis before we conclude.

## II. MODEL DESCRIPTION AND COSMOLOGICAL CONSTRAINTS

To accommodate light sterile neutrino with cosmology, we extend the standard model by introducing a left-handed sterile neutrino ( $\nu_s$ ), which is charged under an additional gauge symmetry  $U(1)_X$ . The new gauge boson ( $X_\mu$ ) would acquire its mass through spontaneous symmetry breaking in the hidden sector. The scalar responsible for the phase transition can also thermalize the sterile sector in the early universe through Higgs' portal. The requirement of anomaly cancellation needs additional fermions in the spectrum that can be a dark matter candidate. However, for our analysis, we only focus on the sterile neutrino and its interactions.

The relevant part of the Lagrangian is the gauge interaction of the sterile neutrino, which is given by

$$-\mathcal{L}_s = g_X \bar{\nu}_s \gamma^\mu P_L \nu_s X_\mu. \quad (2)$$

In terms of mass eigenstates,

$$-\mathcal{L}_s = \sum_{i,j} g_{ij} \bar{\nu}_i \gamma^\mu P_L \nu_j X_\mu, \quad (3)$$

where  $g_{ij} = g_X U_{si}^* U_{sj}$ . The  $4 \times 4$  Pontecorvo-Maki-Nakagawa-Sakata matrix is parametrized as

$$U = R_{34} R_{24} R_{14} R_{23} R_{13} R_{12}, \quad (4)$$

where  $R_{ij}$  is the rotation matrix in the  $i$ - $j$  plane. We assume that the elements of the mixing matrix are real as a contribution of the phases is negligible for the discussion that follows. We also fix the active neutrino mixing angles to the best-fit values from the oscillation measurements [36],

$$\theta_{12} = 33.62^\circ \quad \theta_{23} = 47.2^\circ \quad \theta_{13} = 8.54^\circ. \quad (5)$$

We have six free parameters in our model,

$$\mathcal{P} = \{\theta_{14}, \theta_{24}, \theta_{34}, m_4, g_X, M_X\}, \quad (6)$$

where  $m_4$  is the mass of the fourth (mostly sterile) mass eigenstate and  $M_X$  is the mass of the new gauge boson.

The introduction of self-interactions generates a finite temperature effective potential for the sterile neutrino of the form [10]

$$V_{\text{eff}} = \begin{cases} -\frac{28\pi^3 \alpha_X E T_s^4}{45 M_X^4} & E, T_s \ll M \\ +\frac{\pi \alpha_X T_s^2}{2E} & E, T_s \gg M, \end{cases} \quad (7)$$

which modifies the effective mixing angle given by

$$\sin^2(2\theta_m) = \frac{\sin^2(2\theta_0)}{(\cos(2\theta_0) + \frac{2E}{\Delta m^2} V_{\text{eff}})^2 + \sin^2(2\theta_0)}. \quad (8)$$

In the early universe when the temperature is high, the mixing angle is suppressed and the production rate of the sterile neutrino is negligible. As the Universe cools, the sterile sector recouples to the standard model bath. If the recoupling temperature is  $> \text{MeV}$ , then the sterile neutrinos are thermalized before the big bang nucleosynthesis takes place. Since they are relativistic during BBN, there are very stringent constraints from Planck. Hence, one requires the recoupling temperature to be less than an MeV. In [14] it was shown that the entire parameter space for the scenario is ruled out for  $m_4 \geq 1 \text{ eV}$ . However, it was also pointed out that there are several possible new physics effects that can alleviate these bounds. One of the plausible scenarios is where one adds new lighter particles in the model.

## III. NEUTRINO ABSORPTION BY COSMIC NEUTRINO BACKGROUND

Until very recently, the source of ultrahigh energy neutrinos was unknown. Advances in multimessenger astronomy have pointed towards blazars as possible sources [37]. During propagation through the cosmic media, these neutrinos can get resonantly scattered off the cosmic neutrino background, which results in an absorption line in the neutrino spectrum. If only standard model interactions are considered, the absorption line ( $\sim 10^{13} \text{ GeV}$ ) is undetectable at neutrino telescopes [38]. However, it has been known that secret interaction of the neutrino can also give rise to these lines, which should, in principle, be detectable [39–41]. The absorption lines from sterile neutrino were first pointed out in [42], and the authors of [43] applied it in the context of diffuse supernova background. In this paper, we attempt to explain the two dips in the IceCube spectrum using resonant absorption by heavy (mostly) sterile neutrino and the heaviest active neutrino.

We have assumed that, due to recoupling of the sterile neutrinos, the neutrino background has all four mass eigenstates in equal proportions and at the same temperature. For the benchmark scenarios considered in the paper, the recoupling is guaranteed [6]. The scattering cross section is

$$\sigma_{ij} = \sigma(\bar{\nu}_i \nu_j \rightarrow \bar{\nu} \nu) = \frac{1}{6\pi} |g_{ij}|^2 g_X^2 \frac{s}{(s - m_X^2)^2 + m_X^2 \Gamma_X^2}, \quad (9)$$

where  $\nu_i$  are the mass eigenstates of the four neutrino species and  $\Gamma_X = g_X^2 m_X / 12\pi$  is the decay width of the new boson. The mean free path is

$$\lambda_i(E_i, z) = \left( \sum_j \int \frac{d^3\mathbf{p}}{(2\pi)^3} f_j(p, z) \sigma_{ij}(p, E_i, z) \right)^{-1} \\ \approx \left( n_\nu(z) \sum_j \sigma_{ij}(p, E_i, z) \right)^{-1}, \quad (10)$$

where  $f_i$  is the distribution function for the neutrinos given by

$$f_i(p, z)^{-1} = \exp\left(\frac{p}{T_i(1+z)}\right) + 1 \quad (11)$$

and  $T_i = 1.95$  K for all four components. The approximation in the rhs of Eq. (10) is valid only when the neutrino is nonrelativistic. The oscillation data suggest that at least two active neutrinos are nonrelativistic today. As we see, the lightest neutrino gives the absorption feature for higher energies and is inconsequential to our discussion. For the remainder of the paper, we assume normal hierarchy and neutrino masses to be

$$m_1 = 5 \times 10^{-3} \text{ eV}, \quad m_2 = 1 \times 10^{-2} \text{ eV}, \\ m_3 = 5 \times 10^{-2} \text{ eV}. \quad (12)$$

The case of inverted hierarchy is commented upon at the end of this section. One can see that

$$m_i \gg \langle p \rangle = 3T_\nu \sim 5.3 \times 10^{-4} \text{ eV} \quad \forall i, \quad (13)$$

which allows us to approximate

$$s = 2E_i(1+z)(\sqrt{p^2 + m_i^2} - p \cos[\theta]) \approx 2E_i(1+z)m_i. \quad (14)$$

The  $z$  dependence accounts for redshift during propagation. The survival rate of the neutrino is given as [41,44]

$$R_i = \exp\left[-\int_0^{z_s} \frac{1}{\lambda_i(1+z)} \frac{dL}{dz} dz\right], \quad (15)$$

where  $z_s$  denotes the redshift distance to the source and

$$\frac{dL}{dz} = \frac{c}{H_0 \sqrt{\Omega_m(1+z)^3 + \Omega_\Lambda}}. \quad (16)$$

We have fixed the cosmological parameters to  $\Omega_m = 0.315$ ,  $\Omega_\Lambda = 0.685$ ,  $H_0 = 67.3$  km/s/Mpc using the best-fit values from Planck [4]. We also assume a power-law flux for each neutrino near the source. The flux of neutrino of flavor  $\alpha \in e, \mu, \tau, s$  at Earth is

$$\phi_\alpha = \sum_{j=1}^4 |U_{\alpha j}|^2 \phi_j R_j = (\phi_0 E_\nu^{-\gamma}) \sum_{j=1}^4 |U_{\alpha j}|^2 R_j \equiv (\phi_0 E_\nu^{-\gamma}) R_\alpha. \quad (17)$$

Since the sterile neutrino does not generate any signal at the IceCube detector, the flux of neutrinos that can be seen by IceCube is simply

$$\phi = \phi_e + \phi_\mu + \phi_\tau \\ = (\phi_0 E_\nu^{-\gamma}) \left( \sum_{f=e,\mu,\tau} \sum_{j=1}^4 |U_{fj}|^2 R_j \right) \\ \equiv \phi_0 E_\nu^{-\gamma} \langle R(\mathcal{P}, E_\nu) \rangle, \quad (18)$$

where the parentheses in the last part indicate that  $\langle R \rangle$  depends on the model parameters and incident neutrino energy only.

In Fig. 1, we have shown the variation of  $R_\alpha$  and  $R_i$  for a benchmark scenario. The gauge coupling is fixed to be  $g_X = 0.1$  and the mass of the gauge boson is fixed to be  $M_X = 25$  MeV. We have assumed that the neutrino sources are localized around  $z_s = 0.3$ . There are three features we would like to highlight: (a) There are two prominent dips in the function. The one at lower neutrino energy is associated with the absorption due to heavy (i.e., mostly sterile) mass eigenstate. The second dip is due to the absorption by the heaviest active neutrino (i.e.,  $m_3$  in NH). (b) The dips are not very sharp and there is a broadening due to redshift during propagation. For a source located at  $z_s$ , the dip in the spectrum occurs for the neutrino energies

$$E_{\text{dip}} : \frac{E^{\text{res}}}{(1+z_s)} \rightarrow E^{\text{res}}, \quad (19)$$

where  $E^{\text{res}} = M_X^2 / 2m_i$ . This allows us to estimate the width of the dip as

$$\Delta^i \approx \frac{M_X^2}{2m_i} \frac{z_s}{1+z_s}. \quad (20)$$

(c) Since the other active neutrinos are lighter, their absorption lines are at much higher neutrino energies. Hence, it is inconsequential for our analysis whether the lightest neutrino is relativistic or nonrelativistic today.

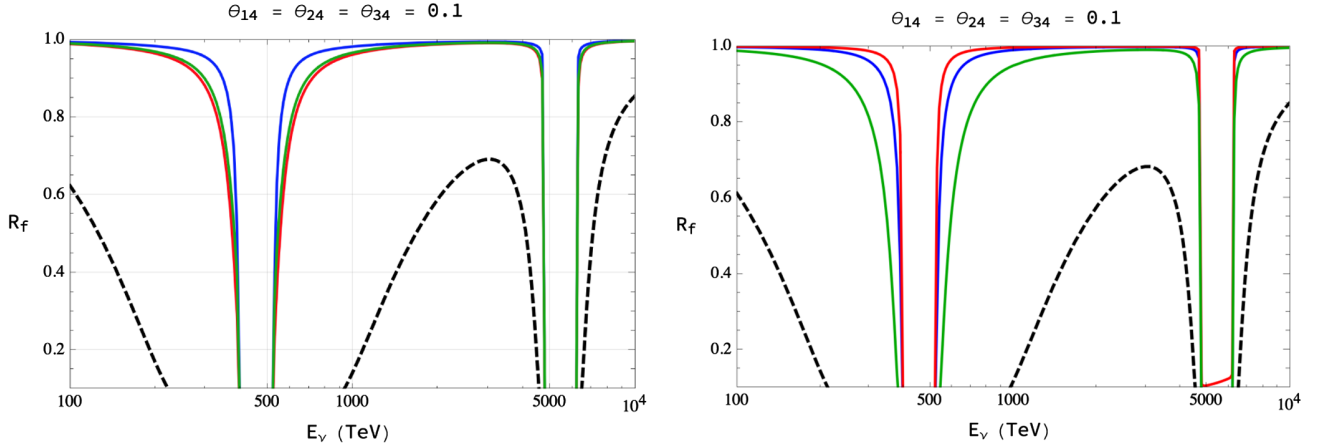


FIG. 1. Left: This plot shows variation of  $R_e$  (blue),  $R_\mu$  (red),  $R_\tau$  (green), and  $R_s$  (black, dashed) with neutrino energy. Right: This plot shows variation of  $R_1$  (blue),  $R_2$  (red),  $R_3$  (green), and  $R_4$  (black, dashed) with neutrino energy. See text for details.

The absorption lines are sensitive to the distance to the source. It can be inferred from (20) that the further the source, the broader the absorption line. We have assumed that the ultra-high energy (UHE) neutrinos originate from blazars and non-blazar active galactic nuclei as opposed to spatially distributed sources like dark matter decay [37,45–48]. Future multimessenger observations will help us verify this hypothesis. For this analysis we assume that the sources are localized around a particular redshift,  $\langle z_s \rangle$ , which makes the calculations simple. The complete analysis that also considers distribution of the sources is beyond the scope of this work. Also note that any source located very far from Earth ( $z_s > 5$ ) will have too broad absorption lines and contribute negligibly to the flux at high energies ( $> 200$  TeV). This may be compatible with the fact that IceCube rarely sees events of such high energies. This inference cannot be made in the standard picture without secret interactions. Thus, if future multimessenger observations infer that almost all the sources of UHE neutrinos are localized within a sphere, it will strongly hint at resonant absorption.

#### IV. CONSTRAINTS FROM FLUX OF NEUTRINOS AT ICECUBE

In IceCube six-year HESE data, 82 events passed the selection criterion of which two are co-incident with atmospheric muons and left out [20]. The best fit for single power-law flux is

$$E_\nu^2 \phi = (2.46 \pm 0.8) \times 10^{-8} \left( \frac{E_\nu}{100 \text{ TeV}} \right)^{-0.92} \text{ GeV cm}^{-2} \text{ s}^{-1} \text{ sr}^{-1}, \quad (21)$$

which has a softer spectral index than the 3-year ( $\gamma = 2.3$ ) [18] as well as the 4-year ( $\gamma = 2.58$ ) data [19]. One can attribute this to the pileup of low energy events along with

the lack of high energy events in the new data. A prominent feature that still remains is the apparent lack of neutrinos with energy 400–800 TeV. From one point of view, one should be able to see these neutrinos with more exposure. However, this may also hint at new physics. Another puzzling mystery is the absence of Glashow resonance. In the standard model, the astrophysical neutrino can interact with the electrons in the detector volume and produce an on-shell W-boson. This happens for neutrino energy  $\sim 6.3$  PeV. Around this energy, the cross section for neutrino-electron scattering is several orders of magnitude larger than the charged and neutral current interactions with nucleons. Thus we expect more numbers of events in the 3.6 to 7.5 PeV bin. Because of this, the best fits to the data hint towards a softer spectral index. Several scenarios have been proposed to address the absence of Glashow events including active neutrino decay,  $\Delta^+$  resonance, and novel flux [49–51].

Now we examine the  $m_s - M_X$  parameter space that can explain the observed IceCube spectrum. The following constraints are imposed.

- (1) If  $E^{\text{res}} \sim \text{PeV}$ , one cannot explain the observed PeV events at IceCube unless exceptional circumstances are evoked. To be general, we constrain the  $m_3$  absorption line to be more than 3 PeV. Because of the broadening during propagation, the constraint depends on  $\langle z_s \rangle$  as

$$M_X^2 \geq 2 \times 3 \text{ PeV } m_3 (1 + \langle z_s \rangle). \quad (22)$$

This is shown in Fig. 2 as a region bounded by green lines.

- (2) Since we wish to explain the dip in the spectrum using the fourth neutrino, we require

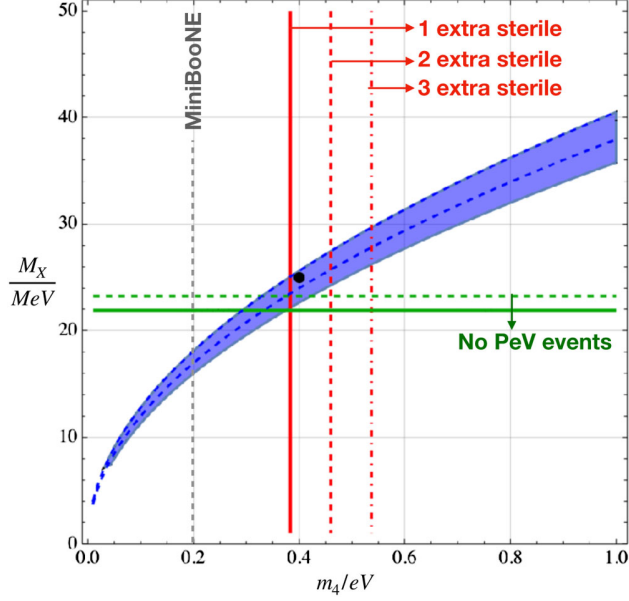


FIG. 2. The shaded blue region with solid (dashed) boundaries can explain the 400–800 TeV dip in the IceCube spectrum assuming that the sources are distributed around  $z = 0.6$  (0.8). The solid (dashed) green lines denote the upper bound on the X boson mass such that the gap due to heaviest active neutrino is above 3 PeV assuming source distribution around  $z = 0.6$  (0.8). The green arrows indicate the region that is disfavored. The red lines (solid, dashed, dot-dashed) denote the number of additional light particles (1, 2, 3) to be added to the theory to evade  $\sum m_\nu$  constraints. The black point shows the benchmark case considered in the paper. The MiniBooNE best fit is highlighted. See the text for more details.

$$E^{\text{res}} \leq 800 \text{ TeV} \quad \& \quad \frac{E^{\text{res}}}{1 + \langle z_s \rangle} \geq 400 \text{ TeV}, \quad (23)$$

which is shown as the blue shaded region in Fig. 2.

- (3) We show the region in the parameter space that requires more than 1, 2, and 3 lighter sterile neutrinos in the full theory [cf., Eq. (10)].

It can be seen from Fig. 2 that only a small portion of the parameter space is compatible with all the constraints. With slightly relaxed assumptions, we chose the representative point

$$m_4 = 0.4 \text{ eV} \quad \& \quad M_X = 25 \text{ MeV} \quad (24)$$

for our analysis. The gauge coupling is constrained from the restrictions on the recoupling temperature. We have chosen the benchmark point  $g_X = 0.1$ , which is consistent.

For the choice of mixing angles, we have considered two scenarios,

$$\text{Case I: } \theta_{14} = \theta_{24} = \theta_{34} = 0.3 \quad \dots (\text{democratic}), \quad (25)$$

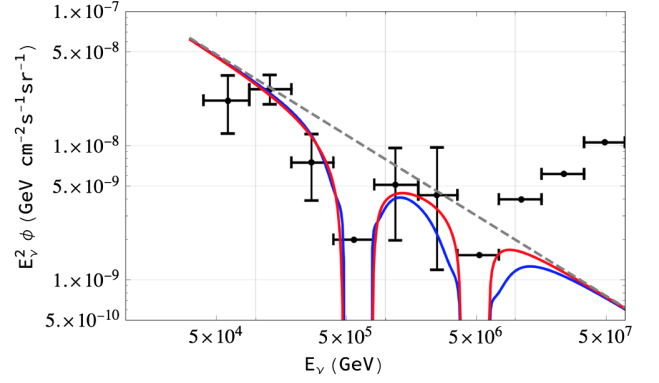


FIG. 3. The flux without attenuation is shown as the dashed gray curve. The blue (red) curve is the flux with attenuation for the democratic (maximal) case. The spectral index is chosen to be 2.6 and the normalization is fixed from the second bin. Sources are assumed to be distributed around  $z = 0.6$ .

$$\text{Case II: } \theta_{14} = \theta_{24} = \pi/4 \quad \& \quad \theta_{34} = 0 \quad \dots (\text{maximal}). \quad (26)$$

For the democratic case, we have checked that the choice 0.3 gives the best fit to the data. The maximal case is motivated by the mixing angles observed by MiniBooNE. We have chosen the spectral index to be 2.6, which is consistent with IceCube best fits. Any softer spectral index will result in reducing the flux of PeV neutrinos, which is unwanted. For harder spectral index, one needs to assume larger values of  $\langle z_s \rangle$  to be compatible. The attenuated flux is shown in Fig. 3.

## V. CONCLUSION

To reconcile a light sterile neutrino of the type observed by MiniBooNE with BBN predictions, one must introduce gauge or scalar mediated interactions between the sterile neutrinos. Because of the lightness of the mediators required, there are observable effects in the spectrum of high energy neutrinos detected by IceCube. We have shown that the gaps in the spectrum at 400–800 TeV as well as beyond 2.6 PeV correspond to resonant absorption of two heaviest mass eigenstates. The prediction for the model at IceCube is peaks beyond 6.3 PeV and dips corresponding to two lighter neutrino mass states. These features may be observable in future IceCube data. A generic feature of absorption during propagation is that energy gap in the spectrum widens with distance to the source. This renders IceCube invisible to  $\nu$  sources beyond a certain  $z_{\text{max}}$ . Future multimessenger observations should be able to confirm this.

- [1] A. A. Aguilar-Arevalo *et al.* (MiniBooNE Collaboration), [arXiv:1805.12028](#).
- [2] A. A. Aguilar-Arevalo *et al.* (LSND Collaboration), *Phys. Rev. D* **64**, 112007 (2001).
- [3] M. Dentler, Á. Hernández-Cabezudo, J. Kopp, P. Machado, M. Maltoni, I. Martínez-Soler, and T. Schwetz, *J. High Energy Phys.* **08** (2018) 010.
- [4] N. Aghanim *et al.* (Planck Collaboration), [arXiv:1807.06209](#).
- [5] S. Hannestad, R. S. Hansen, and T. Tram, *Phys. Rev. Lett.* **112**, 031802 (2014).
- [6] X. Chu, B. Dasgupta, and J. Kopp, *J. Cosmol. Astropart. Phys.* **10** (2015) 011.
- [7] M. Archidiacono, S. Hannestad, R. S. Hansen, and T. Tram, *Phys. Rev. D* **91**, 065021 (2015).
- [8] M. Archidiacono, S. Hannestad, R. S. Hansen, and T. Tram, *Phys. Rev. D* **93**, 045004 (2016).
- [9] M. Archidiacono, S. Gariazzo, C. Giunti, S. Hannestad, R. Hansen, M. Laveder, and T. Tram, *J. Cosmol. Astropart. Phys.* **08** (2016) 067.
- [10] B. Dasgupta and J. Kopp, *Phys. Rev. Lett.* **112**, 031803 (2014).
- [11] N. Saviano, O. Pisanti, G. Mangano, and A. Mirizzi, *Phys. Rev. D* **90**, 113009 (2014).
- [12] A. Mirizzi, G. Mangano, O. Pisanti, and N. Saviano, *Phys. Rev. D* **91**, 025019 (2015).
- [13] F. Forastieri, M. Lattanzi, G. Mangano, A. Mirizzi, P. Natoli, and N. Saviano, *J. Cosmol. Astropart. Phys.* **07** (2017) 038.
- [14] X. Chu, B. Dasgupta, M. Dentler, J. Kopp, and N. Saviano, [arXiv:1806.10629](#).
- [15] B. Chauhan, *Phys. Rev. D* **97**, 123017 (2018).
- [16] T. Bringmann, J. Hasenkamp, and J. Kersten, *J. Cosmol. Astropart. Phys.* **07** (2014) 042.
- [17] M. Ibe and K. Kaneta, *Phys. Rev. D* **90**, 053011 (2014).
- [18] M. G. Aartsen *et al.* (IceCube Collaboration), *Phys. Rev. Lett.* **113**, 101101 (2014).
- [19] M. G. Aartsen *et al.* (IceCube Collaboration), [arXiv:1510.05223](#).
- [20] D. Williams (IceCube Collaboration), *Int. J. Mod. Phys. Conf. Ser.* **46**, 1860048 (2018).
- [21] T. Araki, F. Kaneko, Y. Konishi, T. Ota, J. Sato, and T. Shimomura, *Phys. Rev. D* **91**, 037301 (2015).
- [22] S. Mohanty, A. Narang, and S. Sadhukhan, [arXiv:1808.01272](#).
- [23] A. Bhattacharya, R. Gandhi, A. Gupta, and S. Mukhopadhyay, *J. Cosmol. Astropart. Phys.* **05** (2017) 002.
- [24] A. Bhattacharya, A. Esmaili, S. Palomares-Ruiz, and I. Sarcevic, *J. Cosmol. Astropart. Phys.* **07** (2017) 027.
- [25] M. Dhuria and V. Rentala, *J. High Energy Phys.* **09** (2018) 004.
- [26] C. Rott, K. Kohri, and S. C. Park, *Phys. Rev. D* **92**, 023529 (2015).
- [27] P. S. B. Dev, D. Kazanas, R. N. Mohapatra, V. L. Teplitz, and Y. Zhang, *J. Cosmol. Astropart. Phys.* **08** (2016) 034.
- [28] Y. Sui and P. S. Bhupal Dev, *J. Cosmol. Astropart. Phys.* **07** (2018) 020.
- [29] L. A. Anchordoqui, C. A. Garcia Canal, H. Goldberg, D. Gomez Dumm, and F. Halzen, *Phys. Rev. D* **74**, 125021 (2006).
- [30] V. Barger and W. Y. Keung, *Phys. Lett. B* **727**, 190 (2013).
- [31] P. S. B. Dev, D. K. Ghosh, and W. Rodejohann, *Phys. Lett. B* **762**, 116 (2016).
- [32] U. K. Dey and S. Mohanty, *J. High Energy Phys.* **04** (2016) 187.
- [33] N. Mileo, A. de la Puente, and A. Szykman, *J. High Energy Phys.* **11** (2016) 124.
- [34] B. Chauhan, B. Kindra, and A. Narang, *Phys. Rev. D* **97**, 095007 (2018).
- [35] U. K. Dey, D. Kar, M. Mitra, M. Spannowsky, and A. C. Vincent, *Phys. Rev. D* **98**, 035014 (2018).
- [36] I. Esteban, M. C. Gonzalez-Garcia, M. Maltoni, I. Martínez-Soler, and T. Schwetz, *J. High Energy Phys.* **01** (2017) 087.
- [37] M. G. Aartsen *et al.* (IceCube, Fermi-LAT, MAGIC, AGILE, ASAS-SN, HAWC, H.E.S.S., INTEGRAL, Kanata, Kiso, Kapteyn, Liverpool Telescope, Subaru, Swift NuSTAR, VERITAS, and VLA/17B-403 Collaborations) *Science* **361**, eaat1378 (2018).
- [38] T. J. Weiler, *Phys. Rev. Lett.* **49**, 234 (1982).
- [39] K. C. Y. Ng and J. F. Beacom, *Phys. Rev. D* **90**, 065035 (2014); **90**, 089904(E) (2014).
- [40] K. Ioka and K. Murase, *Prog. Theor. Exp. Phys.* **2014**, 61E01 (2014).
- [41] K. Blum, A. Hook, and K. Murase, [arXiv:1408.3799](#).
- [42] J. F. Cherry, A. Friedland, and I. M. Shoemaker, [arXiv:1605.06506](#).
- [43] Y. S. Jeong, S. Palomares-Ruiz, M. H. Reno, and I. Sarcevic, *J. Cosmol. Astropart. Phys.* **06** (2018) 019.
- [44] A. DiFranzo and D. Hooper, *Phys. Rev. D* **92**, 095007 (2015).
- [45] F. Krau *et al.*, *Astron. Astrophys.* **566**, L7 (2014).
- [46] S. Sahu, L. S. Miranda, and A. Rosales De Len, *Proc. Sci. NEUTEL2017* (2018) 079.
- [47] L. S. Miranda, A. R. de Len, and S. Sahu, *Eur. Phys. J. C* **76**, 402 (2016).
- [48] D. Hooper, T. Linden, and A. Viereg, [arXiv:1810.02823](#).
- [49] S. Pakvasa, A. Joshipura, and S. Mohanty, *Phys. Rev. Lett.* **110**, 171802 (2013).
- [50] S. Sahu and B. Zhang, *J. High Energy Astrophys.* **18**, 1 (2018).
- [51] M. D. Kistler and R. Laha, *Phys. Rev. Lett.* **120**, 241105 (2018).

**Sub-MeV self-interacting dark matter**

Bhavesh Chauhan\*

*Physical Research Laboratory, Ahmedabad 380009, India  
and Indian Institute of Technology Gandhinagar, Palaj 382355, Gandhinagar, India*

(Received 20 November 2017; published 29 June 2018)

In this paper, we present a model for sub-MeV dark matter with strong self-interactions which can solve some of the small-scale crisis of the  $\Lambda$ CDM. The dark matter is a Majorana fermion with only off-diagonal interactions with a hidden  $U(1)_D$  gauge boson. The relic density is obtained by freeze-out of Boltzmann suppressed annihilations to a light fermionic species. The self-interaction is a one-loop process and constrained to be between 0.1 to 1  $\text{cm}^2/\text{g}$ . Severe constraints from the BBN on  $N_{\text{eff}}$  require that the dark and visible sector are not in thermal equilibrium during freeze-out. The effect of this temperature asymmetry is studied.

DOI: 10.1103/PhysRevD.97.123017

**I. INTRODUCTION**

For the past few decades, we have extensively studied the gravitational interaction of Dark Matter (DM) and very little doubt remains of its existence (for an overview, see [1–6] and references therein). However, the particle nature of DM remains a mystery and we have no clue about its mass, spin, and interactions with other elementary particles. During the early days, weakly interacting massive particles (WIMPs) were postulated to be DM candidate but recent bounds from null results of terrestrial experiments have ruled out almost all of the interesting parameter space [7]. Several new candidates have been proposed recently which get the correct relic abundance and are consistent with present detector bounds.

One of the simple solutions is to assume that the DM is light i.e., its mass is in the sub-GeV domain. In this limit, the local DM cannot produce sufficient recoil and thus will remain undetected in the traditional detectors. It has been proposed that electron recoil can be used to probe this parameter space [8–10]. From the model building perspective, it was recently proposed that the 3-to-2 and 4-to-2 annihilations may be important for MeV and keV scale DM respectively [11]. Several interesting follow ups to this paradigm can be found in [12–23]. One of the biggest issues with a sub-MeV DM is the conflict with the effective number of relativistic species ( $N_{\text{eff}}$ ) during the big bang nucleosynthesis (BBN) era [24]. To be consistent, one can

assume that the dark sector has lower temperature than the standard model (SM) bath [25–28], or that it freezes-in after the BBN [29].

The standard model of cosmology,  $\Lambda$ CDM, has been hugely successful in explaining majority of the observed astrophysical phenomenon. However, the assumption of cold collision-less DM runs into what is dubbed as the “small-scale crisis.” The most prominent issues are the “core vs cusp” problem, the missing satellite problem, and the “too-big-to-fail” problem. While individual resolutions to all the problems are possible, the assumption of self-interacting DM can solve some of these problems simultaneously [30–40]. However, observation of galaxy cluster collisions puts a strong bound on this self-interaction. For a recent review, one can refer to [41] and references therein. For our analysis, we take the often used limit  $\sigma_{\text{SI}}/m \sim 0.1\text{--}1 \text{ cm}^2/\text{g}$ .

The outline of this paper is as follows. In Sec. II, we define the low-energy limit of the interaction Lagrangian and find the relic density and self-interaction in the model. In Sec. III, we study the results and discuss the allowed parameter space before we conclude in Sec. IV.

**II. MODEL DESCRIPTION**

In this paper, we will consider the dark sector to be thermally decoupled from the standard model [42–45]. The temperature asymmetry is characterized by the parameter  $\xi = (T_d/T_{\text{SM}}) \leq 1$ . Such a decoupling can be achieved if the interactions responsible for thermal equilibrium between the two sectors freeze out at high temperatures. In the absence of such interactions, one can postulate that the two sectors have been populated at different temperatures during reheating [46]. Because of this temperature asymmetry, smaller mass for DM are allowed which is otherwise strictly constrained from the BBN  $N_{\text{eff}}$ .

\*bhavesh@prl.res.in

*Published by the American Physical Society under the terms of the Creative Commons Attribution 4.0 International license. Further distribution of this work must maintain attribution to the author(s) and the published article's title, journal citation, and DOI. Funded by SCOAP<sup>3</sup>.*

We take DM to be Dirac fermion charged under a dark Abelian symmetry— $U(1)_D$ . The gauge boson of this new symmetry,  $Z'$ , acquires a mass from a high-scale spontaneous symmetry breaking. This transition is also responsible for generating a Majorana mass term which splits the dark fermion into two Majorana fermions ( $\chi_1$  and  $\chi_2$ ) with a mass gap [47–51]. The lighter of the two Majorana states (say,  $\chi_1$ ) will act as DM in this model. In this mass basis, the coupling of  $Z'$  is purely off-diagonal as the Majorana states cannot carry any conserved quantum number. We add a light (almost massless) right-handed Dirac fermion ( $f$ ) which is also charged under  $U(1)_D$ . The Majorana mass term for this light fermion can be avoided either by charge assignments or by assuming additional global symmetries. A detailed model is presented in the Appendix.

In the simplified picture, the interaction Lagrangian is given by

$$\mathcal{L} \supset -ig_D Z'_\mu (\bar{\chi}_1 \gamma^\mu \chi_2 + \bar{f} \gamma^\mu f), \quad (1)$$

where the coupling constant  $g_D \approx 1$  ( $\alpha_D = g_D^2/4\pi \approx 0.1$ ) for remainder of this paper. We assume the mass hierarchy

$$m_f \approx 0 \ll m_\chi = m_1 < m_2 = m_1(1 + \delta) \ll m_{Z'}. \quad (2)$$

As the fermions masses are in the sub-MeV domain and  $\xi$  are not infinitesimally small, these particles contribute to the effective relativistic degrees of freedom during the BBN era as

$$N_{\text{eff}} = 3.046 + 2 \times \left(\frac{11}{4}\right)^{4/3} \xi^4. \quad (3)$$

The analysis of the Planck data indicated that  $N_{\text{eff}} = 3.15 \pm 0.23$  [52] which translates to  $\xi \leq 0.45(0.52)$  at  $1\sigma(2\sigma)$  level. However, if alternative cosmologies are taken into account, these constraints can be either severe or relaxed [53]. Hence, for our analysis, we take two benchmark scenarios  $\xi = 0.5$  and  $\xi = 0.3$  as we do not comment upon the source of this anisotropy.

### A. Relic density from coannihilation

In this model, the relic density for  $\chi_1$  is obtained from the coannihilations  $\chi_1 \chi_2 \rightarrow f_1 f_2$  (Fig. 1). The importance of coannihilations has been known for a long time [54], and novel applications were recently realized in [55–57]. We follow the prescription in [54] and important steps are mentioned for completeness. As  $\chi_2$  can decay into  $\chi_1$  via  $\chi_2 \rightarrow \chi_1 \bar{f} f$ , the coupled Boltzmann equations for tracking abundances of  $\chi_1$  and  $\chi_2$  are approximated by a single differential equation for the total number density  $n = n_1 + n_2$  where  $n_1$  and  $n_2$  are the number densities of  $\chi_1$  and  $\chi_2$  respectively [58]. During late times,  $n$  is dominated by  $n_1$  as most of  $\chi_2$  has decayed. The Boltzmann equation for  $n$  is

$$\frac{dn}{dt} + 3Hn = -\langle \sigma v \rangle_{\text{eff}} (n^2 - \bar{n}^2), \quad (4)$$

where the bar indicates the equilibrium density and

$$\langle \sigma v \rangle_{\text{eff}} = \sum_{ij} \langle \sigma_{ij} v_{ij} \rangle \frac{\bar{n}_i \bar{n}_j}{\bar{n}^2}. \quad (5)$$

Due to the off-diagonal interactions of  $Z'$ , processes such as  $\chi_1 \chi_1 \rightarrow \bar{f} f$  are forbidden at tree level, and the only annihilation channel is  $\chi_1 \chi_2 \rightarrow \bar{f} f$ . Thus, the effective cross section is given as

$$\langle \sigma v \rangle_{\text{eff}} = 2 \langle \sigma_{12} v_{12} \rangle \frac{\bar{n}_1 \bar{n}_2}{\bar{n}^2} \approx 2 \langle \sigma_{12} v_{12} \rangle \frac{\bar{n}_2}{\bar{n}_1}, \quad (6)$$

where the approximation obtained by using  $\bar{n}_2 \ll \bar{n}_1$  is only indicative, and we use full expression for the numerical analysis. Recently, utilization of such Boltzmann suppression for light DM has been realized in [59,60], but with a small mass gap ( $\delta < 1$ ). In this paper, we have considered a significantly large mass gap between the two states ( $\delta \sim 2-6$ ). We use the following expression for number density,

$$n_i(m, T) = \frac{T}{2\pi^2} m^2 K_2\left(\frac{m}{T}\right), \quad (7)$$

and the thermal averaged cross section in the s-wave limit is given as

$$\langle \sigma_{12} v_{12} \rangle = \frac{1}{32\pi} \frac{g_D^4}{m_{Z'}^4} (m_1 + m_2)^2. \quad (8)$$

One can rewrite (4) using the abundance  $Y = n/s$ , where  $s$  denotes the total entropy density of the standard model and the dark sector. As  $\xi < 1$ , the entropy is dominated by the SM bath and to a very good approximation,

$$s \approx s_{\text{SM}} = \frac{2\pi^2}{45} g_*^s(T_{\text{SM}}) T_{\text{SM}}^3.$$

The equilibrium abundance is given by

$$\bar{Y}(x, \xi) = \xi^3 \frac{d_\chi}{g_*^s(m_\chi/x\xi)} \frac{45}{4\pi^4} x^2 K_2(x), \quad (9)$$

where  $x = m_\chi/T_d$  is a measure of the dark sector temperature. The freeze-out occurs when

$$[\bar{n} \langle \sigma v \rangle_{\text{eff}}]_{x_f} = H(\xi, x_f), \quad (10)$$

i.e., when the interaction rate becomes less than the Hubble rate  $H = 1.66 g_*(T) T^2 / M_{\text{pl}} = 1.66 g_*(T/\xi) m_\chi^2 / (x^2 \xi^2 M_{\text{pl}})$ . The present day abundance,  $Y_\infty$ , is given as

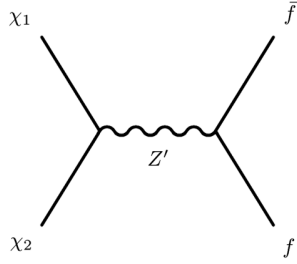


FIG. 1. The annihilation channel for  $\chi_1$  whose freeze-out determines the relic density.

$$Y_\infty = \frac{c\bar{Y}(x_f, \xi)}{1 + \lambda J(x_f) c\bar{Y}(x_f, \xi)}, \quad (11)$$

where  $c$ ,  $\lambda$ , and  $J(x_f)$  are defined in Appendix A. The relic density of DM is given by

$$\begin{aligned} \Omega h^2 &= m_\chi s_0 Y_\infty \frac{h^2}{\rho_c} \\ &\approx 282 \left( \frac{m_\chi}{\text{keV}} \right) \left( \frac{T_\gamma}{2.75 \text{ K}} \right)^3 c\bar{Y}(x_f, \xi), \end{aligned} \quad (12)$$

where the approximation is true in the limit  $\lambda J(x_f) c\bar{Y}(x_f, \xi) \ll 1$ . We use (10) to numerically determine the freeze-out temperature and enforce that  $x_f \geq 3$  so that the nonrelativistic approximation is valid. This restricts us from taking smaller values for  $\xi$  and  $m_1$ . Then we determine the relic density using (9), (11), (12), and compare with the observed value from Planck [52],

$$\Omega_\chi h^2 = 0.118 \pm 0.002. \quad (13)$$

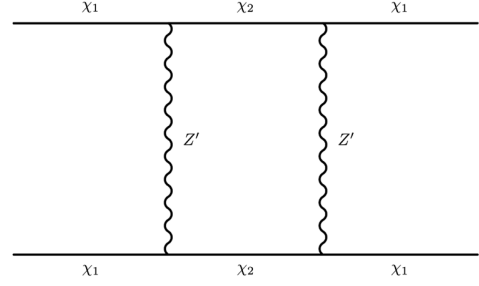


FIG. 2. The Feynman diagram for the self-interaction of DM. There are seven other ‘‘crossed’’ diagrams.

Understanding that such an estimate is only an approximation to solving the complete Boltzmann equations, we conservatively take an error on 5% in our analysis.

### B. One-loop self-interaction

One of the features of this model is that the self-interaction of dark matter is not a tree-level process. At one-loop level, there are eight diagrams that contribute to  $\chi_1 \chi_1 \rightarrow \chi_1 \chi_1$  when  $\chi_2$  and  $Z'$  are in the loop. A representative diagram is shown in Fig. 2. In [61,62], the self-interaction of inelastic DM was studied in the limit of large  $m_\chi$  and light propagator. In this study, we calculate the self-interaction in the limit of small  $m_\chi$  and heavy propagator. Since the loop particles are significantly heavier than the external ones, we use the decoupling limit where we ignore the external momenta while evaluating the loop. We use Package-X [63] and the unitary gauge to calculate the loop function and the cross section. It was checked that the infinities cancel systematically and we are left with a finite part. The self-interaction cross section in the s-wave approximation is given as

$$\frac{\sigma_{SI}}{m_1} = \frac{9}{256\pi^5} g_D^8 \frac{m_1 \left( m_2^6 + 3m_2^2 m_{Z'}^4 + 6m_2^2 m_{Z'}^4 \log\left(\frac{m_2^2}{m_{Z'}^2}\right) - 4m_{Z'}^6 \right)^2}{m_{Z'}^4 (m_{Z'}^2 - m_2^2)^6}. \quad (14)$$

The calculation is detailed in Appendix B. The velocity dependence of the self-interaction is shown in Fig. 3. It can be seen that the change is very small for nonrelativistic case ( $v < 0.1c$ ). Therefore, we use the estimate  $\frac{\sigma_{SI}(0)}{m_1} = 0.1\text{--}1 \text{ cm}^2/\text{g}$  to constrain the parameter space.

### C. A comment on the light fermion

One of the crucial assumption of this model is the existence of a massless fermionic species. One of the possibilities is that it is a part of the radiation component today albeit, the strong self-interactions would prevent it from being hot dark matter candidate. The other interesting possibility is that it is a sterile neutrino which also mixes

with the active neutrinos. It has been pointed out that in presence of self-interactions, the sterile neutrino acquires a large thermal mass in the early Universe and the mixing is suppressed [58,64]. This allows one to have larger mixing angles in the present era and helps resolve some of the short-baseline neutrino anomalies [65]. However, to avoid DM-neutrino scattering in the early universe, we require much smaller vacuum mixing angles that cannot explain these anomalies, but can be probed in future experiments.

The role of the light fermion in cosmology would be similar to that of dark radiation. The most stringent bounds on dark radiation comes from BBN  $N_{\text{eff}}$  which we have considered already. As this light fermion is part of a

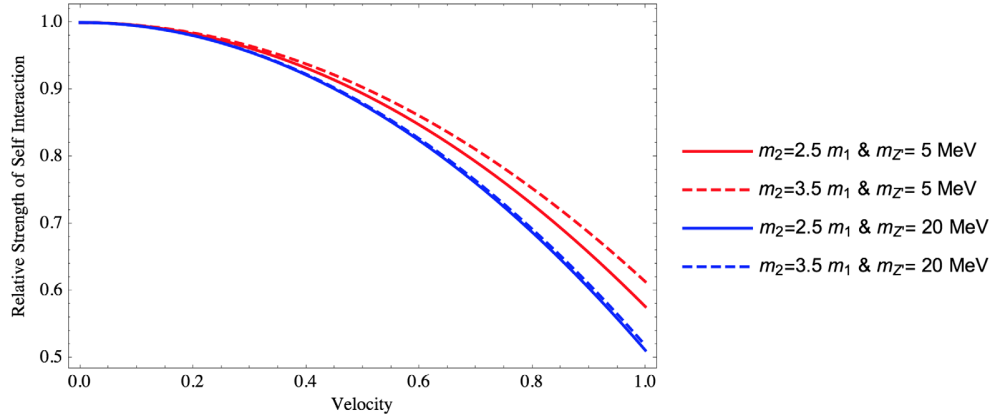


FIG. 3. The relative strength of self-interactions, i.e.,  $\sigma_{SI}(v)/\sigma_{SI}(0)$ , is shown as a function of velocity for various choices of parameters.

secluded and colder sector, it plays very little role in structure formation.

### III. RESULTS AND DISCUSSION

As pointed out before, we take  $g_D \approx 1$  for our analysis. This is a domain where the interactions are strong but perturbativity still holds. In [66], bounds on the mass of warm dark matter from Lyman- $\alpha$  are determined to be  $M_{\text{WDM}} \geq \text{few keV}$ . We only consider  $m_1 > 10$  keV in this work. We analyze the parameter space of  $\delta - m_{Z'}$  for various masses of  $m_1 \in \{10 \text{ keV}, 1 \text{ MeV}\}$  that give the correct relic density and self-interactions (Fig. 4). As the self-interactions do not depend on  $\xi$ , one can see that the limits are same for the two benchmark cases. It is to be noted that a heavier  $Z'$  is associated with smaller self-interaction.

The dependence of relic density on  $\xi$  can be simply understood as follows. From (9) one can see that  $\bar{Y}$  is a

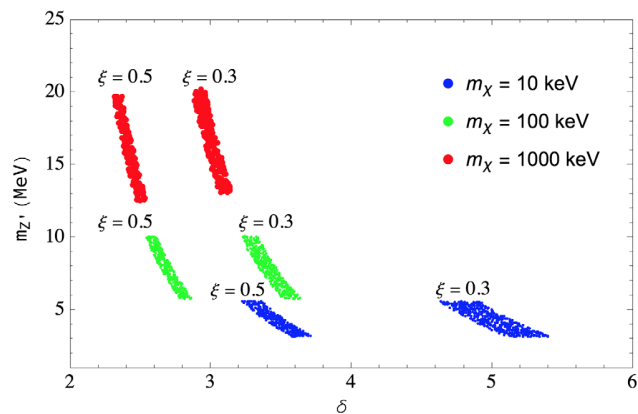


FIG. 4. The allowed parameter space for  $m_{Z'} = 10$  keV (blue), 100 keV (green), and 1 MeV (red) is shown for benchmark models  $\xi = 0.5$  (left) and  $\xi = 0.3$  (right). The upper (lower) limit of  $m_{Z'}$  corresponds to  $\sigma_{SI}/m_1 = 0.1(1.) \text{ cm}^2/\text{g}$ .

monotonically decreasing function of  $x$ . To compensate for small  $\xi$ , one needs a smaller  $x_f$ . This means that the effective cross section should be smaller such that freeze-out occurs earlier. This smallness is brought by a larger Boltzmann suppression due to heavier  $m_2$ . In an analogous way, one can argue the dependence of the relic density on  $c$ .

As the DM is part of a secluded sector, one does not anticipate any signals in direct detection experiments and colliders. This is consistent with the present status of these terrestrial experiments. Such a dark matter can only have gravitational signatures and can be probed through structure formation. Due to the self-interactions, the DM behaves as WDM and is consistent with the present understanding. In the future, as the limits on BBN  $N_{\text{eff}}$  are tightened, there will be less parameter space for the model to thrive.

### IV. CONCLUSION

In this paper, we have seen that one can get the correct relic density and appropriate self-interactions for a sub-MeV dark matter if it has strong off-diagonal interactions with a heavier spin-1 boson. The annihilation cross section is Boltzmann-suppressed and the self-interaction is loop-suppressed, thus allowing the mass scales to go as low as  $\mathcal{O}(10)$  keV while keeping the gauge coupling constant naturally large. Such a light DM must be part of a decoupled sector at a lower temperature in order to be consistent with BBN.

### ACKNOWLEDGMENTS

The author would like to thank Professor Subhendra Mohanty and Professor Namit Mahajan for their insights and several useful discussions. The author is also grateful to Arnab Dasgupta for going through the manuscript and providing valuable suggestions. The author also thanks the anonymous referee for pointing out important constraints.

## APPENDIX A: CALCULATION OF RELIC ABUNDANCE

The calculation of relic abundance of dark matter has been excellently treated in the book *The Early Universe* by E. W. Kolb and M. S. Turner [67]. We follow the general prescription laid by them while making necessary changes due to the temperature asymmetry. Similar calculation is performed in [25] and the only difference is that we use hidden sector temperature to define  $x$  while using SM entropy to define abundance  $Y$ . Such a definition is advantageous in models where the hidden sector entropy is not conserved explicitly (e.g., when a minor component decays into SM particles during late times). In such scenarios, the total entropy density, which is mainly SM entropy, is a good proxy for dilution effect. Otherwise, the treatment is analogous and one can use either definitions.

The Boltzmann equation for the total number density (4) can be conveniently expressed in terms of the abundance,

$$Y = \frac{n}{s}, \quad (\text{A1})$$

which is free from the dilution due to expansion. Note that  $s$  denotes the total entropy density of the dark and visible sectors. However, due to temperature asymmetry, one can ignore the contribution from the dark sector. Also note that, since the total entropy is conserved,  $\dot{s} + 3Hs = 0$ . During the radiation-dominated era, the scale factor  $R \sim t^{1/2}$  which gives us

$$\frac{dx}{dt} = \frac{\tilde{H}(m_\chi, \xi)}{x}, \quad (\text{A2})$$

where  $x = m_\chi/T_d$  and in terms of the Planck mass  $M_{pl} = 1.22 \times 10^{25}$  keV,

$$\tilde{H}(m_\chi, \xi) = 1.66 \sqrt{g_\star} \left( \frac{m_\chi}{x\xi} \right) \frac{1}{\xi^2} \frac{m_\chi^2}{M_{pl}}. \quad (\text{A3})$$

Using (9) and

$$\tilde{s}(m_\chi, \xi) = \frac{2\pi^2}{45} g_\star^s \left( \frac{m_\chi}{x\xi} \right) \frac{m^3}{\xi^3}, \quad (\text{A4})$$

the Boltzmann equation for abundance is

$$\frac{dY}{dx} = -\frac{\tilde{s}}{\tilde{H}} \frac{\langle \sigma v \rangle_{\text{eff}}}{x^2} (Y^2 - \bar{Y}^2). \quad (\text{A5})$$

Note that the temperature (hence,  $x$ ) dependence in the effective cross section comes only from the Boltzmann factor and, hence, one can write

$$\mathcal{M}_1 \sim \frac{g^4 [\bar{u}(k_1) \gamma^\mu (\not{q} + m_2) \gamma^\alpha u(p_1)] [\bar{v}(p_2) \gamma^\beta (\not{q} + m_2) \gamma^\nu v(k_2)] P_{\alpha\beta} P_{\mu\nu}}{(q^2 - m_2^2)(q^2 - m_2^2)}, \quad (\text{B2})$$

$$\langle \sigma v \rangle_{\text{eff}} = \sigma_0 f(x, \delta), \quad (\text{A6})$$

where

$$f(x, \delta) = \frac{(1 + \delta)^2 K_2(x) K_2((1 + \delta)x)}{(K_2(x) + (1 + \delta)^2 K_2((1 + \delta)x))^2}. \quad (\text{A7})$$

Using the dimensionless quantity  $\lambda = \sigma_0 \tilde{s} / \tilde{H}$ , one can simplify (A5) as

$$\frac{dY}{dx} = -\lambda \frac{f(x, \delta)}{x^2} (Y^2 - \bar{Y}^2), \quad (\text{A8})$$

which can be further simplified using the difference  $\Delta = Y - \bar{Y}$  and approximately solved when  $x \gg x_f$  and  $\Delta \approx Y \gg \bar{Y}$ , which gives

$$\Delta' \approx -\lambda \frac{f(x, \delta)}{x^2} \Delta^2. \quad (\text{A9})$$

Upon integration from freeze-out to the present day of (A9), we get

$$\frac{1}{Y_\infty} = \frac{1}{\Delta_\infty} = \frac{1}{\Delta_f} + \lambda \int_{x_f}^{\infty} \frac{f(x, \delta)}{x^2} dx = \frac{1}{\Delta_f} + \lambda J \quad (\text{A10})$$

and the  $J$  integral can be performed numerically once  $x_f$  is determined. It was shown in [25] that the approximation

$$\Delta_f = c \bar{Y}(x_f, \xi) \quad (\text{A11})$$

agrees with the numerical solution of (A8) if  $c = 0.2$  (0.5) for  $\xi = 0.3$  (0.8). This gives us the final result,

$$Y_\infty = \frac{c \bar{Y}(x_f, \xi)}{1 + \lambda J(x_f) c \bar{Y}(x_f, \xi)}, \quad (\text{A12})$$

which is shown in (11). For our analysis, we assume  $c = 0.2$  and note that any change in  $c$  will proportionately scale the relic density.

## APPENDIX B: CALCULATION OF SELF-INTERACTION

We calculate the amplitude for the process,

$$\chi_1(p_1) + \chi_2(p_2) \rightarrow \chi_1(k_1) + \chi_2(k_2), \quad (\text{B1})$$

where  $p_i$  and  $k_i$  are the four momentum of the particles. There are eight Feynman diagrams for this process which are related by crossing to the one shown in Fig. 2. In the decoupling limit, the amplitude is

where  $q$  is the loop momentum and  $P_{\mu\nu}$  in the unitary gauge is given by

$$P_{\mu\nu} = -g_{\mu\nu} + \frac{q_\mu q_\nu}{m_{Z'}^2}. \quad (\text{B3})$$

The other crossed amplitudes ( $\mathcal{M}_2 \rightarrow \mathcal{M}_6$ ) are related to  $\mathcal{M}_1$  by  $\beta \leftrightarrow \mu, \beta \leftrightarrow \nu, k_1 \leftrightarrow k_2$ . There are two diagrams pertaining to the colloquial ‘‘s-channel’’ due to Majorana nature of the incoming fermions. The relative sign of graphs must be taken correctly for cancellation of the infinities. One can evaluate the loop integral using Package-X or any other alternative. The final result can be simply expressed in the  $\{S, V, T, A, P\}$  basis as

$$\begin{aligned} \mathcal{M} = g^4 \sum_{i=S,V,T,A,P} & (C_i [\bar{u}(k_1)\Gamma_i u(p_1)][\bar{v}(p_2)\Gamma_i v(k_2)] \\ & + C'_i [\bar{v}(p_2)\Gamma_i u(p_1)][\bar{u}(k_2)\Gamma_i v(k_1)]). \end{aligned} \quad (\text{B4})$$

Note that the mixed terms (e.g.,  $V - A$ ) are absent. The only nonzero coefficients are

$$C_A = \frac{6m_2^2 m_{Z'}^2 \log\left(\frac{m_2^2}{m_{Z'}^2}\right)}{(m_2^2 - m_{Z'}^2)^3} - \frac{3(m_2^4 - m_2^2 m_{Z'}^2 + 2m_{Z'}^4)}{m_{Z'}^2 (m_2^2 - m_{Z'}^2)^2} \quad (\text{B5})$$

$$C_T = -\frac{m_2^2 (m_2^2 - 3m_{Z'}^2)}{m_{Z'}^2 (m_2^2 - m_{Z'}^2)^2} - \frac{2m_2^2 m_{Z'}^2 \log\left(\frac{m_2^2}{m_{Z'}^2}\right)}{(m_2^2 - m_{Z'}^2)^3} \quad (\text{B6})$$

$$C'_S = \frac{6m_2^2 (m_2^2 - 3m_{Z'}^2)}{m_{Z'}^2 (m_2^2 - m_{Z'}^2)^2} + \frac{12m_2^2 m_{Z'}^2 \log\left(\frac{m_2^2}{m_{Z'}^2}\right)}{(m_2^2 - m_{Z'}^2)^3} \quad (\text{B7})$$

$$C'_A = \frac{3m_2^2 m_{Z'}^2 \log\left(\frac{m_2^2}{m_{Z'}^2}\right)}{(m_2^2 - m_{Z'}^2)^3} - \frac{3(m_2^4 - m_2^2 m_{Z'}^2 + 2m_{Z'}^4)}{2m_{Z'}^2 (m_2^2 - m_{Z'}^2)^2}. \quad (\text{B8})$$

In terms of these coefficients, the nonrelativistic squared amplitude is

$$\begin{aligned} |\overline{\mathcal{M}}|^2 = & 16m_1^4 (3C_A + 2C'_A - 6C_T)^2 \\ & - 16m_1^4 v^2 (C_A + 2C'_A - 6C_T)(3C_A + 2C'_A - 6C_T), \end{aligned} \quad (\text{B9})$$

and the transfer cross section for self-interaction is

$$\begin{aligned} \sigma_{SI} = & \int d\Omega (1 - \cos(\theta)) \left( \frac{d\sigma}{d\Omega} = \frac{1}{64\pi^2 (4m_x^2)} |\overline{\mathcal{M}}|^2 \right) \\ \approx & \frac{1}{64\pi m_x^2} |\overline{\mathcal{M}}|^2. \end{aligned} \quad (\text{B10})$$

## APPENDIX C: POSSIBLE UV COMPLETION

In this section, we consider a possible UV completion of the simplified model presented above. The standard model gauge group is extended by an  $U(1)_D$  symmetry. We add four fermions and a scalar to the model which are singlets under SM gauge symmetry. Their charges under the new symmetry are given in Table I.

The above choice of charges assures that the model is anomaly free. One can chose  $a \approx 1$  but  $\neq 1$  to ensure that  $\phi$  does not have Yukawa-like interaction with  $f_1$  or  $f_2$ . The most general Lagrangian for the dark sector is

$$\begin{aligned} \mathcal{L} = & \bar{\psi}_1 (\not{D} - m)\psi_1 + \bar{\psi}_2 (\not{D} - m)\psi_2 + \bar{f}_1 (\not{D} - m_f)f_1 \\ & + \bar{f}_2 (\not{D} - M_f)f_2 \end{aligned} \quad (\text{C1})$$

$$+ y\phi \bar{\psi}_1 \psi_2 + \text{H.c.} \quad (\text{C2})$$

$$+ (D_\mu \phi)^\dagger (D^\mu \phi) - \frac{1}{4} X^{\mu\nu} X_{\mu\nu} \quad (\text{C3})$$

$$+ \frac{\epsilon}{4} X^{\mu\nu} F_{\mu\nu} + \eta \phi^\dagger \phi H^\dagger H \quad (\text{C4})$$

$$- \mathcal{V}(\phi), \quad (\text{C5})$$

where  $H$  is the SM Higgs field,  $X_{\mu\nu} = \partial_\mu Z'_\nu - \partial_\nu Z'_\mu$  is the field strength for the  $Z'$ , and

$$D_\mu = \partial_\mu - ig_D Q_D Z'_\mu \quad (\text{C6})$$

is the gauge covariant derivative. To begin with, we consider the limit where  $\epsilon \rightarrow 0$  and  $\eta \rightarrow 0$ , which is motivated from the assumption that the dark sector is thermally secluded from the visible sector. Also, these interactions cannot be generated via loops which allows us to take their coefficients to be vanishingly small.

The potential for the new scalar field has the usual form considered for spontaneous symmetry breaking,

$$\mathcal{V}(\phi) = -\mu^2 \phi^\dagger \phi + \lambda (\phi^\dagger \phi)^2. \quad (\text{C7})$$

The symmetry breaking not only gives mass to the new gauge boson, but also generates an off-diagonal mass term from the Yukawa-like interaction. In the  $\psi_1 - \psi_2$  basis, the mass matrix is

$$\hat{M} = \begin{pmatrix} m & yv_\phi \\ yv_\phi & m \end{pmatrix}, \quad (\text{C8})$$

TABLE I. The new fields in the dark sector and their charges under  $U(1)_D$  symmetry.

Fields	$\psi_1$	$\psi_2$	$f_1$	$f_2$	$\phi$
$Q_D$	1	-1	$a$	$-a$	2

which has eigenvalues  $m \pm yv_\phi$ . One can go to the mass eigenstates by the transformation,

$$\psi_1 \rightarrow \frac{\chi_1 + \chi_2}{\sqrt{2}} \quad \text{and} \quad \psi_2 \rightarrow \frac{\chi_1 - \chi_2}{\sqrt{2}}. \quad (\text{C9})$$

The Lagrangian for  $\chi_1$  and  $\chi_2$  is

$$\begin{aligned} \mathcal{L} = & \bar{\chi}_1(\not{\partial} - m_1)\chi_1 + \bar{\chi}_2(\not{\partial} - m_2)\chi_2 \\ & + ig_D(\bar{\chi}_1\mathcal{Z}'\chi_2 + \bar{\chi}_2\mathcal{Z}'\chi_1) + \dots, \end{aligned} \quad (\text{C10})$$

where the ellipses denote interactions with the Higgs scalar of the dark sector. In terms of the free parameters, one can fix  $v_\phi$  given the mass of the  $Z'$  boson. However, by varying  $\lambda$  one can make the scalar sufficiently heavy such that it does not affect the low scale dynamics. Also, one can speculate that if there are other heavy fields in the dark sector, there may be large radiative corrections to the scalar mass. The mass gap between the two states is determined by the Yukawa coupling ( $m_2 = m_1 + 2yv_\phi$ ) and can be considered as a free parameter. In the limit  $M_f \gg m_1, m_2$ , this model essentially reduced to the one considered in the paper.

- 
- [1] K. Garrett and G. Duda, *Adv. Astron.* **2011**, 968283 (2011).  
[2] G. Bertone and D. Hooper, [arXiv:1605.04909](https://arxiv.org/abs/1605.04909).  
[3] M. Lisanti, [arXiv:1603.03797](https://arxiv.org/abs/1603.03797).  
[4] S. Profumo, [arXiv:1301.0952](https://arxiv.org/abs/1301.0952).  
[5] T. Plehn, [arXiv:1705.01987](https://arxiv.org/abs/1705.01987).  
[6] F. S. Queiroz, [arXiv:1605.08788](https://arxiv.org/abs/1605.08788).  
[7] D. S. Akerib *et al.* (LUX Collaboration), *Phys. Rev. Lett.* **118**, 251302 (2017).  
[8] R. Essig, T. Volansky, and T. T. Yu, *Phys. Rev. D* **96**, 043017 (2017).  
[9] G. Cavoto, F. Luchetta, and A. D. Polosa, *Phys. Lett. B* **776**, 338 (2018).  
[10] Y. Hochberg, Y. Kahn, M. Lisanti, K. M. Zurek, A. G. Grushin, R. Ilan, S. M. Griffin, Z.-F. Liu, S. F. Weber, and J. B. Neaton, *Phys. Rev. D* **97**, 015004 (2018).  
[11] Y. Hochberg, E. Kuflik, T. Volansky, and J. G. Wacker, *Phys. Rev. Lett.* **113**, 171301 (2014).  
[12] Y. Hochberg, E. Kuflik, H. Murayama, T. Volansky, and J. G. Wacker, *Phys. Rev. Lett.* **115**, 021301 (2015).  
[13] N. Bernal, C. Garcia-Cely, and R. Rosenfeld, *J. Cosmol. Astropart. Phys.* **04** (2015) 012.  
[14] N. Daci, I. De Bruyn, S. Lowette, M. H. G. Tytgat, and B. Zaldivar, *J. High Energy Phys.* **11** (2015) 108.  
[15] S. M. Choi and H. M. Lee, *J. High Energy Phys.* **09** (2015) 063.  
[16] M. Hansen, K. Langble, and F. Sannino, *Phys. Rev. D* **92**, 075036 (2015).  
[17] N. Bernal, X. Chu, C. Garcia-Cely, T. Hambye, and B. Zaldivar, *J. Cosmol. Astropart. Phys.* **03** (2016) 018.  
[18] N. Bernal and X. Chu, *J. Cosmol. Astropart. Phys.* **01** (2016) 006.  
[19] Y. Hochberg, E. Kuflik, and H. Murayama, *J. High Energy Phys.* **05** (2016) 090.  
[20] U. K. Dey, T. N. Maity, and T. S. Ray, *J. Cosmol. Astropart. Phys.* **03** (2017) 045.  
[21] N. Bernal, X. Chu, and J. Pradler, *Phys. Rev. D* **95**, 115023 (2017).  
[22] S. M. Choi, Y. Hochberg, E. Kuflik, H. M. Lee, Y. Mambrini, H. Murayama, and M. Pierre, *J. High Energy Phys.* **10** (2017) 162.  
[23] G. Krnjaic, *Phys. Rev. D* **94**, 073009 (2016).  
[24] D. Green and S. Rajendran, *J. High Energy Phys.* **10** (2017) 013.  
[25] J. L. Feng, H. Tu, and H. B. Yu, *J. Cosmol. Astropart. Phys.* **10** (2008) 043.  
[26] R. Foot and S. Vagnozzi, *Phys. Rev. D* **91**, 023512 (2015).  
[27] R. Foot and S. Vagnozzi, *Phys. Lett. B* **748**, 61 (2015).  
[28] R. Foot and S. Vagnozzi, *J. Cosmol. Astropart. Phys.* **07** (2016) 013.  
[29] A. Berlin, D. Hooper, and G. Krnjaic, *Phys. Rev. D* **94**, 095019 (2016).  
[30] D. N. Spergel and P. J. Steinhardt, *Phys. Rev. Lett.* **84**, 3760 (2000).  
[31] M. Vogelsberger and J. Zavala, *Mon. Not. R. Astron. Soc.* **430**, 1722 (2013).  
[32] M. Rocha, A. H. G. Peter, J. S. Bullock, M. Kaplinghat, S. Garrison-Kimmel, J. Onorbe, and L. A. Moustakas, *Mon. Not. R. Astron. Soc.* **430**, 81 (2013).  
[33] A. H. G. Peter, M. Rocha, J. S. Bullock, and M. Kaplinghat, *Mon. Not. R. Astron. Soc.* **430**, 105 (2013).  
[34] B. Moore, S. Gelato, A. Jenkins, F. R. Pearce, and V. Quilis, *Astrophys. J.* **535**, L21 (2000).  
[35] N. Yoshida, V. Springel, S. D. M. White, and G. Tormen, *Astrophys. J.* **535**, L103 (2000).  
[36] A. Burkert, *Astrophys. J.* **534**, L143 (2000).  
[37] M. Y. Khlopov, G. M. Beskin, N. E. Bochkarev, L. A. Pustyl'nik, and S. A. Pustyl'nik, *Sov. Astron.* **35**, 21 (1991) [*Astron. Zh.* **68**, 42 (1991)].  
[38] S. I. Blinnikov and M. Y. Khlopov, *Yad. Fiz.* **36**, 809 (1982) [*Sov. J. Nucl. Phys.* **36**, 472 (1982)].  
[39] S. I. Blinnikov and M. Khlopov, *Sov. Astron.* **27**, 371 (1983) [*Astron. Zh.* **60**, 632 (1983)].  
[40] S. Bruggisser, F. Riva, and A. Urbano, *SciPost Phys.* **3**, 017 (2017).  
[41] S. Tulin and H. B. Yu, *Phys. Rep.* **730**, 1 (2018).  
[42] K. Sigurdson, [arXiv:0912.2346](https://arxiv.org/abs/0912.2346).  
[43] S. Hannestad and R. J. Scherrer, *Phys. Rev. D* **62**, 043522 (2000).  
[44] A. Berlin, D. Hooper, and G. Krnjaic, *Phys. Lett. B* **760**, 106 (2016).  
[45] S. Das and K. Sigurdson, *Phys. Rev. D* **85**, 063510 (2012).  
[46] E. Hardy and J. Unwin, *J. High Energy Phys.* **09** (2017) 113.

- [47] D. Tucker-Smith and N. Weiner, *Phys. Rev. D* **64**, 043502 (2001).
- [48] D. Tucker-Smith and N. Weiner, *Phys. Rev. D* **72**, 063509 (2005).
- [49] Y. Cui, D. E. Morrissey, D. Poland, and L. Randall, *J. High Energy Phys.* **05** (2009) 076.
- [50] D. S. M. Alves, S. R. Behbahani, P. Schuster, and J. G. Wacker, *Phys. Lett. B* **692**, 323 (2010).
- [51] S. Chang, N. Weiner, and I. Yavin, *Phys. Rev. D* **82**, 125011 (2010).
- [52] P. A. R. Ade *et al.* (Planck Collaboration), *Astron. Astrophys.* **594**, A13 (2016).
- [53] L. Feng, J. F. Zhang, and X. Zhang, *Sci. China-Phys. Mech. Astron.* **61**, 050411 (2018).
- [54] K. Griest and D. Seckel, *Phys. Rev. D* **43**, 3191 (1991).
- [55] A. Berlin, *Phys. Rev. Lett.* **119**, 121801 (2017).
- [56] E. Izaguirre, Y. Kahn, G. Krnjaic, and M. Moschella, *Phys. Rev. D* **96**, 055007 (2017).
- [57] K. R. Dienes, J. Kumar, B. Thomas, and D. Yaylali, *Phys. Rev. D* **96**, 115009 (2017).
- [58] S. Hannestad, R. S. Hansen, and T. Tram, *Phys. Rev. Lett.* **112**, 031802 (2014).
- [59] R. T. D’Agnolo and J. T. Ruderman, *Phys. Rev. Lett.* **115**, 061301 (2015).
- [60] R. T. D’Agnolo, D. Pappadopulo, and J. T. Ruderman, *Phys. Rev. Lett.* **119**, 061102 (2017).
- [61] M. Blennow, S. Clementz, and J. Herrero-Garcia, *J. Cosmol. Astropart. Phys.* **03** (2017) 048.
- [62] K. Schutz and T. R. Slatyer, *J. Cosmol. Astropart. Phys.* **01** (2015) 021.
- [63] H. H. Patel, *Comput. Phys. Commun.* **218**, 66 (2017).
- [64] B. Dasgupta and J. Kopp, *Phys. Rev. Lett.* **112**, 031803 (2014).
- [65] A. Aguilar-Arevalo *et al.* (LSND Collaboration), *Phys. Rev. D* **64**, 112007 (2001).
- [66] C. Yche, N. Palanque-Delabrouille, J. Baur, and H. du Mas des Bourboux, *J. Cosmol. Astropart. Phys.* **06** (2017) 047.
- [67] E. W. Kolb and M. S. Turner, *The Early Universe* (Springer, 1990).